UNIVERSITY OF SÃO PAULO
Faculty of Pharmaceutical Sciences
Graduation Program in Food Science
Area of Food Science

Evaluation of ethylene-auxin crosstalk and its influence on the volatile compound metabolism during tomato (*Solanum lycopersicum* L.) fruit ripening by comparative metabolomic and proteomic analysis

Eric de Castro Tobaruela

Ph. D. thesis presented for the degree of
DOCTOR OF SCIENCE

Advisor: Prof. Dr. Eduardo Purgatto

São Paulo
2020

UNIVERSITY OF SÃO PAULO
Faculty of Pharmaceutical Sciences
Graduation Program in Food Science
Area of Food Science

Evaluation of ethylene-auxin crosstalk and its influence on the volatile compound metabolism during tomato (*Solanum lycopersicum* L.) fruit ripening by comparative metabolomic and proteomic analysis

Eric de Castro Tobaruela

Original Version

Ph. D. thesis presented for the degree of
DOCTOR OF SCIENCE

Advisor: Prof. Dr. Eduardo Purgatto

São Paulo
2020

Ficha Catalográfica
Elaborada pela Divisão de Biblioteca e
Documentação do Conjunto das Químicas da USP.

Bibliotecária responsável pela orientação de catalogação da publicação:
Marlene Aparecida Vieira - CRB - 8/5562

Tobaruela, Eric de Castro
T628e Evaluation of ethylene-auxin crosstalk and its influence on the volatile compound metabolism during tomato (*Solanum lycopersicum* L.) fruit ripening by comparative metabolomic and proteomic analysis. / Eric de Castro Tobaruela. -- São Paulo, 2020.
198p.

Thesis (doutor) - Faculdade de Ciências Farmacêuticas da Universidade de São Paulo. Departamento de Alimentos e Nutrição Experimental.
Advisor: Purgatto, Eduardo

1. Food science. 2. Fruit ripening. 3. Hormonal regulation. 4. Volatile compounds. I. T. II. Purgatto, Eduardo, advisor.

Eric De Castro Tobaruela

Evaluation of ethylene-auxin crosstalk and its influence on the volatile compound metabolism during tomato (*Solanum lycopersicum* L.) fruit ripening by comparative metabolomic and proteomic analysis

Commission of Thesis
for the
degree of Doctor of Science

_____
Advisor

_____
1st Examiner

_____
2nd Examiner

_____
3rd Examiner

_____
4th Examiner

São Paulo, _____, 2020.

I dedicate this thesis to my loving and supporting parents and my sister, who are always supporting me to accomplish my dreams and cheering for me. Father, mother, and sister, I can not express with words how much you mean to me and how grateful I am for having you in my life. I love you.

ACKNOWLEDGMENT

First, I would like to thank God for all the blessings and for giving me the strength and perseverance to complete this thesis.

I would like to thank my advisor Prof. Eduardo Purgatto for these four years working together. I am thankful for the opportunity to learn from him, for his trust and for allowing me to grow as a research scientist. I admire how passionate he is about scientific research.

I would like to express my gratitude to Dr. Mondher Bouzayen and Dr. Mohamed Zouine, for giving me the opportunity to join the Genomics and Biotechnology of the Fruits (GBF) laboratory as a visiting student at the *Institut national de la recherche agronomique*. I could not imagine how much this experience would make me grow as a scientist and a person. I still can not put in words how grateful I am.

I would also like to thank Prof. João Paulo Fabi, Prof. Luciano Freschi, Prof. Lázaro Eustáquio Pereira Peres, and the postdoctoral researchers Dr. Fernanda Peroni and Dr. Roberta Ghedini for their contributions in my admission and qualification boards, contributing to the developmental this project.

To all LQBQ students and technicians that came and went during my four years here. I want to express my appreciation, for all the work together as a team and for supporting each other. In special, I am so grateful for all the help and friendship of Lúcia Helena Justino, Victor Castro-Alves, Samira Prado, Bruna Lima, Gabriela Schmitz, Elisa Brasili, Florença Borges, Mayra Batista, and Ellen Tyna, without them this thesis would not be finished. To all the other LQBQ members, I would like to thank for all for the moments of fun and for making this journey lighter. I also want to show my appreciation for my friends from different labs who were always there for me and contribute to my project in all sorts of ways.

A special thanks to all the GBF researchers, technicians, and students for their help and assistance, for all the laughter and funny moments, for all the talk and advices. I place on record my deepest gratitude to my GBF best friends, Isabelle Mila, Clementine Dumont, Ximena Chirinos, and Maria Aurineide Rodrigues for all the life lessons, for all the philosophical discussions, and for shared bottles of wine (strictly necessary).

I would like to thank my Brazilian friends from Fortaleza (Camila Barbosa, Marcela Albuquerque, Fabio Neves, and Priscilla Pinho), São Paulo (Roberta Noris and João Leite), and Toulouse (Pedro Gomes, Luiza Vientini, and Carol Camões). As well as to

express my gratitude to my foreign friends with Brazilian hearts (Ximena Chirinos, Guillaume Posé, Jing An, Andra Purdea, and Stefano Neroni) for all the friendship and emotional support during the year at Toulouse. I will never forget our “Brazilian” Night Outs. Thanks for being my piece of Brazil in France. Special thanks to my dear Kevin de Sousa for being an important person since we met in Toulouse...

This work would not be possible without the financial support of FAPESP (grant 2013/07914-8), the scholarships provided by CAPES (88882.376973/2019-01) and CAPES/COFECUB (88881.145838/2017-01), and the commitment from all the employees from the Food and Experimental Nutrition Department.

Obrigado. Merci. Thanks. Gracias. 謝謝你.

“It is not the strongest of the species that survives,
not the most intelligent that survives.
It is the one that is the most adaptable to change.”
Charles Darwin

RESUMO

TOBARUELA EC. **Avaliação da interação etileno-auxina e de sua influência no metabolismo de compostos voláteis durante o amadurecimento de tomates (*Solanum lycopersicum* L.) por análise metabolômica e proteômica comparativa.** 2020. 198f. Tese (Doutorado em Ciência dos Alimentos) – Faculdade de Ciências Farmacêuticas, Universidade de São Paulo, São Paulo, 2020.

Progressos consideráveis têm sido feitos no estudo do amadurecimento de frutos climatéricos. Entretanto, o conhecimento acerca dos fatores dependentes e independentes de etileno que regulam o amadurecimento de frutos climatéricos ainda é limitado e o papel da auxina e de outros hormônios relacionados à regulação do amadurecimento permanece por ser elucidado. Estudos têm avaliado o papel da auxina e da interação etileno-auxina no metabolismo secundário em frutos de tomate e destacado a necessidade de aprofundar o conhecimento já existente e melhorar a compreensão do papel de ambos os hormônios na formação do aroma de frutos climatéricos. Neste contexto, o presente trabalho teve como objetivo avaliar a interação etileno-auxina e sua influência no metabolismo de compostos voláteis durante o amadurecimento de tomates (*Solanum lycopersicum* L.) através de análises metabolômicas e proteômicas comparativas. Para tal, frutos de tomateiro cv. Micro-Tom em estádio *mature green* foram separados em quatro grupos experimentais: CTRL (sem tratamento); ETHY (tratamento com etileno); IAA (tratamento com ácido indol-3-acético); ETHY+IAA (ambos os tratamentos hormonais). A mudança de cor e a emissão de etileno foram determinadas diariamente. Os perfis metabólicos polares e não polares foram determinados separadamente em frutos 0, 8 e 18 dias de amadurecimento por GC-MS enquanto as análises proteômicas foram realizadas em frutos com 0 e 8 dias de amadurecimento por LC-MS. Compostos voláteis foram analisados em dias específicos. Metabolitos primários e secundários tiveram seus níveis significativamente alterados pelos tratamentos hormonais, assim como as enzimas envolvidas em metabolismos relacionados. Análises de enriquecimento evidenciaram as vias metabólicas que foram significativamente influenciadas pelos tratamentos com etileno e auxina, incluindo em metabolismos secundários, como as vias de biossíntese de terpenoides, carotenoides e compostos voláteis derivados de

aminoácidos e ácidos graxos. Por fim, metabólitos primários, metabólitos secundários, enzimas e compostos voláteis importantes para o aroma dos frutos de tomate foram correlacionados em análises de vias metabólicas específicas. Considerando os resultados obtidos, observamos o efeito de cada hormônio estudado na modulação dos metabolismos primário e secundário, e, consequentemente, na formação de compostos voláteis, reforçando não apenas a importância do etileno e da auxina na regulação do amadurecimento, assim como o papel do *crosstalk* entre etileno e auxina no desenvolvimento do aroma do tomate.

Palavras-chave: Frutos climatéricos. Carotenoides. Compostos voláteis. Proteínas. Metabólitos.

ABSTRACT

TOBARUELA EC. **Evaluation of ethylene-auxin crosstalk and its influence on the volatile compound metabolism during tomato (*Solanum lycopersicum* L.) fruit ripening by comparative metabolomic and proteomic analysis.** 2020. 198f. Tese (Doutorado em Ciência dos Alimentos) – Faculdade de Ciências Farmacêuticas, Universidade de São Paulo, São Paulo, 2020.

Considerable progress has been made in studying climacteric fruit ripening. However, knowledge of ethylene-dependent and independent regulatory processes involved in this process is limited, and the roles of auxin and other ripening-related hormones remain to be elucidated. Studies have evaluated the roles of auxin and ethylene-auxin crosstalk in secondary metabolism in tomato fruits and highlighted the need to deepen existing knowledge and improve understanding of the roles of both hormones in regulating aroma formation in climacteric fruits. In this context, the present study aimed to evaluate the ethylene-auxin crosstalk and its influence on the volatile compound metabolism during tomato (*Solanum lycopersicum* L.) fruit ripening by comparative metabolomic and proteomic analysis. Tomato fruits cv. Micro-Tom at the mature green stage were randomly separated into four groups according to hormone treatments: CTRL (without treatment); ETHY (ethylene treatment); IAA (indole-3-acetic acid treatment); and ETHY+IAA (both hormone treatments). The color shift and ethylene emission were determined daily. Polar and non-polar metabolic profiles were obtained separately at 0, 8, and 18 days after harvest (DAH) by GC-MS, while proteomic analysis was conducted at 0 and 8 DAH by LC-MS. Volatile compounds were analyzed on specific days. Hormone treatments significantly altered the levels of both primary and secondary metabolites and the enzymes involved in the related metabolisms. Enrichment analyses showed which pathways were significantly influenced by ethylene and auxin treatments, including those of secondary metabolisms, such as the biosynthetic pathways of terpenoids, carotenoids, and volatile compounds derived from amino acids and fatty acids. Finally, primary and secondary metabolites, enzymes, and volatile compounds important for tomato fruit aroma were correlated in specific pathway analyses. Considering the obtained results, we observed the effect of each studied hormone in modulating primary and secondary metabolisms and

therefore volatile compound formation, reinforcing both the importance of ethylene and auxin in regulating ripening and the role of ethylene-auxin crosstalk in regulating the tomato fruit aroma.

Keywords: Climacteric fruits. Carotenoids. Volatile compounds. Proteins. Metabolites.

LIST OF FIGURES

Figure 1 Ethylene biosynthesis (A) and perception (B)…… 30

Figure 2 Indole-3-acetic acid biosynthesis (A) and perception (B)…… 33

Figure 3 Main metabolic precursors and pathways of volatile compound biosynthesis in plants…..…… 36

CHAPTER 1

Figure 1 Effects of ethylene, auxin, and both treatments on fruit color, ethylene emission, and auxin content during Micro-Tom tomato (*Solanum lycopersicum* L.) fruit ripening…….. 55

Figure 2 Effects of ethylene, auxin, and both treatments on ethylene and auxin-related gene expression during Micro-Tom tomato (*Solanum lycopersicum* L.) fruit ripening……. 56

Figure 3 Effects of ethylene, auxin, and both treatments on VOC contents, carotenoid contents, and related enzyme activities during Micro-Tom tomato (*Solanum lycopersicum* L.) fruit ripening…….. 62

Figure 4 Effects of ethylene, auxin, and both treatments on fruit color, ethylene emission, and VOC contents during Sweet Grape (*Solanum lycopersicum* L.) fruit ripening…… 66

Figure 5 Effects of ethylene, auxin, and both treatments on fruit color, ethylene emission, and VOC contents during Micro-Tom (*Solanum lycopersicum* L.) fruit ripening…..…… 72

Figure S1 Effects of ethylene, auxin, and both treatments on the VOC contents in Micro-Tom tomato (*Solanum lycopersicum* L.) fruits... 75

Figure S2 Effects of ethylene, auxin, and both treatments on the expression of fatty-acid-related genes important to VOC production during Micro-Tom tomato (*Solanum lycopersicum* L.) fruit ripening…….. 77

Figure S3 Relative abundance of significantly changed metabolites in tomato (*Solanum lycopersicum* L. cv. Micro-Tom) fruits after ethylene, auxin, and both treatments throughout ripening.....….. 79

Figure S4 Effects of ethylene, auxin, and both treatments on the VOC contents in Sweet Grape tomato (*Solanum lycopersicum* L.) fruits……... 81
Figure S5 Comparison of VOC profiles of Micro-Tom and Sweet Grape tomato (*Solanum lycopersicum* L.) cultivars at mature green, breaker, and red stages……..… 83

CHAPTER 2

Figure 1 Characterization of Micro-Tom tomato (*Solanum lycopersicum* L.) fruit ripening at two harvests……..……... 103
Figure 2 Polar metabolites of Micro-Tom tomato (*Solanum lycopersicum* L.) fruits at 8 and 18 days after harvest (DAH)……..……... 105
Figure 3 Non-polar metabolites of Micro-Tom tomato (*Solanum lycopersicum* L.) fruits at 8 and 18 days after harvest (DAH)…..…. 106
Figure 4 Metabolic pathways differentially impacted by treatment with ethylene, auxin, or both hormones in Micro-Tom tomato (*Solanum lycopersicum* L.) fruits at 8 and 18 days after harvest (DAH)……. 109
Figure 5 Secondary metabolite biosynthesis panel summarizes the relative levels of individual metabolites involved in the biosynthesis of each secondary metabolite category…..…….. 111
Figure 6 Biosynthesis pathways of the most important volatile compounds with respect to tomato (*Solanum lycopersicum* L.) fruit aroma….. 113
Figure S1 Metabolites of Micro-Tom tomato (*Solanum lycopersicum* L.) fruits at 8 and 18 days after harvest (DAH)……..……. 117

CHAPTER 3

Figure 1 Characterization of tomato (*Solanum lycopersicum* L. cv. Micro-Tom) fruit ripening……..……..… 148
Figure 2 Basic information and functional classification of tomato (*Solanum lycopersicum* L. cv. Micro-Tom) fruit proteome…..... 150
Figure 3 Identity of the tomato (*Solanum lycopersicum* L. cv. Micro-Tom) fruit proteome at two ripening stages (0 and 8 DAH)……..… 153

Figure 4 Identity of the tomato (*Solanum lycopersicum* L. cv. Micro-Tom) fruit proteomes modified by treatment with ethylene, auxin, or both hormones……..……... 156
Figure 5 Tomato (*Solanum lycopersicum* L. cv. Micro-Tom) fruit enzymes involved in hormone and volatile compounds biosynthetic pathways whose abundance changes during fruit ripening or in response to ethylene, auxin, and both treatments……... 162
Figure 6 Tomato (*Solanum lycopersicum* L. cv. Micro-Tom) fruit proteins involved in hormone and volatile compounds biosynthetic pathways whose abundance changes specifically as a result of ethylene, auxin, and both treatments…… 165
Figure S1 Schematic representation of the experiment design and the proteomic analysis workflow……... 173
Figure S2 Differently expressed proteins were grouped according to KEGG pathways……... 175

LIST OF TABLES

CHAPTER 1

Table 1 Identified volatile organic compounds in two tomato (*Solanum lycopersicum* L.) fruit cultivars after ethylene, auxin, and both treatments throughout ripening. Data presented are *p* values for mean comparisons between treated and control fruits (n = 3)…… 59

Table S1 Quantitative PCR primers of all genes analyzed in the study..…... 85

Table S2 Identified volatile organic compounds in tomato (*Solanum lycopersicum* L. cv. Micro-Tom) fruits after ethylene, auxin, and both treatments at breaker and red stages. Data presented are *p* values for mean comparisons between treated and control fruits (n = 3)……... 89

CHAPTER 2

Table S1 Polar metabolites in three ripening stages of Micro-Tom tomato (*Solanum lycopersicum* L.) fruits detected by gas chromatography-mass spectrometry (GC-MS)…….…… 119

Table S2 Non-polar metabolites in three ripening stages of Micro-Tom tomato (*Solanum lycopersicum* L.) fruits detected by gas chromatography-mass spectrometry (GC-MS)…….…… 127

Table S3 Carotenoid contents in three ripening stages of Micro-Tom tomato (*Solanum lycopersicum* L.) fruits detected by high-performance liquid chromatography (HPLC)…….…… 133

Table S4 Metabolic pathways differentially modified by treatment with ethylene, auxin, or both hormones in Micro-Tom tomato (*Solanum lycopersicum* L.) fruits at 8 and 18 days after harvest (DAH)……..…….. 135

CHAPTER 3

Table 1 Summary protein identification data of tomato (*Solanum lycopersicum* L. cv. Micro-Tom) fruit samples at different ripening stages (0 and 8 days after harvest) and hormone treatments…... 151

Table 2 Tomato (*Solanum lycopersicum* L. cv. Micro-Tom) fruit proteins involved in hormone and volatile compounds biosynthesis whose abundance changes specifically as a result of ethylene, auxin, and both treatments……. 160
Table S1 Identification of tomato (*Solanum lycopersicum* L. cv. Micro-tom) fruit protein results…… 171
Table S2 Tomato (*Solanum lycopersicum* L. cv. Micro-Tom) fruit proteins whose abundance changes specifically during ripening or as a result of ethylene, auxin, and both treatments…….. 171
Table S3 Gene ontology classification for tomato (*Solanum lycopersicum* L. cv. Micro-Tom) fruit proteome at 0 and 8 days after harvest (DAH) and different hormone treatments…….. 171
Table S4 Summary of gene ontology and KEGG pathway classifications for tomato (*Solanum lycopersicum* L. cv. Micro-Tom) fruit proteome at 0 and 8 days after harvest (DAH) and different hormone treatments…… 177
Table S5 Gene ontology (GO) and KEGG pathway enrichment analysis of the identified proteins in tomato (*Solanum lycopersicum* L. cv. Micro-Tom) fruit proteomes…… 179
Table S6 Tomato (*Solanum lycopersicum* L. cv. Micro-Tom) fruit proteins involved in primary and secondary metabolisms whose abundance changes specifically during fruit ripening or as a result of ethylene, auxin, and both treatments…….. 171

LIST OF ABBREVIATIONS

AADC	aromatic amino acid decarboxylase
AAT	alcohol acyltransferase
ABA	abscisic acid
ACC	1-aminocyclopropane-1-carboxylic acid
ACO	ACC oxidase
ACS	ACC synthase
ADH2	alcohol dehydrogenase 2
AOC	allene oxide cyclase
AOS2	allene oxide synthase 2
ARF	auxin response factor
Aux/IAA	AUX/IAA proteins
AuxRE	auxin-responsive element
BCAT1	branched-chain-amino-acid aminotransferase 1
CCD1	carotenoid dioxygenase 1
Cel2	endo-1,4- β-glucanase
CTOMT1	catechol-O-methyltransferase 1
CTR	CTR protein
CTRL	control group
CXE1	carboxylesterase 1
DAH	day after harvest
EIL	EIN3-like protein
EIN	ethylene-insensitive protein
ERE	ethylene-responsive element
ERF	ethylene response factor
ETHY	ethylene-treated group
ETHY+IAA	group treated with both hormones
ETR	ethylene receptor
FPPS	farnesyl pyrophosphate synthase
GC-MS	gas chromatography–mass spectrometry
GH3	gretchen hagen 3
GO	gene ontology
HDS	(E)-4-hydroxy-3-methylbut-2-enyl-diphosphate synthase
HPL	hydroperoxide lyase
HPLC	high performance liquid chromatography
IAA	indole-3-acetic acid-treated group
IDI	isopentenyl-diphosphate-isomerase
IspE	4-diphosphocytidyl-2-C-methyl-D-erythritol kinase
IspH	4-hydroxy-3-methylbut-2-en-1-yl diphosphate reductase
LC-MS	liquid chromatography–mass spectrometry

LeEXLA1	expansin-like protein precursor
LeMAN4a	endo-1,4-β-mannosidase 4
LeXYL1	FN3_like domain-containing protein
LoxC	lipoxygenase C
MPDC	diphosphomevalonate decarboxylase
MSTFA	n-methyl-n-(trimethylsilyl) tri-fluoroacetamide
PAL	phenylalanine ammonia-lyase
PAR2	phenylacetaldehyde reductase 2
PG2a	polygalacturonase 2a
PLS-DA	partial least squares discriminant analysis
PME	pectinesterase
PSY1	phytoene synthase 1
SAM	S-adenosyl-l-methionine
SAMS	SAM synthetase
SAMT	salicylic acid methyltransferase
SCF	SKP1–cullin–F-box ubiquitin-ligase complex
SlXTH2	xyloglucan endotransglucosylas
TBG4	β-galactosidase
TIR1	transporter inhibitor response 1
UGT73C4	UDP-glucosyltransferase 73C
VOC	volatile organic compound
ZDS	zeta-carotene desaturase
ZEP	zeaxanthin epoxidase

INDEX

1 INTRODUCTION…….. 29

2 JUSTIFICATION…… 39

3 OBJECTIVE……... 41

4 DESCRIPTION OF CHAPTERS…… 43

CHAPTER 1

ETHYLENE AND AUXIN: HORMONAL REGULATION OF VOLATILE COMPOUND PRODUCTION DURING TOMATO (*SOLANUM LYCOPERSICUM* L.) FRUIT RIPENING……... 45

ABSTRACT…… 46

1 INTRODUCTION……... 46

2 MATERIAL AND METHODS…….. 49

2.1 Plant material and hormone treatments…… 49

2.2 Ethylene emission…….. 50

2.3 Peel color characterization……... 50

2.4 Analysis of volatile compounds…….. 50

2.5 Auxin determination……... 51

2.6 Carotenoid analysis…… 52

2.7 RNA isolation and quantitative RT-PCR analysis…… 53

2.8 Statistical analysis…….. 53

3 RESULTS AND DISCUSSION…… 54

3.1 Ethylene-auxin crosstalk controlling tomato ripening…….. 54

3.2 Hormonal regulation of volatile compound profile during tomato ripening…….. 58

3.3 Cultivar dependence of hormonal regulation of volatile compound production……... 64

3.4 Confirmation of direct hormonal effects on tomato ripening stages…… 69

4 CONCLUSIONS…… 73

SUPPLEMENTARY MATERIAL…… 75

CHAPTER 2

VOLATILE COMPOUND BIOSYNTHESIS: METABOLIC RESPONSES TO ETHYLENE-AUXIN CROSSTALK DURING TOMATO (*SOLANUM LYCOPERSICUM* L.) FRUIT RIPENING……... 93

ABSTRACT…… 94

1 INTRODUCTION……... 95

2 MATERIALS AND METHODS…… 97

2.1 Plant materials and hormone treatments…….. 97

2.2 Ripening characterization…… 98

2.2.1 Ethylene emission……. 98

2.2.2 Fruit surface color…….. 98

2.3 Metabolite profile analysis…… 98

2.3.1 Polar metabolic profile…….. 99

2.3.2 Non-polar metabolic profile…….. 99

2.3.3 GC-MS analysis of derivatized metabolites…….. 100

2.4 Carotenoids…….. 101

2.5 Statistical analysis…….. 101

3 RESULTS AND DISCUSSION…… 102

3.1 Effects of auxin treatment on surface color and ethylene emission during fruit ripening…… 102

3.2 Metabolites showing different concentrations in ethylene and auxin-treated fruits…… 104

3.3 Global metabolic profile and statistical evaluation…… 108

3.4 Changes in volatile compound metabolism…… 111

4 CONCLUSIONS…… 114

DATA AVAILABILITY STATEMENT…… 115

SUPPLEMENTARY MATERIAL…… 117

CHAPTER 3

PROTEOMIC CHANGES IN AROMA METABOLISM DURING TOMATO (*SOLANUM LYCOPERSICUM* L.) FRUIT RIPENING IN RESPONSE TO ETHYLENE AND AUXIN REGULATION…….. 139

ABSTRACT…… 140

1 INTRODUCTION……... 140

2 MATERIALS AND METHODS…… 142
2.1 Plant materials and hormone treatments…….. 142
2.2 Ripening characterization…… 143
2.2.1 Ethylene emission……. 143
2.2.2 Fruit surface color…….. 144
2.3 Total protein extraction…… 144
2.4 Protein quantification…… 144
2.5 In-Gel fractionation, protein digestion and sample clean-up……... 145
2.6 Liquid chromatography-mass spectrometry (LC-MS) analysis….. 145
2.7 Data analysis and label-free quantitation…….. 146
2.8 Bioinformatics analysis…… 146
2.9 Statistical analysis…….. 147
3 RESULTS AND DISCUSSION…… 147
3.1 Tomato ripening changes due to ethylene and auxin treatments... 147
3.2 Label-Free quantification of tomato fruit proteomes……. 149
3.3 Tomato fruit proteomic profiles at early and middle ripening stages……. 152
3.4 Changes of tomato fruit protein levels in response to ethylene and auxin crosstalk……. 155
3.5 Ethylene and auxin effects in tomato aroma reflected by protein expression dynamics……. 159
4 CONCLUSIONS…… 168
SUPPLEMENTARY MATERIAL…… 171

5 CONCLUSIONS…… 187
REFERENCES…….. 189

1 INTRODUCTION

Ripening is a genetically programmed and complex process that determines the quality characteristics of fruit and is evidenced by changes in its chemical composition, color, texture, flavor, and aroma (ROCCO et al., 2006). Ripening directly impacts the fruit quality and, from a biological viewpoint, the protection from post-harvest diseases, attraction of dispersing agents, seed propagation, and animal nutrition (GIOVANNONI, 2004).

Although fruits have different ripening mechanisms and phenotypes, they can be classified into two major groups according to their breathing patterns and ethylene hormone production during ripening: climacteric fruits are characterized by a peak in breathing, concomitant with or preceded by a peak in ethylene production; non-climacteric fruits show no significant variation in respiration rate or ethylene levels (BIALE; YOUNG, 1981). Another important characteristic of climacteric fruits is the differentiation of two ethylene production systems. The first (system I) is responsible for the synthesis of basal levels of hormone and occurs in both climacteric and non-climacteric fruits. System II, however, acts exclusively on climacteric fruits, involving autocatalytic synthesis of, and consequently an increase in, ethylene. In this system, ethylene induces expression of genes that encode enzymes responsible for its own biosynthesis (VAN DE POEL et al., 2012).

Among climacteric fruits, the tomato (*Solanum lycopersicum* L.) fruit has emerged as a widely used model of fruit development and ripening. This is due to (1) the possibility of growing tomatoes under different conditions, allowing understanding of a plant's ability to adapt to different abiotic stresses, such as coldness and dryness; (2) its relatively short life cycle; (3) its high parthenocarpy and homozygosity, an important characteristic for shaping genetic inheritance; (4) the ease of controlled pollination and hybridization; (5) the simplicity and size of its genetic material (the Heinz1706 cultivar, used for tomato genome sequencing, has approximately 900 Mb; THE TOMATO GENOME CONSORTIUM, 2012); and (6) its commercial and economic importance (BERGOUGNOUX, 2014).

The biosynthetic pathway of ethylene, the typical ripening-promoting hormone, was initially described by Yang and Hoffman (1984), and this is well established for most plants (Figure 1A). The first pathway reaction occurs in the L-methionine cycle

(Yang cycle) and involves the conversion of L-methionine to S-adenosyl-L-methionine (SAM), mediated by the enzyme S-adenosylmethionine synthetase (SAMS; Enzyme Commission number (EC): 2.5.1.6), while SAM is converted to 1-aminocyclopropane-1-carboxylic acid (ACC) by the enzyme ACC synthase (ACS; EC: 4.4.1.14). Ethylene is synthesized from ACC by the action of ACC oxidase (ACO; EC: 1.14.17.4), diffuses rapidly through tissues, and binds to its associated receptors, predominantly to the membrane of endoplasmic tissue, triggering the physiological changes that result in fruit ripening and senescence (LELIÈVRE et al., 1997; ARORA, 2005). Ethylene can regulate its own biosynthesis, inducing the *de novo* synthesis of ACS and ACO isoforms. ACC can also be converted to malonyl-ACC by the action of ACC-N-malonyltransferase (NMT; EC: 2.3.1.-) and then transported to the vacuole (THEOLOGIS et al., 1992).

Figure 1 – Ethylene biosynthesis (A) and perception (B)

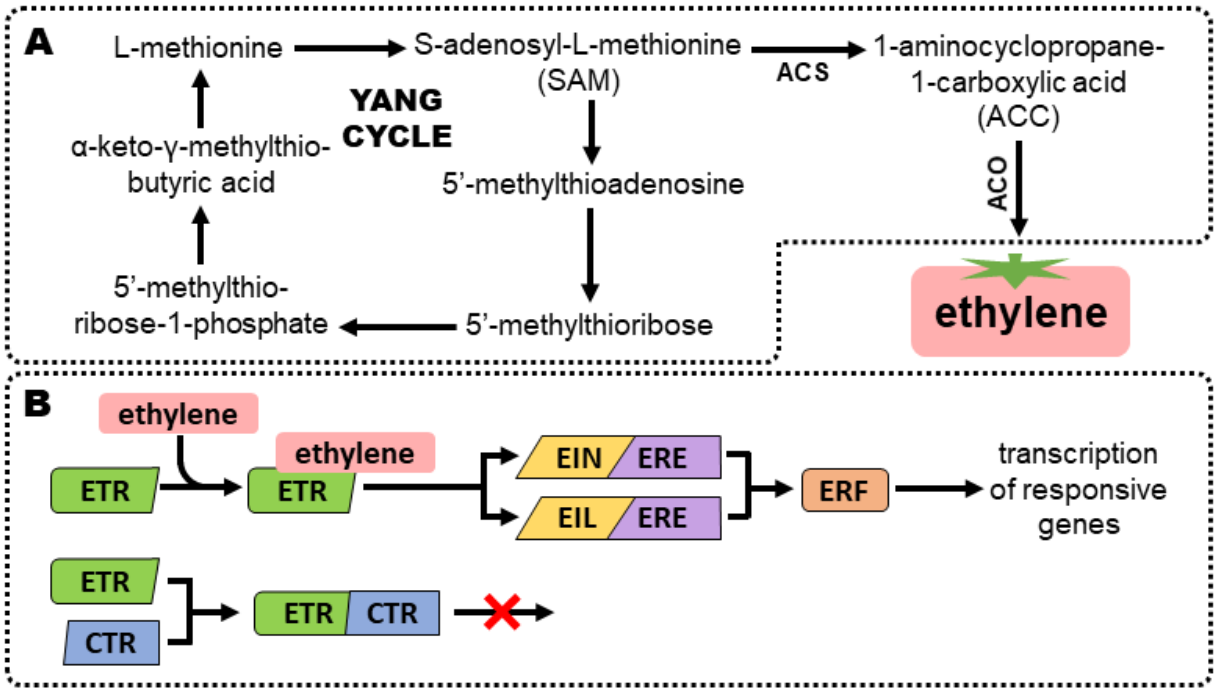

CTR: CTR proteins. EIL: EIN3-like proteins. EIN: ethylene-insensitive protein. ERE: ethylene-responsive element. ERF: ethylene response factor. ETR: ethylene receptor. Adapted from Karlova et al. (2014) and Yang and Hoffman (1984).

Ethylene receptors (ETRs) are the first elements of the hormone-signaling pathway and, in tomatoes, are present in seven isoforms (LeETR1 to LeETR7), which, based on their gene and protein structures, are classified into subfamilies I and II

(TIEMAN; KLEE, 1999; TIEMAN et al., 2000). The accepted model for ethylene signaling involves a mechanism of receptor negative regulation. The interaction of ethylene with the receptor induces its degradation via 26S proteasome, enabling signal transduction, previously inhibited by the receptor activity, leading to the synthesis of new receptors to replace those degraded and promoting low sensitivity to the hormone (negative feedback) (KEVANY et al., 2007). LeETR4, LeETR6, and LeETR3 are the most expressed receptors in the fruit, and their levels increase significantly at the beginning of ripening, indicating that such ETRs play important roles during this period (KEVANY et al., 2007).

In the absence of ethylene, ETRs are physically associated with constitutive triple response (CTR) proteins (KIEBER et al., 1993). In tomatoes, different CTR isoforms (LeCTR1 to LeCTR4) have been identified, whose encoding genes are differentially expressed during fruit development, with LeCTR1 being mainly identified during ripening (ADAMS-PHILLIPS et al., 2004). In studies involving LeCTR1 silencing, it was observed that the fruits ripened more quickly, and the expression of ethylene-induced genes increased, indicating that this CTR protein also acts as an ethylene-signaling negative regulator (LIU; SCHIFF; DINESH-KUMAR, 2002).

In the presence of ethylene, LeCTR1 inactivation occurs, allowing signal transduction. However, it is not yet known whether the ethylene binding causes conformational changes that decrease the interaction between ETRs and LeCTR1 or whether this is also due to the kinase activity of these proteins. The interaction of the hormone with the receptors results in CTR1 uncoupling and the activation of proteins such as ethylene-insensitive 2 (EIN2). Ju et al. (2012) demonstrated that in *Arabidopsis thaliana*, in the absence of ethylene, LeCTR1 acts on EIN2 phosphorylation, preventing migration of the EIN2 C-terminal domain to the nucleus. Once in the nucleus, this domain stabilizes the ethylene-insensitive 3 (EIN3) and EIN3-like (EIL) proteins, preventing their degradation. These proteins induce the transcription of ethylene response factors (ERFs), by connecting to the ethylene-responsive elements (EREs) located in the ERF-promoting region (POTUSCHAK et al., 2003; YANAGISAWA; YOO; SHEEN, 2003). After translation, ERFs directly suppress or stimulate mRNA transcription by binding to fractions, known as GCC-box, of promoter regions of several ripening-related genes (YANG et al., 2009) (Figure 1B).

Although ethylene is an important hormone in the ripening of climacteric fruits, mainly at the beginning of this process, other hormones are also involved, directly or

indirectly, in ripening: for example, auxins, jasmonates, and abscisic acid (LÈLIEVRE et al., 1997). Among these hormones, auxins play an important role in regulating many aspects of plant development, such as cell division, expansion and differentiation, gravitropism, apical dominance, and fruit establishment and development (DAVIES, 1995). Auxins have also been considered relevant to ripening control; however, their role is not yet well defined.

The effects of auxin on fruit ripening were firstly observed in strawberries (*Fragaria ananassa* Duch.) when removal of the tissues producing this hormone accelerated fruit ripening, and subsequent application of synthetic auxin at the removal site delayed it (GIVEN; VENIS; GIERSON, 1988). In bananas (*Musa acuminata* AAA), the application of exogenous auxin provided inhibition of β-amylase activity during ripening, with a consequent delay in starch degradation and sucrose production (PURGATTO et al., 2001). Recent studies highlight the importance of auxin at the beginning of ripening and in the transition between ethylene-production systems I and II (ROSS et al., 2011; GRIERSON, 2013; MCATEE et al., 2013; SEYMOUR et al., 2013).

In studies on mango (*Mangifera indica* L.) and grape (*Vitis vinifera* L.) fruits, it was observed that a reduction in auxin levels appears fundamental to the beginning of ripening (BÖTTCHER et al., 2010; ZAHARAH et al., 2012). In tomato (*S. lycopersicum* L.) and peach (*Prunus persica* L.) fruits, some auxin-related genes, such as those that encode enzymes involved in hormone biosynthesis, transport, and signaling, increase their expression levels during the ripening transition (TRAINOTTI; TADIELLO; CASADORO, 2007; PATTISON; CATALÁ, 2012).

Indole-3-acetic acid is the main auxin found in most plants and is synthesized in young leaves, seeds, and fruits during development. Its biosynthesis ideally occurs via tryptophan-dependent pathways but can also occur via independent pathways (TAIZ; ZEIGER, 2004) (Figure 2A). Since indole-3-acetic acid is only synthesized in some tissues, its transport and distribution to other parts of the plant occur actively, cell by cell or through phloem, via a mechanism responsible for transporting large amounts of the hormone across larger distances (DAVIES et al., 2004).

Endogenous auxin levels are controlled by oxidation reactions or conjugation with amino acids and carbohydrates, as free indole-3-acetic acid is the active form. Therefore, auxin conjugation, mediated by *Gretchen Hagen 3* (*GH3*) genes, regulates its homeostasis in the cell. However, *de novo* biosynthesis and hydrolysis from its

conjugates also contribute to balancing the auxin levels in tissues (KORASICK; ENDERS; STRADER, 2013).

Figure 2 – Indole-3-acetic acid biosynthesis (A) and perception (B)

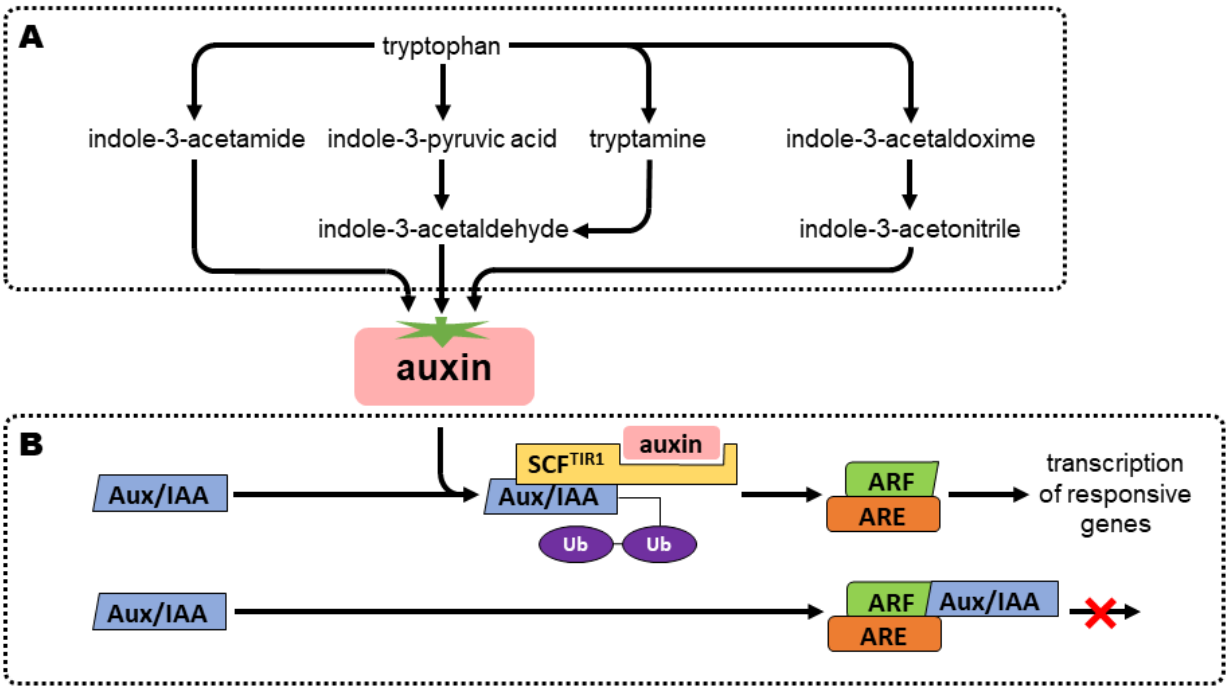

ARE: Auxin response element. ARF: Auxin response factor. Aux/IAA: Aux/IAA proteins. SCF: Part of SCF/TIR1 protein complex. TIR1: Transporter inhibitor response 1. Adapted from Teale, Paponov, and Palme (2006) and Normanly, Slovin, and Cohen (1995).

The molecular interactions that mediate auxin perception and signaling have been extensively studied during the past decade (BARGMANN; ESTELLE, 2014). The most accepted model is based on the activation and repression of auxin response genes through a signal transduction mechanism involving three types of transcriptional regulators: auxin response factor (ARF), Aux/IAAs (transcriptional repressors that also act as part of the hormone-perception complex), and TOPLESS (corepressor) proteins (LIU; KARMARKAR, 2008). Aux/IAAs have four well-conserved domains (I to IV) and act as negative regulators, suppressing the auxin response. When auxin levels are low, these proteins form heterodimers with ARFs due to the interaction of domains III and IV with the ARF C-terminal domain. Such interaction causes inactivation of ARFs, which can bind to specific DNA regions called auxin-responsive elements (AuxREs) through their DBD N-terminal domain (DNA-binding domain). These elements are located in the auxin-related genes (HAYASHI, 2012) (Figure 2B). The Aux/IAA

degradation and consequent ARF activation occurs in the presence of auxin, allowing the transcription of auxin-responsive genes. This initially happens through auxin binding to transporter inhibitor response 1 (TIR1) and auxin-signaling F-box (AFB), F-box proteins that act as receptors. They are associated with a Skp1–Cullin–F-box (SCF) ubiquitin-ligase complex called $SCF^{TIR1/AFB}$, which binds to Aux/IAA domain II, being responsible for ubiquitinating Aux/IAA for 26S proteasome recognition and degradation (HAYASHI, 2012; ZOUINE et al., 2014).

The intricate mechanisms underlying auxin regulation, and even their exact role in ripening control, remain largely unclear, especially in relation to their interaction with other hormone signals. The ethylene-auxin crosstalk may involve several components of the signaling pathways of both hormones, resulting in different physiological responses. In the primary crosstalk, genes containing ethylene and auxin-responsive elements (EREs and AuxREs, respectively) in their promoting regions can be regulated by both hormones, activating the metabolic pathways controlled by these genes. Additionally, the secondary crosstalk involves hormone-responsive genes that can regulate the synthesis, transport, signaling, and response of other hormones (MUDAY; RAHMAN; BINDER, 2012). Kumar et al. (2012) and Yue et al. (2019) showed that ethylene can promote auxin reduction by promoting *GH3* gene expression in tomato (*S. lycopersicum* L.) and pear (*Pyrus ussuriensis*), respectively. Simultaneously, Zouine et al. (2014) confirmed that tomato ARFs respond to exogenous ethylene treatment due to the presence of EREs in their promoter regions, suggesting that these transcription factors can mediate both auxin and ethylene responses, presenting a specific role in ethylene-auxin crosstalk. In tomatoes, the ethylene-auxin crosstalk has also been studied in other organs, with effects observed on root development and on the abscission process, among others (NEGI et al., 2010; MEIR et al., 2010). Few studies have explored this crosstalk during fruit ripening.

Comparative transcriptomic analysis (RNA-seq) performed by Prof. Dr. Eduardo Purgatto in partnership with Prof. Dr. Mondher Bouzayen (Genomics and Biotechnology of Fruit Laboratory, Toulouse, France) (unpublished data) was used to evaluate changes in gene transcription patterns in tomato (cv. Micro-Tom) fruits treated with exogenous ethylene and indole-3-acetic acid; this indicated crosstalk between the two hormones, suggesting that ethylene-related genes were affected by auxin treatment. Recent study results (unpublished data) evidenced the role of auxin in delaying the beginning of ripening and its interaction with ethylene. Several ethylene-

signaling components, including other ripening-related genes, were also affected by auxin. Simultaneously, ethylene played an important role in auxin regulation, since exogenous ethylene treatment induced auxin conjugate activation of GH3 coding genes.

Several studies have focused on ethylene and auxin effects on secondary metabolisms of climacteric fruits during ripening (EGEA et al., 2011; SU et al., 2015; Li et al., 2016). Among these metabolisms, the processes related to color and aroma formation are among the most important, since they strongly impact fruit quality parameters and therefore acceptance.

Fruit color change is one of the first ripening signs and is an important quality criterion. During tomato ripening, this change results from the biosynthesis of carotenoids and the chloroplast-to-chromoplast transition. Chloroplasts contain chlorophyll, while chromoplasts are rich in lycopene and β-carotene (EGEA et al., 2011). Many processes involved in carotenoid biosynthesis are mediated by hormones. Ethylene also plays an essential role in the mechanism of chloroplast differentiation into chromoplasts, mainly in climacteric fruits (EGEA et al., 2011). In relation to the role of auxin in promoting color change, this hormone was already associated with decreased transcription of genes involved in the carotenoid metabolism, which delays the tomato fruit color change. Su et al. (2015) studied the carotenoid profile changes of tomato (cv. Micro-Tom) fruits treated with exogenous ACC and indole-3-acetic acid and observed that auxin treatment delayed the transition from green to orange, with fruits never reaching the full red color. Related genes (*Psy, Ziso, Pds,* and *Crtiso*) presented decreased transcription levels. Jones et al. (2002) showed that ARF4 plays an important role in the tomato fruit color change, since a decrease in the expression of this ARF increased the number of chloroplasts and the chlorophyll content, consequently producing fruits with a dark green color.

In addition to being responsible for the characteristic ripe fruit color, carotenoids are important precursors in biosynthetic pathways of several classes of volatile organic compounds (VOCs), including alcohols, ketones, esters, and aldehydes (Figure 3). These VOC pathways are well established, but the hormone regulation in this process remains poorly understood.

Several studies have been conducted to establish the processes of synthesis, conjugation, and release of aroma compounds in climacteric fruits, highlighting the main volatile metabolites formed during ripening. Approximately 400 VOCs have been

detected in tomato fruits; among these, fewer than 10% show increased concentrations during ripening, produced in sufficient quantities to be perceived by humans, and are crucial in conferring the characteristic tomato aroma (BALDWIN et al., 2000; MATHIEU et al., 2009; DU et al., 2015; TIEMAN et al., 2017). The other compounds may provide background odors that impact the overall aroma quality (TANDON et al., 2001; KLEE; GIOVANNONI, 2011). Another function of aroma compounds is to enhance the main flavor components, such as soluble sugars and organic acids (KLEE; TIEMAN, 2013; TIEMAN et al., 2017).

Figure 3 – Main metabolic precursors and pathways of volatile compound biosynthesis in plants

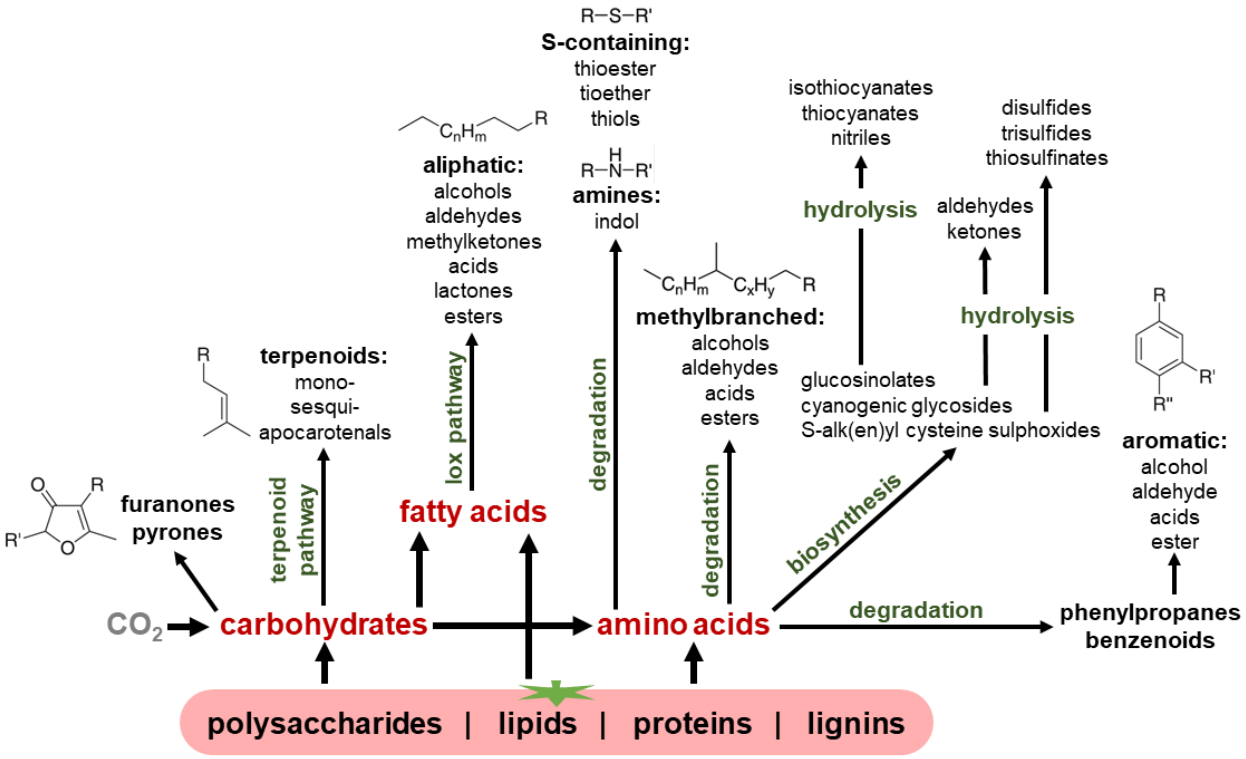

Adapted from Schwab, Rikanati, and Lewinsohn (2008)

Tieman et al. (2017) evaluated the VOC profiles and sensory preferences of 398 tomato varieties and showed that among the 400 detectable compounds, 23 were responsible for forming the characteristic tomato aroma, with only 13 identified as important for consumer acceptance: β-ionone; 1-nitro-3-methylbutane; 1-octen-3-one; 2-isobutylthiazole; 2-methylbutanol; 3-methylbutanal; 3-methylbutanol; 3-methylbutanoic acid; 6-methyl-5-hepten-2-one; methional; (E,E)-2,4-decadienal; and (E)-2-heptenal. Klee and Tieman (2018) described other important contributors to the

ripe tomato flavor that positively correlates with consumer preferences: β-damascenone; 1-hexanal; 1-hexanol; 1-pentanal; 1-pentanol; 1-penten-3-one; 2-phenylethanol; 3-pentanone; 6-methyl-5-hepten-2-ol; benzaldehyde; citral; furaneol; geranyl acetone; guaiacol; heptaldehyde; isobutyl acetate; isovaleraldehyde; isovaleric acid; isovaleronitrile; methyl salicylate; nonyl aldehyde; phenylacetaldehyde; (E)-2-hexenal; (E)-2-pentenal; (E)-3-hexen-1-ol; (Z)-3-hexen-1-ol; (Z)-3-hexenal; and (Z)-4-decenal. Additionally, Tieman et al. (2017) highlighted the importance of the glucose, fructose, citric acid, and malic acid contents in forming the intense characteristic tomato fruit flavor.

Generally, there are three major groups of fruit aroma precursors: carbohydrates, amino acids, and fatty acids. From the carbohydrate metabolism, mainly terpenes and furanones are formed. Amino acid metabolism is involved in the biosynthesis of volatile alcohols (aliphatic, branched, and aromatic), carbonyls, acids, and esters. However, fatty acids are considered the most important VOC precursors, being catabolized by two oxidative pathways: β-oxidation and lipoxygenase (Lox; EC: 1.13.11.12) pathways. Fatty acid β-oxidation forms acyl-CoAs, which are used by alcohol acyltransferases (AAT; EC: 2.3.1.84) to generate volatile esters. Most alcohols, aldehydes, acids, and esters responsible for fruit aromas are generated by the oxidative degradation of linoleic and linolenic acids, the main Lox substrates (PÉREZ; SANZ, 2008).

Other enzymes involved in VOC metabolism were already identified, together with the associated volatile products: aromatic amino acid decarboxylases (AADC; EC: 4.1.1.53) are associated with the biosynthesis of phenylacetaldehyde, 2-phenylethanol, 1-nitro-2-phenylethane, and 2-phenylacetonitrile (TIEMAN et al., 2006); phenylacetaldehyde reductases (PARs) with the synthesis of 2-phenylethanol (TIEMAN et al., 2007); 13-lipoxygenase (LoxC; EC: 1.13.11.12) with the synthesis of (Z)-3-hexenal, (Z)-3-hexenol, hexanal, and hexanol (CHEN et al., 2004); salicylic acid methyltransferase (SAMT; EC: 2.1.1.274) with the synthesis of methyl salicylate (TIEMAN et al., 2010); catechol-O-methyltransferase 1 (CTOMT1; EC: 2.1.1.6) with the synthesis of guaiacol (MAGEROY et al., 2012); carotenoid dioxygenase 1 (CCD1; EC: 1.14.99.4) with the synthesis of apocarotenoids (SIMKIN et al., 2004); and carboxylesterase 1 (CXE1; EC: 3.1.1.1) with the synthesis of alcohols (GOULET et al., 2012).

The biosynthesis of important volatiles is associated with fruit ripening (TIEMAN et al., 2006) and, at the molecular level, the regulation of VOC synthesis can theoretically occur in several ways. Thus, the enzymes responsible for their synthesis are controlled, directly or indirectly, by the same transcription factors that control other ripening processes (GIOVANNONI; KLEE, 2011). A study by Baldwin et al. (2000) showed that fruits of non-ripening tomato mutants, *ripening inhibitor* (*rin*) and *non-ripening* (*nor*), presented deficiencies in VOC biosynthesis.

Previous studies performed by our research group (unpublished data) directly evaluated (targeted) the ethylene-auxin crosstalk and its influence on VOC formation, showing that fruits treated with ethylene, indole-3-acetic acid, and both hormones presented different VOC profiles, with delays in the accumulation of aroma compounds as well as in the transcription of related genes. These results and those obtained by the RNA-seq analysis described above inspired more in-depth and comprehensive studies concerning the roles of auxin and ethylene-auxin crosstalk in tomato fruit ripening, with an emphasis on their influence on the VOC metabolism. In this context, recent advances in omics approaches allow assessment of the general internal fruit metabolism at different biological system levels.

Metabolomic and proteomic analyses have been used as analytical tools in studies related to climacteric (OMS-OLIU et al., 2011; BARSAN et al., 2012) and non-climacteric (ARAGÜEZ; FERNÁNDEZ, 2013) fruit ripening. Therefore, an integrated study of metabolites produced by the primary and secondary metabolisms and the enzymes related to VOC pathways during fruit ripening is an interesting strategy for deepening existing knowledge and improving understanding of the role of these hormones in aroma formation, which is considered one of the most important fruit quality parameters. The large amount of generated data enables visualization of the internal state of the fruit together with a broader and more detailed view of the regulation involved in ripening, which would have been inconceivable a few years ago.

2 JUSTIFICATION

Considerable progress has been made in studying climacteric fruit ripening; however, the roles of auxins and other ripening-related hormones remain to be elucidated. Indole-3-acetic acid, the main auxin found in plants, has been identified as an important compound in this process, since it delays some ripening parameters modulating specific fruit metabolisms, such as carotenoid metabolism.

Although knowledge of the individual role of auxin has been deepened, the importance of ethylene-auxin crosstalk in this regulatory process is unclear. In this context, the RNA-seq analysis previously realized was at the frontiers of knowledge, enabling analysis of the transcription patterns of hundreds of genes and transcription factors directly involved in the metabolic ripening process. However, it is important to note that an increase in mRNA levels does not always correlate with an increase in protein or metabolite levels, as translated proteins may or may not be active. Due to these factors, changes in fruit transcriptome do not always correspond to proteomic, metabolomic, and therefore phenotypic changes.

In this context, for the present study, metabolomics and proteomics approaches were proposed, with an emphasis on VOC metabolism. The biosynthesis of aroma compounds also appears to be regulated by both hormones, at least as a consequence of primary and secondary metabolism regulation. The comparative metabolic evaluation of fruits treated with exogenous ethylene, auxin, and both hormones allows identification of responsive metabolites and enzymes involved, directly and indirectly, in this regulatory process and provides a broad view of hormonal regulation of ripening at enzymatic and metabolic levels. Thus, characterization of the metabolic response in the presence of increased doses of ethylene and auxin can provide presumptive explanations of the role of each hormone, the interaction between them, and the mechanisms by which they regulate aroma formation in tomato fruits.

3 OBJECTIVE

The main objective of this study was to evaluate the ethylene-auxin crosstalk and its influence on the volatile compound metabolism during tomato (*Solanum lycopersicum* L.) fruit ripening by comparative metabolomic and proteomic analysis.

4 DESCRIPTION OF CHAPTERS

To achieve the main aim of this thesis, the study was divided into three parts with specific aims, and the manuscripts of each part are presented as chapters. Chapter 1 was submitted to Foods (ISSN 2304-8158) and Chapter 2 to Metabolomics (ISSN 1573-3890). The final chapter is still being revised for submission to Plant Physiology and Biochemistry (ISSN 0981-9428) as soon as possible.

CHAPTER 1 - ETHYLENE AND AUXIN: HORMONAL REGULATION OF VOLATILE COMPOUND PRODUCTION DURING TOMATO (*SOLANUM LYCOPERSICUM* L.) FRUIT RIPENING

The importance of ethylene and auxin in regulating climacteric fruit ripening has been studied; however, the roles of these hormones and the crosstalk between them in regulating tomato fruit aroma formation requires clarification. In this chapter, the influences of ethylene, auxin, and ethylene-auxin crosstalk on the VOC metabolism in tomato (*Solanum lycopersicum* L.) fruits were evaluated at different ripening stages. In addition to emphasizing VOC profile changes, this study compares the change patterns of two tomato cultivars (Micro-Tom and Sweet Grape) to determine whether the VOC profile changes are cultivar independent. Finally, a second experimental design was applied to confirm whether aroma changes occur due to the direct effect of the exogenous hormone treatment or indirectly due to temporal changes caused by the treatments.

CHAPTER 2 - VOLATILE COMPOUND BIOSYNTHESIS: METABOLIC RESPONSES TO ETHYLENE-AUXIN CROSSTALK DURING TOMATO (*SOLANUM LYCOPERSICUM* L.) FRUIT RIPENING

Tomato fruit ripening is a genetically coordinated process regulated by phytohormones such as ethylene and auxin. Due to primary and secondary

metabolism regulation, the VOC biosynthesis also appears to be regulated by both hormones. In this chapter, the metabolic responses to ethylene-auxin crosstalk during tomato (*Solanum lycopersicum* L.) fruit ripening are evaluated, with an emphasis on VOC metabolism. Polar and non-polar metabolites were measured by GC-MS, and the presented results describe primary and secondary metabolic pathways that were significantly influenced by ethylene and auxin treatments, evidencing how each hormone and its crosstalk affected tomato fruit metabolic profiles and therefore the fruit aroma.

CHAPTER 3 - PROTEOMIC CHANGES IN AROMA METABOLISM DURING TOMATO (*SOLANUM LYCOPERSICUM* L.) FRUIT RIPENING IN RESPONSE TO ETHYLENE AND AUXIN REGULATION

Knowledge of the proteins involved in the metabolic changes characterizing fruit ripening is extensive, but their hormone regulation remains unclear. The study presented in this chapter evaluated the proteomic responses to ethylene-auxin crosstalk during tomato (*Solanum lycopersicum* L.) fruit ripening, focusing on VOC metabolism. Proteomic profiles obtained by LC-MS were identified and compared, including 1,547 proteins differently expressed ($p < 0.05$) between at least two ripening stages or hormone treatments. Proteins involved in metabolic processes and that participates in catalytic activities were identified and classified according to the KEGG pathway. Abundances of overlapped proteins were compared, enabling identification of the enzymes related to VOC biosynthesis affected by ethylene and auxin treatments and reinforcing both the effects of individual hormonal regulation and the role of the ethylene-auxin crosstalk in regulating the tomato fruit aroma.

CHAPTER 1

ETHYLENE AND AUXIN: HORMONAL REGULATION OF VOLATILE COMPOUND PRODUCTION DURING TOMATO (*SOLANUM LYCOPERSICUM* L.) FRUIT RIPENING

Eric de Castro Tobaruela[1,2,§], Bruna Lima Gomes[1,2,§], Vanessa Caroline de Barros Bonato[1,2,§], Elis Silva de Lima[1,2], Luciano Freschi[3], Eduardo Purgatto[1,2,*]

[1]Department of Food and Experimental Nutrition, Faculty of Pharmaceutical Sciences, University of São Paulo (USP), São Paulo, SP, Brazil; [2]Food Research Center (FoRC), São Paulo, SP, Brazil; Food and Nutrition Research Center (NAPAN) – USP; [3]Department of Botanic, Institute of Bioscience, University of São Paulo (USP), São Paulo, SP, Brazil;

[§]These authors contributed equally

Author contributions:
LF provided and generated the plant material. ECT, BLG, VCBB and ESL conducted experiments and analyzed the data. ECT prepared figures and tables, and wrote the paper. EP designed experiments, supervised and reviewed drafts of the paper.

Submitted to Foods (ISSN 2304-8158).

ABSTRACT

As the auxin-ethylene interaction in climacteric fruit ripening have been highlighted, the hormonal regulation of aroma changes in climacteric fruits requires clarification. The influence of both hormones on the volatile organic compound (VOC) metabolism were evaluated during tomato (*Solanum lycopersicum* L.) fruit ripening. Tomato fruits cv. Micro-Tom and Sweet Grape at the mature green stage were randomly grouped according to ethylene (ETHY), auxin (IAA) or both hormones (ETHY+IAA) treatments. At middle ripening, Micro-Tom ETHY+IAA fruits present VOC profiles like those of ETHY fruits, while Sweet Grape present VOC profiles closer to IAA fruits. At full ripeness, Micro-Tom and Sweet Grape ETHY+IAA fruits show profiles closer to those of IAA fruits, suggesting that auxin overlap ethylene effects. The transcription of genes related to important tomato VOCs biosynthesis evidence their regulation by both hormones. In conclusion, ethylene and auxin regulate specific VOC pathways that affect different VOC levels, impacting on tomato aroma formation during ripening.

KEYWORDS

Climacteric fruit. Crosstalk. Carotenoids. Aromatic volatiles. Fruit quality.

1 INTRODUCTION

Tomato (*Solanum lycopersicum* L.) fruits have been extensively studied as a reference for climacteric fruits and a model system for fleshy fruit development due to their advantages over other species of agronomic interest (GAPPER; MCQUINN; GIOVANNONI, 2013). The ripening changes in tomato fruit result from genetic programming that leads to wide alteration of gene expression, encoding proteins related to several metabolic pathways and determining the fruit traits and physiological responses. Dynamic interplay between multiple hormones in conjunction with a set of developmental non-hormonal factors is required for regulating these processes (KLEE; GIOVANNONI, 2011; KARLOVA et al., 2014).

During tomato ripening, the accumulation of volatile organic compounds (VOCs), mostly produced from fatty acids, carotenoids, and amino acids, produces the

fruit aroma. Several hundred VOCs have been identified in tomato fruits, while only 23 of these were identified as responsible for the characteristic aroma of tomatoes and 13 as important to consumer acceptance: methional; 3-methylbutanenitrile; 2-methyl-1-butanol; 3-methyl-1-butanol; 2-isobutylthiazole; 1-octen-3-one; β-ionone; 3-methylbutanoic acid; (E,E)-2,4-decadienal; 3-methylbutanal; (E)-2-heptenal; and 6-methyl-5-hepten-2-one (TIEMAN et al., 2017). The tomato aroma quality is strictly ripening-dependent; most of the VOCs accumulate at the onset of tomato ripening and peak at either full ripening or shortly before. This occurs because the enzymes responsible for their synthesis are controlled, directly or indirectly, by the same transcription factors that control other ripening processes (KLEE; GIOVANNONI, 2011).

Ethylene is a typical ripening-promotion hormone, especially in climacteric fruits; these show a burst of ethylene production and a rapid rise in respiration at the onset of ripening. Ethylene is biosynthesized from S-adenosylmethionine in two steps by using two enzymes: aminocyclopropane-1-carboxylic acid (ACC) synthase (ACS) and ACC oxidase (ACO). In tomatoes, ACS2, ACS4, ACO1, and ACO4 display the most ripening-associated expression patterns, while ACS1a and ACS6 have been associated with the preclimacteric phase (LIU et al., 2015). According to the accepted model for ethylene signaling, ethylene is perceived by specific receptors, triggering a cascade of signal transduction and comprising a complex network of transcriptional regulation. Based on a genome-wide search, there are seven ethylene receptors (ETRs) in tomato, which are named ETR1 to ETR7 (CHEN et al., 2018). The binding of ethylene to its receptors activates the signal transduction, ultimately activating the ethylene response factors (ERFs) that directly control different metabolic pathways.

Despite the emphasis on the role of ethylene and its importance in fruit ripening, new perspectives have been introduced on ripening regulation that indicate coordinated action between ethylene and other hormones. Auxin was shown to significantly affect the interplay between other hormones, and it is now commonly accepted as a main regulator of fruit ripening (MUDAY; RAHMAN; BINDER et al., 2012; KUMAR; KHURANA; SHARMA et al., 2014). An increasing number of studies have demonstrated that auxin plays a critical role in various developmental processes, from embryo patterning to plant responses to environmental stimuli, including fruit set and development (ZOUINE et al., 2014). Furthermore, fruit ripening studies have shown that auxin has the opposite effect to ethylene (KUMAR; KHURANA; SHARMA

et al., 2014; SU et al., 2015; LI et al., 2016). Interestingly, studies have also indicated that auxin is crucial for triggering ripening and acting on the transition between systems I and II of ethylene production and therefore does not necessarily inhibit fruit ripening (ROSS et al., 2011; MCATEE et al., 2013; SEYMOUR et al., 2013). Moreover, genes related to auxin synthesis, transport, and signaling enhance their expression at the onset of ripening in fruits such as tomatoes and peaches (EXPOSITO-RODRÍGUEZ et al., 2011; PATTISON; CATALÁ, 2012).

Indole-3-acetic acid is the main auxin in plants that is synthesized through both tryptophan-dependent and independent pathways (KORASICK; ENDERS; STRADER, 2013). The metabolism of auxin involves converting active free IAA by mediated conjugation by *Gretchen Hagen 3* (*GH3*) genes into carbohydrates or amino acids as the inactive forms. The rapid conversion of storage forms into active free IAA therefore regulates the auxin homeostasis in the cell (KORASICK; ENDERS; STRADER, 2013). Auxin is perceived by the TIR1/AFB receptors, which leads to the transcriptional control of auxin-responsive genes. The auxin response is mediated by auxin response factors (ARFs): transcription factors that directly control auxin-responsive genes through binding to their promoters. Three types of transcriptional regulators are required to control auxin-responsive genes: ARFs, Aux/IAAs (transcriptional repressors that also act as part of the hormone-perception complex), and TOPLESS (co-repressor) proteins (LIU; KARMARKAR, 2008). In the absence of auxin, Aux/IAA proteins form dimers with ARFs to inhibit their activity by recruiting the TPL co-repressors. In the presence of auxin, Aux/IAAs bind to the $SCF^{TIR1/AFB}$ complex and subsequently become ubiquitinated and degraded by the 26S proteasome. The ARFs are then released and can regulate the transcription of their target auxin-responsive genes (ZOUINE et al., 2014).

The intricate mechanisms underlying auxin regulation, and even their exact role in ripening control, remain largely unclear, especially in relation to their interaction with other hormone signals. A multiple-hormone interplay that regulates metabolic pathways involved in fruit ripening can occur at the molecular level through interaction between components of hormone signal transduction (MUDAY; RAHMAN; BINDER, 2012). Regarding the crosstalk between ethylene and auxin, recent reports have elucidated antagonistic effects of the two hormones, including auxin acting as a ripening repressor and thereby opposing the known role of ethylene in inducing ripening in tomato fruit (SU et al., 2015; LI et al., 2016).

Few studies exist on the crosstalk between ethylene and auxin, and their effects on aroma formation during tomato fruit ripening remain almost unknown. In this study, the interactions between ethylene and auxin are explored, together with the role of each hormone in the metabolism of VOCs. The effects of exogenous ethylene and auxin on the production of both hormones; auxin conjugation; the profiles of VOCs; the activities of some enzymes; and the expression of key genes related to the regulation of ethylene, auxin, and the metabolism of tomato aroma are analyzed. The information provided in this study is valuable in illuminating the contributions of ethylene, auxin, and their interactions to the regulation of aroma metabolism during tomato fruit ripening.

2 MATERIAL AND METHODS

2.1 Plant material and hormone treatments

Tomato plants (*Solanum lycopersicum* cv. Micro-Tom and Sweet Grape) were grown under standard greenhouse conditions. Fruit samples were harvested at the mature green stage and randomly separated into four groups according to hormone treatments: CTRL (without treatment); ETHY (ethylene treatment); IAA (indole-3-acetic acid treatment); and ETHY+IAA (both hormone treatments). During the experiments, fruits were left to ripen spontaneously in 323 L chamber at 22°C, for a 16 hour-day/8 hour-night cycle and at 80% relative humidity. Ethylene treatments were performed using a gaseous hormone at 10 $\mu L.L^{-1}$ for 12 hours. The indole-3-acetic acid solutions were prepared at 100 µM in 10 mM MES buffer at pH 5.6 using 3% sorbitol and injected through the calyx end as described by Su et al. (2015). Fruits from the IAA group received indole-3-acetic acid solution, while fruits from the ETHY+IAA group were exposed to gaseous ethylene before being infiltrated with auxin solution. Two experimental blocks were performed with Micro-Tom fruits, while one experimental block was performed with Sweet Grape fruits. In the first Micro-Tom and Sweet Grape experiments, fruits were frozen in relation to the ripening stage of the CTRL group. The second Micro-Tom experiment had a different experimental design, with samples frozen on independent days when each group reached the defined ripening stages. To

maintain a consistent injection method for all samples, fruits from the ETHY and CTRL groups were injected with a buffer solution only. During all the experiments, the ethylene emission and the peel color shift were evaluated daily as ripening parameters. For further analyses, at least five fruits from each group were collected at different points, covering three ripening stages: mature green, breaker, and red. Samples were then frozen in liquid nitrogen and stored at −80°C.

2.2 Ethylene emission

Five fruits from each group were individually placed in airtight glass containers and left at 25°C. After 1 hour, 1 mL samples were collected from the headspace with a gas-tight syringe through a rubber septum for ethylene analysis. This was performed by gas chromatography (Agilent Technologies Inc., Santa Clara, USA, model HP-6890). A flame ionization detector was employed, and an HP-Plot Q column (30 m × 0.53 mm × 40 µm, Agilent Technologies) was used. Injector and detector temperatures were both set at 250°C, and the oven temperature was set at 30°C. The injections were performed in pulsed splitless mode. Helium was used as carrier gas (1 $mL.min^{-1}$).

2.3 Peel color characterization

The peel color was measured using a HunterLab ColorQuest XE instrument (Hunter Associates Laboratories) in terms of L (lightness), A (redness and greenness), and B (yellowness and blueness). The hue value was used to represent color variations and was defined as described by Fabi et al. (2007). At least five representative measurements were taken from each experimental group.

2.4 Analysis of volatile compounds

The headspace volatile production of tomato fruit was determined by solid-phase microextraction (SPME). A pool of five fresh fruits was homogenized with

sodium chloride solution 30% (Merck). Aliquots of 10 g were placed in vials and frozen at −20°C. Samples were thawed under agitation at 40°C just before analysis. The headspace equilibrium time was 10 min and the adsorption time was 50 min. The SPME fiber (PDMS/DVB/CAR 50 µm, Supelco Co.) was injected directly into a HP-6890 gas chromatograph (Agilent Technologies) coupled to a mass selective detector (HP-5973, Agilent Technologies) and held for 10 min for desorption of VOCs. The injector temperature was 200°C. Components were then separated using a Supelcowax 10 capillary column (30 m × 0.25 mm × 0.25 µm), and the oven temperature was programmed to increase from 40°C to 150°C at 2°C.min^{-1}. These conditions were previously optimized and were selected according to the higher number of peaks and the greater total area of the chromatogram. VOCs were identified by comparison using the NIST (NIST98, version 2.0, Gaithersburg, USA) and MassBank of North America (MoNA - http://mona.fiehnlab.ucdavis.edu/) libraries, considering 75% similarity as the cut-off and further confirming the results with the retention indexes. Some of the compounds were also identified using the retention indexes and spectral mass of authentic external standards. All analyses were performed in triplicate.

2.5 Auxin determination

The free auxin was determined using the method proposed by Ludwig-Müller, Georgiev, and Bley (2008), with modifications. Fruit tissues (500 mg) were extracted with isopropanol:acetic acid (95:5) under incubation at 4°C for 2 h, with 2 µg of [$^{13}C_6$]-IAA (Cambridge Isotopes, Andover, MA, USA) added as internal standard (IS). After centrifugation at 4°C and 13,000 × g for 10 minutes, the supernatant was concentrated to 50 µL using a vacuum concentrator. The pH was adjusted to between 2.5 and 3.5 by adding 1 M HCl and 500 µL of ethyl acetate, followed by centrifugation at 4°C and 13,000 × g for 5 minutes. The organic phase was collected, and the procedure was repeated twice in the aqueous phase. Samples were dried by vacuum concentration and then resuspended in 100 µL of methanol. After drying again under vacuum, 25 µL of pyridine and 25 µL of N-Methyl-N-tert-butyldimethylsilyltrifluoroacetamide (MTBSTFA, Sigma-Aldrich) were added, followed by incubation at 92°C for 1 h.

Conjugated forms were assessed by solid phase extraction according to an adapted method based on that of Chen et al. (1988). Aliquots of 500 mg of fruit tissues were added to 2 mL of extraction solution (65% isopropanol in imidazole buffer 0.2 M pH 7.0), and 2 µg of [$^{13}C_6$]-IAA (Cambridge Isotopes), followed by centrifugation at room temperature and 13,000 × g for 10 minutes. The isopropanol was evaporated, and 500 µL of 1 M NaOH was added to the remaining solution, which was incubated at room temperature for 1 hour (IAA-ester fraction). The remaining solution (500 µL) was transferred to a reaction vial to which 500 µL of 7 M NaOH was added before incubating at 100°C for 3 h (IAA-amide fraction).

The resins (500 mg) used for sample clean-up were C18 (Supelclean – LC – C_{18}) and aminopropyl (Supelclean – LC – NH_2). Before elution, the pH of both fractions (ester and amide) was adjusted to 2.5. After loading the sample on the C18 cartridge, the resin was washed with ultrapure water and the IAA fraction eluted with 2 mL of acetonitrile. This solution was diluted with 18 mL of imidazole buffer 0.02 M (pH 7.0) and then applied to the NH_2 cartridge. The sample was percolated by gravity, and the resin was sequentially washed with 2 mL of hexane, 2 mL of ethyl acetate, 2 mL of acetonitrile, and 2 mL of methanol. Finally, 3 mL of 2% acetic acid in methanol was added, and the partially purified IAA fraction was collected. Samples were completely dried using a vacuum concentrator and resuspended with 100 µL of methanol.

Auxin was quantified using a HP-6890 gas chromatograph (Agilent Technologies Inc.) coupled to a HP-5973 mass selective detector (Agilent Technologies Inc.). Samples (1 µL) were automatically injected (ALS 7693, Agilent Technologies) in splitless mode, with helium flux at 0.83 mL.min^{-1}, through a DB-5ms column (30 m × 0.25 mm × 0.50 µm). The monitored ions for endogenous IAA (m/z 130 and 232) and labelled IS (m/z 136 and 238) were used in the extracted chromatograms, and the concentration was obtained from the ratios of the chromatogram areas (Sample/IS).

2.6 Carotenoid analysis

Representative samples for each experimental group were used for carotenoid extractions. The frozen tissues were powdered, and analyses were performed according to the method developed by Sérino et al. (2009).

2.7 RNA isolation and quantitative RT-PCR analysis

Gene expression analyses were performed according to Fabi et al. (2012), following the “Minimum Information for Publication of Quantitative Real-Time PCR Experiments – MIQE” (BUSTIN et al., 2009). All the primers used for amplification are listed in Table S1.

Total RNAs from five individual fruits at each experimental stage were extracted using Concert™ Plant RNA Reagent (Invitrogen™) and treated with the “Ambion® DNA-free™ DNase Treatment & Removal Reagents” kit (Invitrogen™) for genomic DNA removal. RNAs were verified by agarose gel electrophoresis. For the cDNA synthesis, 1 µg of RNAs, measured spectrophotometrically, was used in reverse transcription reactions according to the instructions for the “ImProm-II™ Reverse Transcription System” kit (Promega). A total 10 µL of real-time PCR reactions were set using the “Power SYBR Green Master Mix” kit (Applied Biosystems), and reactions were run in a QuantStudio 7 Flex system (Applied Biosystems) programmed to 95°C for 5 min, 60 cycles of 95°C for 15 s, 60°C for 30 s, and 72°C for 30 s. The TIP41-like protein (TIP) and expressed unknown protein (EXP) genes were used as the internal controls, and the relative expressions were calculated according to the method developed by Pfaffl (2001), setting the first ripening time as 1.

2.8 Statistical analysis

SPSS Version 19.0 (SPSS Inc., Chicago, IL, USA) was used to perform statistical analysis. Data were analyzed by Student's T-tests or one-way ANOVA with a subsequent Tukey’s test to evaluate the effects of hormone treatments on VOCs and other evaluated parameters at different ripening stages. Differences were considered significant at $p < 0.05$.

VOC data were uploaded to MetaboAnalyst 4.0 (CHONG; WISHART; XIA, 2019) for a heatmap, hierarchical clustering, partial least squares discriminant analysis (PLS-DA), and variable importance in projection (VIP) score after normalization by median, log transformation, and Pareto scaling.

Linear regression analysis was applied to gene expression during fruit ripening with hormone treatment data used as predictor variables (x) and transcript levels as response variables (y), assuming a significance level of $p < 0.05$.

3 RESULTS AND DISCUSSION

3.1 Ethylene-auxin crosstalk controlling tomato ripening

Fruit ripening is driven by dynamic interplay among ethylene, auxin, other hormones, and several key developmental factors. Despite the concurrence of multiple hormones controlling ripening being a common theme in plant development, the mechanisms underlying ethylene-auxin crosstalk are not always clear. In this study, the ripening of tomato (*Solanum lycopersicum* L. cv. Micro-Tom) fruits treated with ethylene (ETHY), auxin (IAA), and a combination of both hormones (ETHY+IAA) was monitored daily using peel color characterization and ethylene emission as primary analyses. For this first experiment, samples were frozen and analyzed using untreated fruits (CTRL) as reference.

As expected, the color shift (Figure 1A and 1B) and ethylene emission (Figure 1C) were accelerated by ethylene treatment. ETHY fruits showed ethylene emission approximately four times higher than that of CTRL fruits on the first day after harvest (DAH) and showed higher concentrations between two and four DAH. The IAA and ETHY+IAA groups showed delays at the beginning of the color shift; however, the climacteric peak was advanced in relation to that of the CTRL group. Fruits treated with both hormones showed less variation in ethylene levels over the evaluated ripening days. On the fourteenth DAH, CTRL and ETHY fruits had already reached full ripeness, while auxin-treated fruits (IAA and ETHY+IAA) did not show the observed red color.

Indeed, the expression patterns of ethylene-related genes indicated that auxin has an opposing role in regulating key effectors of ripening (Figure 2A). ACS1a and ACS6, genes associated with system I of ethylene production, were induced by auxin during the first days after treatment, whereas ACS2 and ACS4, known to be related to system II and upregulated by ethylene, were downregulated by auxin until the

breaker stage (fourth DAH). Furthermore, in ETHY+IAA fruits, the responses were similar to those in IAA fruits, revealing that the presence of auxin repressed ethylene-inducible genes. This highlights the epistatic effects of auxin over ethylene.

Figure 1 – Effects of ethylene, auxin, and both treatments on fruit color, ethylene emission, and auxin content during Micro-Tom tomato (*Solanum lycopersicum* L.) fruit ripening

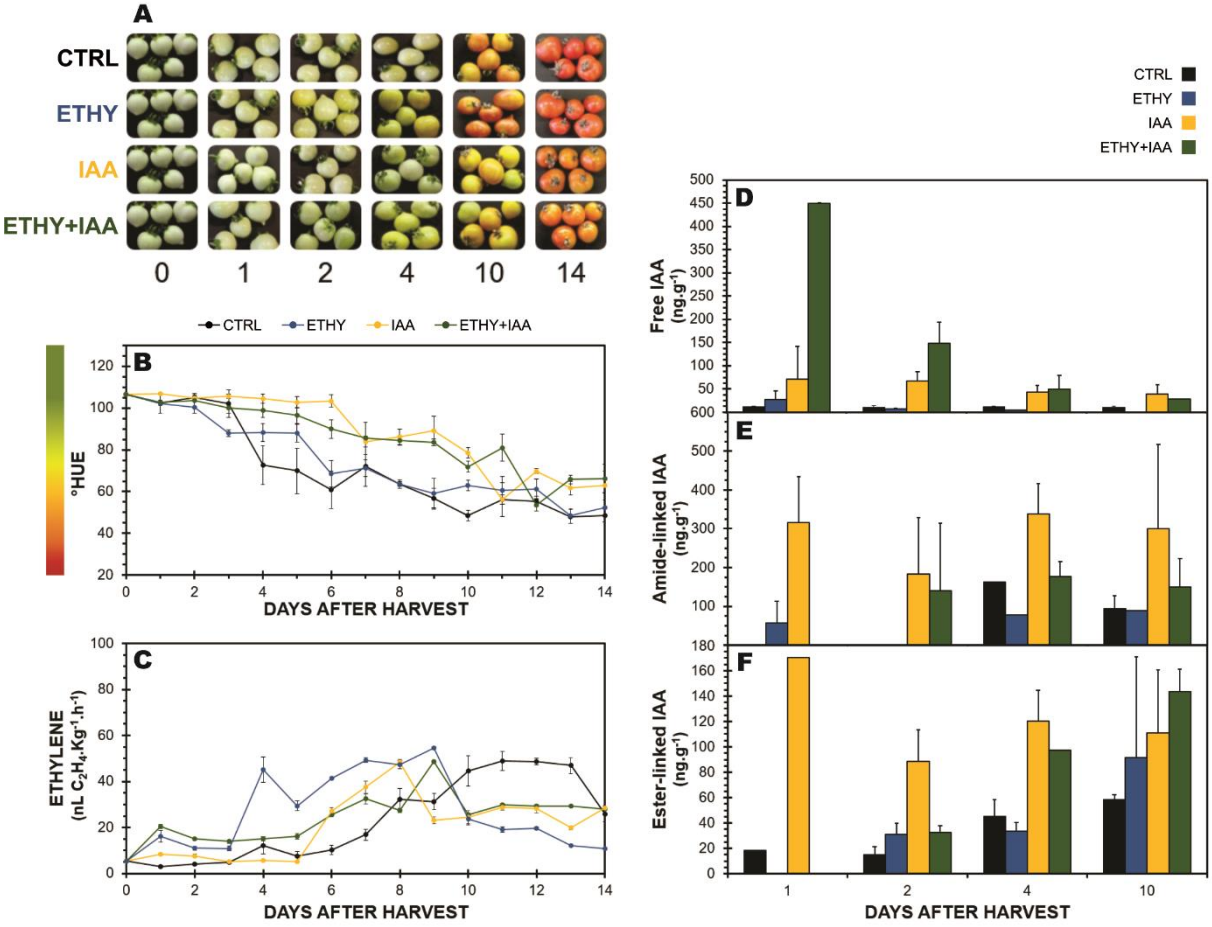

(A) Pictures of tomato fruits. (B) Peel color expressed by hue angle. (C) Ethylene emission. (D) Free auxin content. (E) Amide-linked auxin content. (F) Ester-linked auxin content. CTRL: Control group. ETHY: Ethylene-treated group. IAA: Indole-3-acetic acid-treated group. ETHY+IAA: Group treated with both hormones. The contents of free, ester-linked, and amide-linked auxin are given in micrograms per gram of fruit on fresh weight basis. Vertical bars represent the standard deviation of three replicates (n = 3).

It is particularly notable that the transcript levels of ACO1, related to tomato ripening (VAN DE POEL et al., 2012), were induced by ethylene treatment on the first DAH, whereas auxin treatment apparently did not affect its expression at the transcriptional level. However, ACO4 expression, also associated with tomato ripening (KUMAR; KHURANA; SHARMA, 2014), was upregulated by auxin, suggesting that this hormone affected its regulation.

Figure 2 – Effects of ethylene, auxin, and both treatments on ethylene and auxin-related gene expression during Micro-Tom tomato (*Solanum lycopersicum* L.) fruit ripening

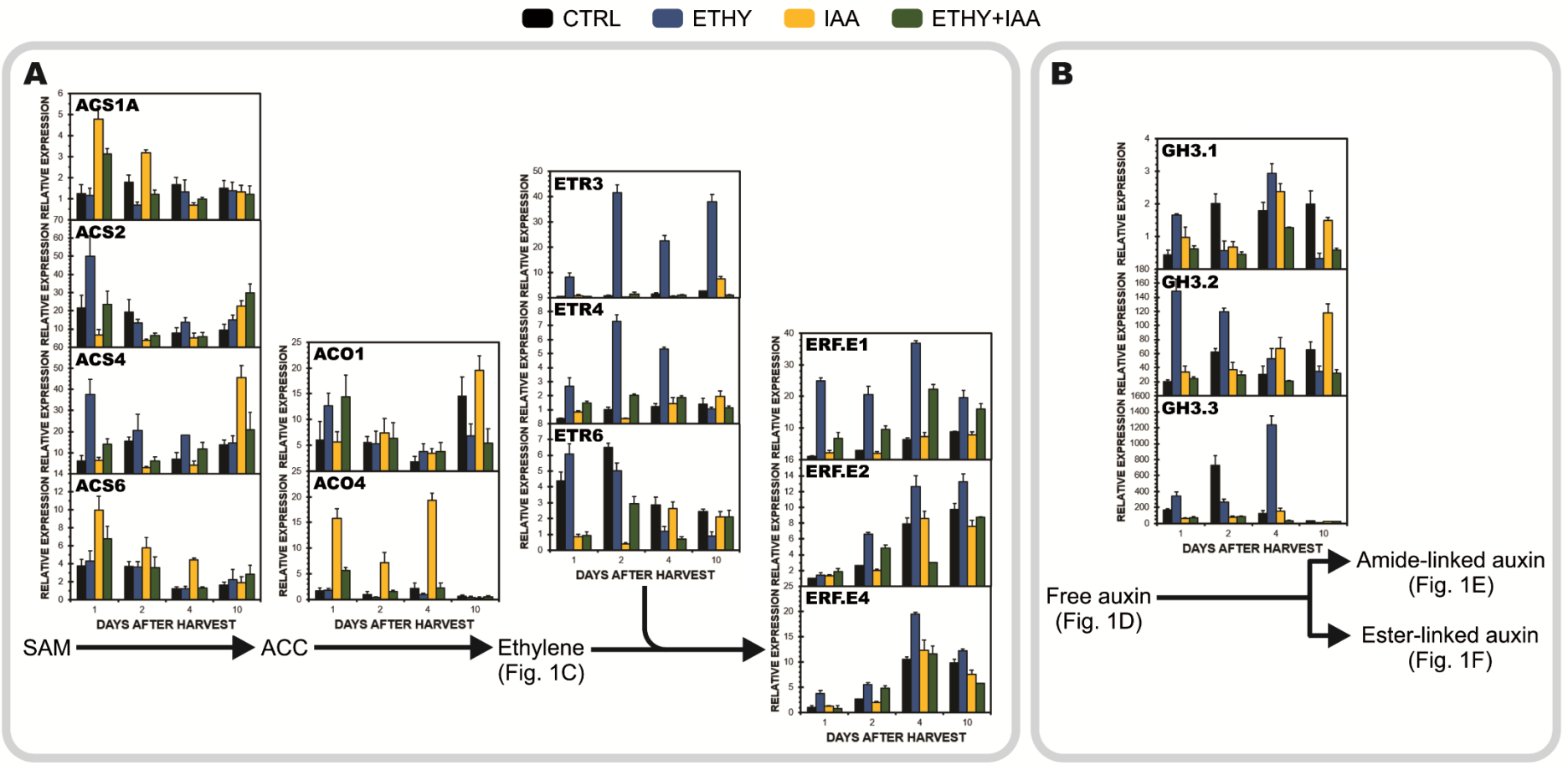

CTRL: Control group. ETHY: Ethylene-treated group. IAA: Indole-3-acetic acid-treated group. ETHY+IAA: Group treated with both hormones. ACS: 1-aminocyclopropane-1-carboxylic acid (ACC) synthase. ACO: ACC oxidase. ERF: Ethylene response factor. ETR: Ethylene receptor. GH3: Gretchen Hagen protein 3. Vertical bars represent the standard deviation of three replicates (n = 3).

The results revealed that auxin affected ethylene perception, which is consistent with the ripening delay. The transcription of the ETRs predominantly expressed in tomato fruit ripening (ETR3, ETR4, and ETR6) (KEVANY et al., 2007), was downregulated in IAA fruits (Figure 2A). Moreover, these genes are known to be ethylene-regulated, confirming the induction observed in ETHY fruits. However, in ETHY+IAA fruits, the ethylene effect was repressed, potentially indicating direct regulation by auxin of the ethylene perception and downstream signal transduction.

ERFs were also affected by auxin. Liu et al. (2016) reported that ERF.E1, ERF.E2, and ERF.E4 are important transcription factors of the ERF family in tomatoes, displaying a consistent ripening-associated expression pattern. In this study, results concerning the expression of these three genes revealed upregulation by ethylene during the first days of ripening until the breaker stages, whereas auxin treatments were found to block the ethylene effect, repressing the transcription. Once these genes can directly regulate ripening events associated with several metabolisms such as color shift, ethylene biosynthesis, or volatile production, these findings can be correlated with the overall ripening delay observed for auxin treatments.

In relation to the endogenous auxin contents, free auxin (Figure 1D) levels in CTRL fruits were reduced during the first days of ripening, whereas the amide-linked (Figure 1E) and ester-linked auxin (Figure 1F) forms increased during the same time period, indicating that active auxin removal is required for normal ripening. IAA and ETHY+IAA fruits presented increased values of free auxin and both conjugated forms. On the first DAH, these two groups of fruits presented free auxin concentrations approximately four and six times higher than those of CTRL fruits, respectively. The results also showed that ETHY fruits presented less active auxin (ten times lower than the CTRL) and increased conjugated forms, especially amide-linked forms, revealing accelerated conjugation.

To verify the auxin and ethylene responsiveness of auxin-associated genes, GH3 transcript levels were assessed for three GH3 genes (GH3.1, GH3.2, and GH3.3) (Figure 2B). These genes have shown a ripening-related expression pattern and upregulation by ethylene in the first days after harvest. Notably, auxin treatments appear to have no induction effects during the first ripening stages but only after four DAH. Together, these results suggest that ethylene might induce auxin conjugation, possibly through upregulation of ethylene-inducible GH3 genes, illuminating an important crosstalk point between auxin and ethylene.

3.2 Hormonal regulation of volatile compound profile during tomato ripening

To investigate how treatment with ethylene, auxin, and a combination of both hormones affected aroma components, VOC analysis was performed by SPME. A total of 66 VOCs was identified and confirmed, of which 40 contributed to the aroma through odor notes and varying odor thresholds (Table 1). These compounds were mostly aldehydes (8), ketones (7), and terpenoids (7); however, esters (5), furans (4), benzene compounds (4), alcohols (3), carboxylic acids (1), and sulfur compounds (1) were also found (Figure S1A). In relation to the metabolic precursors, 16 compounds had fatty-acid precursors, 11 were obtained through amino-acid degradation, 9 were derived from isoprenoids, and 4 were derived from carbohydrates (Figure S1B).

To obtain an overall description of the effects of exogenous hormones on VOC profiles during tomato ripening, hierarchical cluster analysis (HCA), PLS-DA, and VIP were performed at 01, 04 and 14 DAH (Figure 3). At the beginning of ripening, the tomatoes presented VOC profiles comprising 32 of the 40 previously selected compounds, and 19 of these presented abundances with significant differences ($p < 0.05$) between at least two groups. PLS-DA explained 69.5% (component 1, 42.6%; component 2, 26.9%) of the total variance between the CTRL and the treated samples. As shown in Figure 3A, the differences in VOC profiles among the CTRL, ETHY, and ETHY+IAA groups were separated primarily by component 1, while component 2 separated the ETHY and ETHY+IAA groups. HCA reinforced differences visualized by PLS-DA, showing that the IAA and ETHY+IAA groups presented similar VOC profiles, both being more similar to the CTRL than to the ETHY group. Based on PLS-DA, terpenoids, furans, and benzene compounds were the most important in distinguishing the CTRL and the treated samples.

The two terpenoids found at the beginning of ripening (α-cubebene; linalool) were found with higher contents in the CTRL and ETHY fruits. These compounds were not found in the ETHY+IAA fruits. In relation to the furans, the 2-pentylfuran, 2-ethylfuran, and 2-propylfuran contents were higher in the ETHY+IAA fruits, while the 2-acetyl-5-methylfuran content was higher in the ETHY than in the other groups. Toluene, m-xylene, benzaldehyde, and butylated hydroxytoluene, the four benzene compounds found at 01 DAH, were induced in the ETHY fruits; however, only toluene and butylated hydroxytoluene were induced in the ETHY+IAA fruits.

Table 1 – Identified volatile organic compounds in two tomato (*Solanum lycopersicum* L.) fruit cultivars after ethylene, auxin, and both treatments throughout ripening. Data presented are *p* values for mean comparisons between treated and control fruits (n = 3)

ID[a]	Volatile organic compound	RI[b]	Functional group	Odor type	Micro-Tom						Sweet Grape					
					4 DAH			14 DAH			4 DAH			8 DAH		
					E[c]	A[d]	E+A[e]	E[c]	A[d]	E+A[e]	E[c]	A[d]	E+A[e]	E[c]	A[d]	E+A[e]
Amino acids																
Ald.01	2-methylbutanal	<1000	aldehyde	chocolate	-	-	-	-	-	-	0.81	0.83	0.46	0.64	0.93	0.70
Benz.01	Toluene	1041	benzenic compound	sweet	**0.01**	0.14	**0.02**	0.89	0.50	0.87	0.38	0.14	0.72	0.11	0.48	0.56
Ald.03	2-methylbut-2-enal	1095	aldehyde	green	-	-	-	-	-	-	0.26	0.74	0.45	0.47	**0.03**	0.06
Benz.02	m-xylene	1131	benzenic compound	plastic	**0.00**	0.11	**0.00**	0.80	0.15	0.19	-	-	-	-	-	-
Benz.03	Styrene	1250	benzenic compound	balsamic	0.27	0.11	**0.03**	0.14	0.14	0.14	-	-	-	-	-	-
Est.03	Methyl heptanoate	1283	ester	fruity	0.01	0.10	**0.00**	0.76	0.65	0.50	0.06	0.23	**0.01**	**0.05**	**0.02**	**0.03**
Ket.05	2,2,6-trimethylcyclohexan-1-one	1303	ketone	thujonic	0.36	0.74	0.64	0.42	0.95	0.55	-	-	-	-	-	-
Est.04	(Z)-3-hexenyl (E)-2-butenoate	1361	ester	green	**0.01**	0.36	0.13	0.78	0.24	0.84	**0.00**	0.09	0.26	0.61	0.98	0.60
Sulf.01	2-isobutylthiazole*****	1391	sulfur compound	tomato	**0.01**	0.61	**0.00**	0.41	0.16	0.90	0.26	0.74	0.45	**0.05**	0.93	0.12
Alc.08	6-methyl-5-hepten-2-ol	1458	alcohol	green	-	-	-	-	-	-	0.26	0.74	0.45	0.76	0.09	0.06
Alc.09	2-ethylhexan-1-ol	1484	alcohol	citrus	**0.01**	**0.01**	**0.01**	0.77	0.16	0.69	0.69	0.82	0.77	0.84	0.70	0.24
Benz.04	Benzaldehyde	1506	benzenic compound	fruity	-	-	-	-	-	-	**0.01**	0.93	0.95	**0.01**	0.93	0.70
Ald.13	2-phenylacetaldehyde	1622	aldehyde	green	-	-	-	-	-	-	**0.00**	**0.01**	**0.02**	0.97	0.25	0.86
Sulf.02	2-thiolpropionic acid	1697	sulfur compound	sulfurous	-	-	-	-	-	-	0.26	0.74	0.45	0.30	0.33	0.18
Est.05	Methyl salicylate*****	1760	ester	minty	0.06	0.11	0.16	0.65	**0.04**	0.12	0.26	0.74	0.45	0.64	0.93	0.70
Est.06	Ethyl salicylate	1850	ester	minty	**0.01**	**0.01**	**0.01**	0.77	0.16	0.69	-	-	-	-	-	-
Alc.10	Phenylethyl Alcohol*****	1888	alcohol	floral	-	-	-	-	-	-	0.01	0.49	0.03	0.64	0.96	0.92
Benz.05	Butylated hydroxytoluene (BHT)	1905	benzenic compound	phenolic	0.25	0.61	0.14	**0.05**	**0.05**	**0.05**	-	-	-	-	-	-
Carbohydrates																
Fur.01	2-acetyl-5-methylfuran	1081	furan	nutty	0.25	**0.01**	**0.04**	0.77	0.16	0.69	-	-	-	-	-	-
Fur.02	2-pentylfuran	1217	furan	fruity	**0.01**	0.40	**0.00**	0.80	0.40	0.36	-	-	-	-	-	-
Fur.03	2-ethylfuran	1400	furan	sweet	**0.05**	**0.01**	**0.02**	0.77	0.16	0.69	**0.02**	**0.01**	0.08	0.28	0.41	0.09
Fur.04	2-pentanoylfuran	1458	furan	caramellic	-	-	-	-	-	-	0.26	0.74	0.45	0.40	0.16	0.81
Fur.05	2-propylfuran	1461	furan	fruity	0.06	**0.02**	**0.04**	0.77	0.16	0.69	0.22	**0.01**	**0.02**	0.64	0.93	0.70
Fatty acids																
Ket.01	3-pentanone*****	<1000	ketone	ethereal	0.48	0.63	0.67	0.32	0.10	**0.04**	0.07	0.19	0.44	0.13	0.35	0.84
Est.01	Ethyl acetate	<1000	ester	fruity	-	-	-	-	-	-	0.06	**0.03**	**0.03**	0.64	0.93	0.70
Ket.02	1-penten-3-one	1027	ketone	spicy	**0.03**	0.06	0.07	0.82	0.07	0.10	0.12	**0.05**	**0.01**	0.29	0.11	0.12
Ald.02	Hexanal*****	1084	aldehyde	green	0.09	0.58	**0.03**	0.73	**0.02**	0.13	**0.02**	0.70	0.71	0.24	0.11	0.21

Table 1 – (continued)

ID[a]	Volatile compound	RI[b]	Functional group	Odor type	Micro-Tom						Sweet Grape					
					4 DAH			14 DAH			4 DAH			8 DAH		
					E[c]	A[d]	E+A[e]	E[c]	A[d]	E+A[e]	E[c]	A[d]	E+A[e]	E[c]	A[d]	E+A[e]
Fatty acids																
Ald.04	(E)-2-pentenal	1130	aldehyde	green	-	-	-	-	-	-	0.07	**0.01**	**0.01**	0.14	0.93	0.70
Ald.05	3-hexenal	1151	aldehyde	green	**0.00**	**0.00**	**0.00**	**0.01**	**0.01**	**0.01**	**0.01**	**0.04**	0.69	0.63	0.90	0.69
Ket.03	4-hexen-3-one	1152	ketone	acidic	-	-	-	-	-	-	0.09	**0.05**	0.81	0.88	0.58	0.67
Est.02	Propanoyl propanoate	1173	ester	ethereal	0.06	0.61	**0.02**	0.55	**0.02**	**0.02**	0.06	0.57	0.72	0.65	0.39	0.67
Ald.06	Heptanal	1185	aldehyde	green	-	-	-	-	-	-	0.12	0.74	0.45	0.64	0.93	0.70
Ald.07	(E)-2-hexenal*	1219	aldehyde	green	0.28	0.14	0.88	0.53	0.87	0.58	0.11	0.42	0.19	0.43	0.64	0.30
Alc.01	1-pentanol*	1246	alcohol	fermented	-	-	-	-	-	-	**0.01**	**0.01**	0.39	**0.02**	0.93	**0.03**
Ket.04	1-hepten-3-one	1296	ketone	metallic	0.70	0.88	0.14	0.68	0.25	0.34	0.28	0.23	0.14	0.56	0.46	0.51
Alc.02	(Z)-2-penten-1-ol	1314	alcohol	green	-	-	-	-	-	-	0.14	0.70	0.52	0.64	0.93	0.70
Ket.06	(E)-2-heptenal	1319	ketone	thujonic	0.11	0.34	0.11	0.82	0.23	0.98	**0.05**	0.77	0.59	0.66	0.97	0.70
Alc.03	1-hexanol*	1348	alcohol	herbal	-	-	-	-	-	-	**0.00**	0.29	**0.00**	**0.00**	0.93	0.70
Ald.08	2-propenal	1352	aldehyde	fruity	**0.01**	0.17	0.48	0.39	0.22	0.63	0.44	0.24	0.10	0.96	0.73	0.62
Alc.04	(E)-3-hexen-1-ol*	1357	alcohol	green	-	-	-	-	-	-	**0.00**	0.07	0.12	0.69	0.99	0.47
Alc.05	(Z)-3-hexen-1-ol	1379	alcohol	green	0.11	0.12	0.22	0.73	0.27	0.49	**0.02**	0.27	0.14	0.94	0.41	1.00
Ald.09	Nonanal	1391	aldehyde	aldehydic	0.56	0.64	0.91	0.64	0.36	0.53	-	-	-	-	-	-
Ald.10	(E,E)-2,4-hexadienal	1401	aldehyde	green	**0.02**	**0.02**	**0.02**	0.77	0.16	0.69	0.07	0.06	0.72	0.64	0.93	0.26
Ket.08	1-octen-3-one	1421	ketone	earthy	-	-	-	-	-	-	0.64	0.92	0.70	0.92	0.38	0.48
Ald.11	(E)-2-octenal*	1423	aldehyde	fatty	0.11	1.00	0.10	0.73	0.22	0.32	0.64	0.01	**0.01**	0.64	0.93	0.70
Alc.06	1-octen-3-ol	1447	alcohol	earthy	0.25	**0.00**	**0.02**	0.30	0.09	0.97	0.22	0.50	0.30	0.64	0.93	0.70
Alc.07	1-heptanol	1448	alcohol	green	-	-	-	-	-	-	**0.00**	**0.01**	**0.01**	0.64	0.93	0.70
Ald.12	Decanal	1493	aldehyde	aldehydic	**0.01**	0.61	0.14	0.12	**0.01**	**0.05**	-	-	-	-	-	-
Carb.01	Pentanoic acid	1889	carboxilic acid	cheesy	0.25	0.61	0.14	0.21	0.11	0.41	0.26	**0.02**	**0.00**	**0.03**	0.93	**0.01**
Isoprenoids																
Ket.07	6-methyl-5-hepten-2-one*	1333	ketone	citrus	**0.03**	**0.02**	**0.03**	0.95	0.17	0.21	**0.04**	0.26	**0.03**	0.88	0.56	0.28
Terp.01	α-cubebene	1456	terpenoid	herbal	0.25	0.61	0.08	0.77	0.16	0.69	-	-	-	-	-	-
Terp.02	Linalool	1543	terpenoid	floral	0.25	0.61	0.14	0.77	0.16	0.69	0.11	0.25	0.40	0.07	0.07	0.07
Terp.03	Linalyl butanoate	1548	terpenoid	floral	0.25	0.61	0.14	0.77	0.16	0.69	-	-	-	-	-	-
Terp.04	o-guaiacol*	1597	terpenoid	woody	-	-	-	-	-	-	0.11	0.29	0.15	0.15	0.76	0.15
Terp.05	β-cyclocitral	1601	terpenoid	tropical	1.00	**0.05**	**0.05**	0.68	0.14	0.59	-	-	-	-	-	-
Terp.06	Citral*	1724	terpenoid	citrus	0.25	0.61	0.14	0.88	**0.03**	0.07	0.26	0.74	0.45	0.64	0.06	0.06

Table 1 – (continued)

ID[a]	Volatile compound	RI[b]	Functional group	Odor type	Micro-Tom						Sweet Grape					
					4 DAH			14 DAH			4 DAH			8 DAH		
					E[c]	A[d]	E+A[e]	E[c]	A[d]	E+A[e]	E[c]	A[d]	E+A[e]	E[c]	A[d]	E+A[e]
Isoprenoids																
Terp.07	Photocitral A	1729	terpenoid	herbal	0.25	0.61	0.14	0.10	**0.00**	**0.02**	-	-	-	-	-	-
Ket.09	Geranyl acetone*****	1850	ketone	floral	**0.04**	0.61	0.14	0.84	0.09	0.61	-	-	-	-	-	-
Terp.08	β-ionone*****	1924	terpenoid	floral	**0.03**	0.61	0.14	0.36	0.61	0.36	-	-	-	-	-	-

[a]ID: Volatile compound identification.

[b]RI: Retetion index. relative to n-alkanes (C_{10}-C_{30}) on the SupelcoWax capillary column.

[c]E: *p* value for T-test between control and ethylene treated fruits.

[d]A: *p* value for T-test between control and auxin treated fruits.

[e]E+A: *p* value for T-test between control and ethylene-auxin treated fruits.

DAH: Days after harvest.

*Compound confirmed by mass spectrum comparison with external standard.

Values in bold letters show significant differences ($p < 0.05$) between the control and treated fruits.

Figure 3 – Effects of ethylene, auxin, and both treatments on VOC contents, carotenoid contents, and related enzyme activities during Micro-Tom tomato (*Solanum lycopersicum* L.) fruit ripening

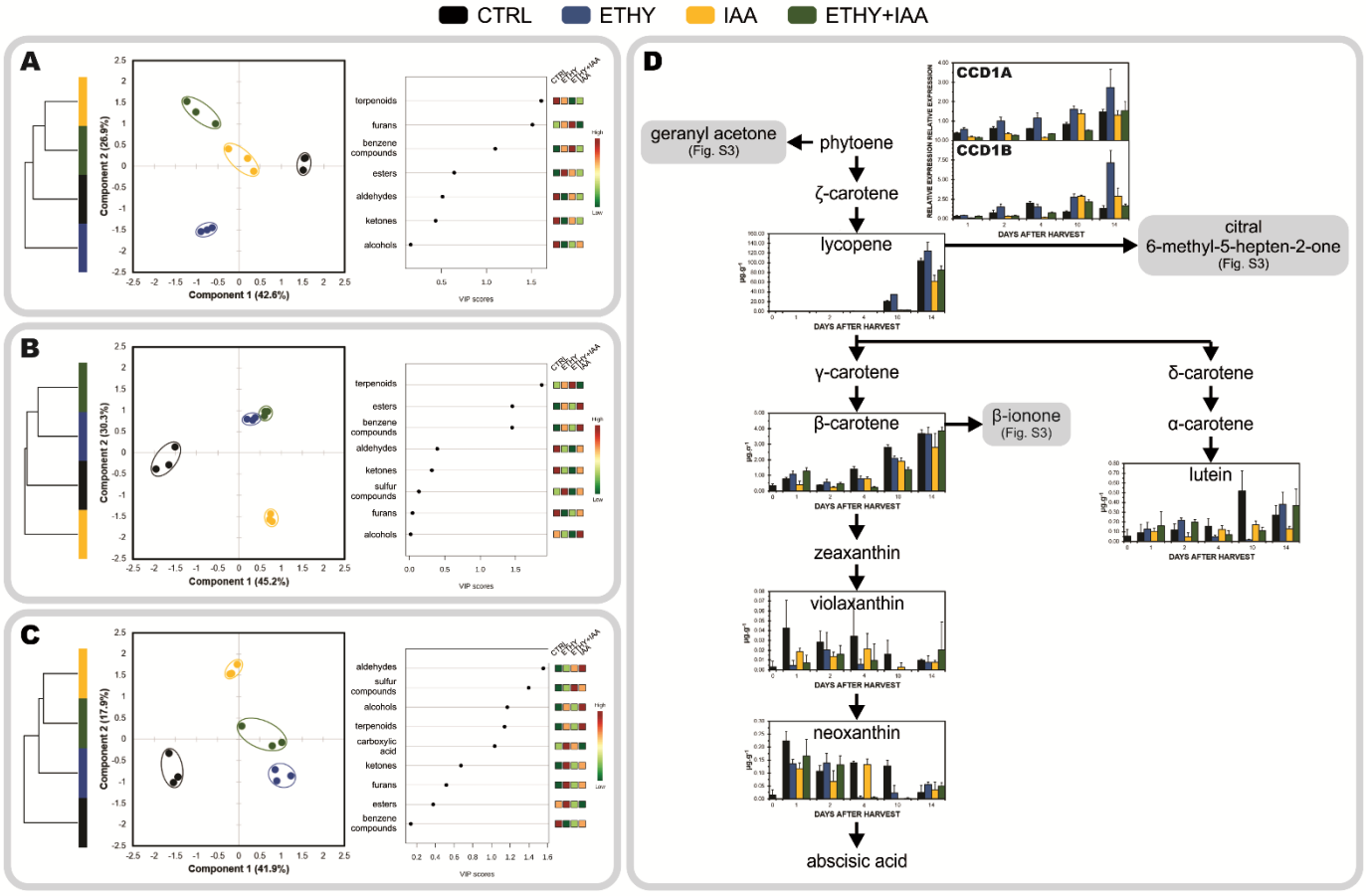

(A, B, and C) Hierarchical clustering, partial least squares discriminant analysis (PLS-DA), and variable importance in projection (VIP) of VOCs produced after 01, 04 (breaker stage), and 14 (red stage) days after harvest. (D) Carotenoid content and CCD gene expression. CTRL: Control group. ETHY: Ethylene-treated group. IAA: Indole-3-acetic acid-treated group. ETHY+IAA: Group treated with both hormones. CCD: Carotenoid cleavage dioxygenase. The contents of carotenoids are given in micrograms per gram of fruit on fresh weight basis. Vertical bars represent the standard deviation of three replicates (n = 3).

After 3 DAH, when the CTRL fruits reached the breaker stage, their VOC profiles comprised 34 compounds, and 28 of them presented abundances with significant differences ($p < 0.05$) between at least two groups. PLS-DA explained 75.5% of the total variation between samples (Figure 3B). Component 1 (45.2%) separated the CTRL from the other groups, and component 2 (30.3%) separated the ETHY and ETHY+IAA groups from the IAA group. In addition to PLS-DA, HCA showed that the ETHY and ETHY+IAA groups have more similar VOC profiles to each other, and both were more similar to the CTRL than to the IAA group. Hexanal, (E)-2-hexenal, (E)-2-heptenal, 6-methyl-5-hepten-2-one, and 2-isobutylthiazole, aroma compounds important to consumer acceptance (TIEMAN et al., 2017), were found with higher

contents in ETHY and ETHY+IAA fruits. Other important VOCs, including 2-ethylhexan-1-ol and (E,E)-2,4-hexadienal, were found only in the CTRL fruits, while decanal and β-ionone were exclusive to ETHY fruits. Previously found with higher contents in CTRL and ETHY, and not in ETHY+IAA, α-cubebene was found only in ETHY+IAA fruits, suggesting that exogenous auxin treatment delayed the metabolic pathway of this compound.

Finally, when the CTRL group was completely ripe (Figure 3C), the VOC profiles comprised 31 compounds, and only 12 of them presented abundances with significant differences ($p < 0.05$) between at least two groups. PLS-DA explained 59.8% of the total variation between samples. Component 1 (41.9%) separated the CTRL and IAA from the ETHY and ETHY+IAA groups, while component 2 (17.9%) separated the IAA from the CTRL and ETHY groups. Additionally, HCA showed that the IAA and ETHY+IAA fruits presented more similar VOC profiles to each other, and both were more similar to the ETHY than to the CTRL fruits. With respect to fatty-acid-derived volatiles, the accumulation of (Z)-3-hexen-1-ol, 2-propenal, hexanal, (E)-2-hexenal, (E)-2-octenal, 1-penten-3-one, and 1-hepten-3-one was affected by exogenous ethylene and auxin treatment during ripening. Hexanal and 2-propenal were found in higher contents in IAA and ETHY+IAA than in ETHY fruits. However, 1-penten-3-one, 1-hepten-3-one, (Z)-3-hexen-1-ol, and (E)-2-octenal were fatty-acid-derived volatiles with higher contents in ETHY than in IAA and ETHY+IAA fruits. Hexanal, (E)-2-hexenal, and (Z)-3-hexen-1-ol were fatty-acid-related volatiles found with higher contents in the tomato aroma profiles, at 10, 3, and 2 times higher than the other VOCs, respectively. Other compounds, including citral, 6-methyl-5-hepten-2-one, and methyl salicylate, were found with higher contents in ETHY and ETHY+IAA than in IAA fruits.

As observed in tomato fruit aroma profiles carbohydrates and isoprenoid-derived compounds showed greater importance in distinguishing CTRL and exogenous hormone-treated fruits at the early ripening stage. Throughout ripening, isoprenoid derivatives remained important, while fatty-acid derivatives became more important than carbohydrate derivatives. At the final ripening stage, fatty-acid and amino-acid-derived compounds were the most important in distinguishing between the volatile profiles of CTRL and treated fruits.

To investigate the origin of the observed changes in tomato fruit aromas and to identify the effects of exogenous auxin and ethylene treatments on the metabolic

pathways of VOC precursors, the expression profiles of major genes involved in the biosynthesis of VOCs during tomato fruit ripening were analyzed, as well as the contents of tomato fruit carotenoids (Figure 3D and Figure S2). Lycopene contents on DAH 10 and DAH 14 were lower in IAA and ETHY+IAA, and higher in ETHY fruits, in accordance with the peel color measurements and the pictures shown in Figure 1A–B. Additionally, no significant differences in the β-carotene levels were found between the groups. Su et al. (2015) achieved similar results concerning the carotenoid levels once auxin exposure had affected only the lycopene contents in tomato fruit. Carotenoid cleavage dioxygenase (CCD), specifically CCD1A and CCD1B, transcript levels were also downregulated by auxin and upregulated by ethylene, whereas treatment with both hormones led to a similar expression pattern for IAA fruits. Thus, the delay in the production of the VOCs derived from isoprenoid in hormone-treated fruits (Figure S3) can by correlated with the modulation of CCDs genes, once the enzymes encoded by these genes use carotenoids as substrates for aroma compounds biosynthesis. These results are consistent with the lower carotenoid contents and the downregulation of the related genes.

Fatty-acid volatiles are the most abundant VOCs in tomato fruits (KLEE, 2010), and most of these are derived from the lipoxygenase pathway via LoxC, HPL, and ADH2 enzymes and the corresponding genes (LIBIN et al., 2016). These enzymes were identified and shown to be associated with aroma development during tomato fruit ripening (JIYUAN et al., 2014). In this study, this volatile-related gene expression was also found to be upregulated by ethylene, especially at the breaker stage (04 DAH). Conversely, auxin delayed the increase in the transcriptional levels until 10 DAH (Figure S2).

Altogether, these results support the delaying effects of the exogenous auxin treatment on the tomato fruit volatile profiles and consolidate the role of this hormone in delaying ripening. However, considering that the observed effects could be cultivar-dependent, tomatoes (*Solanum lycopersicum*) cv. Sweet Grape were chosen for further investigations on the role of ethylene and auxin in the VOC metabolism.

3.3 Cultivar dependence of hormonal regulation of volatile compound production

Tomatoes (*Solanum lycopersicum*) cv. Sweet Grape were subjected to the same hormone treatments to confirm whether the effects of exogenous ethylene and auxin treatments would be cultivar-dependent or independent. As observed in the Micro-Tom experiment, the color shift (Figure 4A and 4B) and the ethylene emission (Figure 4C) were accelerated by ethylene treatment and retarded by auxin. However, Sweet Grape tomatoes treated with both hormones showed results closer to those of ETHY than of IAA fruits. On the sixth DAH, ETHY fruits had already reached full ripeness, while the same stage was reached on the eighth DAH for the CTRL and ETHY+IAA fruits, and those treated only with auxin did not show the observed red color.

In relation to the VOC profiles, a total of 52 compounds were identified and confirmed, of which 44 had the odoriferous note described in the literature (Table 1). These compounds were mostly aldehydes (11), alcohols (10), and ketones (7); however, esters (5), terpenoids (3), furans (3), benzene compounds (2), sulfur compounds (2), and carboxylic acids (1) were also found (Figure S4A). In relation to the metabolic precursors, 24 compounds had fatty-acid as precursors, 13 were obtained through amino-acid degradation, 4 were directly derived from isoprenoids, and 3 were derived from carbohydrates (Figure S4B). To identify the similarities and differences between Micro-Tom and Sweet Grape tomato fruits, the VOC profiles of untreated tomato fruits were compared at mature green, breaker, and red stages (Figure S5). Although the two cultivars present differences in their aroma profiles, these are more evident after complete ripening (red stage) than at the beginning (mature green stage).

PLS-DA (Figure S5A) and heatmap analysis (Figure S5B) showed that the same ripening stages of different cultivars are strongly similar and that tomatoes presented more similar VOC profiles at the mature green and breaker stages than at the red stage. According to PLS-DA, linalool, (E,E)-2,4-hexadienal, methyl salicylate, 2-ethylfuran, 2-ethylhexan-1-ol, and 2-isobutylthiazole were the most important compounds in distinguishing the ripening stages in the two cultivars (Figure S5C). Knowing that the cultivars are strongly similar at the same ripening stages, it was possible to identify the treatment effects of exogenous ethylene and auxin on Sweet Grape tomato fruits and compare their results with those on Micro-Tom tomato fruits.

Figure 4 – Effects of ethylene, auxin, and both treatments on fruit color, ethylene emission, and VOC contents during Sweet Grape (*Solanum lycopersicum* L.) fruit ripening

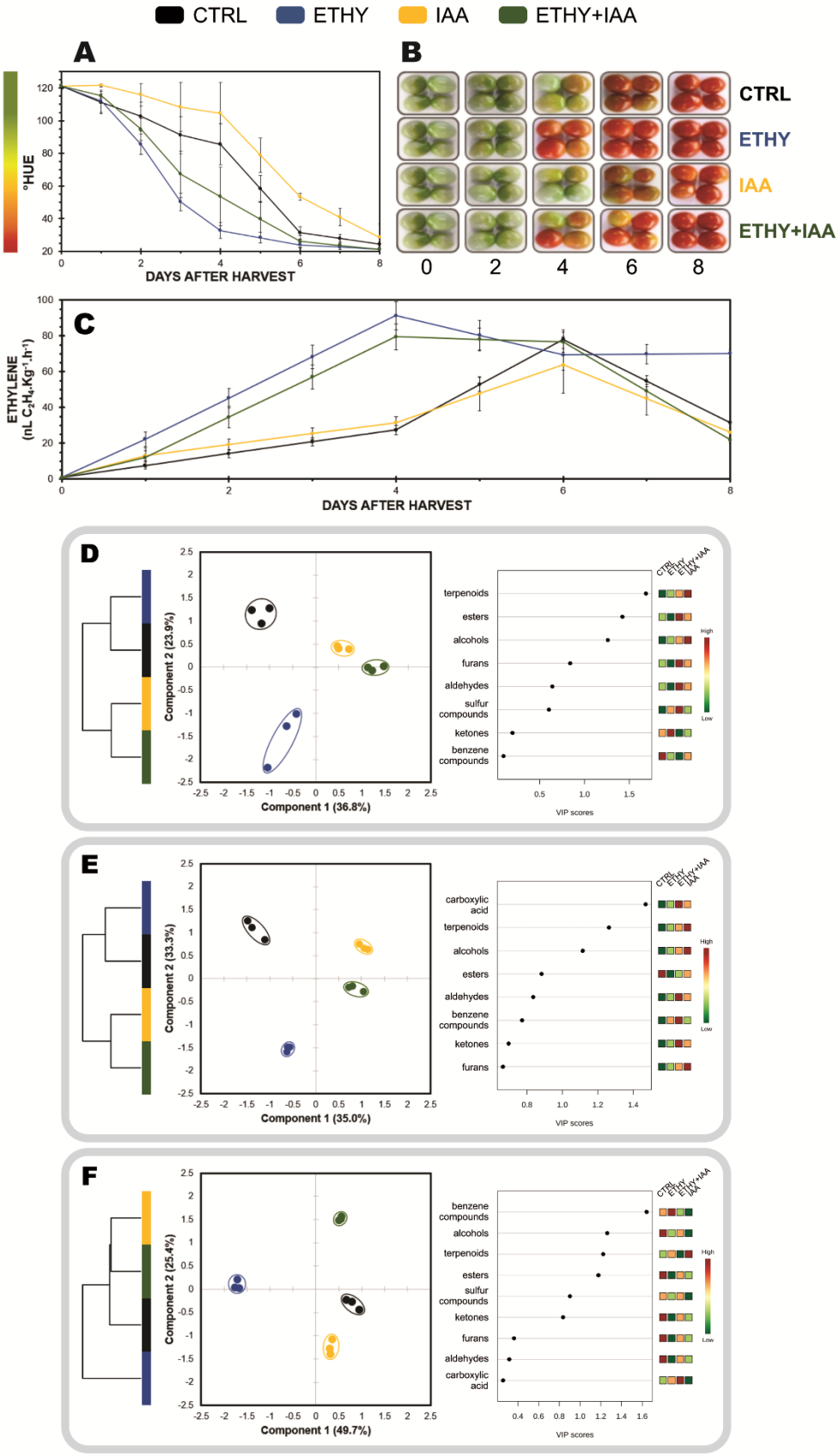

(A) Peel color expressed by hue angle. (B) Pictures of tomato fruits. (C) Ethylene emission. (D, E, and F) Hierarchical clustering, partial least squares discriminant analysis (PLS-DA), and variable importance

in projection (VIP) of VOCs produced at days 01, 04 (breaker stage), and 08 (red stage). CTRL: Control group. ETHY: Ethylene-treated group. IAA: Indole-3-acetic acid-treated group. ETHY+IAA: Group treated with both hormones. Vertical bars represent the standard deviation of three replicates (n = 3).

On the first DAH (Figure 4D), Sweet Grape tomatoes presented VOC profiles comprising 29 of the 44 previously selected compounds, and only 10 of them presented abundances with significant differences ($p < 0.05$) between at least two groups. PLS-DA explained 60.7% (component 1, 36.8%; component 2, 23.9%) of the total variance between the CTRL and the treated samples. As shown in Figure 4D, component 1 separated the CTRL and ETHY from the IAA and ETHY+IAA groups, while the differences in VOC profiles among the CTRL, IAA, and ETHY groups were separated by component 2. HCA reinforced the differences visualized by PLS-DA, in which the CTRL and ETHY groups presented more similar VOC profiles, as did the IAA and ETHY+IAA groups.

At this stage, some important fatty-acid-derived volatiles, including 3-pentanone, hexanal, and (E)-2-hexenal, were affected by the hormone treatments and showed higher contents in the CTRL than in treated fruits. Other fatty-acid derivatives were found in higher levels only in the CTRL and ETHY (3-hexenal and 4-hexen-3-one) or in IAA and ETHY+IAA fruits (ethyl acetate). Treatment with auxin (IAA group) increased the contents of some compounds in the tomato fruits, including (Z)-2-penten-1-ol, 6-methyl-5-hepten-2-one, (E)-3-hexen-1-ol, and linalool, but a different result was found for ETHY+IAA fruits, again suggesting that the ethylene and auxin responses already overlapped within hours of treatment. Additionally, other compounds were important in distinguishing CTRL and treated fruits due to their presence in specific groups. Benzaldehyde was found only in CTRL fruits, while 2-methylbutanal was exclusive to ETHY and 1-hexanol to ETHY+IAA fruits; 1-penten-3-one and (E,E)-2,4-hexadienal were found only in CTRL and ETHY fruits.

When the CTRL fruits reached the breaker stage, VOC profiles comprised 37 compounds, and 29 of them presented abundances with significant differences ($p < 0.05$) between at least two groups. PLS-DA explained 68.3% of the total variation between samples. Component 1 (35.0%) separated the CTRL and ETHY from the IAA and ETHY+IAA groups, while component 2 (33.3%) separated the CTRL and IAA from the other groups (Figure 4E). HCA showed that CTRL and treated fruits presented the same dispersion as the previous analysis, in which the CTRL and ETHY groups

presented more similar VOC profiles, as did the IAA and ETHY+IAA groups. Apart from 3-pentanone, which was inhibited by both exogenous treatments, fatty-acid-derived compounds were found in higher contents in treated fruits. The accumulation of hexanal, 3-hexenal, 4-hexen-3-one, (E)-2-hexenal, (E,E)-2,4-hexadienal, and (E)-2-octenal was induced by ethylene treatment, while (Z)-2-penten-1-ol, (E)-3-hexen-1-ol, and (Z)-3-hexen-1-ol were affected by auxin treatment and showed higher contents in the IAA and ETHY+IAA groups. With respect to amino-acid-derived volatiles, the accumulation of 2-methylbutanal, 2-ethylhexan-1-ol, benzaldehyde, and phenylethyl alcohol was more affected by exogenous ethylene treatment, and the (Z)-3-hexenyl and (E)-2-butenoate contents were higher in IAA and ETHY+IAA fruits. The accumulation of VOCs derived from carotenoids was separately affected by ethylene (6-methyl-5-hepten-2-one) and auxin (linalool), suggesting that each hormone regulated different sites in the geranyl diphosphate pathway. Regarding the other volatiles, heptanal, 2-propylfuran, and 2-phenylacetaldehyde were important in distinguishing ETHY fruits from the others due to their presence in this specific group. Ethyl acetate, (E)-2-pentenal, and 2-propylfuran were also important because they were exclusive to the CTRL and ETHY fruits, while 1-hexanol was exclusive to the CTRL and IAA fruits, and 1-pentanol was only found in the CTRL and ETHY+IAA fruits.

After the CTRL fruits ripened, VOC profiles comprised 35 compounds, and 19 of them presented abundances with significant differences ($p < 0.05$) between at least two groups. PLS-DA explained 75.1% (component 1, 49.7%; component 2, 25.4%) of the total variance between samples. As shown in Figure 4F, the first component separated the ETHY from the other groups, while the second component separated the CTRL and IAA from the ETHY+IAA group. HCA reinforced differences visualized by PLS-DA, showing that the IAA and ETHY+IAA groups presented similar VOC profiles, both being more similar to the CTRL than to the ETHY group.

Fatty-acid-derived compounds had an important role in the VOC profiles of Sweet Grape tomato fruits; 3-hexenal, 2-propenal, and (E)-3-hexen-1-ol were affected by ethylene treatment, while the accumulation of propanoyl propanoate and (Z)-3-hexen-1-ol was induced by exogenous auxin. Hexanal was found in higher contents in CTRL and ETHY+IAA fruits, and 3-pentanone and 4-hexen-3-one accumulation was affected by both treatments, although these had not shown higher contents in ETHY+IAA fruits. Regarding amino-acid-derived volatiles, 6-methyl-5-hepten-2-ol and 2-phenylacetaldehyde accumulation was more affected by exogenous ethylene

treatment, and the 2-isobutylthiazole and 2-ethylhexan-1-ol contents were higher in IAA fruits. Additionally, other compounds were important in distinguishing CTRL and treated fruits due to their presence in specific groups. Linalool was found only in CTRL fruits, while 2-methylbut-2-enal, (E)-2-pentenal, and benzaldehyde were exclusive to ETHY and (E,E)-2,4-hexadienal to ETHY+IAA fruits. Citral was found only in CTRL and ETHY fruits, and 1-pentanol and pentanoic acid were found only in ETHY and ETHY+IAA fruits.

The VOC profiles of Sweet Grape tomato fruits were initially similar to those of Micro-Tom, with carbohydrates and isoprenoid-derived compounds showing greater importance in distinguishing CTRL and exogenous hormone-treated fruits. Although VOC profiles change considerably during ripening, isoprenoids continued to be important in distinguishing the samples. Consistent with the Micro-Tom results, fatty-acid-derived compounds were the most important in distinguishing the volatile profiles at the final ripening stage; however, carbohydrate derivatives continued to have different contents and, consequently, played an important role in distinguishing Sweet Grape fruits after exogenous hormone treatments.

Based on these results, the levels of some tomato aromatic volatiles were influenced by exogenous ethylene and auxin treatments in both tomato cultivars. Therefore, both hormones could be considered as important aroma regulators, their interaction also being important in controlling the final tomato aroma. However, the observed changes could result from indirect hormone treatment effects, such as the acceleration and delay of the entire ripening process and, specifically, the color metabolism. To minimize these indirect effects, the experimental design was adjusted in a second experiment with Micro-Tom tomato fruits to compare the same ripening stages.

3.4 Confirmation of direct hormonal effects on tomato ripening stages

The sampling performed in the preview experiments was consistent with the model most commonly used in studies evaluating hormonal regulation during ripening. Samples were collected from experimental groups using the ripening stages of CTRL

fruits as reference. However, this model raises questions regarding the changes observed in the fruit phenotype and genotype, particularly whether the changes observed in the VOC profiles after treatment occurred due to the direct effect of hormonal regulation or to the change in the “natural” ripening process. Thus, a new experiment was performed with Micro-Tom tomato fruits to answer this question. This new sampling directly compared the same maturation stages.

To confirm the effectiveness of the treatments, the ethylene emission and peel color shift were analyzed daily (Figure 5A and 5B). Both parameters showed that ethylene treatment accelerated the tomato ripening, while IAA and ETHY+IAA groups showed the opposite effect. These results corroborate those previously obtained. Compared with the first Micro-Tom experiment, CTRL fruits took on average 5 more days to reach the red stage (19 DAH), while ETHY fruits took 18 DAH and IAA and ETHY+IAA fruits took 21 DAH to fully ripen. The breaker stage was identified on the eighth DAH in CTRL fruits, on the sixth day in ETHY fruits, and on the ninth and tenth days in IAA and ETHY+IAA fruits.

For each experimental group, fruits at the mature green, breaker, and red stages were sampled (on their specific DAH) and their VOC profiles were analyzed after SPME. By adopting the inclusion criteria previously described, a total of 97 VOCs were identified and confirmed, of which 53 had the odoriferous note described in the literature (Table S2). To better visualize and understand the influence of ethylene, auxin, and the ethylene-auxin interaction on the VOC profiles during and after ripening, univariate and multivariate statistical methods were applied equally to each stage.

At the breaker stage (Figure 5C), VOC profiles comprised 46 compounds, and 23 of them presented abundances with significant differences ($p < 0.05$) between at least two groups. PLS-DA explained 57.3% of the total variation between samples. Component 1 (29.6%) separated the CTRL and ETHY groups from the IAA group, while component 2 (27.7%) separated the IAA and ETHY groups from the CTRL and ETHY+IAA groups. HCA reinforced differences visualized by PLS-DA, showing that the CTRL and ETHY+IAA groups presented similar VOC profiles, both being more similar to the IAA group than to the ETHY group.

Apart from methanethiol and 3-methylbutanal, which were inhibited by both exogenous treatments, the VOC profiles of ETHY fruits were characterized by high levels of fatty-acid-derived compounds, including hexanal, (Z)-2-hexenal, (E)-2-hexenal, and 1-octen-3-ol, besides the amino-acid derivatives 3-methyl-1-butanol and

benzaldehyde. The accumulation of ethyl acetate, limonene, 3-methyl-1-pentanol, and nonanal was induced in the IAA fruits, while ETHY+IAA fruits only showed higher levels of o-guaiacol when compared with the other tomato fruits. Other fatty-acid and amino-acid derivatives had important roles in differentiating the VOC profiles. Pentanal and 1-pentanol were found in their lowest contents in IAA and ETHY+IAA fruits, in addition to 6-methyl-5-hepten-2-one, an important carotenoid-derived volatile. Normal accumulation of (E)-3-hexenal, 2-isobutylthiazole, and five benzene compounds (toluene, o-xylene, m-xylene, pseudocumene, and styrene) was observed in in IAA fruits, with lower contents in ETHY and ETHY+IAA fruits. Ethylene and auxin treatment affected accumulation of 2-methylfuran, 1-penten-3-one, and 2,3-pentanedione, but these showed normal levels in ETHY+IAA fruits.

Upon reaching full ripening (Figure 5D), the VOC profiles comprised 49 compounds, and 38 of them presented abundances with significant differences ($p < 0.05$) between at least two groups. PLS-DA explained 62.9% of the total variation between samples. Component 1 (37.9%) separated the CTRL group from the IAA and ETHY groups, while component 2 (25.0%) separated the ETHY+IAA group from the other groups. HCA reinforced differences visualized by PLS-DA, where the CTRL and ETHY+IAA groups presented more similar VOC profiles as did the ETHY and IAA groups.

When compared with treated tomatoes, CTRL fruits were better characterized by higher contents of ethyl acetate, 3-methylbutanal, 1-hexanol, and 2-isobutylthiazole. However, citral, methyl salicylate, geranyl acetone, and pentanoic acid levels were higher in ETHY and IAA fruits. With its characteristic tomato aroma, 2-isobutylthiazole is one of the most important VOCs for the tomato aroma formation (TIEMAN et al., 2017). Treated fruits showed altered contents of several compounds, mainly those derived from fatty acids and amino acids. The accumulation of 2,3-pentanedione, pseudocumene, (E)-4-nonenal, and 1-octen-3-one was more affected by exogenous ethylene treatment, and the content of 3-methyl-1-pentanol was higher in IAA fruits. ETHY+IAA fruits showed higher levels of 1-penten-3-one and hexanal, two important fatty-acid-derived compounds. Benzene compounds derived from amino acids (toluene, o-xylene, m-xylene, styrene, benzaldehyde, and 1-phenylethanone) showed higher accumulation in fruits treated with ethylene and auxin, while aldehyde compounds derived from fatty acids were found in higher contents in ETHY and ETHY+IAA aromatic profiles, including (Z)-3-hexenal, heptanal, octanal, and nonanal.

Additionally, methyl salicylate, 6-methyl-5-hepten-2-one, and 2-ethylfuran were also found in higher contents in ETHY and ETHY+IAA fruits.

Figure 5 – Effects of ethylene, auxin, and both treatments on fruit color, ethylene emission, and VOC contents during Micro-Tom (*Solanum lycopersicum* L.) fruit ripening

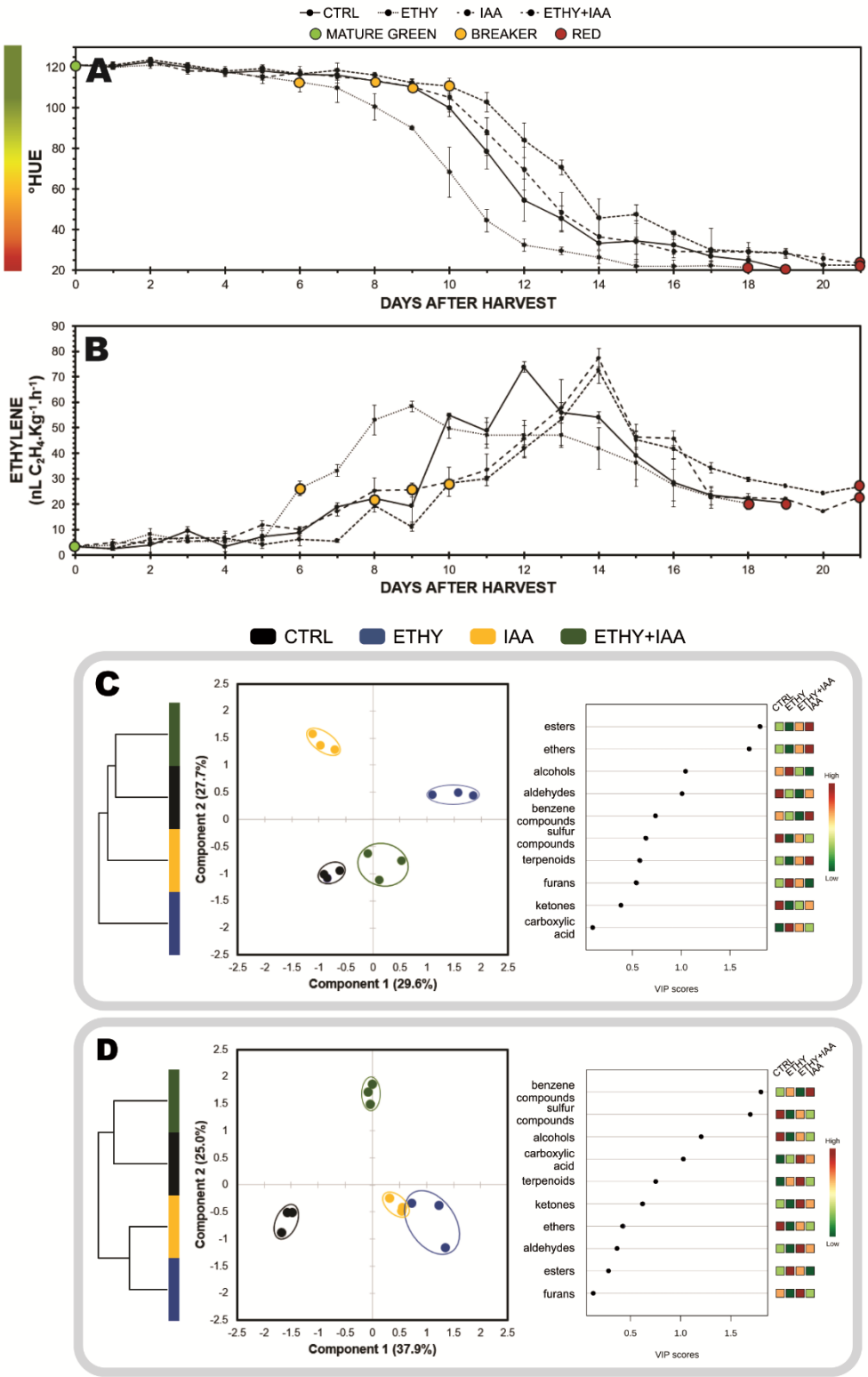

(A) Peel color expressed by hue angle. (B) Ethylene emission. (C and D) Hierarchical clustering, partial least squares discriminant analysis (PLS-DA), and variable importance in projection (VIP) of VOCs

produced at breaker (C) and red (D) stages. CTRL: Control group. ETHY: Ethylene-treated group. IAA: Indole-3-acetic acid-treated group. ETHY+IAA: Group treated with both hormones. Vertical bars represent the standard deviation of three replicates (n = 3).

Generally, the VOC profiles observed during the ripening of Micro-Tom tomato fruits were dissimilar to that identified in the first experiment. The new experimental design allowed confirmation that amino-acid-derived compounds played a more important role in tomato fruit aroma distinction than was previously observed. However, after all the fruits completely ripened, the VOC precursors presented the same impacts on aroma profile distinction as those previously observed. Fatty-acid and amino-acid-derived compounds were the most important in distinguishing between the VOC profiles of CTRL and treated fruits. Carbohydrate derivatives showed no strong differences in their contents and, consequently, did not play an important role in tomato fruit distinction after ethylene and auxin treatments.

The results obtained with this sampling model thus reaffirmed the importance of ethylene and auxin in regulating VOC metabolisms, even as the interaction between ethylene and auxin. It was possible to observe the direct effect of each hormone on fruit metabolism, ruling out possible changes resulting from advancing or delaying the natural ripening process. The VOC profiles were directly affected by each hormone treatment, while fruits treated with both hormones presented VOC profiles more similar to that of untreated fruits. Secondary metabolism changes indicate that ethylene and auxin present opposite regulatory effects and that crosstalk is important in restoring the metabolism of tomato fruits.

4 CONCLUSIONS

Ethylene and auxin play important roles in VOC formation in tomato fruits, regulating this metabolism in different ways, especially in relation to carotenoid and fatty-acid-derived compounds and the enzymes involved in the formation of these metabolites.

The analyses of ethylene and auxin hormones (free and conjugated), as well as genes involved in the regulation of these hormones, contribute to the hypothesis that ethylene regulates auxin conjugation, while this hormone regulates ethylene

perception. This possible mechanism explains why both hormones mainly act antagonistically.

The results also indicate that the observed effects on the VOC metabolism are not peculiar to the Micro-Tom cultivar, as these are also observed in the Sweet Grape cultivar. Additionally, the results suggest that ethylene and auxin directly regulate the metabolic pathways related to VOC formation, since fruits apparently at the same maturation stage have different aromas.

SUPPLEMENTARY MATERIAL

Figure S1 – Effects of ethylene, auxin, and both treatments on the VOC contents in Micro-Tom tomato (*Solanum lycopersicum* L.) fruits

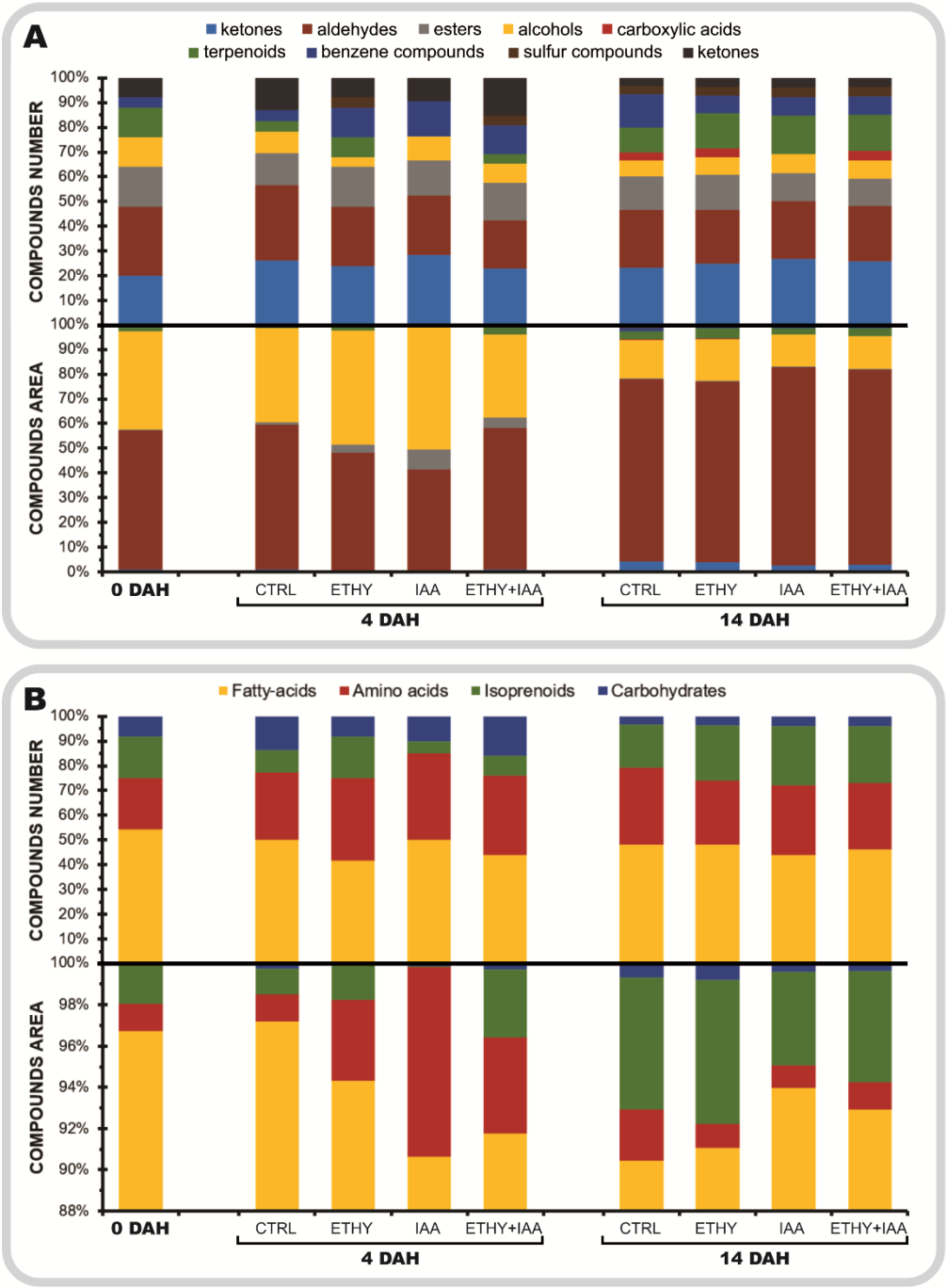

(A) number and relative area of VOC classes at 0 (mature green), 04 (breaker stage), and 14 (red stage) days after harvest. (B) number and relative area of VOCs obtained from the same precursors at 0 (mature green), 04 (breaker stage), and 14 (red stage) days after harvest. CTRL: Control group. ETHY: Ethylene-treated group. IAA: Indole-3-acetic acid-treated group. ETHY+IAA: Group treated with both hormones. Each value is presented as the mean of three replicates (n = 3).

Figure S2 – Effects of ethylene, auxin, and both treatments on the expression of fatty-acid-related genes important to VOC production during Micro-Tom tomato (*Solanum lycopersicum* L.) fruit ripening

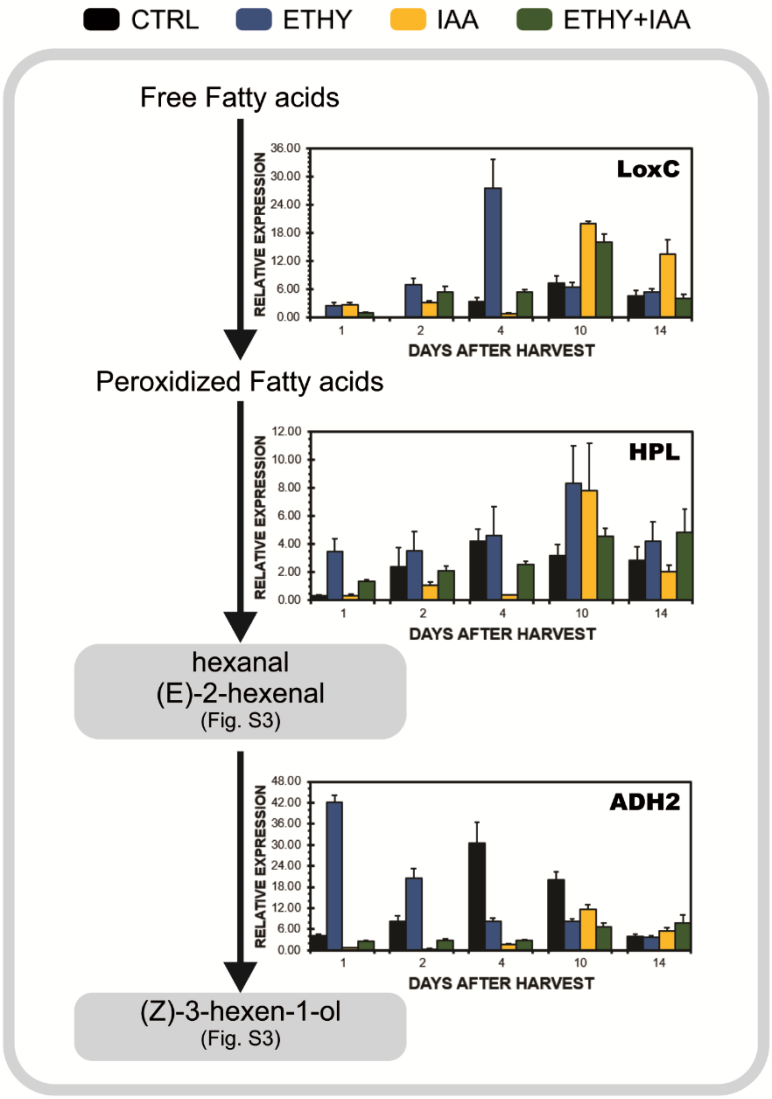

CTRL: Control group. ETHY: Ethylene-treated group. IAA: Indole-3-acetic acid-treated group. ETHY+IAA: Group treated with both hormones. LoxC: Lipoxygenase C. HPL: Hydroperoxide lyase. ADH2: Alcohol dehydrogenase. Vertical bars represent the standard deviation of three replicates (n = 3).

Figure S3 – Relative abundance of significantly changed metabolites in tomato (*Solanum lycopersicum* L. cv. Micro-Tom) fruits after ethylene, auxin, and both treatments throughout ripening

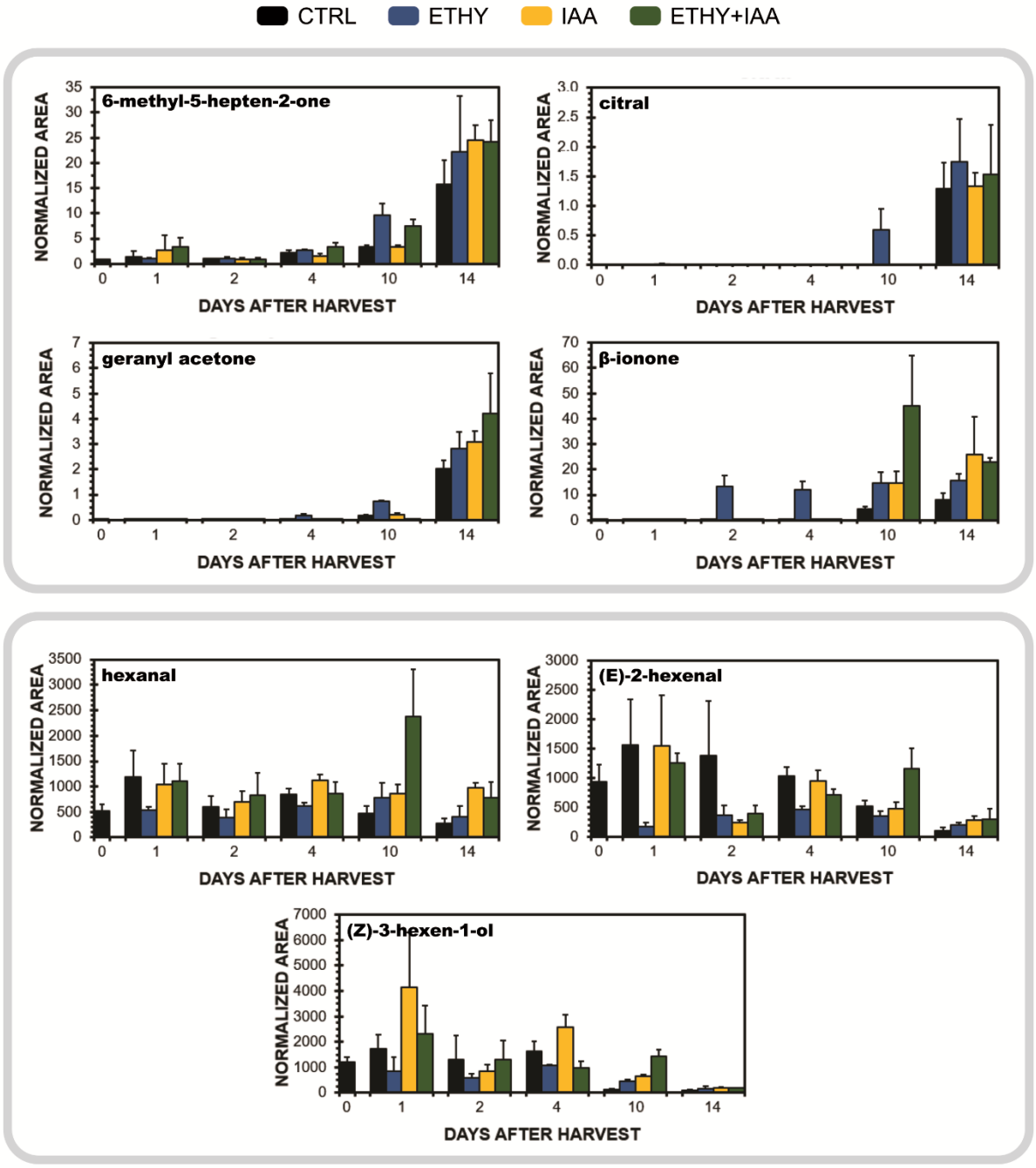

CTRL: Control group. ETHY: Ethylene-treated group. IAA: Indole-3-acetic acid-treated group. ETHY+IAA: Group treated with both hormones. Each value is presented as the mean, and vertical bars represent the standard deviation of three replicates (n = 3).

Figure S4 – Effects of ethylene, auxin, and both treatments on the VOC contents in Sweet Grape tomato (*Solanum lycopersicum* L.) fruits

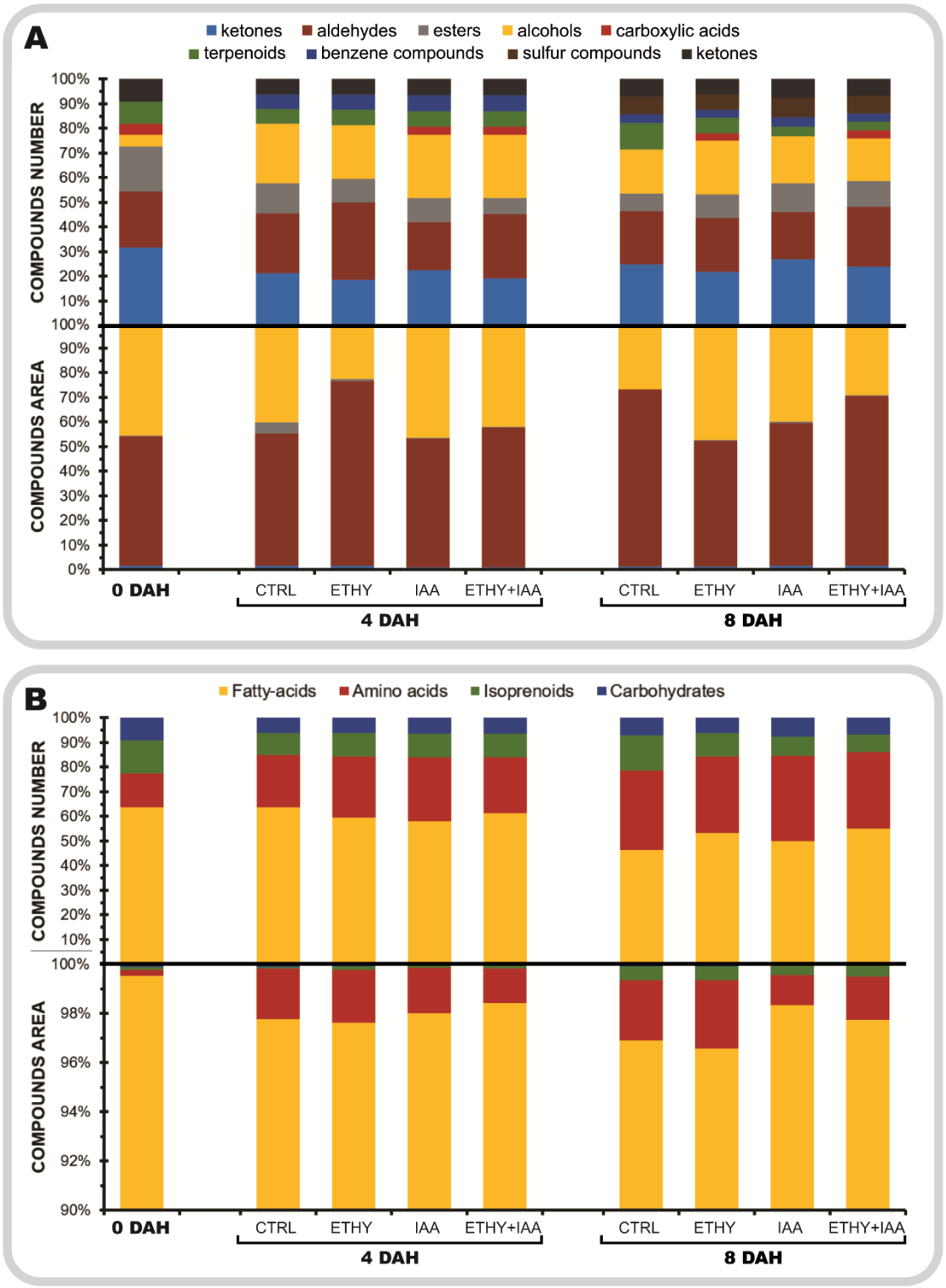

(A) number and relative area of VOC classes at 0 (mature green), 04 (breaker stage), and 14 (red stage) days after harvest. (B) number and relative area of VOCs obtained from the same precursors at 0 (mature green), 04 (breaker stage), and 14 (red stage) days after harvest. CTRL: Control group. ETHY: Ethylene-treated group. IAA: Indole-3-acetic acid-treated group. ETHY+IAA: Group treated with both hormones. Each value is presented as the mean of three replicates (n = 3).

Figure S5 – Comparison of VOC profiles of Micro-Tom and Sweet Grape tomato (*Solanum lycopersicum* L.) cultivars at mature green, breaker, and red stages

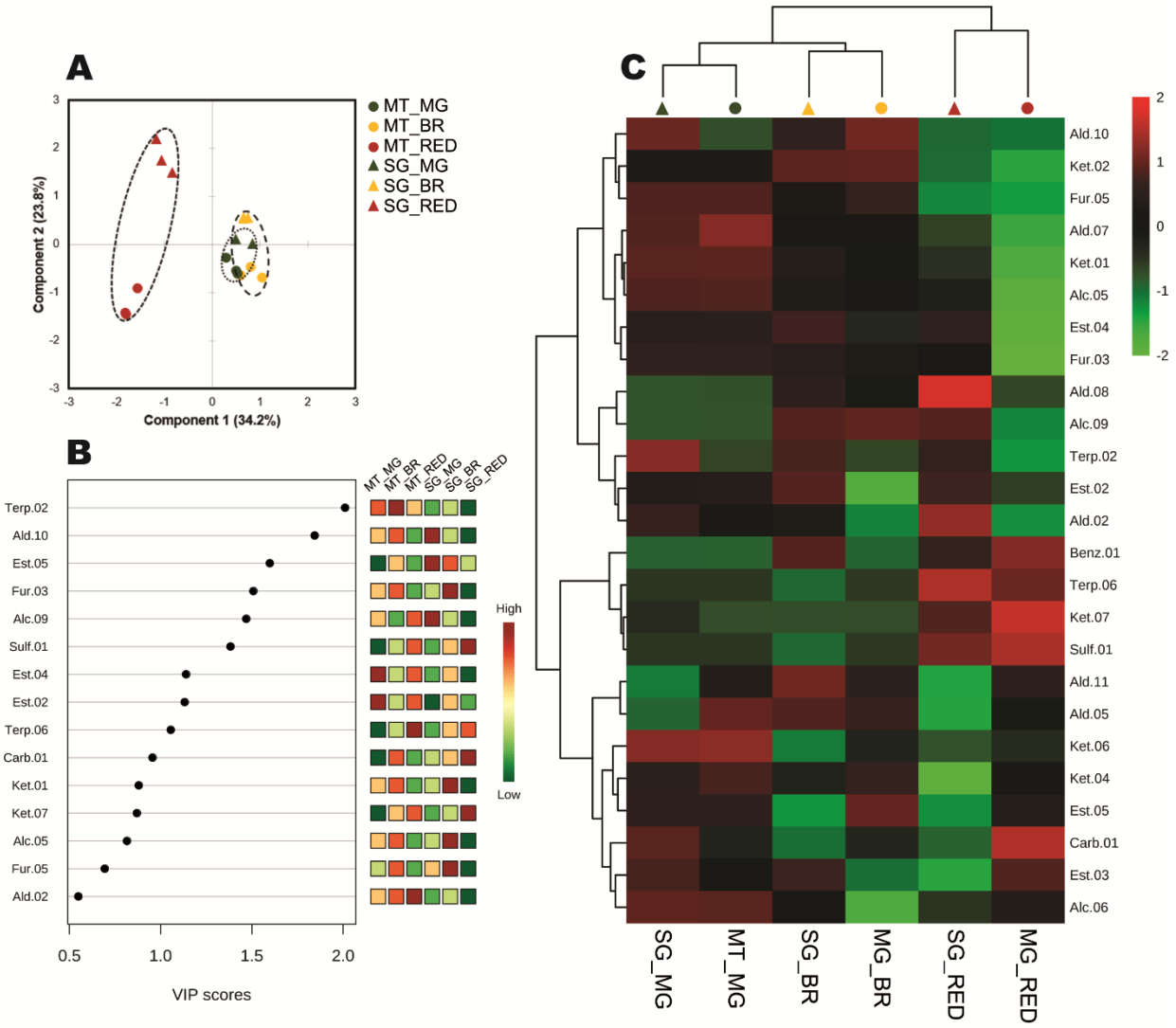

(A) Partial least squares discriminant analysis (PLS-DA). (B) Heatmap with hierarchical clustering. (C) Variable importance in projection (VIP). MG: Mature green stage. BR: Breaker stage. RED: Red stage. Each value is presented as the mean (n = 3).

Table S1 – Quantitative PCR primers of all genes analyzed in the study

GeneID	Gene name	Gene symbol	Primer	Sequence	Reference
Solyc07g025390	Expressed unknown protein	*Expressed*	F	5'-GCTAAGAACGCTGGACCTAATG-3'	Exposito-Rodriguez et al. (2008)
			R	5'-TGGGTGTGCCTTTCTGAATG-3'	
Solyc10g049850	TIP41-like protein	TIP41	F	5'-ATGGAGTTTTTGAGTCTTCTGC-3'	Exposito-Rodriguez et al. (2008)
			R	5'-GCTGCGTTTCTGGCTTAGG-3'	
Solyc08g081540	ACC synthase 1A	ACS1A	F	5'-AAGGTTTATGGAGAAAGTGAGAGG-3'	NA
			R	5'-AAAGGCATCACCAGGATCAG-3'	
Solyc01g095080	ACC synthase 2	ACS2	F	5'-GGTTAGGTAAAAGGCACAAACAT-3'	Rugkong et al. (2011)
			R	5'-GAATAGGTGACGAAAGTGGTGAC-3'	
Solyc05g050010	ACC synthase 4	ACS4	F	5'-GATTTGCGGTCATTGTTGAAAG-3'	Rugkong et al. (2011)
			R	5'-GCCTGGGCGAATCTAGTTTATTT-3'	
Solyc08g008100	ACC synthase 6	ACS6	F	5'-CTCCTATGGTCCAAGCAAGG-3'	Liu et al. (2013)
			R	5'-CGACATGTCCATAATTGAACG-3'	
Solyc06g073580	ACC oxidase 1	ACO1	F	5'-GCCAAAGAGCCAAGATTTGA-3'	Liu et al. (2013)
			R	5'-TTTTTAATTGAATTGGGATCTAAGC-3'	
Solyc02g081190	ACC oxidase 4	ACO4	F	5'-GGAGCCTAGGTTTGAAGCAA-3'	Liu et al. (2013)
			R	5'-AAACAAATTCCCCCTTGAAAA-3'	
Solyc09g075440	Ethylene receptor 3	ETR3	F	5'-AGGGAACCACTGTCACGTTTG-3'	Kevany et al. (2008)
			R	5'-TCTGGGAGGCATAGGTAGCA-3'	
Solyc06g053710	Ethylene receptor 4	ETR4	F	5'-GTAATCCCAAATCCAGAAGGTTT-3'	Kevany et al. (2008)
			R	5'-CAATTGATGGCCGCAGTTG-3'	

Table S1 – (continued)

GeneID	Gene name	Gene symbol	Primer	Sequence	Reference
Solyc09g089610	Ethylene receptor 6	ETR6	F	5’-ATTCCAAAGGCAGCCGTTAA-3’	Kevany et al. (2008)
			R	5’-GATGTGGATATGTGGGATTAGAA-3’	
Solyc06g063070	Ethylene response factor E1	ERF.E1	F	5'-GTTCCTCTCAACCCCAAACG-3'	Liu et al. (2016)
			R	5'-TTCATCTGCTCACCACCTGTAGA-3'	
Solyc09g075420	Ethylene response factor E2	ERF.E2	F	5'-ACTTCGTGAGGAAACCCTGAAC-3'	Liu et al. (2016)
			R	5'-GTTACTAATATAAGTCATGTTGGGCTGAA-3'	
Solyc01g065980	Ethylene response factor E4	ERF.E4	F	5'-AGGCCAAGGAAGAACAAGTACAGA-3'	Liu et al. (2016)
			R	5'-CCAAGCCAAACGCGTACAC-3'	
Solyc01g095580	Gretchen hagen protein 3.1	GH3.1	F	5’-AGACAATGAGGGCAATGCAAAC-3’	NA
			R	5’-CAAGAGATGGCAGTACAAAGATTGG-3’	
Solyc01g107390	Gretchen hagen protein 3.2	GH3.2	F	5'-CAATGTTGTTTAGCGATGGAAGAG-3'	NA
			R	5'-AATGGACCAATTGAGTTACAAGCA-3'	
Solyc02g064830	Gretchen hagen protein 3.3	GH3.3	F	5'-TTCATCTCCTTTTGATCCCTCT-3'	NA
			R	5'-CATTTTGTCGGATAACATCAACA-3'	
Solyc01g087250	Carotenoid cleavage dioxygenase 1A	CCD1A	F	5'-ATGGGGAGAAAAGAAGATGATGGA-3'	Ilg et al. (2014)
			R	5'-ATTCAAGAACAAGCCAAACTGTGA-3'	
Solyc01g087260	Carotenoid cleavage dioxygenase 1B	CCD1B	F	5'-ATGGGGATGAATGAAGAAGATGGA-3'	Ilg et al. (2014)
			R	5'-ATTCAGGAGCAAGCCAAAATGTGA-3'	
Solyc01g006540	Lipoxygenase C	LoxC	F	5'-GAGTTTGGAGTTCCAGGAGCAT-3'	Qin et al. (2012)
			R	5'-CATCTTCGAGTGTGAGTGACTTGA-3'	

Table S1 – (continued)

GeneID	Gene name	Gene symbol	Primer	Sequence	Reference
Solyc07g049690	Hydroperoxide llyase	HPL	F	5'-GTCCACCAGTACCAAGTCAATATGC-3'	Bai et al. (2011)
			R	5'-GCTCCCCTTTCTTGATTTCGTAA-3'	
Solyc06g059740	Alcohol dehydrogenase-2	ADH2	F	5'-TGAGTACACCGTGGTTCATGTTG-3'	Qin et al. (2012)
			R	5'-TCCAAGGCCTGTCGAAATTC-3'	

NA: not applicable. PCR primers were designed in accordance this study specificity.

Table S2 – Identified volatile organic compounds in tomato (*Solanum lycopersicum* L. cv. Micro-Tom) fruits after ethylene, auxin, and both treatments at breaker and red stages. Data presented are *p* values for mean comparisons between treated and control fruits (n = 3)

ID[a]	Volatile organic compound	RI[b]	Functional group	Odor type	Micro-Tom					
					Breaker			Red		
					ETHY	IAA	ETHY+IAA	ETHY	IAA	ETHY+IAA
Amino acids										
Sulf.01	Methanethiol	<900	sulfur compound	sulfurous	0.40	0.31	0.39	0.15	0.17	0.46
Ald.02	3-methylbutanal	<900	aldehyde	aldehydic	**0.05**	0.10	0.11	**0.04**	0.13	**0.05**
Ket.03	2-butyl acetate	969	ketone	fruity	**0.03**	0.30	0.26	**0.01**	**0.01**	**0.02**
Benz.01	Toluene	1041	benzenic compound	sweet	0.26	0.76	0.26	0.41	**0.02**	0.41
Ket.06	Artemesia	1080	ketone	herbal	**0.05**	**0.01**	0.72	0.06	0.33	0.27
Benz.02	o-xylene	1114	benzenic compound	geranium	**0.02**	0.74	0.61	1.00	0.20	**0.04**
Benz.03	m-xylene	1131	benzenic compound	plastic	**0.01**	0.67	0.94	0.72	0.34	0.07
Alc.01	3-methyl-1-butanol	1213	alcohol	fermented	**0.05**	0.09	**0.05**	0.17	0.24	**0.01**
Benz.04	Pseudocumene	1250	benzenic compound	plastic	**0.04**	0.95	**0.00**	0.10	0.17	0.16
Benz.05	Styrene	1250	benzenic compound	balsamic	**0.03**	**0.04**	0.63	0.20	0.12	0.31
Alc.03	3-methyl-1-pentanol	1324	alcohol	fruity	**0.03**	0.15	0.18	0.06	**0.02**	0.13
Sulf.02	2-isobutylthiazole*****	1391	sulfur compound	tomato	**0.00**	**0.01**	**0.02**	**0.00**	**0.01**	**0.03**
Benz.06	Benzaldehyde	1506	benzenic compound	fruity	**0.05**	0.09	0.26	0.09	**0.03**	0.06
Benz.07	1-phenylethanone	1632	benzenic compound	floral	0.50	0.13	0.83	**0.05**	**0.00**	0.15
Carb.03	3-methylbutanoic acid	1657	carboxilic acid	cheesy	0.18	0.58	0.97	0.12	0.65	0.08
Est.04	Methyl salicylate*****	1760	ester	minty	0.18	0.18	0.17	0.13	0.60	0.45
Alc.06	Phenylethyl alcohol*****	1888	alcohol	floral	**0.03**	**0.00**	0.26	0.22	0.18	0.14
Carbohydrates										
Fur.01	2-methylfuran	<900	furan	chocolate	0.33	**0.10**	0.41	0.29	0.13	0.95
Fur.02	2-ethylfuran	1400	furan	sweet	0.33	0.97	0.80	0.66	0.16	0.35
Fur.03	2-propylfuran	1442	furan	fruity	**0.03**	0.30	0.26	0.06	0.42	0.13
Fatty acids										
Est.01	Ethyl ether	<900	ether	ethereal	0.18	0.33	0.35	0.15	0.22	0.32
Ald.01	Propanal	<900	aldehyde	ethereal	**0.00**	0.96	**0.03**	0.70	0.79	0.16
Ket.01	Propan-2-one	<900	ketone	solvent	0.29	0.99	0.76	**0.03**	0.71	0.29
Ket.02	Methyl acetate	<900	ketone	ethereal	**0.05**	0.61	0.76	**0.04**	**0.04**	0.08

Table S2 – (continued)

ID[a]	Volatile compound	RI[b]	Functional group	Odor type	Micro-Tom					
					Breaker			Red		
					ETHY	IAA	ETHY+IAA	ETHY	IAA	ETHY+IAA
Fatty acids										
Est.02	Ethyl acetate	<900	ester	fruity	0.24	0.58	0.67	0.34	0.34	0.39
Ald.03	Pentanal*	958	aldehyde	fermented	**0.03**	0.16	0.37	0.27	0.37	**0.01**
Ket.04	1-penten-3-one	1027	ketone	spicy	0.11	0.06	0.89	0.15	0.55	0.68
Ket.05	2,3-pentanedione	1044	ketone	buttery	**0.01**	**0.01**	0.82	0.55	**0.01**	0.39
Carb.01	Methyl pentanoate	1072	carboxilic acid	fruity	**0.03**	0.30	0.08	0.06	0.42	0.13
Ald.04	Hexanal*	1084	aldehyde	green	0.10	0.79	0.49	0.14	0.28	0.50
Ald.05	(E)-3-hexenal	1120	aldehyde	green	**0.03**	0.50	0.09	0.72	0.25	0.38
Ald.06	(Z)-3-hexenal*	1126	aldehyde	green	**0.02**	0.14	0.13	0.78	0.30	0.64
Ket.07	4-hexen-3-one	1152	ketone	acidic	0.42	0.58	0.89	0.06	0.42	0.13
Est.03	Propanoyl propanoate	1173	ester	ethereal	**0.03**	0.30	0.26	**0.03**	0.42	**0.01**
Ald.07	Heptanal	1185	aldehyde	green	0.39	0.18	0.22	0.77	0.74	0.41
Ald.08	(Z)-2-hexenal	1200	aldehyde	green	0.15	0.74	0.73	**0.05**	0.19	0.13
Ald.09	(E)-2-hexenal*	1219	aldehyde	green	0.65	0.41	0.43	0.24	0.70	0.34
Alc.02	1-pentanol*	1246	alcohol	fermented	**0.03**	0.16	0.42	0.08	0.85	0.62
Ald.10	Octanal	1268	aldehyde	aldehydic	0.08	0.82	0.19	**0.03**	0.47	0.32
Alc.04	1-hexanol*	1348	alcohol	herbal	**0.02**	0.30	0.26	**0.02**	**0.03**	**0.05**
Ald.11	Nonanal	1391	aldehyde	aldehydic	**0.04**	**0.01**	0.06	**0.01**	**0.01**	**0.04**
Ald.12	(E)-4-nonenal	1416	aldehyde	fruity	**0.03**	0.30	0.26	**0.03**	**0.01**	0.17
Ket.09	1-octen-3-one	1421	ketone	earthy	0.21	**0.02**	0.33	0.94	0.86	0.06
Ald.13	(E)-2-octenal*	1423	aldehyde	fatty	**0.00**	0.30	0.11	0.11	**0.00**	**0.03**
Carb.02	Acetic acid	1439	carboxilic acid	acidic	0.08	0.51	0.57	**0.00**	**0.03**	**0.02**
Alc.05	1-octen-3-ol	1447	alcohol	earthy	**0.01**	0.28	0.46	**0.01**	**0.01**	0.29
Carb.04	Pentanoic acid	1889	carboxilic acid	cheesy	0.29	0.13	**0.03**	0.24	0.39	0.57
Isoprenoids										
Terp.01	α-pinene	1005	terpenoid	herbal	**0.03**	0.30	0.26	0.06	0.42	0.13
Terp.02	Limonene	1161	terpenoid	citrus	**0.01**	0.19	0.53	**0.02**	0.42	0.13
Ket.08	6-methyl-5-hepten-2-one*	1333	ketone	citrus	0.16	0.10	0.66	0.22	0.55	0.03
Terp.03	o-guaiacol*	1597	terpenoid	woody	0.12	0.28	**0.04**	0.06	0.42	0.07

Table S2 **–** (continued)

ID[a]	Volatile compound	RI[b]	Functional group	Odor type	Micro-Tom					
					Breaker			Red		
					ETHY	IAA	ETHY+IAA	ETHY	IAA	ETHY+IAA
Isoprenoids										
Terp.04	Citral*****	1724	terpenoid	citrus	**0.03**	0.30	0.26	**0.05**	0.33	**0.02**
Ket.10	Geranyl acetone*****	1850	ketone	floral	**0.03**	0.30	0.26	0.44	0.18	0.15

[a]ID: Volatile compound identification.

[b]RI: Retetion index. relative to n-alkanes (C10-C30) on the SupelcoWax capillary column.

ETHY: *p* value for T-test between control and ethylene treated fruits.

IAA: *p* value for T-test between control and auxin treated fruits.

ETHY+IAA: *p* value for T-test between control and ethylene-auxin treated fruits.

*****Compound confirmed by mass spectrum comparison with external standard.

Values in bold letters show significant differences ($p < 0.05$) between the control and treated fruits.

CHAPTER 2

VOLATILE COMPOUNDS BIOSYNTHESIS: METABOLIC RESPONSES TO ETHYLENE-AUXIN CROSSTALK DURING TOMATO (*SOLANUM LYCOPERSICUM* L.) FRUIT RIPENING

Eric de Castro Tobaruela[1,2], Isabel Louro Massaretto[1,2], Silvia Leticia Rivero Meza[1,2], Grazieli Benedetti Pascoal[2,3], Luciano Freschi[4], Eduardo Purgatto[1,2,*]

[1]Department of Food and Experimental Nutrition, Faculty of Pharmaceutical Sciences, University of São Paulo (USP), São Paulo, SP, Brazil; [2]Food Research Center (FoRC), São Paulo, SP, Brazil; [3]Faculty of Medicine, Federal University of Uberlândia (UFU), Uberlândia, MG, Brazil; [4]Department of Botanic, Institute of Bioscience, University of São Paulo (USP), São Paulo, SP, Brazil.

Author contributions:

LF provided and generated the plant material. ECT conducted experiments and analyzed data. ILM, SLRM and GBP contributed during metabolomic experiments. ECT wrote the paper, prepared figures and tables. ILM, SLRM and GBP reviewed drafts of the paper. EP designed experiments, supervised and reviewed drafts of the paper.

Submitted to Metabolomics (ISSN 1573-3890).

ABSTRACT

Introduction Tomato fruit ripening is a genetically coordinated process regulated by phytohormones such as ethylene and auxin. Biochemical changes in color, texture, flavor, and aroma render the ripe fruit attractive to seed-dispersing organisms and human consumers. Due to primary and secondary metabolism regulation, the biosynthesis of volatile organic compounds (VOCs) also appears to be regulated by both hormones; however, the importance of ethylene-auxin crosstalk in this regulatory process is unclear.

Objectives This study evaluates metabolic responses to ethylene-auxin crosstalk during tomato (*Solanum lycopersicum* L.) fruit ripening, with an emphasis on VOC metabolism.

Methods Tomato fruits cv. Micro-Tom at the mature green stage are randomly separated into four groups according to hormone treatments: CTRL (without treatment); ETHY (ethylene treatment); IAA (indole-3-acetic acid treatment); and ETHY+IAA (both hormone treatments). The color shift and ethylene emission are determined daily. Polar and non-polar metabolic profiles are separately obtained by GC-MS after metabolite extraction and derivatization.

Results Polar (79) and non-polar metabolites (47) are measured by GC-MS; the levels of some of these are significantly changed by hormone treatments. Enrichment analysis evidences metabolic pathways (39–48) that are significantly influenced by ethylene and auxin treatments, including secondary metabolisms, such as terpene and sugar derivative biosynthesis. Primary metabolites (8) and VOCs (20) that are important to the tomato fruit aroma are correlated by pathway analysis.

Conclusion This study describes how ethylene and auxin change primary and secondary metabolic profiles and, consequently, the tomato fruit aroma.

Keywords

Climacteric fruit. Carotenoids. Aroma compounds. Metabolomic. Lipidomic. GC-MS

1 INTRODUCTION

Fruit ripening is a genetically coordinated process accompanied by significant biochemical changes in color, texture, flavor, aroma, and nutritional content that render the ripe fruit attractive to seed-dispersing organisms (SEYMOUR et al., 1993; GOFF; KLEE, 2006). These changes coincide with seed maturation in the final phase of fruit development and are precisely regulated by plant hormones such as ethylene and auxin (KUMAR; KHURANA; SHARMA, 2014; PESARESI et al., 2014).

Tomato (*Solanum lycopersicum* L.) fruits have been extensively studied as a reference for fleshy fruit development and a model plant for studying climacteric fruit ripening, in which ethylene is the most important regulator (GIOVANNONI, 2007; GAPPER; MCQUINN; GIOVANNONI, 2013). Despite the emphasis on the role of ethylene and its importance in climacteric fruit ripening, recent reports have indicated that the coordinated action of ethylene and auxin may be crucial in fruit ripening (SEYMOUR et al., 2013; SU et al., 2015).

Ethylene is biosynthesized from S-adenosyl-methionine (LIU et al., 2015), while indole-3-acetic acid, the main auxin in plants, is synthesized through both tryptophan-dependent and independent pathways (KORASICK; ENDERS; STRADER, 2013). Mechanisms underlying ethylene regulation have been extensively studied, while even the exact role of auxin in ripening control remains unclear. Regarding ethylene-auxin crosstalk in fruit ripening, recent studies have elucidated antagonistic effects of the two hormones, such as auxin acting as a ripening repressor and thereby opposing the known role of ethylene as a ripening inducer in tomato fruit (KUMAR; KHURANA; SHARMA, 2014; SU et al., 2015; LI et al., 2016). Interestingly, studies have also indicated that auxin is crucial for triggering ripening and acting on the transition between systems I and II of ethylene production, suggesting that it may not inhibit fruit ripening (ROSS et al., 2011; MCATEE et al., 2013; SEYMOUR et al., 2013).

During ripening, chlorophyll degradation, lycopene accumulation, and other changes in primary and secondary metabolites are known to be controlled by regulatory mechanisms involving ethylene and auxin, although these mechanisms are not fully understood (KLEE; GIOVANNONI, 2011; SU et al., 2015). Due to their regulation of primary and secondary metabolisms, the biosynthesis of volatile organic compounds (VOCs) also appears to be regulated by both hormones.

Aroma compounds have been extensively studied, and approximately 400 of them have been identified in tomato fruit (BALDWIN et al., 2000). Among these, fewer than 10% are produced in sufficient quantities to be perceived by humans (BALDWIN et al., 2000; MATHIEU et al., 2009), and these are crucial in conferring the characteristic tomato aroma (DU et al., 2015). The other compounds may provide background odors that impact the overall aroma quality (TANDON et al., 2001; KLEE; GIOVANNONI, 2011). Another function of aroma volatiles is to enhance the main flavor components, such as soluble sugars and organic acids (KLEE; TIEMAN, 2013; TIEMAN et al., 2017). These aroma compounds are derived from diverse precursors, including amino acids, fatty acids, and carotenoids (KLEE; TIEMAN, 2013; BAUCHET et al., 2017). Tieman et al. (2017) and Klee and Tieman (2018) described the principal contributors to the ripe tomato flavor that positively correlates with consumer preferences: 1-nitro-3-methylbutane; 1-penten-3-one; 1-octen-3-one; 2-isobutylthiazole; 2-methylbutanol; 3-methylbutanol; 2-phenylethanol; 3-pentanone; 6-methyl-5-hepten-2-ol; 6-methyl-5-hepten-2-one; benzaldehyde; heptaldehyde; nonyl aldehyde; phenylacetaldehyde; β-damascenone; citral; furaneol; geranyl acetone; guaiacol; β-ionone; isobutyl acetate; isovaleraldehyde; isovaleronitrile; isovaleric acid; methional; methyl salicylate; 1-pentanal; 1-pentanol; (E)-2-pentenal; 1-hexanal; 1-hexanol; (E)-3-hexen-1-ol; (Z)-3-hexen-1-ol; (E)-2-hexenal; (Z)-3-hexenal; (E)-2-heptenal; (E,E)-2,4-decadienal; and (Z)-4-decenal. Changes in the VOC profiles occur during fruit ripening in response to hormonal regulation and several intrinsic and extrinsic factors. This process promotes changes in the compound ratios as well as their interactions, resulting in changes in the tomato aroma (KLEE; GIOVANNONI, 2011; WANG et al., 2015). In this context, the integrated study of metabolites produced by the primary and secondary metabolisms and the VOCs emitted by the fruit during ripening is an interesting strategy to deepen existing knowledge and improve understanding of the role of these hormones in aroma formation, which is considered one of the most important fruit quality parameters. Metabolomic approaches to fruit ripening studies allow visualization of the internal state of the fruit, and the large amount of data generated enables a broader and more detailed understanding of the regulation involved in the ripening process.

Considering that identifying and understanding how hormone treatments affect metabolic pathways is key to knowledge of hormonal regulation, this study evaluates the metabolic responses to ethylene and auxin crosstalk during tomato (*Solanum*

lycopersicum L.) fruit ripening, with an emphasis on VOC metabolism. This study highlights the important role that ethylene-auxin crosstalk plays in regulating tomato aroma.

2 MATERIALS AND METHODS

2.1 Plant materials and hormone treatments

Tomato plants (*Solanum lycopersicum* cv. Micro-Tom) were grown under standard greenhouse conditions. Two biological replicates (400 fruits/replicate) were harvested in December 2016 at the mature green stage (approximately 40 days after anthesis), while two other biological replicates were harvested in April 2017 at the same stage. Each biological replicate comprised at least 100 plants. Fruits were randomly separated into four groups according to hormone treatments: CTRL (without treatment); ETHY (ethylene treatment); IAA (indole-3-acetic acid treatment); and ETHY+IAA (both hormone treatments). Each group comprised at least 100 fruits. During the experiments, fruits were left to ripen spontaneously in a 323 L chamber at 22°C for a 16-hour-day/8-hour-night cycle at 80% relative humidity. Ethylene treatments were performed using a gaseous hormone at 10 $\mu L.L^{-1}$ for 12 hours. The indole-3-acetic acid solutions were prepared at 100 µM in 10 mM 2-(N-morpholino)ethanesulfonic acid buffer at pH 5.6 with 3% sorbitol and were injected through the calyx end as described by Su et al. (2015). Fruits from the IAA group received indole-3-acetic acid solution, while fruits from the ETHY+IAA group were exposed to gaseous ethylene before infiltration with indole-3-acetic acid solution. To maintain a consistent injection method across all samples, fruits from the ETHY and CTRL groups were injected only with buffer solution. During the experiment, ethylene emission and surface color were evaluated daily as ripening parameters. For further analysis, at least five fruits from each experimental group were collected, considering the ripening stages (breaker and red) of the CTRL group as reference. Samples were then frozen in liquid nitrogen and stored at −80°C.

2.2 Ripening characterization

2.2.1 Ethylene emission

Five intact tomato fruits from each experimental group were placed in airtight glass containers and left at 25°C. After 1 h, five 1 mL samples were collected from the headspace with gas-tight syringes through a rubber septum. Ethylene emission was analyzed by gas chromatography with a flame ionization detector (GC-FID) (Agilent Technologies, HP-6890). A HP-Plot Q column (30 m × 0.53 mm × 40 µm) was used. The injector and detector temperatures were both set at 250°C, and the oven temperature was set at 30°C. The injections were performed in pulsed splitless mode. Helium was used as carrier gas (1 $mL.min^{-1}$).

2.2.2 Fruit surface color

The fruit surface color was assessed using a HunterLab ColorQuest XE instrument (Hunter Associates Laboratories) in terms of L, a, b space, and the data were processed to obtain the °hue values as described by Fabi et al. (2007). Three measures were taken at the equators of five fruits (from each experimental group), and average values were calculated.

2.3 Metabolite profile analysis

Polar and non-polar metabolic profiles were separately obtained by GC-MS analysis (as described below) of samples comprising five fruits for each biological replicate. Polar metabolites were extracted and derivatized as described by Lisec et al. (2006), while non-polar metabolites were prepared according to the Bligh-Dyer protocol (BLIGH; DYER, 1959) and derivatized as described by Ichihara et al. (2010) and Fiehn et al. (2010). Trimethylsilyl (TMS) derivatives were analyzed by GC-MS

according to the protocol described by Kind et al. (2009), including periodic analysis for experimental quality control.

2.3.1 Polar metabolic profile

For metabolite extraction, 100 mg of ground frozen tomato fruits was mixed with 1,400 µL of 100% distilled methanol (pre-cooled at −20°C), vortexed for 10 s, and then added to 60 µL of ribitol (200 µg.mL^{-1}, internal quantitative standard). The samples were briefly vortexed, incubated in a thermomixer at 950 rpm for 10 min at 70°C, centrifuged at 11,000 g for 10 min, and the supernatant was collected. Next, 750 µL of chloroform (pre-cooled at −20°C) and 1,500 µL of Milli-Q water were added to the upper phase, vigorously mixed, and centrifuged for 15 min at 2,200 g. After phase separation, 150 µL of the upper hydrophilic phases was collected and dried under vacuum. Samples were derivatized by adding 40 µL of 20 mg.mL^{-1} methoxyamine hydrochloride (Sigma–Aldrich Chemical Co., St. Louis, MO, USA) dissolved in pyridine followed by incubation for 2 h in an orbital shaker at 1,000 rpm and 37°C. Next, 70 µL of N-methyl-N-(trimethylsilyl) tri-fluoroacetamide (MSTFA) was added to each sample followed by incubation for 30 min in an orbital shaker at 1,000 rpm and 37°C. The derivatized samples were then transferred to glass vials and subjected to GC-MS for no more than 24 h. A pool of the following polar metabolite standards (1 mg.mL^{-1}, Sigma–Aldrich) was prepared and derivatized for use in identifying the compounds by mass spectral comparison: D-glucose; D-fructose; maltose; sucrose; D-galactose; myo-inositol; citric acid; L-alanine; L-serine; L-proline; L-aspartate; and L-glutamate (KIND et al., 2009).

2.3.2 Non-polar metabolic profile

Briefly, 1,000 mg ground frozen tomato fruits was mixed with 1,250 µL of chloroform and 2,500 µL of methanol, vortexed for 10 s, and then added to 20 µL of n-tridecane (800 µg.mL^{-1}, internal quantitative standard). The mixture was vortexed for 10 s, incubated on ice for 30 min, added to 1,250 µL of 1.5% sodium sulfate and

another 1,250 µL of chloroform, and incubated on ice for another 5 min. The solvent phases were separated by centrifugation at 1,000 rpm for 5 min at 4°C. The upper polar phase was removed with a pipette and dried with nitrogen gas. Samples were reconstituted with 1,000 µL of hexane, 200 µL of toluene, 1,500 µL of methanol, and 300 µL of 8% hydrochloric acid, vortexed for 10 s, and then incubated at 100°C for 1.5 h. After cooling at room temperature, samples were added to 1,000 µL of hexane and Milli-Q water, and vortexed. The hexane phases were then collected, dried with nitrogen gas, reconstituted with hexane (80 µL) and pyridine (20 µL), and derivatized by adding 40 µL of MSTFA. The derivatized samples were then transferred to glass vials and subjected to GC-MS for no more than 24 h. A pool of the following fatty acid methyl ester (FAME) standards (Sigma–Aldrich) was prepared and derivatized for use in confirming the compounds identification by mass spectral comparison: methyl laurate (C12:0, 0.8 $mg.mL^{-1}$); methyl tetradecanoate (C14:0, 0.8 $mg.mL^{-1}$); methyl palmitate (C16:0, 0.8 $mg.mL^{-1}$); methyl octadecanoate (C18:0, 0.4 $mg.mL^{-1}$); methyl arachidate (C20:0, 0.4 $mg.mL^{-1}$); methyl docosanoate (C22:0, 0.4 $mg.mL^{-1}$); methyl lignocerate (C24:0, 0.4 $mg.mL^{-1}$); methyl linoleate (C18:2, 0.4 $mg.mL^{-1}$); (Z)-9-oleyl methyl ester (C18:1, 0.4 $mg.mL^{-1}$); methyl linolenate (C18:3, 0.4 $mg.mL^{-1}$); and methyl palmitoleate (C16:1, 0.8 $mg.mL^{-1}$) (KIND et al., 2009).

2.3.3 GC-MS analysis of derivatized metabolites

Derivatized samples were immediately analyzed using an Agilent GC-MS 5977 instrument (Agilent Technologies, CA, USA) under optimized conditions based on those described by Kind et al. (2009). A HP5ms column (30 m × 0.25 m × 0.25 µm) was used. Helium was used as carrier gas with an inlet flow rate (constant mode) of 2 $mL.min^{-1}$. In total, 1 µL of TMS derivatives was injected into an injector at 230°C in splitless mode. The oven temperature program for the GC analysis of derivatized compounds was as follows: initial temperature 80°C, held for 2 min; heated at 15°C.min^{-1} to 330°C, held for 6 min. The electron impact ionization mass spectrometer was operated as follows: ionization voltage, 70 eV; ion source temperature, 250°C; injection port temperature, 250°C; scan mode, mass range 70–600 m/z at 20 $scans.s^{-1}$. Data acquisition, deconvolution, and analysis were conducted using MassHunter

software (Agilent Technologies), and the NIST mass spectral library (NIST, 2011, Gaithersburg, MD, USA) was used for retention index (RI) comparison and data validation. Some of the identified metabolites were also confirmed by mass spectral comparison with the authentic external standards previously described. Metabolites were normalized to ribitol as an internal standard and presented as relative areas.

2.4 Carotenoids

Carotenoids were extracted in triplicate according to the methods described by Sérino et al. (2009). Briefly, a liquid-liquid extraction was performed with 100 µL of saturated NaCl solution, 200 µL of dichloromethane, and 500 µL of hexane:ethyl ether (1:1, v:v), and further centrifugation was performed at 13,000 rpm for 5 min at 4°C. The resulting supernatant was collected, and the procedure was repeated three times until the residue no longer exhibited the characteristic carotenoid color. The total extract was dried under vacuum and resuspended using ethyl acetate. Quantitative determination of carotenoids was performed using an Infinity 1260 high performance liquid chromatography (HPLC) system (Agilent Technologies) coupled to a diode array detector (DAD) equipped with a YMC Carotenoid HPLC C30 (5 µm × 250 mm × 4.6 mm) column under optimized conditions as described by Souza et al. (2020). Peak identification was performed by comparing the retention time and absorption spectrum with those of authentic external standards. Lycopene, β-carotene, and lutein (Sigma–Aldrich) were used as reference standards.

2.5 Statistical analysis

The results are presented as mean ± standard deviation. One-way ANOVA with Tukey's *post hoc* test was performed to determine the effects of hormone treatment on metabolic and carotenoid profiles. Statistical significance was indicated by $p < 0.05$. Heatmap, hierarchical clustering, and partial least squares discriminant analysis (PLS-DA) were performed on peak areas after normalization by an internal standard area (for metabolites) or median (for carotenoids), and the resulting data were log-

transformed and Pareto-scaled using MetaboAnalyst 4.0 (CHONG; WISHART; XIA, 2019). Pathway impact analysis was performed on the metabolic data using MetaboAnalyst 4.0 against all *Arabidopsis thaliana* pathways (as *Solanum lycopersicum* pathways were not available), considering an enrichment analysis based on the GlobalTest method and a pathway topology analysis based on degree centrality measurement. The TomatoCyc omics dashboard was used to visualize the metabolic data according to biological function categories (PALEY et al., 2017).

3 RESULTS AND DISCUSSION

3.1 Effects of auxin treatment on surface color and ethylene emission during fruit ripening

Characterization of the control (CTRL) fruit ripening stages was based on daily analysis of surface color (Figure 1C and 1D) and ethylene emission (Figure 1E and 1F). CTRL fruits from the four biological replicates reached the breaker stage on the eighth day after harvest (DAH) and reached full ripeness after 18 DAH, as shown in the pictures in Figure 1A and 1B.

As shown in the ethylene emission and surface color graphs, ethylene treatments (ETHY) accelerated the ripening of fruits, while indole-3-acetic acid treatment (IAA) and ethylene and indole-3-acetic acid treatment (ETHY+IAA) produced the opposite effect. At 18 DAH, IAA and ETHY+IAA fruits did not yet show the characteristic red color of fully ripe tomatoes, while ETHY fruits were already losing moisture, a characteristic of senescence. The antagonistic roles of these two hormones are already well established in many biological processes in tomato plants (SEYMOUR et al., 2013). Similar results have been observed during fruit ripening in previous studies by this research group and by Li et al. (2017).

Although IAA and ETHY+IAA fruits had similar ethylene emission profiles, the surface color curves and visual aspects of the fruits suggested that the ETHY+IAA fruits had an intermediate profile between those of CTRL and IAA fruits. In accordance with Su et al. (2015), these results indicate that both hormones simultaneously interfered with the carotenoid metabolism.

Figure 1 – Characterization of Micro-Tom tomato (*Solanum lycopersicum* L.) fruit ripening at two harvests

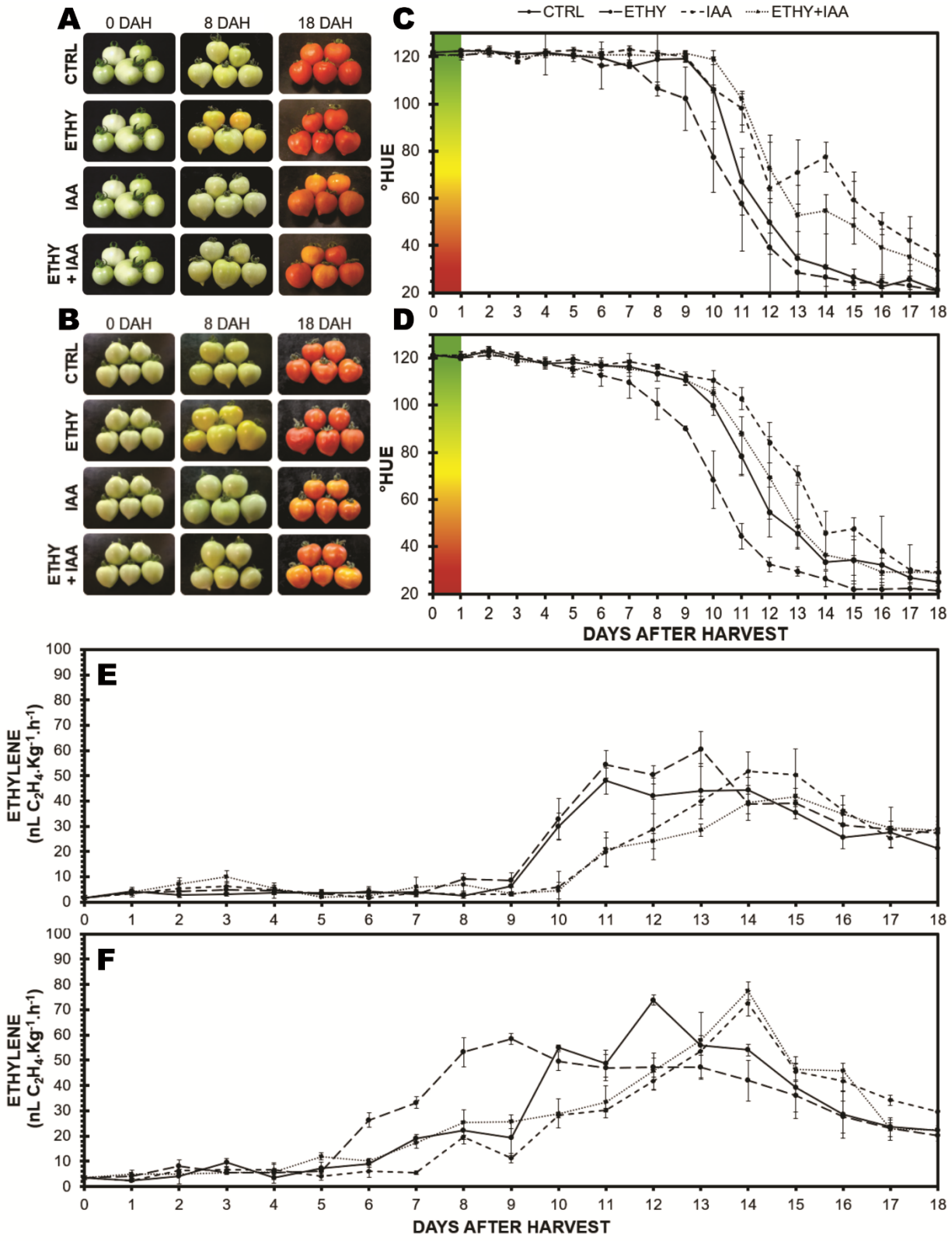

Effects of ethylene, auxin, and both treatments on fruit color and ethylene emission during fruit ripening. (A and B) Pictures of tomato fruits. (C and D) Surface color expressed by hue angle. (E and F) Ethylene emission. CTRL: Control group. ETHY: Ethylene-treated group. IAA: Indole-3-acetic acid-treated group. ETHY+IAA: Group treated with both hormones.

Additionally, the similar results observed for ETHY+IAA and IAA fruits suggest that auxin regulation overlaps the ethylene regulatory system. Metabolic analysis was then performed to investigate the effects of ethylene-auxin treatment on the global metabolism and specific metabolic systems, including aroma compounds.

3.2 Metabolites showing different concentrations in ethylene and auxin-treated fruits

Fruits from each experimental group were sampled at 0 (early ripening stage), 8 (middle ripening stage), and 18 DAH (full ripening stage) for polar and non-polar metabolic profile analysis. A total of 126 metabolites was identified in the samples using GC-MS. Among these, 79 compounds were measured using the polar approach (Table S1); 45 of these were identified according to the criteria described above as amino acids, carbohydrates, or organic acids. Unidentified compounds were described as “unknown”. Additionally, the non-polar approach enabled the quantification of 47 metabolites (Table S2), which were fatty acids (saturated and unsaturated), sterols, and derivatives. This approach was also adopted by Li et al. (2017), who obtained only 41 metabolites, confirming that the strategy adopted and developed in the current study was successful.

To evaluate the measurement reproducibility for the different biological replicates, the metabolites originating from both approaches were subjected to PLS-DA. The results indicated that the biological replicates for each group were always clustered together (Figure S1), simultaneously demonstrating the high reproducibility of the different treatments and the significance of their effects on the metabolite levels. The PLS-DA score plots revealed a clear separation according to the ripening stage (0, 8, and 18 DAH) and the treatment (CTRL, ETHY, IAA, and ETHY+IAA), from higher to lower separation (Figure S1). Further PLS-DA, for polar and non-polar approaches, were performed to evaluate the overall differences in the metabolic profiles between treated and CTRL tomato fruits (Figure 2 and Figure 3). Heatmap analysis was performed to evaluate the changes in each metabolite class after the hormone treatments. Simultaneously, bar graphs of the total normalized area were obtained for metabolite classes to simplify the visualization of metabolite abundances for treated and CTRL fruits.

Figure 2 – Polar metabolites of Micro-Tom tomato (*Solanum lycopersicum* L.) fruits at 8 and 18 days after harvest (DAH)

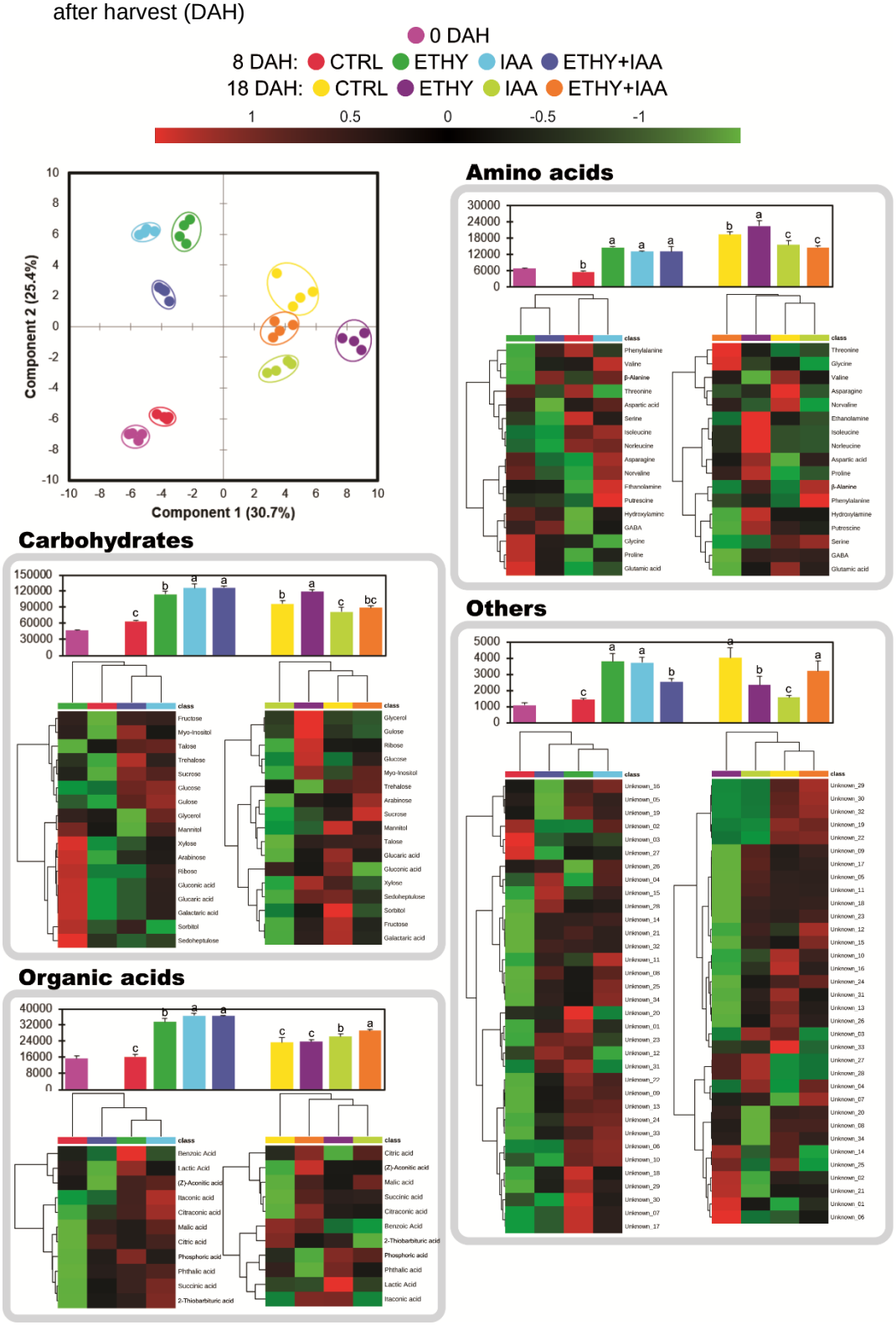

Partial least squares discriminant analysis (PLS-DA) of global polar metabolite changes after treatment with ethylene, auxin, and both hormones. Total normalized area, heatmap, and hierarchical clustering of carbohydrates, organic acids, amino acids, and other compounds. CTRL: Control group. ETHY: Ethylene-treated group. IAA: Indole-3-acetic acid-treated group. ETHY+IAA: Group treated with both hormones. Vertical bars represent the mean values of four replicates (n = 4). Different letters represent significant differences ($p < 0.05$) between treatments at the same DAH.

Figure 3 – Non-polar metabolites of Micro-Tom tomato (*Solanum lycopersicum* L.) fruits at 8 and 18 days after harvest (DAH)

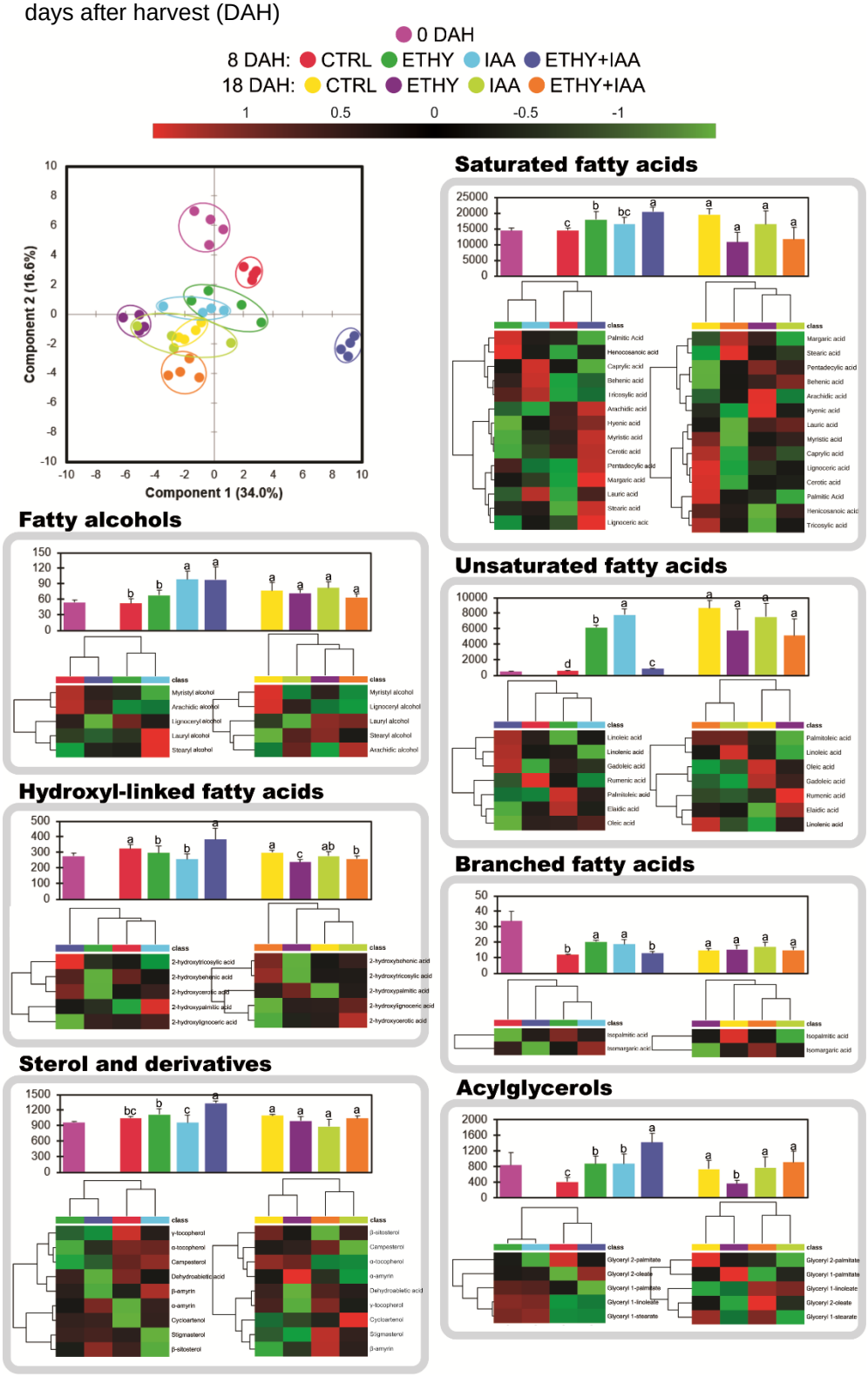

Partial least squares discriminant analysis (PLS-DA) of global non-polar metabolite changes after treatment with ethylene, auxin, and both hormones. Total normalized area, heatmap, and hierarchical clustering of saturated fatty acids, unsaturated fatty acids, branched fatty acids, acylglycerols, fatty alcohols, hydroxyl-linked fatty acids, sterols, and derivatives. CTRL: Control group. ETHY: Ethylene-treated group. IAA: Indole-3-acetic acid-treated group. ETHY+IAA: Group treated with both hormones. Vertical bars represent the mean values of four replicates (n = 4). Different letters represent significant differences ($p < 0.05$) between treatments at the same DAH.

The PLS-DA for metabolites originated from the polar approach displayed a similar tendency to that for the global analysis but did not reveal the same separation. Polar metabolic profiles obtained by GC-MS comprised 17 amino acids, 17 carbohydrates, and 11 organic acids. Among these, 27 polar metabolites (11 amino acids, 10 carbohydrates, and 6 organic acids) presented levels with significant differences in at least one ripening stage (Table S1). Generally, treated fruits presented significantly higher total normalized areas of polar metabolic classes when compared to the CTRL at 8 DAH (Figure 2). Dramatic increases in free amino acid (SORREQUIETA et al., 2010), carbohydrate (LI et al., 2017), and organic acid (OMS-OLIU et al., 2011) contents were observed in tomato fruit during ripening, and Li et al., 2017 previously reported that exogenous auxin treatment significantly increased these metabolic classes in tomato fruits (cv. Xin-taiyang). At the final ripening stage (18 DAH), the total normalized areas of amino acids and carbohydrates were increased by ethylene and decreased by auxin. ETHY+IAA and IAA fruits presented total normalized areas without significant differences, suggesting that the auxin regulation overlapped that of ethylene. However, the total normalized areas of organic acids were increased by ethylene and decreased by auxin. ETHY+IAA fruits also presented total normalized areas of organic acids increased by ethylene, but these were significantly different from those of IAA fruits.

PLS-DA for non-polar metabolites revealed that the hormone treatments did not cause significant differences between the score plots of these compound classes during fruit ripening. Saturated fatty acids, unsaturated fatty acids, branched fatty acids, fatty alcohols, hydroxyl-linked fatty acids, acylglycerols, and sterol derivatives comprised the non-polar metabolic profiles obtained by GC-MS. However, only 12 non-polar metabolites (2 saturated, 3 unsaturated, 1 branched, 2 hydroxyl-linked fatty acids, 1 fatty alcohol, 1 acylglycerol, and 2 sterol derivatives) presented levels with significant differences in at least one ripening stage (Table S2). During the middle ripening stage (8 DAH), the total normalized areas of saturated fatty acids, unsaturated fatty acids, branched fatty acids, and acylglycerols were increased by ethylene and auxin. The total normalized areas of saturated fatty acids and acylglycerols also increased for ETHY+IAA fruits, but the same did not occur with unsaturated and branched fatty acids. At the same stage, the total normalized areas of fatty alcohols increased only for IAA and ETHY+IAA fruits, while the total normalized areas of hydroxyl-linked fatty acids and sterols increased only for ETHY+IAA fruits. However,

CTRL and treated fruits did not present significant differences between their total normalized areas at the final ripening stage (18 DAH) for any of the non-polar metabolic classes, except for acylglycerols and hydroxyl-linked fatty acids (Figure 3). However, the metabolites from these classes do not participate directly in secondary metabolic pathways or aroma formation. These results suggest that both hormones influenced the metabolism of carbohydrates, amino acids, and organic acids more than that of fatty acids.

Except for linoleic acid, identified metabolite precursors of VOCs presented significant differences in at least one ripening stage. IAA fruits showed significantly higher levels ($p < 0.05$) of valine (8 DAH), isoleucine (8 DAH), and phenylalanine (18 DAH) when compared to the other fruits. Other compounds are important for tomato fruits because they participate in the global metabolism or secondary metabolic pathways, some of which indirectly affect the aroma of tomatoes (QUINET et al., 2019).

3.3 Global metabolic profile and statistical evaluation

The polar and non-polar metabolites were assessed in a combined and integrated analysis. The carotenoid (lycopene, β-carotene, and lutein) contents of tomato fruits were analyzed by HPLC and included in this analysis (Table S3). As well as being responsible for the final red color of tomato fruits, carotenoids are precursors of VOCs that are important to the tomato aroma: geranyl acetone; citral; 6-methyl-5-hepten-2-one; guaiacol; β-damascenone; and β-ionone (SU et al., 2015; TIEMAN et al., 2017). A total of 95 metabolites was considered for the pathway enrichment analysis and pathway impact analysis, and the pathways affected by the hormone treatments are shown in Figure 4 and described in Table S4. The number of pathways significantly influenced by hormone treatment ranged from 39 to 48, with 17 pathways being altered under all conditions analyzed (ripening stages and treatments). Additionally, 18 pathways were significantly influenced only at 8 DAH and 6 pathways only at 18 DAH. This increased value at the middle stage (8 DAH) suggests that some of the changes caused by hormone treatment were reestablished over the ripening. At 8 DAH, 16 of these significantly changed pathways were amino acid metabolism pathways, indicating a significant alteration in amino acid biosynthesis and metabolism.

Figure 4 – Metabolic pathways differentially impacted by treatment with ethylene, auxin, or both hormones in Micro-Tom tomato (*Solanum lycopersicum* L.) fruits at 8 and 18 days after harvest (DAH)

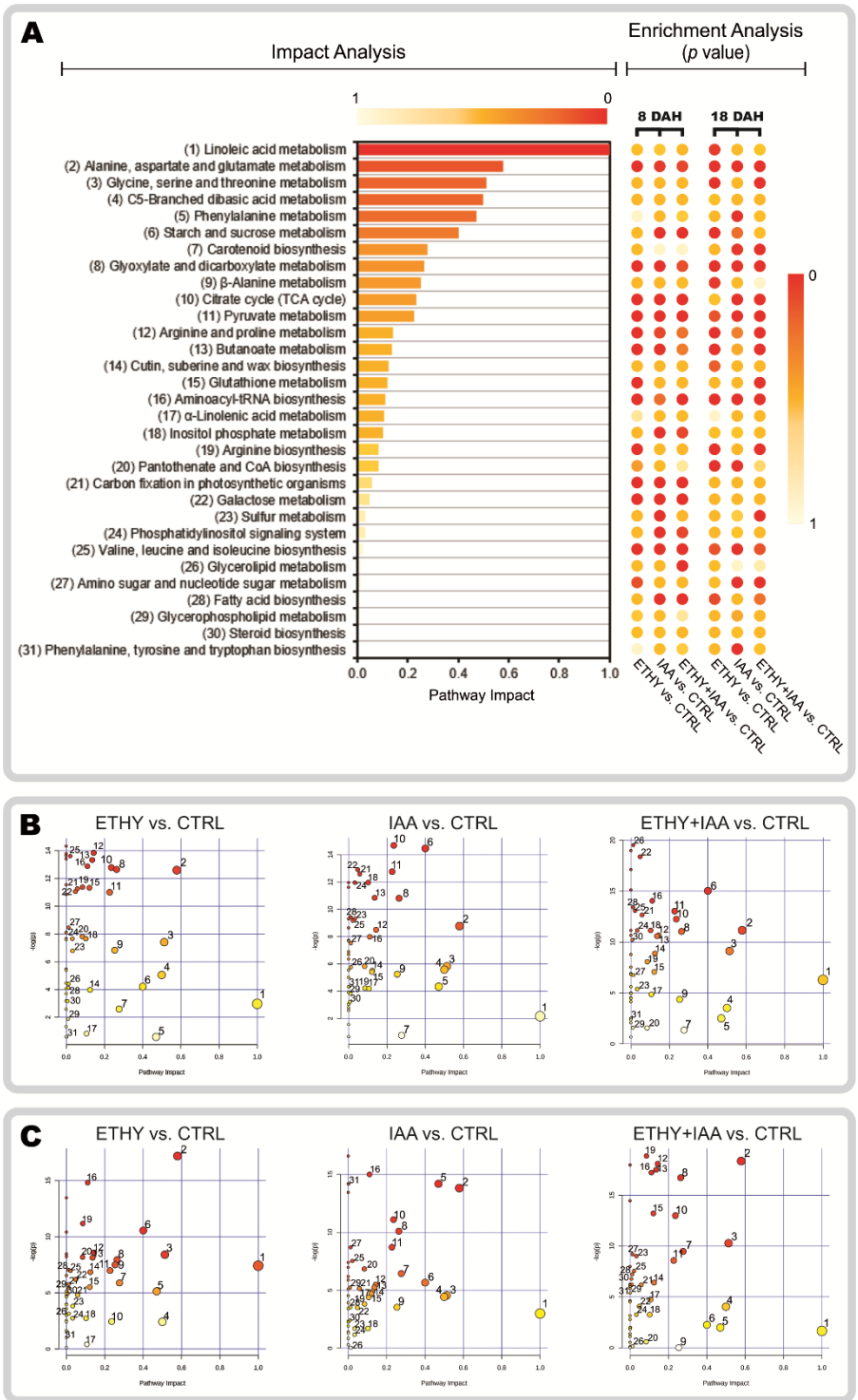

(A) Pathways differentially impacted by hormone treatments ordered by impact score and p-value from enrichment analysis between each treated and control group at the same DAH. (B) Pathway impact analysis based on 91 metabolites found in treated and control fruits at 8 DAH. Y-axis is the −log p-value from pathway enrichment analysis. X-axis is the pathway impact value from pathway topology analysis. The node color and radius are based on the p-value and pathway impact value, respectively. (C) Pathway impact analysis based on 91 metabolites found in treated and control fruits at 18 DAH. ETHY: Ethylene-treated group. IAA: Indole-3-acetic acid-treated group. ETHY+IAA: Group treated with both hormones.

Pathways related to carbohydrate (8), organic acid (7), and fatty acid (4) metabolisms were significantly altered to a lesser extent, supporting the results described above. The metabolic changes induced by ethylene, auxin, and ethylene-auxin crosstalk imply that both hormones may influence VOC biosynthesis in tomato fruits.

To deepen the understanding of how ethylene and auxin affect the tomato fruit metabolism, metabolite profile data were transferred to the TomatoCyc omics dashboard (PALEY et al., 2017) to visualize the differences between treated and CTRL fruits within annotated secondary metabolite biosynthesis systems (Figure 5).

During ripening (Figure 5A), the secondary metabolism was positively affected by the hormone treatments, except for the pathways related to biosynthesis of fatty acid derivatives and N-containing compounds. The biosynthesis of S-containing compounds and derivatives of L-pipecolite and phenylpropanoid was affected by ethylene. Pathways related to the biosynthesis of terpenes, furaneol, and mesifurane derivatives were affected by ethylene more than by auxin, and ETHY+IAA fruits presented a response closer to that of the fruits treated only with auxin. Metabolites associated with sugar derivative biosynthesis were particularly increased in IAA and ETHY+IAA fruits. At 18 DAH (Figure 5B), metabolites associated with the biosynthesis of fatty acid derivatives and N-containing compounds continued to be apparently unaffected by any hormone treatment. Pathways related to the biosynthesis of furaneol and mesifurane derivatives were only affected by ethylene, while terpene pathways were positively affected by ethylene and depleted by auxin. ETHY+IAA fruits presented a response more similar to those treated only with auxin. Metabolites associated with sugar derivative biosynthesis were depleted in ETHY and IAA fruits but increased in ETHY+IAA fruits. The biosynthesis of S-containing compounds and derivatives of L-pipecolite and phenylpropanoid was negatively affected by ethylene and auxin treatments.

These results are consistent with the traditional statistical analysis but build a more comprehensive picture of ethylene and auxin effects on primary and secondary metabolisms. Ethylene and auxin upregulated secondary metabolite pathways in different ways during ripening. Additionally, the auxin response apparently overlapped ethylene response. However, to further clarify the role of each hormone in regulating the tomato fruit aroma, the direct links between primary and secondary metabolisms and VOC profiles need to be better understood.

Figure 5 – Secondary metabolite biosynthesis panel summarizes the relative levels of individual metabolites involved in the biosynthesis of each secondary metabolite category

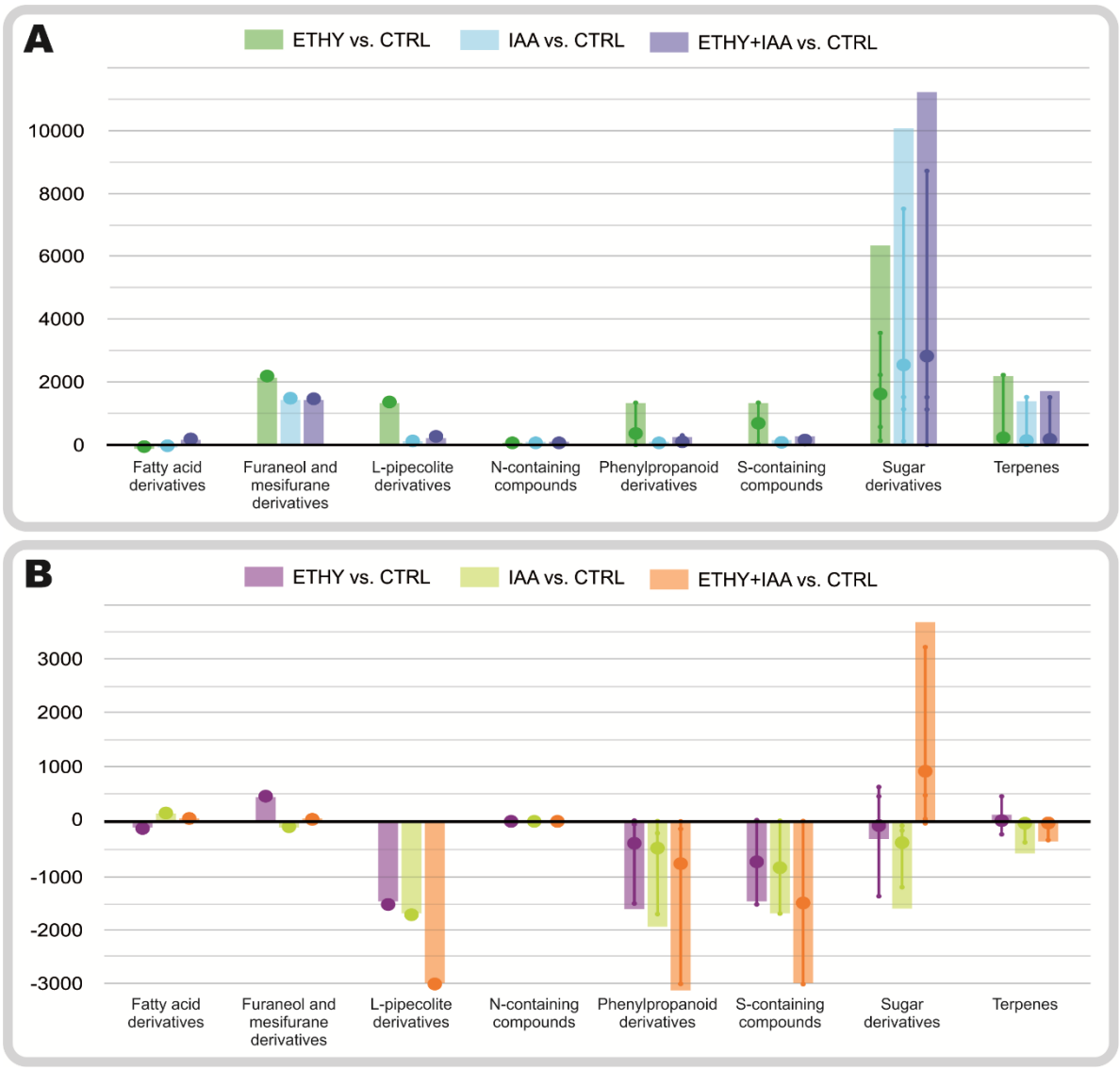

Panel visualized using TomatoCyc omics dashboard (PALEY et al., 2017). (A) Relative comparison of secondary metabolite categories based on 93 metabolites found in treated and control fruits at 8 DAH. (B) Relative comparison of secondary metabolite categories based on 93 metabolites found in treated and control fruits at 18 DAH. ETHY: Ethylene-treated group. IAA: Indole-3-acetic acid-treated group. ETHY+IAA: Group treated with both hormones.

3.4 Changes in volatile compound metabolism

In this study, the levels of metabolite precursors of VOCs were changed by ethylene or auxin treatments. Some of these even showed different responses when treated with both hormones. Figure 6 shows biosynthetic pathways of 20 VOCs that are important to the tomato aroma and consumer acceptance and their 8 metabolic precursors (TIEMAN et al., 2017; KLEE; TIEMAN, 2018).

The class of VOCs derived from fatty acids (Figure 6A) constitute the most abundant volatiles produced in tomato fruits: C6 volatiles (hexanal, 1-hexanol, (Z)-3-hexenal, (E)-2-hexenal, and (Z)-3-hexen-1-ol) and C5 volatiles (1-pentanal, 1-pentanol, and 1-penten-3-one) (RAMBLA et al., 2014). These compounds are classified as green-leaf volatiles due to their characteristic aroma of freshly cut grass, and their production increases during fruit ripening (RAMBLA et al., 2014). The biosynthesis of these fatty acid derivatives begins with linoleic and linolenic acids (main precursors), which are first oxidized to 13-hydroperoxides (13-HPO) by the action of lipoxygenase C (LoxC) followed by oxidative cleavage catalyzed by 13-hydroperoxide lyase to generate hexanal and (Z)-3-hexenal (BAI et al., 2011; CHEN et al., 2004); (Z)-3-hexenal could then be isomerized to (E)-2-hexenal (RAMBLA et al., 2014). Finally, alcohol dehydrogenase 2 participates in the reduction of hexanal, (Z)-3-hexenal, and (E)-2-hexenal to 1-hexanol, (Z)-3-hexen-1-ol, and (E)-2-hexen-1-ol, respectively (SPEIRS et al., 1998).

Linoleic and linolenic acid levels were changed by both hormones. Linoleic acid accumulation was induced in IAA fruits at 18 DAH and in ETHY+IAA fruits during both ripening stages. Ethylene treatment decreased linoleic acid levels. Linolenic acid levels decreased in IAA fruits and increased in ETHY+IAA fruits during both ripening stages. However, ETHY fruits presented higher levels of linolenic acid at 18 DAH than did the CTRL. In addition to regulating the free fatty acid concentrations, ethylene regulation of LoxC gene expression was also revealed in tomato (GRIFFITHS et al., 1999), supporting the importance of this hormone for this VOC class.

A significant number of amino acid-derived VOCs are important for tomato aroma (SELLI et al., 2014**;** RAMBLA et al., 2014). Volatiles from this class can be grouped into two categories (phenolic and branched-chain compounds) and include compounds directly derived from phenylalanine (phenylacetaldehyde, 2-phenylethanol, methyl salicylate), leucine (3-methylbutanal, 3-methylbutanol), isoleucine (2-methylbutanal, 2-methylbutanol), and valine (isobutyl acetate, 2-isobutylthiazole) (RAMBLA et al., 2014). In this study (Figure 6B), the accumulation of phenylalanine, isoleucine, and valine was induced by auxin and repressed by ethylene during ripening, but only phenylalanine maintained high levels until IAA fruits were fully ripe. At 18 DAH, isoleucine and valine presented higher contents in ETHY fruits. Valine presented similar contents in IAA and ETHY+IAA fruits during ripening, while no clear pattern was observed for the other metabolites.

Figure 6 – Biosynthesis pathways of the most important volatile compounds with respect to tomato (*Solanum lycopersicum* L.) fruit aroma

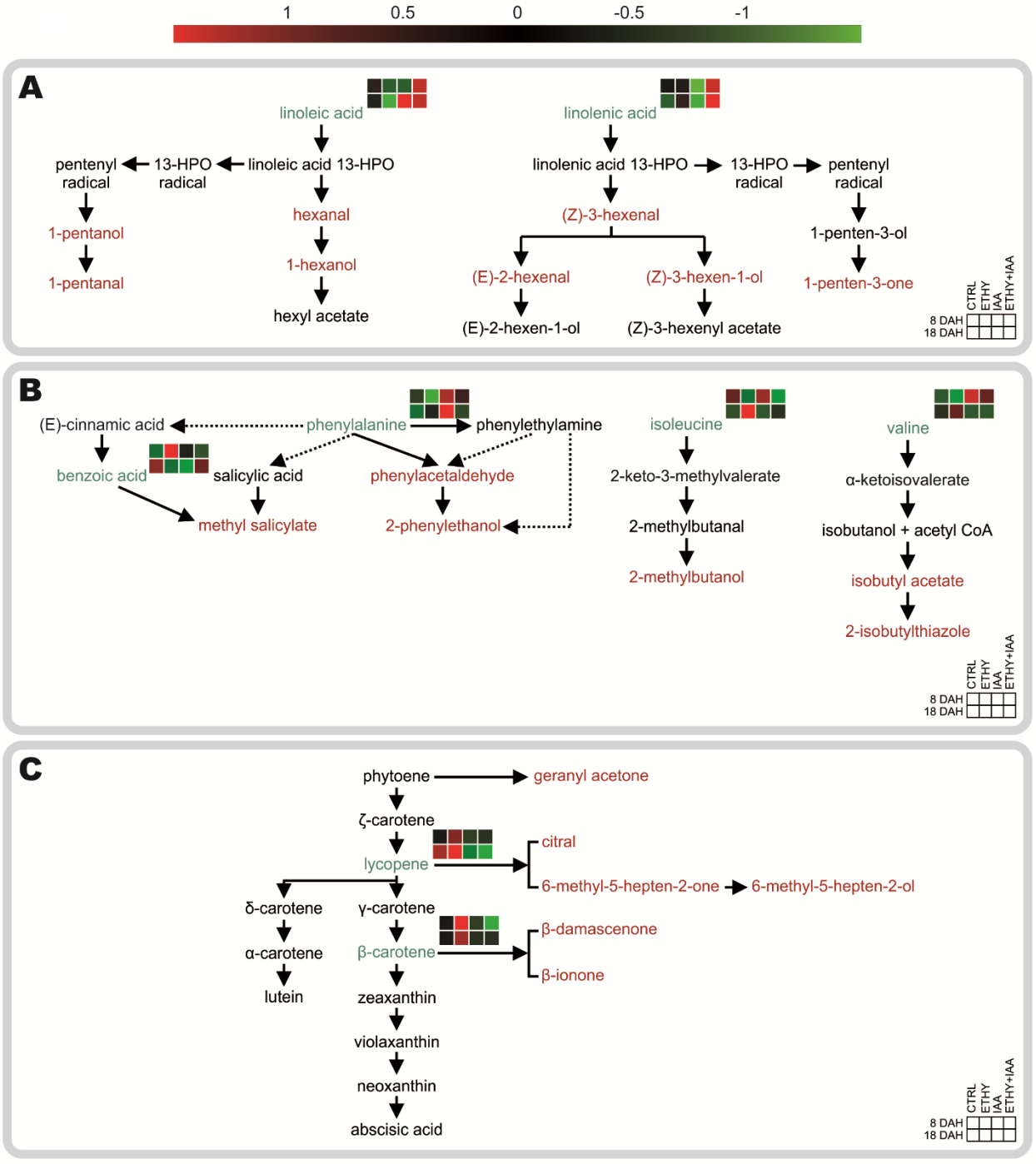

Metabolites found using the adopted metabolic approaches are shown in green. Important volatile compounds (TIEMAN et al., 2017; KLEE; TIEMAN, 2018) are shown in red. Color-coded squares illustrate the relative levels of metabolites and volatile compounds after each hormone treatment. (A) Carotenoid pathways and respective volatile compounds. (B) Amino acid pathways and respective volatile compounds. (C) Fatty acid pathways and respective volatile compounds. ETHY: Ethylene-treated group. IAA: Indole-3-acetic acid-treated group. ETHY+IAA: Group treated with both hormones. Adapted from Klee and Tieman (2018).

Biosynthetic pathways of VOCs derived from amino acids have not yet been completely elucidated in fruits (RAMBLA et al., 2014), and nor has their regulation by ethylene and auxin. However, these compounds contribute significantly to the tomato aroma with distinct aromatic notes, especially 2-isobutylthiazole, which individually presents a characteristic tomato-like aroma (BALDWIN et al., 1998).

Finally, carotenoid-derived VOCs are also positively associated with flavor and overall liking of tomato fruit (TIEMAN et al., 2017). Geranyl acetone is derived from phytoene, while citral, 6-methyl-5-hepten-2-one, and 6-methyl-5-hepten-2-ol are derived from lycopene; β-damascenone and β-ionone are both important apocarotenoids derived from β-carotene (RAMBLA et al., 2014). These compounds are produced at low levels in ripe fruit but are important in tomato aroma and flavor perception due to their low perception threshold (BUTTERY et al., 1971; VOGEL et al., 2010; RAMBLA et al., 2014). By analyzing tomato color changes, Su et al. (2015) and Li et al. (2016) showed that ethylene induces lycopene and β-carotene accumulation by key gene induction, while auxin downregulates the same genes and decreases the levels of the same carotenoids. The current study observed similar results (Figure 6C) for both hormones and additionally showed that ETHY+IAA fruits presented similar results to fruits treated only with auxin, suggesting that auxin regulation overlaps the ethylene regulatory system. In tomato fruits, the carotenoid-derived VOCs described above are produced by the action of carotenoid cleavage dioxygenases (CCD1A and CCD1B) (SIMKIN et al., 2004), and although it is not yet known whether both hormones can regulate CCD1A and CCD1B-related genes, the change in precursor accumulation could consequently change the final aroma of tomato fruits.

4 CONCLUSIONS

Knowledge of hormonal regulation is extensive; however, the role of each hormone in fruit aroma formation remains unclear. This study describes how different hormone treatments changed the primary and secondary metabolic profiles and, consequently, the tomato fruit aroma. The metabolic approaches described above were highly effective in elucidating ethylene and auxin regulatory mechanisms in VOC pathways. Although the tomato fruits were visually similar when fully ripe, we identified

significant changes in various metabolite classes, indicating reprogramming of specific pathways after ethylene and auxin treatments. A systemic view of the primary and secondary metabolite changes during infection indicated different reactions for each hormone as well as for the crosstalk between them. Furthermore, the findings in this study encourage the application of other “omics” approaches to studying hormonal regulation of secondary metabolisms, such as enzymatic profile changes after hormone treatments.

DATA AVAILABILITY STATEMENT

Files and metadata reported in this paper are available via Metabolights and study identifier MTBLS1535. (https://www.ebi.ac.uk/metabolights/MTBLS1535).

SUPPLEMENTARY MATERIAL

Figure S1 – Metabolites of Micro-Tom tomato (*Solanum lycopersicum* L.) fruits at 8 and 18 days after harvest (DAH)

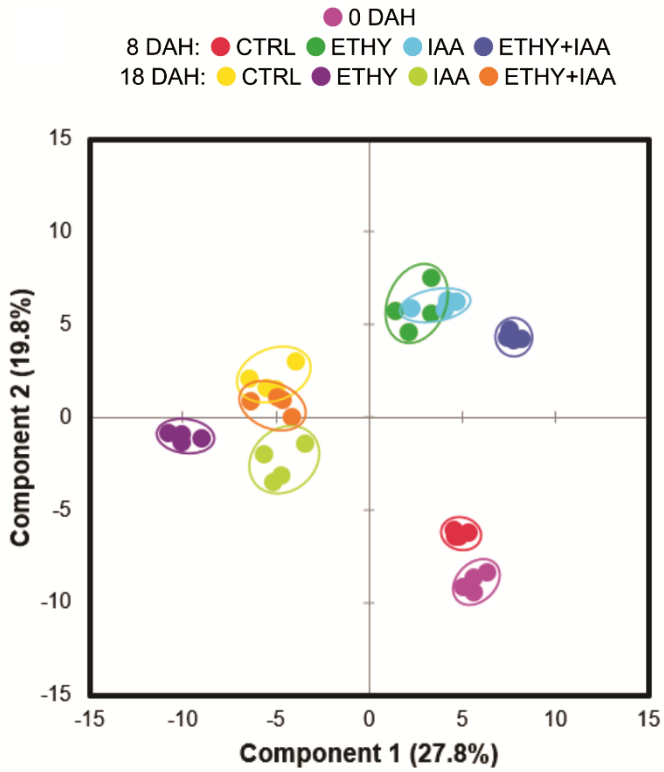

Partial least squares discriminant analysis (PLS-DA) of global metabolite changes after ethylene, auxin, and both treatments. CTRL: Control group. ETHY: Ethylene-treated group. IAA: Indole-3-acetic acid-treated group. ETHY+IAA: Group treated with both hormones.

Table S1 – Polar metabolites in three ripening stages of Micro-Tom tomato (*Solanum lycopersicum* L.) fruits detected by gas chromatography-mass spectrometry (GC-MS)

Class	Metabolite	RI	DAH	Hormone treatment				One-way ANOVA	
				CTRL	ETHY	IAA	ETHY+IAA	*F* value	*p* value
Amino acids	Valine	1101	0	41.43 ± 10.49					
			8	**16.71 ± 3.27^{b}**	**3.74 ± 0.77^{c}**	**40.94 ± 8.34^{a}**	**19.89 ± 8.29^{b}**	**20.1**	**5.73E-05**
			18	6.93 ± 0.96	7.10 ± 1.28	5.84 ± 1.60	6.02 ± 1.43	0.6	6.31E-01
	Hydroxylamine	1124	0	89.37 ± 2.52					
			8	**79.38 ± 7.33^{c}**	**176.93 ± 8.88^{a}**	**151.69 ± 5.14^{b}**	**164.55 ± 23.60^{ab}**	**61.7**	**1.46E-07**
			18	168.82 ± 15.56	263.67 ± 48.05	159.34 ± 15.58	178.43 ± 51.90	1.2	3.36E-01
	Isoleucine	1185	0	45.27 ± 10.39					
			8	**29.94 ± 8.41^{a}**	**0.32 ± 0.10^{b}**	**65.93 ± 15.24^{a}**	**0.30 ± 0.04^{b}**	**96.1**	**1.17E-08**
			18	nd	nd	nd	nd	-	-
	Serine	1266	0	133.65 ± 26.02					
			8	76.82 ± 28.21	45.05 ± 1.55	101.18 ± 24.50	37.47 ± 6.40	1.3	3.28E-01
			18	73.85 ± 6.05	37.65 ± 16.00	103.39 ± 63.71	31.34 ± 10.21	4.4	2.58E-02
	Ethanolamine	1274	0	24.52 ± 2.55					
			8	31.60 ± 3.51	38.02 ± 7.05	50.78 ± 12.26	36.90 ± 6.70	1.5	2.75E-01
			18	55.69 ± 3.71	72.37 ± 6.78	44.77 ± 3.48	39.83 ± 4.48	1.2	3.54E-01
	Norleucine	1282	0	11.27 ± 4.39					
			8	**8.71 ± 1.98^{a}**	**0.32 ± 0.10^{b}**	**13.03 ± 2.79^{a}**	**0.30 ± 0.04^{b}**	**10.5**	**1.12E-03**
			18	nd	nd	nd	nd	-	-
	Threonine	1300	0	142.31 ± 21.67					
			8	166.55 ± 25.79	138.56 ± 17.95	187.39 ± 56.18	77.41 ± 6.82	0.6	5.99E-01
			18	243.33 ± 40.84	88.82 ± 10.61	82.33 ± 19.36	72.22 ± 7.20	0.2	8.72E-01
	Glycine	1316	0	30.99 ± 3.87					
			8	28.74 ± 0.51	33.82 ± 2.40	53.43 ± 7.63	39.66 ± 10.38	1.0	4.43E-01
			18	34.12 ± 11.03	51.58 ± 10.22	45.71 ± 5.51	41.98 ± 4.17	0.2	8.84E-01
	Aspartic acid	1429	0	217.10 ± 19.60					
			8	277.14 ± 29.80	591.51 ± 96.04	409.07 ± 14.06	439.00 ± 10.36	2.0	1.61E-01
			18	1052.60 ± 75.71	1732.09 ± 442.08	1466.53 ± 714.73	1064.54 ± 226.44	1.9	1.87E-01
	β-Alanine	1434	0	119.28 ± 13.38					
			8	**85.73 ± 27.70^{c}**	**66.09 ± 14.25^{c}**	**127.91 ± 19.53^{b}**	**139.25 ± 51.03^{a}**	**5.4**	**1.42E-02**
			18	19.70 ± 0.52	29.01 ± 1.85	42.03 ± 10.97	19.90 ± 4.90	2.6	9.99E-02

Table S1 – (Continued)

Class	Metabolite	RI	DAH	Hormone treatment				One-way ANOVA	
				CTRL	ETHY	IAA	ETHY+IAA	*F* value	*p* value
Amino acids	Proline	1527	0	1460.50 ± 279.29					
			8	**1341.16 ± 86.37^{d}**	**5156.62 ± 536.32^{a}**	**2401.01 ± 202.65^{c}**	**3190.57 ± 343.41^{b}**	**156.2**	**7.02E-10**
			18	8650.50 ± 1160.67	12975.02 ± 1628.32	6626.63 ± 738.28	8127.16 ± 426.19	2.6	1.01E-01
	GABA	1542	0	4372.58 ± 269.83					
			8	3221.51 ± 279.51	6708.95 ± 213.82	8949.18 ± 296.02	8367.01 ± 1760.63	2.6	9.74E-02
			18	**5740.66 ± 376.74^{a}**	**5412.24 ± 307.41^{a}**	**5469.17 ± 617.14^{a}**	**4762.50 ± 148.68^{b}**	**11.0**	**9.24E-04**
	Asparagine	1601	0	56.41 ± 22.12					
			8	62.42 ± 49.20	125.62 ± 51.28	174.89 ± 93.90	51.17 ± 4.31	2.7	9.60E-02
			18	**60.40 ± 8.61^{a}**	**0.76 ± 0.19^{b}**	**0.40 ± 0.09^{b}**	**0.44 ± 0.14^{b}**	**16.6**	**1.43E-04**
	Phenylalanine	1636	0	39.02 ± 14.37					
			8	17.26 ± 6.48	14.66 ± 4.77	32.10 ± 4.39	24.70 ± 3.50	0.4	7.31E-01
			18	**0.29 ± 0.10^{b}**	**0.76 ± 0.19^{b}**	**17.40 ± 0.74^{a}**	**0.44 ± 0.14^{b}**	**11.0**	**9.26E-04**
	Glutamic acid	1635	0	22.69 ± 11.49					
			8	**113.77 ± 38.33^{c}**	**1449.06 ± 291.70^{a}**	**215.10 ± 77.76^{c}**	**362.59 ± 65.45^{b}**	**10.7**	**1.05E-03**
			18	**3224.74 ± 401.33^{a}**	**1698.51 ± 181.01^{a}**	**1501.83 ± 692.89^{a}**	**220.23 ± 12.10^{b}**	**10.9**	**9.60E-04**
	Putrescine	1742	0	9.62 ± 20					
			8	49.76 ± 1.35	102.27 ± 2.6	118.92 ± 8.01	100.04 ± 11.07	1.0	4.43E-01
			18	83.36 ± 15.63	101.41 ± 2.21	64.31 ± 8.06	74.17 ± 4.47	1.5	2.55E-01
	Norvaline	2273	0	3.85 ± 0.51					
			8	3.91 ± 0.48	13.71 ± 4.44	8.29 ± 3.01	8.23 ± 0.94	0.7	5.82E-01
			18	**9.43 ± 3.23^{a}**	**0.76 ± 0.19^{b}**	**0.40 ± 0.09^{b}**	**4.56 ± 0.95^{a}**	**9.7**	**1.54E-03**
Carbohydrates	Glycerol	1290	0	8.63 ± 1.12					
			8	**8.89 ± 0.44^{a}**	**15.20 ± 4.01^{a}**	**28.62 ± 10.58^{a}**	**0.30 ± 0.04^{b}**	**12.8**	**4.82E-04**
			18	30.12 ± 5.10	40.19 ± 5.95	30.36 ± 5.14	29.43 ± 2.79	4.0	3.57E-02
	Xylose	1678	0	nd					
			8	**38.29 ± 11.33^{c}**	**86.32 ± 15.17^{a}**	**56.08 ± 2.48^{b}**	**41.98 ± 5.01^{c}**	**14.1**	**3.04E-04**
			18	**57.72 ± 4.45^{a}**	**70.39 ± 6.8^{a}**	**28.45 ± 5.81^{b}**	**34.37 ± 4.14^{b}**	**41.2**	**1.35E-06**
	Arabinose	1690	0	30.99 ± 0.40					
			8	**185.77 ± 25.73^{d}**	**460.55 ± 79.50^{a}**	**312.38 ± 18.49^{b}**	**252.33 ± 27.76^{c}**	**35.4**	**3.05E-06**
			18	325.30 ± 12.78	354.05 ± 20.32	202.15 ± 26.19	251.65 ± 16.04	0.4	7.26E-01

Table S1 – (Continued)

Class	Metabolite	RI	DAH	Hormone treatment				One-way ANOVA	
				CTRL	ETHY	IAA	ETHY+IAA	*F* value	*p* value
Carbohydrates	Ribose	1717	0	9.04 ± 1.16					
			8	13.76 ± 1.51	33.35 ± 3.14	24.85 ± 2.38	24.37 ± 1.66	2.2	1.41E-01
			18	**30.45 ± 9.48^{ab}**	**47.08 ± 17.77^{a}**	**20.93 ± 0.44^{b}**	**30.99 ± 4.70^{ab}**	**5.2**	**1.58E-02**
	Fructose	1914	0	21965.24 ± 455.93					
			8	28931.57 ± 605.81	54337.22 ± 1344.57	55692.08 ± 3329.82	57095.05 ± 779.04	4.4	2.59E-02
			18	56562.83 ± 4598.14	65299.89 ± 1411.30	47119.60 ± 4254.88	47314.42 ± 1817.60	1.1	3.76E-01
	Talose	1940	0	16255.04 ± 234.41					
			8	18837.82 ± 365.61	32627.96 ± 1718.83	37484.59 ± 1592.60	36238.81 ± 1858.66	2.4	1.18E-01
			18	21695.98 ± 2977.34	34905.75 ± 3252.50	20951.52 ± 2268.71	21967.96 ± 1697.41	1.9	1.88E-01
	Glucose	1953	0	3717.59 ± 83.51					
			8	4096.39 ± 195.53	6758.81 ± 798.66	8579.33 ± 473.53	8042.14 ± 429.57	2.0	1.70E-01
			18	4195.53 ± 802.14	6991.35 ± 241.69	3936.31 ± 665.54	4579.87 ± 729.08	1.6	2.39E-01
	Mannitol	1967	0	4.86 ± 0.91					
			8	**73.55 ± 18.96^{a}**	**171.72 ± 22.85^{a}**	**139.26 ± 46.71^{a}**	**53.89 ± 5.64^{b}**	**7.8**	**3.74E-03**
			18	173.55 ± 39.06	98.89 ± 13.06	93.53 ± 29.06	142.81 ± 55.44	3.4	5.43E-02
	Sorbitol	1981	0	nd					
			8	4271.64 ± 367.78	7707.88 ± 1023.92	6555.70 ± 1118.05	6233.32 ± 445.64	1.4	3.03E-01
			18	8643.61 ± 1010.40	7130.56 ± 696.13	6431.89 ± 1097.17	6660.45 ± 1244.05	3.0	7.44E-02
	Glucaric acid	1988	0	nd					
			8	nd	nd	nd	nd	-	-
			18	274.68 ± 45.31	211.28 ± 11.54	54.75 ± 24.21	136.76 ± 17.59	3.5	5.09E-02
	Trehalose	1994	0	126.58 ± 30.87					
			8	189.28 ± 29.56	411.51 ± 229.94	644.67 ± 43.53	618.94 ± 152.35	2.0	1.68E-01
			18	**276.68 ± 170.40^{a}**	**0.76 ± 0.19^{c}**	**33.44 ± 5.33^{b}**	**284.66 ± 50.34^{a}**	**51.8**	**3.88E-07**
	Galactaric acid	2004	0	nd					
			8	nd	nd	nd	nd	-	-
			18	64.96 ± 7.12	45.07 ± 6.37	35.14 ± 13.08	31.73 ± 4.00	2.0	1.75E-01
	Gluconic acid	2042	0	15.13 ± 0.73					
			8	15.86 ± 2.16	28.68 ± 2.49	33.67 ± 3.58	34.00 ± 1.56	0.6	6.49E-01
			18	68.54 ± 9.82	90.86 ± 42.86	60.55 ± 14.77	45.60 ± 7.29	0.8	4.95E-01

Table S1 – (Continued)

Class	Metabolite	RI	DAH	Hormone treatment				One-way ANOVA	
				CTRL	ETHY	IAA	ETHY+IAA	*F* value	*p* value
Carbohydrates	Gulose	2072	0	472.76 ± 9.31					
			8	**564.39 ± 32.40^{c}**	**664.01 ± 9.76^{b}**	**1202.34 ± 78.72^{a}**	**1089.88 ± 126.54^{a}**	**101.9**	**8.37E-09**
			18	458.80 ± 108.20	775.56 ± 142.66	431.44 ± 94.18	397.78 ± 97.94	1.7	2.28E-01
	Myo-Inositol	2120	0	1404.98 ± 33.71					
			8	724.57 ± 79.08	1265.61 ± 143.99	1795.76 ± 93.26	1830.91 ± 162.73	2.6	9.99E-02
			18	**1000.74 ± 206.19^{c}**	**1631.96 ± 529.23^{a}**	**817.61 ± 143.89^{c}**	**1474.95 ± 318.40^{b}**	**6.5**	**7.51E-03**
	Sedoheptulose	2177	0	6.06 ± 0.52					
			8	16.29 ± 2.36	43.20 ± 11.68	28.34 ± 2.59	27.66 ± 5.29	0.1	9.36E-01
			18	**245.65 ± 85.62^{a}**	**226.21 ± 65.61^{a}**	**67.36 ± 17.94^{b}**	**80.79 ± 90^{b}**	**9.6**	**1.62E-03**
	Sucrose	2704	0	3588.77 ± 663.47					
			8	**6175.54 ± 126.05^{c}**	**9720.73 ± 1562.78^{b}**	**13656.21 ± 2287.52^{a}**	**14831.22 ± 807.91^{a}**	**40.4**	**1.50E-06**
			18	**2603.73 ± 869.47^{a}**	**1237.57 ± 579.45^{ab}**	**1364.32 ± 362.97^{b}**	**5803.12 ± 2085.60^{a}**	**7.0**	**5.49E-03**
Organic acids	Lactic Acid	<1100	0	116.58 ± 6.39					
			8	111.98 ± 14.63	157.54 ± 3.94	93.73 ± 4.54	127.10 ± 6.25	3.2	6.21E-02
			18	160.44 ± 10.35	377.26 ± 86.21	293.84 ± 64.93	282.25 ± 41.08	1.1	3.84E-01
	Benzoic Acid	1248	0	18.69 ± 2.52					
			8	15.48 ± 0.92	52.34 ± 15.70	33.00 ± 1.39	27.43 ± 2.80	1.7	2.26E-01
			18	**35.77 ± 3.74^{a}**	**0.76 ± 0.19^{b}**	**0.40 ± 0.09^{b}**	**40.55 ± 8.99^{a}**	**25.8**	**1.63E-05**
	Phosphoric acid	1287	0	2290.15 ± 21.86					
			8	**2247.86 ± 241.37^{c}**	**4412.92 ± 108.80^{a}**	**3707.37 ± 217.03^{b}**	**3708.58 ± 206.28^{b}**	**69.7**	**7.31E-08**
			18	4195.74 ± 675.64	4651.75 ± 411.85	4093.29 ± 188.84	4230.44 ± 97.92	1.8	2.08E-01
	Succinic acid	1320	0	13.95 ± 2.86					
			8	**10.51 ± 0.57^{c}**	**20.53 ± 0.93^{ab}**	**22.95 ± 3.55^{a}**	**17.71 ± 3.67^{b}**	**25.0**	**1.90E-05**
			18	16.66 ± 1.40	20.79 ± 4.85	20.85 ± 1.34	23.18 ± 2.81	1.7	2.14E-01
	Itaconic acid	1355	0	140.67 ± 8.20					
			8	141.62 ± 53.48	433.30 ± 154.74	276.65 ± 35.04	262.12 ± 36.17	0.6	6.31E-01
			18	250.76 ± 67.12	686.67 ± 139.37	433.71 ± 68.40	718.44 ± 235.79	3.1	6.55E-02
	Citraconic acid	1363	0	60.88 ± 9.35					
			8	69.24 ± 19.62	209.53 ± 75.04	144.56 ± 11.08	108.92 ± 10.83	1.3	3.25E-01
			18	99.62 ± 39.33	153.35 ± 16.92	260.10 ± 70.66	239.69 ± 76.89	2.7	9.30E-02

Table S1 – (Continued)

Class	Metabolite	RI	DAH	Hormone treatment				One-way ANOVA	
				CTRL	ETHY	IAA	ETHY+IAA	*F* value	*p* value
Organic acids	Malic acid	1506	0	3837.84 ± 169.93					
			8	**2280.62 ± 146.26^{c}**	**4916.12 ± 542.29^{b}**	**5873.68 ± 87.25^{a}**	**5381.68 ± 223.80^{ab}**	**158.9**	**6.37E-10**
			18	**1784.11 ± 358.63^{b}**	**2241.74 ± 229.24^{a}**	**3490.88 ± 186.15^{a}**	**3128.12 ± 151.85^{a}**	**5.2**	**1.55E-02**
	(Z)-Aconitic acid	1766	0	77.61 ± 5.67					
			8	82.23 ± 16.71	170.70 ± 7.85	182.79 ± 35.23	116.20 ± 8.81	0.9	4.84E-01
			18	117.20 ± 10.63	99.71 ± 22.11	180.08 ± 24.81	152.37 ± 4.44	0.8	5.31E-01
	Citric acid	1797	0	8739.41 ± 1287.93					
			8	**11214.77 ± 1333.40^{c}**	**22921.44 ± 1132.77^{b}**	**25962.41 ± 1229.05^{a}**	**26544.72 ± 148.51^{a}**	**132.7**	**1.82E-09**
			18	16254.72 ± 1933.15	15211.63 ± 480.79	17237.44 ± 1635.92	20095.51 ± 589.01	1.0	4.10E-01
	Phthalic acid	1863	0	7.05 ± 0.72					
			8	4.39 ± 0.29	8.31 ± 1.02	8.83 ± 1.04	7.43 ± 1.24	3.8	3.85E-02
			18	10.58 ± 1.08	12.11 ± 1.96	9.19 ± 0.34	9.17 ± 1.06	1.4	3.00E-01
	2-Thiobarbituric acid	1893	0	89.31 ± 11.55					
			8	**117.98 ± 5.80^{d}**	**247.12 ± 29.11^{b}**	**291.79 ± 7.53^{a}**	**219.73 ± 10.94^{c}**	**128.1**	**2.23E-09**
			18	397.65 ± 69.38	342.27 ± 33.01	344.96 ± 100.66	304.83 ± 34.49	1.4	3.02E-01
Others	Unknown_01	1118	0	23.16 ± 1.16					
			8	17.18 ± 4.64	76.56 ± 18.49	94.10 ± 13.68	47.49 ± 7.29	4.0	3.56E-02
			18	85.81 ± 21.53	237.01 ± 27.11	106.51 ± 18.24	182.9 ± 73.94	0.2	8.98E-01
	Unknown_02	1157	0	219.24 ± 58.67					
			8	231.18 ± 8.72	224.37 ± 27.06	376.87 ± 69.53	224.79 ± 24.00	0.4	7.74E-01
			18	298.91 ± 67.00	485.42 ± 92.78	317.10 ± 6.15	318.08 ± 24.68	2.2	1.45E-01
	Unknown_03	1191	0	57.67 ± 8.37					
			8	**8.02 ± 0.75^{a}**	**0.32 ± 0.10^{b}**	**0.24 ± 0.00^{b}**	**0.30 ± 0.04^{b}**	**35.3**	**3.11E-06**
			18	**148.00 ± 23.61^{a}**	**0.53 ± 0.23^{b}**	**112.46 ± 55.72^{a}**	**0.44 ± 0.14^{c}**	**21.1**	**4.41E-05**
	Unknown_04	1406	0	6.68 ± 1.90					
			8	7.54 ± 0.71	11.26 ± 2.95	13.63 ± 0.83	16.17 ± 0.15	1.9	1.90E-01
			18	11.59 ± 3.25	22.03 ± 2.25	30.01 ± 8.94	28.41 ± 12.13	2.4	1.20E-01
	Unknown_05	1494	0	8.55 ± 1.53					
			8	**7.71 ± 0.14^{a}**	**16.85 ± 4.47^{a}**	**19.37 ± 1.12^{a}**	**0.30 ± 0.04^{b}**	**25.0**	**1.91E-05**
			18	**12.73 ± 1.41^{a}**	**0.53 ± 0.23^{b}**	**19.23 ± 3.71^{a}**	**12.19 ± 3.53^{a}**	**38.3**	**2.01E-06**

Table S1 – (Continued)

Class	Metabolite	RI	DAH	Hormone treatment				One-way ANOVA	
				CTRL	ETHY	IAA	ETHY+IAA	*F* value	*p* value
Others	Unknown_06	1507	0	23.64 ± 6.01					
			8	**0.15 ± 0.01^{b}**	**45.68 ± 9.49^{a}**	**79.92 ± 41.92^{a}**	**0.30 ± 0.04^{b}**	**99.0**	**9.88E-09**
			18	nd	nd	nd	nd	-	-
	Unknown_07	1538	0	nd					
			8	nd	nd	nd	nd	-	-
			18	168.64 ± 39.87	110.86 ± 3.08	123.01 ± 9.07	135.26 ± 22.15	0.2	8.95E-01
	Unknown_08	1573	0	5.22 ± 1.13					
			8	**0.15 ± 0.01^{c}**	**19.40 ± 2.48^{a}**	**12.74 ± 0.26^{b}**	**12.37 ± 2.30^{b}**	**42.1**	**1.21E-06**
			18	13.94 ± 3.11	18.70 ± 1.38	12.70 ± 1.23	13.67 ± 1.00	1.8	2.02E-01
	Unknown_09	1644	0	7.90 ± 1.60					
			8	6.00 ± 1.16	15.23 ± 2.75	12.11 ± 1.18	8.10 ± 1.43	3.9	3.75E-02
			18	**8.84 ± 2.12^{a}**	**0.53 ± 0.23^{b}**	**9.79 ± 2.88^{a}**	**7.81 ± 2.37^{a}**	**12.7**	**4.95E-04**
	Unknown_10	1670	0	9.91 ± 0.67					
			8	9.95 ± 1.69	23.34 ± 7.62	24.37 ± 0.97	13.10 ± 1.99	3.8	4.06E-02
			18	14.31 ± 1.51	11.58 ± 2.28	9.36 ± 1.20	10.47 ± 2.71	1.0	4.38E-01
	Unknown_11	1778	0	18.10 ± 2.62					
			8	8.40 ± 0.31	18.61 ± 2.35	23.98 ± 4.29	19.19 ± 2.07	2.2	1.46E-01
			18	**12.89 ± 1.52^{a}**	**0.53 ± 0.23^{b}**	**18.02 ± 3.82^{a}**	**12.68 ± 1.40^{a}**	**39.3**	**1.76E-06**
	Unknown_12	1787	0	6.29 ± 0.86					
			8	11.06 ± 0.97	26.33 ± 4.52	38.08 ± 1.98	31.24 ± 3.09	1.6	2.35E-01
			18	23.59 ± 5.53	12.08 ± 5.83	15.83 ± 0.66	17.94 ± 4.49	0.5	7.05E-01
	Unknown_13	1863	0	nd					
			8	**0.15 ± 0.01^{c}**	**23.03 ± 5.05^{a}**	**47.73 ± 6.43^{a}**	**12.60 ± 1.14^{b}**	**29.7**	**7.71E-06**
			18	**73.11 ± 24.71^{a}**	**0.53 ± 0.23^{b}**	**22.36 ± 1.79^{a}**	**23.03 ± 10.86^{a}**	**16.5**	**1.46E-04**
	Unknown_14	1873	0	30.04 ± 3.79					
			8	**54.52 ± 3.67^{b}**	**136.27 ± 45.38^{a}**	**143.84 ± 46.58^{a}**	**128.09 ± 19.55^{a}**	**5.6**	**1.23E-02**
			18	153.79 ± 29.15	113.63 ± 32.94	108.35 ± 32.12	77.86 ± 12.25	0.9	4.64E-01
	Unknown_15	2021	0	20.54 ± 2.64					
			8	**15.56 ± 1.81^{b}**	**20.64 ± 4.47^{b}**	**31.27 ± 2.50^{a}**	**40.86 ± 9.13^{a}**	**20.7**	**4.92E-05**
			18	**10.96 ± 1.40^{a}**	**0.53 ± 0.23^{b}**	**21.92 ± 4.54^{a}**	**14.22 ± 4.96^{a}**	**4.8**	**2.02E-02**

Table S1 – (Continued)

Class	Metabolite	RI	DAH	Hormone treatment				One-way ANOVA	
				CTRL	ETHY	IAA	ETHY+IAA	*F* value	*p* value
Others	Unknown_16	2029	0	nd					
			8	**6.76 ± 1.09^{b}**	**18.07 ± 6.58^{a}**	**29.89 ± 4.91^{a}**	**0.30 ± 0.04^{c}**	**31.8**	**5.41E-06**
			18	50.90 ± 15.74	16.84 ± 6.62	13.35 ± 2.64	18.91 ± 2.09	1.2	3.61E-01
	Unknown_17	2037	0	nd					
			8	nd	nd	nd	nd	-	-
			18	**10.15 ± 1.76^{a}**	**0.53 ± 0.23^{b}**	**20.92 ± 3.10^{a}**	**14.17 ± 5.62^{a}**	**35.3**	**3.10E-06**
	Unknown_18	2122	0	216.20 ± 98.56					
			8	**114.31 ± 17.44^{c}**	**447.91 ± 121.64^{a}**	**233.72 ± 7.63^{b}**	**196.03 ± 7.96^{b}**	**38.8**	**1.88E-06**
			18	**344.72 ± 133.19^{a}**	**0.53 ± 0.23^{b}**	**234.58 ± 35.19^{a}**	**382.77 ± 142.69^{a}**	**38.2**	**2.03E-06**
	Unknown_19	2131	0	48.33 ± 5.58					
			8	**29.83 ± 3.45^{b}**	**148.25 ± 55.55^{a}**	**59.69 ± 7.86^{a}**	**0.30 ± 0.04^{c}**	**54.3**	**2.97E-07**
			18	**193.92 ± 74.37^{a}**	**0.53 ± 0.23^{b}**	**0.40 ± 0.09^{b}**	**115.06 ± 30.38^{a}**	**69.4**	**7.49E-08**
	Unknown_20	2161	0	29.06 ± 2.79					
			8	36.65 ± 3.14	81.41 ± 24.52	52.61 ± 6.51	68.60 ± 9.25	1.0	4.11E-01
			18	71.73 ± 12.07	48.04 ± 36.32	61.00 ± 9.27	73.33 ± 7.09	0.8	5.34E-01
	Unknown_21	2179	0	nd					
			8	**0.15 ± 0.01^{c}**	**43.21 ± 11.68^{a}**	**26.44 ± 5.50^{b}**	**27.56 ± 4.98^{b}**	**588.5**	**2.77E-13**
			18	392.59 ± 102.09	435.56 ± 103.29	121.54 ± 57.32	159.72 ± 8.38	2.3	1.30E-01
	Unknown_22	2255	0	89.63 ± 13.96					
			8	**91.53 ± 5.15^{c}**	**226.74 ± 48.85^{a}**	**198.91 ± 3.56^{a}**	**149.48 ± 28.62^{b}**	**31.3**	**5.87E-06**
			18	**140.34 ± 13.55^{a}**	**0.76 ± 0.19^{b}**	**0.40 ± 0.09^{b}**	**169.63 ± 38.29^{a}**	**60.8**	**1.58E-07**
	Unknown_23	2266	0	70.74 ± 16.22					
			8	59.23 ± 5.65	138.64 ± 41.43	169.30 ± 11.12	130.82 ± 24.93	2.2	1.41E-01
			18	**101.63 ± 28.98^{a}**	**0.76 ± 0.19^{b}**	**78.29 ± 13.92^{a}**	**98.94 ± 34.95^{a}**	**36.1**	**2.75E-06**
	Unknown_24	2329	0	62.12 ± 30.77					
			8	71.85 ± 17.23	159.23 ± 54.15	154.51 ± 22.48	70.65 ± 10.09	3.3	5.77E-02
			18	**134.00 ± 109.69^{a}**	**0.76 ± 0.19^{b}**	**68.10 ± 45.65^{a}**	**52.09 ± 36.14^{a}**	**5.1**	**1.70E-02**
	Unknown_25	2473	0	10.10 ± 2.65					
			8	12.01 ± 1.90	20.96 ± 10.40	32.68 ± 13.37	23.45 ± 7.82	3.3	5.60E-02
			18	40.03 ± 14.41	29.52 ± 21.21	13.62 ± 3.81	6.62 ± 2.20	1.2	3.42E-01

Table S1 – (Continued)

Class	Metabolite	RI	DAH	Hormone treatment				One-way ANOVA	
				CTRL	ETHY	IAA	ETHY+IAA	*F* value	*p* value
Others	Unknown_26	2571	0	1.85 ± 1.32					
			8	**6.65 ± 0.90^{b}**	**0.32 ± 0.10^{c}**	**12.85 ± 1.24^{a}**	**10.01 ± 2.31^{a}**	**297.8**	**1.58E-11**
			18	**15.48 ± 7.20^{a}**	**0.76 ± 0.19^{b}**	**12.10 ± 1.17^{a}**	**6.14 ± 1.67^{a}**	**8.9**	**2.19E-03**
	Unknown_27	2587	0	9.08 ± 4.74					
			8	**16.37 ± 4.30^{a}**	**11.41 ± 3.61^{b}**	**10.42 ± 0.84^{b}**	**8.02 ± 1.49^{b}**	**5.8**	**1.11E-02**
			18	nd	nd	nd	nd	-	-
	Unknown_28	2817	0	22.96 ± 10.84					
			8	13.54 ± 3.59	42.8 ± 7.89	47.53 ± 13.47	41.82 ± 7.64	2.1	1.48E-01
			18	nd	nd	nd	nd	-	-
	Unknown_29	2958	0	nd					
			8	35.83 ± 2.77	172.10 ± 47.90	60.82 ± 8.72	42.39 ± 3.77	2.3	1.26E-01
			18	**16.49 ± 6.90a**	**0.76 ± 0.19^{b}**	**0.51 ± 0.12^{b}**	**20.23 ± 6.64^{a}**	**14.3**	**2.84E-04**
	Unknown_30	2976	0	nd					
			8	9.47 ± 1.85	34.91 ± 8.76	23.33 ± 3.56	13.83 ± 1.23	0.7	5.95E-01
			18	**19.19 ± 5.07^{a}**	**0.76 ± 0.19^{b}**	**0.51 ± 0.12^{b}**	**10.59 ± 4.80^{a}**	**6.4**	**7.79E-03**
	Unknown_31	>3000	0	9.69 ± 2.33					
			8	6.67 ± 0.64	31.18 ± 9.39	21.38 ± 4.59	14.46 ± 3.46	0.9	4.88E-01
			18	**17.38 ± 7.13^{a}**	**0.76 ± 0.19^{c}**	**7.15 ± 3.53^{a}**	**3.61 ± 1.76^{b}**	**13.5**	**3.79E-04**
	Unknown_32	>3000	0	23.14 ± 4.83					
			8	**9.94 ± 0.81^{b}**	**38.43 ± 10.19^{a}**	**34.92 ± 2.61^{a}**	**40.55 ± 13.36^{a}**	**27.4**	**1.19E-05**
			18	**18.19 ± 3.64^{a}**	**0.76 ± 0.19^{b}**	**0.51 ± 0.12^{b}**	**17.15 ± 7.96^{a}**	**16.5**	**1.48E-04**
	Unknown_33	>3000	0	64.24 ± 8.73					
			8	**19.79 ± 4.71^{c}**	**63.16 ± 16.93^{a}**	**73.98 ± 15.49^{a}**	**39.37 ± 4.64^{b}**	**24.3**	**2.20E-05**
			18	**27.27 ± 9.05^{a}**	**0.76 ± 0.19^{b}**	**0.51 ± 0.12^{b}**	**0.44 ± 0.14^{b}**	**24.2**	**2.25E-05**
	Unknown_34	>3000	0	nd					
			8	502.70 ± 88.04	1454.20 ± 350.43	1562.06 ± 346.79	1107.46 ± 257.51	3.1	6.81E-02
			18	**1393.78 ± 306.82^{a}**	**792.82 ± 606.58^{a}**	**510.13 ± 12.17^{b}**	**1199.10 ± 510.54^{a}**	**50.4**	**4.46E-07**

RI: Retention index, relative to n-alkanes (C10-C30) on the SupelcoWax capillary column. DAH: Days after harvest. CTRL: Control fruits. ETHY: Ethylene-treated fruits. IAA: Indole-3-acetic acid-treated fruits. ETHY+IAA: Fruits treated with both hormones. nd: not determined. *F* value and *p* value (fold discovery rate) were calculated using one-way ANOVA analysis (Tukey HSD). Values in bold letters and different superscript letters indicate statistical significance ($p < 0.05$) at the same DAH (mean ± standard deviation, n = 4).

Table S2 – Non-polar metabolites in three ripening stages of Micro-Tom tomato (*Solanum lycopersicum* L.) fruits detected by gas chromatography-mass spectrometry (GC-MS)

Class	Metabolite	RI	DAH	Hormone treatment				One-way ANOVA	
				CTRL	ETHY	IAA	ETHY+IAA	*F* value	*p* value
Saturated fatty acids	Caprylic acid	1127	0	1.16 ± 0.53					
			8	0.90 ± 0.14	0.93 ± 0.19	1.80 ± 0.64	0.80 ± 0.04	0.9	4.64E-01
			18	0.59 ± 0.14	0.47 ± 0.06	0.32 ± 0.08	0.48 ± 0.13	1.9	1.89E-01
	Lauric acid	1520	0	14.50 ± 1.26					
			8	11.62 ± 0.61	15.84 ± 0.57	46.81 ± 3.48	59.43 ± 3.38	5.3	1.46E-02
			18	46.72 ± 0.62	60.08 ± 6.36	64.25 ± 0.74	72.95 ± 22.54	3.1	6.74E-02
	Myristic acid	1719	0	45.93 ± 3.76					
			8	55.95 ± 1.26	52.73 ± 11.17	41.55 ± 7.84	74.35 ± 0.41	2.2	1.36E-01
			18	63.13 ± 2.58	50.89 ± 8.79	57.72 ± 13.1	56.68 ± 7.52	1.1	3.90E-01
	Pentadecylic acid	1819	0	12.87 ± 0.51					
			8	16.39 ± 1.14	17.81 ± 0.96	18.02 ± 1.77	22.55 ± 2.23	1.1	3.97E-01
			18	13.07 ± 0.86	11.34 ± 1.2	16.79 ± 1.58	14.11 ± 0.61	0.7	5.93E-01
	Palmitic Acid	1933	0	9728.55 ± 372.11					
			8	10583.34 ± 1100.29	8024.17 ± 1828.56	5609.39 ± 1141.75	13555.11 ± 857.40	3.8	3.88E-02
			18	7528.92 ± 742.96	3153.86 ± 1041.23	5837.10 ± 1685.62	4021.81 ± 1343.20	2.9	7.67E-02
	Margaric acid	2020	0	23.49 ± 2.89					
			8	24.66 ± 2.66	32.24 ± 2.34	28.78 ± 3.09	26.10 ± 1.81	0.3	8.19E-01
			18	26.46 ± 2.06	27.20 ± 2.89	20.65 ± 5.49	21.36 ± 1.68	0.6	6.32E-01
	Stearic acid	2135	0	2304.95 ± 165.21					
			8	2068.75 ± 243.88	1759.55 ± 492.87	1214.58 ± 312.38	3004.92 ± 339.60	1.1	3.69E-01
			18	1516.00 ± 221.15	527.96 ± 195.84	1309.56 ± 609.42	673.17 ± 241.11	2.3	1.26E-01
	Arachidic acid	2322	0	203.47 ± 6.36					
			8	**237.35 ± 14.59[a]**	**168.86 ± 37.31[b]**	**147.62 ± 29.19[b]**	**286.83 ± 5.05[a]**	**14.3**	**2.87E-04**
			18	132.20 ± 13.41	92.25 ± 21.00	122.33 ± 34.88	130.14 ± 35.90	1.5	2.72E-01
	Henicosanoic acid	2421	0	9.21 ± 2.04					
			8	**12.34 ± 0.94[a]**	**8.01 ± 1.43[b]**	**10.42 ± 2.02[a]**	**17.00 ± 1.93[a]**	**7.1**	**5.29E-03**
			18	6.80 ± 0.25	3.99 ± 1.24	6.33 ± 1.35	5.71 ± 1.47	3.0	7.04E-02
	Behenic acid	2523	0	83.55 ± 1.53					
			8	118.04 ± 3.21	99.42 ± 12.71	91.62 ± 20.57	148.22 ± 0.94	2.9	8.03E-02
			18	78.95 ± 4.16	66.64 ± 9.21	71.26 ± 8.20	60.04 ± 6.75	0.5	7.13E-01

Table S2 – (Continued)

Class	Metabolite	RI	DAH	Hormone treatment				One-way ANOVA	
				CTRL	ETHY	IAA	ETHY+IAA	*F* value	*p* value
Saturated fatty acids	Tricosylic acid	2623	0	32.88 ± 2.44					
			8	65.44 ± 4.30	48.72 ± 6.36	61.00 ± 6.75	76.55 ± 3.65	0.6	6.13E-01
			18	41.83 ± 0.92	42.24 ± 1.44	47.95 ± 15.53	48.17 ± 5.77	0.7	5.86E-01
	Lignoceric acid	2725	0	147.25 ± 8.69					
			8	227.46 ± 5.70	202.42 ± 37.52	154.63 ± 24.60	264.54 ± 18.81	0.9	4.54E-01
			18	175.32 ± 4.53	146.53 ± 14.29	156.12 ± 28.46	137.69 ± 20.82	2.4	1.21E-01
	Hyenic acid	2824	0	34.40 ± 0.94					
			8	50.23 ± 4.14	48.86 ± 7.08	56.52 ± 7.77	66.31 ± 2.79	2.1	1.55E-01
			18	54.04 ± 1.57	49.71 ± 2.32	34.25 ± 15.63	44.78 ± 11.26	0.5	7.02E-01
	Cerotic acid	2925	0	34.68 ± 0.97					
			8	46.38 ± 1.32	44.75 ± 5.51	32.68 ± 4.81	57.58 ± 2.29	1.9	1.90E-01
			18	42.01 ± 0.25	28.16 ± 2.56	27.91 ± 8.45	35.17 ± 0.27	1.1	3.91E-01
Unsaturated fatty acids	Palmitoleic acid	1898	0	89.73 ± 2.92					
			8	**122.28 ± 11.41^{a}**	**79.75 ± 21.44^{b}**	**64.12 ± 13.50^{b}**	**132.90 ± 3.80^{a}**	**6.8**	**6.09E-03**
			18	87.39 ± 14.23	37.88 ± 8.76	63.31 ± 13.83	61.98 ± 9.54	3.2	6.04E-02
	Elaidic acid	2113	0	3.54 ± 0.04					
			8	4.62 ± 0.48	5748.14 ± 199.51	7361.75 ± 726.01	5.51 ± 0.97	0.4	7.36E-01
			18	8156.67 ± 961.71	5537.70 ± 2734.82	6873.68 ± 1616.81	4571.85 ± 2170.65	0.3	7.94E-01
	Oleic acid	2216	0	91.19 ± 3.33					
			8	**95.28 ± 4.64^{b}**	**59.89 ± 18.36^{b}**	**69.66 ± 15.20^{b}**	**150.34 ± 17.76^{a}**	**5.9**	**1.05E-02**
			18	72.89 ± 11.26	42.50 ± 14.27	128.25 ± 42.83	96.09 ± 11.18	1.3	3.22E-01
	Rumenic acid	2119	0	15.03 ± 1.31					
			8	6.10 ± 0.36	14.34 ± 3.27	15.00 ± 0.82	22.07 ± 7.88	1.6	2.30E-01
			18	16.75 ± 1.20	6.34 ± 2.50	14.49 ± 4.44	16.12 ± 6.38	2.5	1.05E-01
	Linoleic acid	2211	0	287.42 ± 23.06					
			8	314.24 ± 44.55	210.26 ± 60.46	247.39 ± 53.98	478.64 ± 40.61	5.3	1.48E-02
			18	261.04 ± 32.18	132.97 ± 22.58	408.37 ± 137.48	306.63 ± 52.97	1.7	2.27E-01
	Linolenic acid	2279	0	14.54 ± 0.73					
			8	**21.88 ± 3.56^{b}**	**23.53 ± 2.59^{b}**	**15.28 ± 2.19^{c}**	**29.90 ± 1.49^{a}**	**21.4**	**4.13E-05**

		18	17.68 ± 1.37	16.96 ± 4.22	12.10 ± 2.32	22.29 ± 2.15	0.5	7.17E-01

Table S2 – (Continued)

Class	Metabolite	RI	DAH	Hormone treatment				One-way ANOVA	
				CTRL	ETHY	IAA	ETHY+IAA	*F* value	*p* value
Unsaturated fatty acids	Gadoleic acid	2295	0	43.91 ± 2.33					
			8	54.39 ± 6.36	40.45 ± 7.04	27.00 ± 8.07	59.81 ± 6.38	0.9	4.79E-01
			18	44.28 ± 0.94	33.49 ± 2.72	28.21 ± 5.19	33.19 ± 5.39	1.1	3.71E-01
Branched fatty acids	Isopalmitic acid	1882	0	11.53 ± 0.06					
			8	0.11 ± 0.00	8.81 ± 1.09	7.47 ± 0.95	12.66 ± 1.16	4.6	2.35E-02
			18	7.03 ± 1.05	4.34 ± 0.40	9.54 ± 2.54	8.08 ± 2.31	0.8	5.17E-01
	Isomargaric acid	1991	0	22.34 ± 5.93					
			8	**11.75 ± 0.45[a]**	**11.66 ± 0.20[a]**	**11.33 ± 2.54[a]**	**0.14 ± 0.01[b]**	**8.6**	**2.56E-03**
			18	7.69 ± 0.47	11.12 ± 2.60	7.55 ± 2.02	6.73 ± 0.55	1.8	2.09E-01
Acylglycerols	Glyceryl 2-palmitate	2566	0	15.09 ± 3.00					
			8	20.26 ± 7.54	13.94 ± 0.45	12.13 ± 2.07	15.96 ± 3.27	4.2	3.00E-02
			18	10.53 ± 1.00	23.00 ± 6.65	14.89 ± 6.57	18.24 ± 1.84	0.6	6.02E-01
	Glyceryl 1-palmitate	2598	0	134.59 ± 50.53					
			8	45.25 ± 24.08	129.76 ± 32.84	130.03 ± 37.01	202.23 ± 36.81	0.0	9.97E-01
			18	95.52 ± 22.68	50.86 ± 17.05	102.65 ± 61.55	124.31 ± 40.08	0.7	5.97E-01
	Glyceryl 2-oleate	2731	0	58.46 ± 27.02					
			8	31.12 ± 11.6	54.11 ± 14.67	59.85 ± 18.86	91.72 ± 8.05	3.2	6.38E-02
			18	45.45 ± 9.19	21.18 ± 8.17	49.43 ± 29.79	65.47 ± 15.29	0.9	4.70E-01
	Glyceryl 1-linoleate	2768	0	555.25 ± 243.15					
			8	189.64 ± 92.83	605.99 ± 179.17	593.83 ± 189.04	999.68 ± 183.75	1.1	3.76E-01
			18	520.77 ± 154.78	210.74 ± 74.72	591.64 ± 204.47	669.90 ± 249.12	1.6	2.38E-01
	Glyceryl 1-stearate	2793	0	73.26 ± 13.26					
			8	**118.08 ± 57.78[a]**	**67.93 ± 14.64[b]**	**74.20 ± 20.97[b]**	**104.27 ± 12.27[a]**	**6.4**	**7.75E-03**
			18	66.30 ± 30.14	60.94 ± 5.10	10.35 ± 3.55	32.93 ± 9.08	0.2	8.61E-01
Fatty alcohols	Lauryl alcohol	1569	0	15.46 ± 1.41					
			8	11.20 ± 5.21	18.58 ± 4.58	36.88 ± 9.46	31.35 ± 11.79	1.1	3.89E-01
			18	17.96 ± 7.30	19.05 ± 3.93	20.48 ± 6.74	18.21 ± 4.69	0.5	7.01E-01
	Myristyl alcohol	1763	0	19.09 ± 4.90					
			8	5.59 ± 2.47	15.01 ± 4.76	21.28 ± 6.36	30.26 ± 11.28	2.1	1.49E-01
			18	24.91 ± 7.77	12.57 ± 5.46	31.72 ± 14.17	16.44 ± 1.69	0.3	8.54E-01

Table S2 – (Continued)

Class	Metabolite	RI	DAH	Hormone treatment				One-way ANOVA	
				CTRL	ETHY	IAA	ETHY+IAA	*F* value	*p* value
Fatty alcohols	Stearyl alcohol	2159	0	5.53 ± 1.69					
			8	10.68 ± 3.64	13.00 ± 2.27	19.9 ± 4.12	12.73 ± 1.87	0.4	7.46E-01
			18	18.44 ± 5.22	18.49 ± 1.24	17.96 ± 5.63	14.47 ± 2.27	0.5	6.67E-01
	Arachidic alcohol	2350	0	12.80 ± 1.46					
			8	**20.95 ± 2.35^{a}**	**16.85 ± 0.19^{b}**	**17.13 ± 1.94^{b}**	**19.55 ± 0.48^{a}**	**6.5**	**7.30E-03**
			18	11.44 ± 1.24	18.17 ± 0.39	9.09 ± 3.54	10.55 ± 1.71	1.3	3.08E-01
	Lignoceryl alcohol	2744	0	1.37 ± 0.28					
			8	3.58 ± 0.58	4.49 ± 0.79	3.32 ± 0.29	4.11 ± 0.89	1.1	4.00E-01
			18	3.99 ± 0.56	4.08 ± 0.61	3.19 ± 0.45	3.87 ± 0.57	0.6	6.38E-01
Hydroxyl-linked fatty acids	2-hydroxypalmitic acid	2136	0	147.65 ± 8.48					
			8	162.90 ± 21.54	132.03 ± 40.00	88.80 ± 27.78	169.14 ± 67.71	1.6	2.41E-01
			18	**134.36 ± 9.62^{a}**	**77.13 ± 9.60^{b}**	**95.76 ± 33.24^{b}**	**57.61 ± 13.80^{b}**	**10.3**	**1.23E-03**
	2-hydroxybehenic acid	2716	0	21.87 ± 2.36					
			8	26.73 ± 1.46	22.76 ± 0.77	21.18 ± 2.83	25.83 ± 1.52	1.4	3.01E-01
			18	21.62 ± 1.02	24.2 ± 1.38	24.5 ± 1.60	27.12 ± 0.78	1.2	3.51E-01
	2-hydroxytricosylic acid	2814	0	12.23 ± 2.33					
			8	**15.79 ± 1.50^{b}**	**15.07 ± 1.55^{ac}**	**13.49 ± 1.17^{c}**	**20.74 ± 1.81^{a}**	**15.7**	**1.89E-04**
			18	**16.37 ± 1.35^{b}**	**11.69 ± 1.58^{c}**	**16.44 ± 1.81^{b}**	**19.26 ± 0.91^{a}**	**18.1**	**9.45E-05**
	2-hydroxylignoceric acid	2913	0	77.67 ± 13.41					
			8	98.49 ± 6.80	103.67 ± 7.93	108.30 ± 13.09	140.91 ± 7.50	0.3	7.97E-01
			18	105.23 ± 3.97	104.80 ± 7.73	113.52 ± 9.69	126.05 ± 8.72	0.2	9.23E-01
	2-Hydroxycerotic acid	>3000	0	16.65 ± 0.53					
			8	20.20 ± 2.13	23.15 ± 1.20	23.34 ± 3.19	25.82 ± 2.80	1.0	4.17E-01
			18	21.91 ± 0.71	19.73 ± 1.16	25.86 ± 4.92	28.55 ± 3.32	0.5	6.66E-01
Sterols and derivated	Dehydroabietic acid	2387	0	nd					
			8	6.62 ± 1.07	5.44 ± 1.91	6.41 ± 1.80	3.86 ± 0.28	2.6	1.00E-01
			18	5.51 ± 1.65	2.72 ± 1.10	4.69 ± 0.28	5.85 ± 1.62	4.3	2.80E-02
	γ--tocopherol	>3000	0	34.67 ± 5.06					
			8	61.87 ± 5.52	44.29 ± 6.34	30.04 ± 3.76	64.64 ± 8.43	0.7	5.53E-01
			18	36.59 ± 1.71	28.23 ± 2.43	40.30 ± 13.25	46.40 ± 14.25	1.3	3.12E-01

Table S2 – (Continued)

Class	Metabolite	RI	DAH	Hormone treatment				One-way ANOVA	
				CTRL	ETHY	IAA	ETHY+IAA	*F* value	*p* value
Sterols and derivated	α-tocopherol	>3000	0	123.97 ± 16.12					
			8	130.13 ± 3.34	177.64 ± 6.74	126.14 ± 11.76	142.84 ± 6.29	0.8	5.06E-01
			18	205.75 ± 15.64	188.39 ± 31.90	118.60 ± 20.95	215.06 ± 25.41	2.0	1.74E-01
	Campesterol	>3000	0	61.22 ± 2.55					
			8	42.94 ± 0.89	51.80 ± 5.06	44.96 ± 1.54	56.83 ± 7.29	0.3	8.13E-01
			18	39.24 ± 1.94	41.37 ± 0.58	42.59 ± 5.13	45.84 ± 3.07	1.0	4.40E-01
	Stigmasterol	>3000	0	190.17 ± 15.96					
			8	282.85 ± 2.11	322.66 ± 45.78	205.29 ± 43.69	337.6 ± 19.10	5.2	1.60E-02
			18	444.64 ± 3.21	401.06 ± 39.23	347.71 ± 81.55	413.49 ± 49.35	0.5	6.99E-01
	β-sitosterol	>3000	0	489.80 ± 43.79					
			8	450.56 ± 28.79	442.09 ± 64.60	460.37 ± 96.45	638.5 ± 26.57	2.2	1.47E-01
			18	275.58 ± 16.61	213.97 ± 21.17	250.87 ± 30.31	210.34 ± 35.36	1.5	2.61E-01
	β-amyrin	>3000	0	28.84 ± 11.28					
			8	27.16 ± 5.82	20.32 ± 8.79	26.99 ± 5.32	28.67 ± 4.66	0.5	7.20E-01
			18	51.39 ± 6.56	60.85 ± 7.52	43.05 ± 14.45	49.36 ± 7.83	0.3	8.38E-01
	α-amyrin	>3000	0	30.50 ± 0.03					
			8	**30.06 ± 0.76^{b}**	**39.54 ± 8.53^{a}**	**41.88 ± 2.00^{a}**	**44.46 ± 3.50^{a}**	**8.8**	**2.37E-03**
			18	25.24 ± 3.45	42.53 ± 8.43	32.46 ± 4.26	40.43 ± 5.06	0.7	5.74E-01
	Cycloartenol	>3000	0	5.05 ± 1.96					
			8	13.08 ± 2.23	15.09 ± 3.72	14.93 ± 2.24	15.25 ± 2.46	1.4	2.86E-01
			18	**11.04 ± 0.78^{b}**	**13.19 ± 1.93^{b}**	**6.08 ± 1.30^{c}**	**16.12 ± 0.57^{a}**	**129.6**	**2.09E-09**

RI: Retention index, relative to n-alkanes (C10-C30) on the SupelcoWax capillary column. DAH: Days after harvest. CTRL: Control fruits. ETHY: Ethylene-treated fruits. IAA: Indole-3-acetic acid-treated fruits. ETHY+IAA: Fruits treated with both hormones. nd: not determined. *F* value and *p* value (fold discovery rate) were calculated using one-way ANOVA analysis (Tukey HSD). Values in bold letters and different superscript letters indicate statistical significance ($p < 0.05$) at the same DAH (mean ± standard deviation, n = 4).

Table S3 – Carotenoid contents in three ripening stages of Micro-Tom tomato (*Solanum lycopersicum* L.) fruits detected by high-performance liquid chromatography (HPLC)

Metabolite	DAH	Hormone treatment				One-way ANOVA	
		CTRL	ETHY	IAA	ETHY+IAA	*F* value	*p* value
Lutein	0	3.66 ± 0.45					
	8	3.29 ± 0.38	2.72 ± 0.48	3.64 ± 0.71	2.94 ± 1.04	1.3	3.10E-01
	18	**2.17 ± 0.08^{b}**	**2.04 ± 0.02^{c}**	**2.02 ± 0.02^{d}**	**2.73 ± 0.05^{a}**	**189.6**	**2.26E-10**
Lycopene	0	9.23 ± 0.43					
	8	8.65 ± 0.44	8.32 ± 0.93	9.12 ± 0.77	8.44 ± 0.84	0.5	6.71E-01
	18	**578.01 ± 53.41^{a}**	**337.62 ± 65.73^{b}**	**190.5 ± 78.35^{d}**	**225.46 ± 63.93^{c}**	**0.8**	**5.38E-01**
β-carotene	0	2.52 ± 0.21					
	8	**2.89 ± 0.38^{b}**	**3.55 ± 0.51^{a}**	**2.66 ± 0.2^{b}**	**2.41 ± 0.27^{b}**	**7.5**	**4.43E-03**
	18	**3.91 ± 0.16^{b}**	**4.27 ± 0.48^{a}**	**3.39 ± 0.35^{d}**	**3.59 ± 0.24^{c}**	**1.2**	**3.55E-01**

DAH: Days after harvest. CTRL: Control fruits. ETHY: Ethylene-treated fruits. IAA: Indole-3-acetic acid-treated fruits. ETHY+IAA: Fruits treated with both hormones. *F* value and *p* value (fold discovery rate) were calculated using one-way ANOVA analysis (Tukey HSD). Values in bold letters and different superscript letters indicate statistical significance ($p < 0.05$) at the same DAH (mean ± standard deviation, n = 4).

Table S4 - Metabolic pathways differentially modified by treatment with ethylene, auxin, or both hormones in Micro-Tom tomato (*Solanum lycopersicum* L.) fruits at 8 and 18 days after harvest (DAH)

ID	Pathway name	Match	Impact	8 DAH						18 DAH					
				ETHY *vs*. CTRL		IAA *vs*. CTRL		ETHY+IAA *vs*. CTRL		ETHY *vs*. CTRL		IAA *vs*. CTRL		ETHY+IAA *vs*. CTRL	
				-LOG(p)	FDR	-LOG(p)	FDR	-LOG(p)	FDR	-LOG(p)	FDR	-LOG(p)	FDR	-LOG(p)	FDR
1	Linoleic acid metabolism	1/4	1.000	2.967	6.29E-02	2.163	1.22E-01	**6.289**	**3.00E-03**	**7.419**	**2.06E-03**	**2.991**	**7.08E-02**	1.648	2.35E-01
2	Alanine, aspartate and glutamate metabolism	5/22	0.579	**12.597**	**1.69E-05**	**8.773**	**5.32E-04**	**11.156**	**4.94E-05**	**17.184**	**1.89E-06**	**13.815**	**7.86E-06**	**18.361**	**1.71E-07**
3	Glycine, serine and threonine metabolism	4/33	0.513	**7.410**	**1.11E-03**	**5.827**	**5.45E-03**	**9.126**	**2.72E-04**	**8.399**	**1.24E-03**	**4.562**	**1.98E-02**	**10.280**	**1.57E-04**
4	C5-Branched dibasic acid metabolism	1/6	0.500	**5.046**	**1.01E-02**	**5.577**	**6.48E-03**	**3.524**	**3.60E-02**	2.421	9.77E-02	**4.432**	**2.11E-02**	**4.038**	**2.85E-02**
5	Phenylalanine metabolism	1/11	0.471	0.587	5.56E-01	**4.332**	**1.76E-02**	2.507	9.15E-02	**5.136**	**1.04E-02**	**14.183**	**6.35E-06**	1.982	1.76E-01
6	Starch and sucrose metabolism	3/22	0.401	**4.206**	**2.16E-02**	**14.467**	**1.43E-05**	**15.034**	**2.71E-06**	**10.549**	**2.75E-04**	**5.654**	**9.63E-03**	2.247	1.49E-01
7	Carotenoid biosynthesis	3/43	0.277	2.593	8.68E-02	0.761	4.76E-01	1.354	2.63E-01	**5.884**	**6.38E-03**	**6.442**	**5.16E-03**	**9.471**	**3.26E-04**
8	Glyoxylate and dicarboxylate metabolism	7/29	0.264	**12.649**	**1.69E-05**	**10.812**	**1.01E-04**	**11.044**	**5.17E-05**	**7.950**	**1.39E-03**	**10.092**	**2.28E-04**	**16.728**	**3.74E-07**
9	β-Alanine metabolism	2/18	0.254	**6.829**	**1.92E-03**	**5.243**	**8.07E-03**	**4.366**	**1.62E-02**	**7.496**	**2.04E-03**	**3.535**	**4.46E-02**	0.010	9.90E-01
10	Citrate cycle (TCA cycle)	4/20	0.236	**12.785**	**1.69E-05**	**14.684**	**1.43E-05**	**12.255**	**2.18E-05**	2.449	9.77E-02	**11.094**	**9.29E-05**	**12.993**	**1.14E-05**
11	Pyruvate metabolism	2/22	0.228	**11.003**	**5.39E-05**	**12.761**	**3.77E-05**	**13.040**	**1.19E-05**	**6.981**	**2.73E-03**	**8.709**	**7.63E-04**	**8.581**	**6.45E-04**
12	Arginine and proline metabolism	3/34	0.144	**13.844**	**1.27E-05**	**8.500**	**6.22E-04**	**10.661**	**6.79E-05**	**8.589**	**1.24E-03**	**5.496**	**1.08E-02**	**18.087**	**1.71E-07**
13	Butanoate metabolism	3/17	0.136	**13.334**	**1.27E-05**	**10.847**	**1.01E-04**	**10.579**	**7.00E-05**	**8.126**	**1.25E-03**	**5.227**	**1.28E-02**	**17.508**	**2.28E-07**
14	Cutin, suberine and wax biosynthesis	3/18	0.125	**3.973**	**2.52E-02**	**5.509**	**6.55E-03**	**8.876**	**3.25E-04**	**6.845**	**2.93E-03**	**4.866**	**1.63E-02**	**6.404**	**4.34E-03**
15	Glutathione metabolism	2/26	0.122	**11.324**	**4.74E-05**	**5.408**	**7.04E-03**	**7.071**	**1.61E-03**	**5.513**	**8.54E-03**	**4.716**	**1.82E-02**	**13.214**	**1.00E-05**
16	Aminoacyl-tRNA biosynthesis	10/46	0.111	**12.881**	**1.69E-05**	**7.987**	**9.84E-04**	**14.055**	**6.18E-06**	**14.815**	**1.01E-05**	**14.992**	**6.35E-06**	**17.227**	**2.59E-07**
17	α-Linolenic acid metabolism	1/28	0.107	0.821	4.74E-01	**4.192**	**1.93E-02**	**4.850**	**1.08E-02**	0.422	6.68E-01	**4.382**	**2.15E-02**	**4.713**	**1.70E-02**
18	Inositol phosphate metabolism	1/28	0.103	**7.662**	**9.24E-04**	**11.960**	**4.40E-05**	**11.150**	**4.94E-05**	2.734	7.77E-02	1.702	2.18E-01	**3.254**	**5.90E-02**
19	Arginine biosynthesis	2/18	0.085	**11.375**	**4.74E-05**	**4.233**	**1.90E-02**	**8.071**	**6.36E-04**	**11.170**	**1.94E-04**	**3.812**	**3.58E-02**	**18.860**	**1.71E-07**
20	Pantothenate and CoA biosynthesis	2/23	0.084	**7.814**	**8.89E-04**	**5.818**	**5.45E-03**	1.562	2.18E-01	**8.176**	**1.25E-03**	**6.838**	**3.69E-03**	0.588	6.36E-01
21	Carbon fixation in photosynthetic organisms	2/21	0.058	**11.257**	**4.74E-05**	**12.584**	**3.77E-05**	**12.673**	**1.57E-05**	**4.797**	**1.34E-02**	**5.154**	**1.32E-02**	**6.188**	**4.71E-03**
22	Galactose metabolism	5/27	0.048	**11.055**	**5.39E-05**	**12.909**	**3.77E-05**	**18.386**	**1.90E-07**	**6.190**	**4.90E-03**	**3.506**	**4.46E-02**	**4.086**	**2.80E-02**
23	Sulfur metabolism	2/15	0.033	**6.784**	**1.94E-03**	**9.309**	**3.60E-04**	**5.382**	**7.02E-03**	**3.820**	**2.94E-02**	1.165	3.50E-01	**9.010**	**4.48E-04**
24	Phosphatidylinositol signaling system	1/26	0.033	**7.662**	**9.24E-04**	**11.960**	**4.40E-05**	**11.150**	**4.94E-05**	2.734	7.77E-02	1.702	2.18E-01	**3.254**	**5.90E-02**
25	Valine, leucine and isoleucine biosynthesis	4/22	0.021	**13.610**	**1.27E-05**	**9.171**	**3.82E-04**	**13.068**	**1.19E-05**	**6.966**	**2.73E-03**	**7.525**	**2.28E-03**	**7.557**	**1.60E-03**

Table S4 – (Continued)

ID	Pathway name	Match	Impact	8 DAH						18 DAH					
				ETHY *vs*. CTRL		IAA *vs*. CTRL		ETHY+IAA *vs*. CTRL		ETHY *vs*. CTRL		IAA *vs*. CTRL		ETHY+IAA *vs*. CTRL	
				-LOG(p)	FDR	-LOG(p)	FDR	-LOG(p)	FDR	-LOG(p)	FDR	-LOG(p)	FDR	-LOG(p)	FDR
26	Glycerolipid metabolism	1/21	0.013	**4.406**	**1.81E-02**	**5.759**	**5.60E-03**	**19.532**	**1.55E-07**	**3.153**	**5.47E-02**	0.053	9.48E-01	0.142	9.54E-01
27	Amino sugar and nucleotide sugar metabolism	3/50	0.013	**8.467**	**5.78E-04**	**7.508**	**1.26E-03**	**6.753**	**1.95E-03**	**5.774**	**6.84E-03**	**8.700**	**7.63E-04**	**9.197**	**3.98E-04**
28	Fatty acid biosynthesis	6/56	0.011	**4.126**	**2.28E-02**	**9.427**	**3.60E-04**	**13.418**	**1.02E-05**	**7.054**	**2.73E-03**	**3.523**	**4.46E-02**	**7.218**	**2.12E-03**
29	Glycerophospholipid metabolism	1/37	0.009	1.879	1.71E-01	**3.827**	**2.66E-02**	1.584	2.17E-01	**5.447**	**8.77E-03**	**5.235**	**1.28E-02**	**6.213**	**4.71E-03**
30	Steroid biosynthesis	3/45	0.007	**3.171**	**5.25E-02**	**3.206**	**4.85E-02**	**10.208**	**9.66E-05**	**4.927**	**1.21E-02**	2.380	1.27E-01	**6.767**	**3.17E-03**
31	Phenylalanine, tyrosine and tryptophan biosynthesis	1/22	0.002	0.587	5.56E-01	**4.332**	**1.76E-02**	2.507	9.15E-02	**5.136**	**1.04E-02**	**14.183**	**6.35E-06**	1.982	1.76E-01
32	Biosynthesis of unsaturated fatty acids	6/22	0.000	**3.695**	**3.26E-02**	**6.356**	**3.41E-03**	**10.666**	**6.79E-05**	**8.213**	**1.25E-03**	**3.927**	**3.28E-02**	**6.242**	**4.71E-03**
33	Cyanoamino acid metabolism	5/29	0.000	**4.045**	**2.41E-02**	**5.013**	**9.89E-03**	**4.462**	**1.51E-02**	**13.467**	**2.60E-05**	**16.581**	**3.46E-06**	**14.457**	**3.22E-06**
34	Glucosinolate biosynthesis	3/65	0.000	**13.790**	**1.27E-05**	**6.895**	**2.23E-03**	**18.993**	**1.55E-07**	**4.926**	**1.21E-02**	**13.444**	**9.97E-06**	1.832	2.00E-01
35	Cysteine and methionine metabolism	2/46	0.000	**7.598**	**9.51E-04**	**3.913**	**2.50E-02**	**6.912**	**1.83E-03**	**4.640**	**1.40E-02**	0.303	7.54E-01	**5.807**	**6.12E-03**
36	Valine, leucine and isoleucine degradation	2/37	0.000	**13.648**	**1.27E-05**	**7.685**	**1.10E-03**	**17.127**	**5.02E-07**	-	-	-	-	-	-
37	Pentose phosphate pathway	2/19	0.000	**14.327**	**1.27E-05**	**11.616**	**5.51E-05**	**15.134**	**2.71E-06**	1.507	2.34E-01	2.316	1.32E-01	**3.144**	**6.41E-02**
38	Ascorbate and aldarate metabolism	2/18	0.000	-	-	-	-	-	-	**3.571**	**3.69E-02**	**6.194**	**6.24E-03**	**6.131**	**4.78E-03**
39	Lysine biosynthesis	1/9	0.000	**8.064**	**7.21E-04**	**7.727**	**1.10E-03**	**8.782**	**3.25E-04**	**4.703**	**1.35E-02**	0.849	4.53E-01	0.029	9.90E-01
40	Tropane, piperidine and pyridine alkaloid biosynthesis	1/8	0.000	0.587	5.56E-01	**4.332**	**1.76E-02**	2.507	9.15E-02	**5.136**	**1.04E-02**	**14.183**	**6.35E-06**	1.982	1.76E-01
41	Monobactam biosynthesis	1/8	0.000	**8.064**	**7.21E-04**	**7.727**	**1.10E-03**	**8.782**	**3.25E-04**	**4.703**	**1.35E-02**	0.849	4.53E-01	0.029	9.90E-01
42	Nitrogen metabolism	1/12	0.000	**10.858**	**5.57E-05**	2.585	8.13E-02	**6.830**	**1.86E-03**	**8.458**	**1.24E-03**	**4.529**	**1.98E-02**	**17.977**	**1.71E-07**
43	Nicotinate and nicotinamide metabolism	1/13	0.000	**8.064**	**7.21E-04**	**7.727**	**1.10E-03**	**8.782**	**3.25E-04**	**4.703**	**1.35E-02**	0.849	4.53E-01	0.029	9.90E-01
44	Pentose and glucuronate interconversions	1/16	0.000	**5.478**	**6.97E-03**	**3.054**	**5.52E-02**	0.674	5.10E-01	**3.935**	**2.69E-02**	**7.394**	**2.42E-03**	**7.990**	**1.10E-03**
45	Sphingolipid metabolism	1/17	0.000	**3.187**	**5.25E-02**	1.560	2.18E-01	**4.141**	**1.99E-02**	**4.003**	**2.57E-02**	0.301	7.54E-01	**5.979**	**5.35E-03**
46	Ascorbate and aldarate metabolism	1/18	0.000	**7.662**	**9.24E-04**	**11.960**	**4.40E-05**	**11.150**	**4.94E-05**	-	-	-	-	-	-
47	Propanoate metabolism	1/20	0.000	**13.408**	**1.27E-05**	**9.299**	**3.60E-04**	**5.619**	**5.70E-03**	1.649	2.07E-01	**5.115**	**1.32E-02**	**5.375**	**9.10E-03**
48	Fructose and mannose metabolism	1/20	0.000	**8.123**	**7.21E-04**	**5.550**	**6.48E-03**	**7.543**	**1.04E-03**	**2.985**	**6.32E-02**	**3.420**	**4.74E-02**	2.771	9.06E-02
49	Thiamine metabolism	1/22	0.000	**5.399**	**7.31E-03**	**8.641**	**5.72E-04**	2.392	1.01E-01	2.422	9.77E-02	1.917	1.84E-01	1.377	3.02E-01
50	Fatty acid elongation	1/23	0.000	2.580	8.68E-02	**6.688**	**2.54E-03**	**5.003**	**9.73E-03**	**6.540**	**3.61E-03**	2.262	1.33E-01	**4.522**	**1.87E-02**
51	Brassinosteroid biosynthesis	1/26	0.000	**4.466**	**1.76E-02**	2.793	6.87E-02	**4.943**	**1.01E-02**	2.545	9.19E-02	1.307	3.10E-01	**4.632**	**1.78E-02**
52	Valine, leucine and isoleucine degradation	1/37	0.000	-	-	-	-	-	-	0.124	8.83E-01	1.409	2.86E-01	1.104	3.88E-01

Table S4 – (Continued)

ID	Pathway name	Match	Impact	8 DAH						18 DAH					
				ETHY *vs*. CTRL		IAA *vs*. CTRL		ETHY+IAA *vs*. CTRL		ETHY *vs*. CTRL		IAA *vs*. CTRL		ETHY+IAA *vs*. CTRL	
				-LOG(p)	FDR	-LOG(p)	FDR	-LOG(p)	FDR	-LOG(p)	FDR	-LOG(p)	FDR	-LOG(p)	FDR
53	Fatty acid degradation	1/37	0.000	2.580	8.68E-02	**6.688**	**2.54E-03**	**5.003**	**9.73E-03**	**6.540**	**3.61E-03**	2.262	1.33E-01	**4.522**	**1.87E-02**
54	Pyrimidine metabolism	1/38	0.000	1.327	2.92E-01	**3.033**	**5.52E-02**	2.071	1.36E-01	**10.415**	**2.75E-04**	**5.884**	**8.06E-03**	0.093	9.82E-01
55	Ubiquinone and other terpenoid-quinone biosynthesis	1/38	0.000	**11.546**	**4.43E-05**	0.659	5.17E-01	**4.534**	**1.44E-02**	1.022	3.74E-01	**6.970**	**3.45E-03**	0.536	6.57E-01
56	Phenylpropanoid biosynthesis	1/46	0.000	0.587	5.56E-01	**4.332**	**1.76E-02**	2.507	9.15E-02	**5.136**	**1.04E-02**	**14.183**	**6.35E-06**	1.982	1.76E-01
57	Porphyrin and chlorophyll metabolism	1/48	0.000	**10.858**	**5.57E-05**	2.585	8.13E-02	**6.830**	**1.86E-03**	**8.458**	**1.24E-03**	**4.529**	**1.98E-02**	**17.977**	**1.71E-07**

Values in bold letters indicate statistical significance ($p < 0.05$) at the same DAH (mean ± standard deviation, n = 4).

CHAPTER 3

PROTEOMIC CHANGES IN AROMA METABOLISM DURING TOMATO (*SOLANUM LYCOPERSICUM* L.) FRUIT RIPENING IN RESPONSE TO ETHYLENE AND AUXIN REGULATION

Eric de Castro Tobaruela[1,2], Isabel Louro Massaretto[1,2], Silvia Leticia Rivero Meza[1,2], Grazieli Benedetti Pascoal[2,3], Luciano Freschi[4], Eduardo Purgatto[1,2,*]

[1]Department of Food and Experimental Nutrition, Faculty of Pharmaceutical Sciences, University of São Paulo (USP), São Paulo, SP, Brazil; [2]Food Research Center (FoRC), São Paulo, SP, Brazil; [3]Faculty of Medicine, Federal University of Uberlândia (UFU), Uberlândia, MG, Brazil; [4]Department of Botanic, Institute of Bioscience, University of São Paulo (USP), São Paulo, SP, Brazil.

Author contributions:

LF provided and generated the plant material. ECT conducted experiments and analyzed data. ILM, SLRM and GBP contributed during proteomic experiments. ECT wrote the paper, prepared figures and tables. ILM, SLRM and GBP reviewed drafts of the paper. EP designed experiments, supervised, and reviewed drafts of the paper.

Future submission to Plant Physiology and Biochemistry (ISSN 0981-9428).

ABSTRACT

Fruit ripening is a complex process controlled by regulatory mechanisms not fully understood involving ethylene and auxin. Primary and secondary metabolic modifications promote the biosynthesis of volatile organic compounds (VOC), resulting in changes in fruit aroma. However, the hormonal regulation of aroma formation in climacteric fruits requires clarification. The present study evaluated the proteomic responses to ethylene-auxin crosstalk during tomato (*Solanum lycopersicum* L.) fruit ripening, with an emphasis on VOC metabolism. Tomato fruits cv. Micro-Tom at the mature green stage were randomly separated into four groups according to hormone treatments: CTRL (without treatment); ETHY (ethylene treatment); IAA (indole-3-acetic acid treatment); and ETHY+IAA (both hormone treatments). The color shift and ethylene emission were determined daily. Proteomic profiles were obtained by LC-MS after proteome extraction, fractioning, tryptic digestion, and cleaning-up. A total of 3704 proteins was identified, but only 1807 were reliably measured at least in one of the analyzed ripening stages or treatment conditions, including 1547 proteins differently expressed ($p < 0.05$) between at least two groups. The identification of proteins involved in metabolic processes and that participates in catalytic activities, using Gene Ontology, as well as the classification of them by KEGG pathway and comparison of overlapped protein abundances enabled the identification of the enzymes related to VOC biosynthesis affected by ethylene and auxin treatments, as the enzymes of terpenoid pathway upregulated by auxin. The obtained results reinforce not only the effects of ethylene and auxin regulation, but also the role of the ethylene-auxin crosstalk in regulating the tomato fruit aroma.

Keywords

Climacteric fruit. Carotenoids. Aroma compounds. Proteomic. LC-MS.

1 INTRODUCTION

Fruit ripening is a complex, genetically programmed, and developmentally regulated process accompanied by massive biological and biochemical changes which lead to the final ripe fruit. These changes coincide with seed maturation in the final

phase of fruit development and are precisely regulated by plant hormones such as ethylene and auxin (KUMAR; KHURANA; SHARMA, 2014; PESARESI et al., 2014). During ripening, chlorophyll degradation, carotenoid accumulation, and other changes in primary and secondary metabolites are known to be controlled by regulatory mechanisms involving ethylene and auxin, although these mechanisms are not fully understood (KLEE; GIOVANNONI, 2011; SU et al., 2015). The biosynthesis of volatile organic compounds (VOC) also appears to be regulated by both hormones, and most of them are accumulated at the onset of ripening and peak at full ripening (KLEE; GIOVANNONI, 2011).

Tomato (*Solanum lycopersicum* L.) fruit aroma compounds have been extensively studied, and approximately 400 of them have been identified in tomato fruit during ripening of an intact fruit (primary aroma compounds) and during tissue disruption (secondary aroma compounds) (BALDWIN et al., 2000; DÍAZ DE LEÓN-SÁNCHEZ et al., 2009). Among these, fewer than 10% are produced in sufficient quantities to be perceived by humans (BALDWIN et al., 2000; MATHIEU et al., 2009), and these are crucial in conferring the characteristic tomato aroma (DU et al., 2015). The other VOC may provide background odors that impact the overall aroma quality (TANDON et al., 2001; KLEE; GIOVANNONI, 2011). These aroma compounds are derived from diverse precursors, including amino acids, fatty acids, and carotenoids (KLEE; TIEMAN, 2013; BAUCHET et al., 2017). Tieman et al. (2017) and Klee and Tieman (2018) described the principal contributors to the ripe tomato flavor that positively correlates with consumer preferences (such as 2-methylbutanol, 3-methylbutanol, 2-isobutylthiazole, 2-phenylethanol, 1-hexanol, (E)-3-hexen-1-ol, guaiacol, β-ionone and 6-methyl-5-hepten-2-one) and, although the enzymes involved in the biosynthesis of these VOC are well known, the knowledge about how their expressions are regulated by ethylene and auxin is not extensive.

Tomato is one of the most widely studied plant species, largely since its fruit serve as a reference for investigation of fleshy fruit development and a model for studying climacteric fruit ripening, in which ethylene is the most important regulator (GIOVANNONI, 2007; GAPPER; MCQUINN; GIOVANNONI, 2013). Despite the emphasis on the role of ethylene and its importance in climacteric fruit ripening, recent reports have indicated that the coordinated action of ethylene and auxin may be crucial in fruit ripening (SEYMOUR et al., 2013; SU et al., 2015). Mechanisms underlying ethylene regulation have been extensively studied, while even the exact role of auxin

in ripening control remains unclear. Regarding ethylene-auxin crosstalk in fruit ripening, recent studies have elucidated antagonistic effects of the two hormones, such as auxin acting as a ripening repressor and thereby opposing the known role of ethylene as a ripening inducer in tomato fruit (KUMAR; KHURANA; SHARMA, 2014; SU et al., 2015; LI et al., 2016). Interestingly, studies have also indicated that auxin is crucial for triggering ripening and acting on the transition between systems I and II of ethylene production, suggesting that it may not inhibit fruit ripening (ROSS et al., 2011; MCATEE et al., 2013; SEYMOUR et al., 2013).

Changes in the VOC profiles occur during fruit ripening in response to hormonal regulation and several intrinsic and extrinsic factors. This process promotes changes in the compound ratios as well as their interactions, resulting in changes in the tomato aroma (KLEE; GIOVANNONI, 2011; WANG et al., 2015). However, the dynamic patterns of ripening and volatile production in tomato fruit during ripening, from mature green to full ripe, remains unclear. In this context, a proteomic approach has importance to study the major physiological modifications that affect gene regulation, hormonal signaling and metabolic processes during fruit ripening. Differential proteomics at different stages of fruit ripening is an interesting strategy to deepen existing knowledge and improve understanding of these hormones in aroma formation, once it gives information on the concomitant molecular changes during this important process. The aim of this study was to evaluate the proteomic responses to ethylene-auxin crosstalk during tomato (*Solanum lycopersicum* L.) fruit ripening. This study highlights the important role that ethylene and auxin plays in regulating tomato aroma.

2 MATERIALS AND METHODS

2.1 Plant materials and hormone treatments

Tomato plants (*Solanum lycopersicum* cv. Micro-Tom) were grown under standard greenhouse conditions. Four biological replicates (400 fruits/replicate) were harvested between December 2016 and April 2017 at the mature green stage (approximately 40 days after anthesis). Each biological replicate comprised at least 100 plants. Fruits were randomly separated into four groups according to hormone

treatments: CTRL (without treatment); ETHY (ethylene treatment); IAA (indole-3-acetic acid treatment); and ETHY+IAA (both hormone treatments). Each group comprised at least 100 fruits. During the experiments, fruits were left to ripen spontaneously in a 323 L chamber at 22°C for a 16-hour-day/8-hour-night cycle at 80% relative humidity. Ethylene treatments were performed using a gaseous hormone at 10 $\mu L.L^{-1}$ for 12 hours. The indole-3-acetic acid solutions were prepared at 100 µM in 10 mM 2-(N-morpholino)ethanesulfonic acid buffer at pH 5.6 with 3% sorbitol and were injected through the calyx end as described by Su et al. (2015). Fruits from the IAA group received indole-3-acetic acid solution, while fruits from the ETHY+IAA group were exposed to gaseous ethylene before infiltration with indole-3-acetic acid solution. To maintain a consistent injection method across all samples, fruits from the ETHY and CTRL groups were injected only with buffer solution. During the experiment, ethylene emission and surface color were evaluated daily as ripening parameters. For further analysis, at least five fruits from each experimental group were collected, considering the mature green and breaker ripening stages of the CTRL group as reference. Samples were then frozen in liquid nitrogen and stored at −80°C.

2.2 Ripening characterization

2.2.1 Ethylene emission

Five intact tomato fruits from each experimental group were placed in airtight glass containers and left at 25°C. After 1 h, five 1 mL samples were collected from the headspace with gas-tight syringes through a rubber septum. Ethylene emission was analyzed by gas chromatography with a flame ionization detector (GC-FID) (Agilent Technologies, HP-6890). A HP-Plot Q column (30 m × 0.53 mm × 40 µm) was used. The injector and detector temperatures were both set at 250°C, and the oven temperature was set at 30°C. The injections were performed in pulsed splitless mode. Helium was used as carrier gas (1 $mL.min^{-1}$).

2.2.2 Fruit surface color

The fruit surface color was assessed using a HunterLab ColorQuest XE instrument (Hunter Associates Laboratories) in terms of L, a, b space, and the data were processed to obtain the °hue values as described by Fabi et al. (2007). Three measures were taken at the equators of five fruits (from each experimental group), and average values were calculated.

2.3 Total protein extraction

A plant total protein extraction kit (PE0230; Sigma-Aldrich, St.Louis, MO) was used for total protein extraction and the entire procedure followed the manufacturer's manual. Ground frozen tomato fruits (250 mg) was vortexed with 1,500 µL of pre-cooled methanol solution with protease inhibitor was added to the powder for 30 seconds. The mixture was incubated at -20°C then centrifuged at 16,000 g for 5 min at 4°C. Supernatant was removed and the pellet was washed by pre-cooled methanol solution for two more times. The resulting pellet was washed by 1,500 µL of pre-cooled acetone, incubated at -20°C and centrifuged at 16,000 g for 5 min at 4°C. Supernatant was removed and the pellet was washed by pre-cooled acetone solution for one more time. A SpeedVac Plus SC 210A (Thermo Fisher Scientific, Waltham, MA, USA) was used to remove residual acetone and 1,000 µL of the protein extraction reagent provided by the kit was used to incubate the pellet for 15 minutes at room temperature. The pellet was then centrifuged at 16,000 g for 30 minutes, and supernatant was collected and stored at -80°C.

2.4 Protein quantification

The protein content in each proteome extract was quantified using the 2-D Quant Kit (GE Healthcare, Uppsala, Sweden) according to the manufacturer’s manual. A standard curve was made using bovine serum albumin as a control.

2.5 In-Gel fractionation, protein digestion and sample clean-up

An aliquot (30 µg of total proteins) of each proteome sample in Laemmli buffer was heated at 37 °C to prevent aggregation of hydrophobic proteins, and then loaded on a 12% SDS polyacrylamide gel for separation by 1D-SDS-PAGE (running two-thirds of the way down the gel). After electrophoresis, proteins were fixed and stained with Coomassie brilliant blue. Each lane was cut into three segments according to the protein maker (70 and 25 kDa) and each section cut into 1mm^3 cubes. Gel pieces were washed with 50mM ammonium bicarbonate (NH_4HCO_3) and acetonitrile before reduction with 20 mM Dithiothreitol in 50 mM NH_4HCO_3 and alkylation with 50 mM iodoacetamide in 50 mM NH_4HCO_3. Then, proteins were digested at 37°C overnight as described by Shevchenko et al. (2006), using Sequencing Grade Modified Trypsin (V511A; Promega, Madison, WI, USA). The digested peptides were recovered from the gel pieces after adding two elution solution (v/v): 1% formic acid/59.4% methanol and 1% formic acid/49.5% acetonitrile. Resulting peptides were cleaned using ZipTip C18 Pipette Tips (Millipore, Bedford, MA, USA). Clean peptide samples were vacuum-dried using a SpeedVac (Thermo Fisher Scientific) and stored at -80°C.

2.6 Liquid chromatography-mass spectrometry (LC-MS) analysis

Peptide mixtures dissolved in 0.1% formic acid were trapped on a C18 pre-column (Acclaim PepMap RSLC Nano-Trap column; 3 µm, 100 Å, 75 µm × 20 mm, Thermo Fisher Scientific) and separated on a C18 analytical column (Acclaim PepMap RSLC column; 2 µm, 100 Å, 75 µm × 150 mm, Thermo Fisher Scientific) using a linear gradient from 5% buffer A (80% ACN, 0.1% FA) to 95% in 120 min, with buffer B containing 0.1% FA. The flow rate was set to 350 nL.min^{-1} and oven temperature to 50°C. The QToF Impact II Bruker mass spectrometer (Bruker Daltonics, Bremen, Germany) was interfaced to the nanoLC system (Thermo Scientific UltiMate™ 3000 RSLCnano system) with the CaptiveSpray nanoBooster source (Bruker Daltonics) using acetonitrile as dopant. LC-MS data were acquired using a Data Dependent Acquisition (DDA) scheme. Briefly, a MS scan at scan speed of 200 ms was followed by 20 MS/MS fragment scans of the most intense precursors (50 ms) in a total cycle

time of 1.2 seconds. The mass range of the MS scan was set from m/z 150 to 2200. Isolation of precursor ions was performed using an m/z isolation window of 2.0 and a dynamic exclusion of 0.4 min. The collision energy was adjusted between 23 and 65 eV as a function of the m/z value. All samples were analyzed in random order.

2.7 Data analysis and label-free quantitation

The MS data were analyzed using MaxQuant software v. 1.6.6.0 and the label-free quantification (LFQ) was performed as described by Tyanova, Temu and Cox (2016). The MS data were searched against the uniprot *Solanum lycopersicum* database (34,648 total entries) in UniProtKB (https://www.uniprot.org/). Carbamidomethylation was specified as fixed modification, while oxidation on methionine and acetylation on protein N-terminal were specified as variable modifications. Mass error was set to 10 ppm for precursor ions and 0.02 Da for fragment ions. The search followed the enzymatic cleavage rule for trypsin/P, allowing up to 2 missing cleavages. Additionally, at least 2 peptide identifications per protein were required, with minimum peptide length of 5. At least 1 peptide had to be unique to the protein group. The cutoff for the global false discovery rate (FDR) in peptide and protein identification was 0.05. All the other parameters in MaxQuant were set to default values.

2.8 Bioinformatics analysis

Bioinformatics analysis was mainly performed using Perseus software v. 1.6.6.0 (TYANOVA et al., 2016). MaxQuant data were filtered for reverse identifications (false positives), contaminants and “only identified by site”. The LFQ intensities were log transformed. For further analysis in the Perseus software, proteins that had LFQ intensity value different from 0 in at least 2 of the 4 biological replicates for at least 1 experimental group were considered. For each group, proteins with 2 data available had the third value imputed using the mean value, while proteins with the 4 data available had the most discrepant data disregarded. Gene ontology (GO) annotation

proteome was derived from the UniProt-GOA database (http://www.ebi.ac.uk/GOA/). Firstly, converting identified protein ID to UniProt ID and then mapping to GO IDs by protein ID. If some identified proteins were not annotated by UniProt-GOA database, the InterProScan soft would be used to annotated protein's GO functional based on protein sequence alignment method. Then proteins were classified by GO annotation based on two categories: biological process and molecular function. Subcellular localization also was predicted using UniprotKB. The SolCyc (http://solcyc.solgenomics.net/) was used to find more information on annotated genes, to obtain detailed information on pathways and biochemical reactions involved. KEGG online service tool KAAS to annotated protein's KEGG database description (https://www.genome.jp/kaas-bin/kaas_main) was used to KEGG pathway annotation. Then, KEGG ID were mapped on the KEGG pathway database using KEGG online service tools KEGG mapper (https://www.kegg.jp/kegg/mapper.html). Enrichment analyses were performed using STRING database version 11.0 (https://string-db.org/).

2.9 Statistical analysis

The ethylene and color data are presented as mean ± standard deviation. MetaboAnalyst 4.0 (CHONG; WISHART; XIA, 2019) was used to perform statistical analysis. Protein data were analyzed by Student's T-tests or one-way ANOVA with a subsequent Tukey’s test to evaluate the effects of ripening or hormone treatments. Differences were considered significant at $p < 0.05$. Heatmap and partial least squares discriminant analysis (PLS-DA) were performed on protein LFQ intensity values after normalization by median, log-transformation and Pareto-scaling.

3 RESULTS AND DISCUSSION

3.1 Tomato ripening changes due to ethylene and auxin treatments

To better understand the ethylene and auxin roles in the control of tomato fruit ripening, it was critical to characterize the normal ripening process and how hormone

treatment was changing it. Characterization of the tomato fruit ripening was based on daily analysis of surface color and ethylene emission (Figure 1). As shown in the ethylene emission and surface color graphs, ethylene treatments (ETHY) accelerated the ripening of fruits, while indole-3-acetic acid treatment (IAA) and ethylene and indole-3-acetic acid treatment (ETHY+IAA) produced the opposite effect. CTRL fruits reached the breaker stage on the eighth day after harvest (DAH) and reached full ripeness after 18 DAH, as shown in the pictures in Figure 1. At 18 DAH, IAA and ETHY+IAA fruits did not yet show the characteristic red color of fully ripe tomatoes, while ETHY fruits were already losing moisture, a characteristic of senescence. The antagonistic roles of these two hormones are already well established in many climacteric fruits, been observed during tomato fruit ripening in previous studies by this research group, by Li et al. (2017) and Seymour et al. (2013).

Figure 1 – Characterization of tomato (*Solanum lycopersicum* L. cv. Micro-Tom) fruit ripening

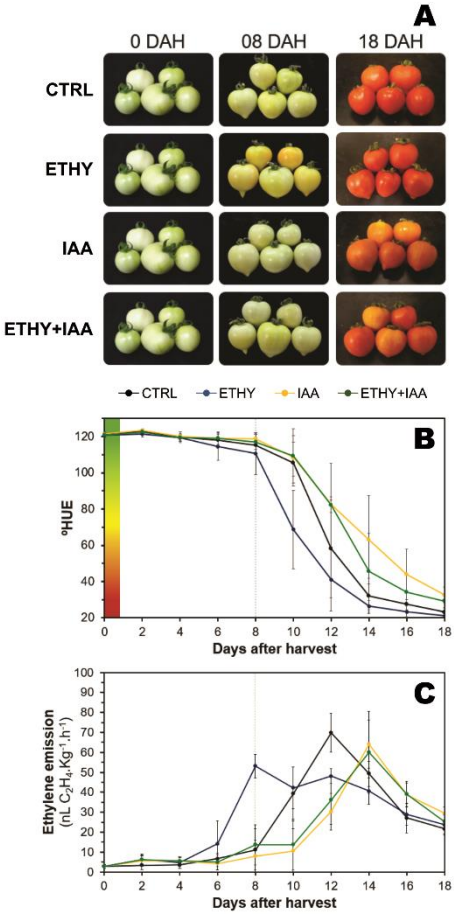

Effects of ethylene, auxin, and both treatments on fruit color and ethylene emission during fruit ripening. (A) Pictures of tomato fruits. (B) Surface color expressed by hue angle. (C) Ethylene emission. CTRL: Control group. ETHY: Ethylene-treated group. IAA: Indole-3-acetic acid-treated group. ETHY+IAA: Group treated with both hormones.

Although IAA and ETHY+IAA fruits had similar ethylene emission profiles, ETHY+IAA fruits appears to have an intermediate profile between those of CTRL and IAA, as observed in surface color curves and visual aspects of fruits. These results are in accordance with those presented by Su et al. (2015), indicating that both hormones simultaneously interfered with the carotenoid metabolism and suggesting that auxin regulation overlaps the ethylene regulatory system.

To investigate proteins levels changes and how they relate to the metabolic shift during fruit ripening, the proteome of the tomato fruits from each experimental group were sampled at 0 (early ripening stage) and 8 DAH (middle ripening stage), stages in which the enzymatic processes that result in the final tomato fruit characteristics would still be in progress. This approach aimed to investigate the effects of ethylene-auxin crosstalk on the global metabolism and specific metabolic systems, including aroma compounds.

3.2 Label-Free quantification of tomato fruit proteomes

In order to obtain a detailed view how ethylene and auxin modulates the enzymatic processes during fruit ripening, proteomes isolated from tomato fruits at 0 and 8 DAH were quantified, fractionated (SDS-polyacrylamide gel) and subjected to in-gel tryptic digestion. Released peptides were analyzed using a LC-MS followed by MaxQuant analysis to identify and quantify the progenitor proteins. All this procedure is schematically depicted in Figure S1. The mass error and the length of the identified peptides were checked to confirm the MS data quality for this proteomic analysis. The distribution of mass error was near 0 and most of them were less than 0.02 Da, which means the mass accuracy of the MS data fit the requirements (Figure 2A). Second, the length of most peptides distributed from 8 to 20 amino acids, which is consistent with the typical size tryptic peptides (Figure 2B), indicating that sample preparation was acceptable.

A total of 3960 proteins were identified, and after filtration for reverse identifications (false positives) and contaminants 3704 remained in the search for dysregulated proteins, although some of these proteins were not found consistently among all for biological replicates of an experimental group (Table S1).

Figure 2 – Basic information and functional classification of tomato (*Solanum lycopersicum* L. cv. Micro-Tom) fruit proteome

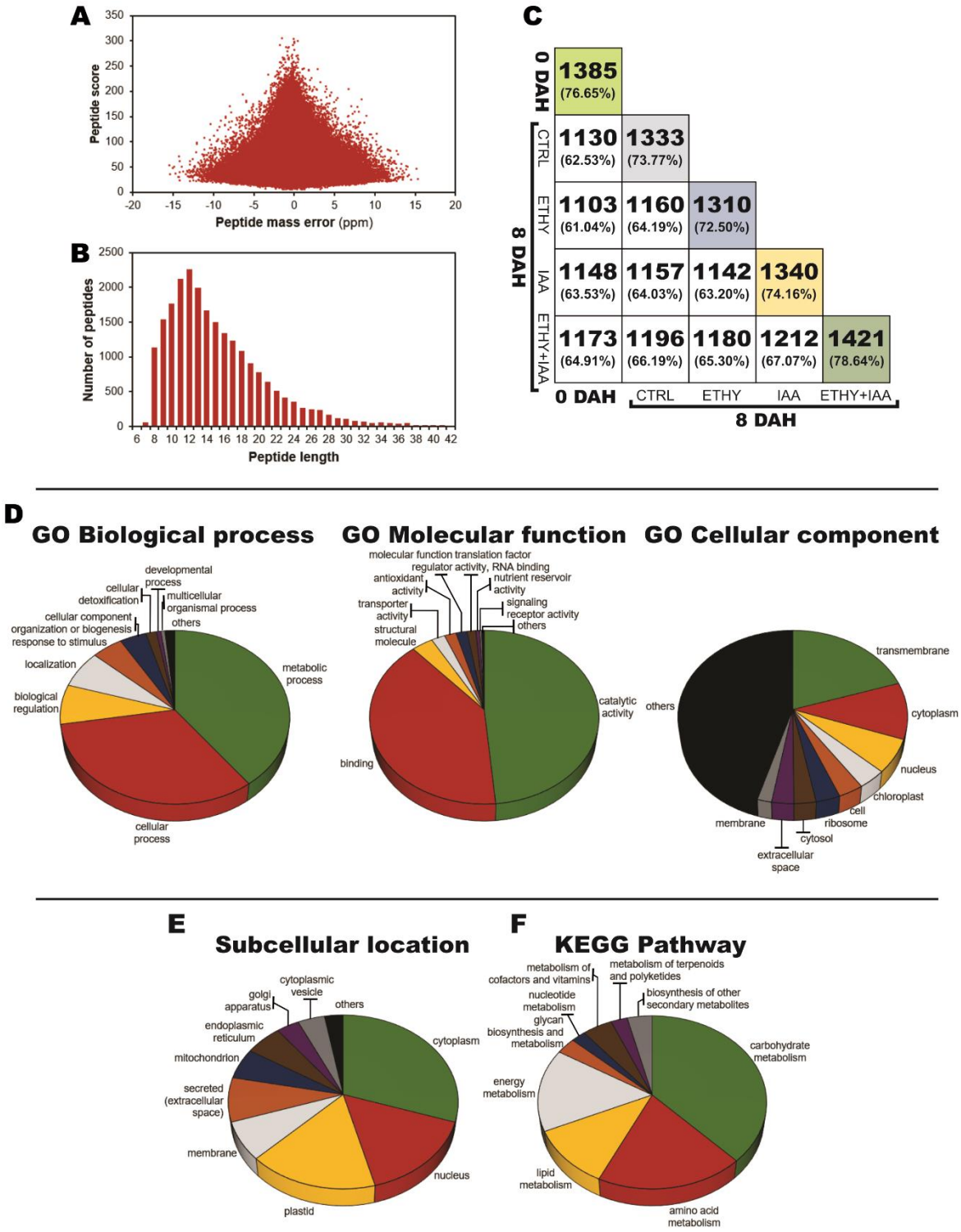

(A) Quality control validation of MS data: mass error distribution of all identified peptides. (B) Distribution of peptide length. (C) Number of proteins identified at different ripening stages (0 and 8 days after harvest) and hormone treatments. The white squares show the pairwise overlap of the proteins identified in experimental group. The diagonals show the total number of identified proteins in each group. (D) Pie chart of the proteins matched to gene ontology (GO) biological process, molecular function, and cellular component using UniProt-GOA database (http://www.ebi.ac.uk/GOA/). (E) Pie chart of the proteins classified by subcellular location using UniProtKB (https://www.uniprot.org/). (F) Pie chart of the proteins classified by KEGG pathway using KEGG mapper (http://www.genome.jp/kegg/mapper.html).

To allow inclusion of these proteins in subsequent analyses the following definitions were used: “Absent” for proteins that were not identified in any of the four replicates; “Marginal” for proteins found in only one replicate; “Present” when found in three or all four replicates. A protein was considered “found” when labeled “present” (Table 1). A total of 1807 proteins were found, which included 1547 proteins differently expressed ($p < 0.05$) between at least two groups (Table S2). In total, all the groups shared 975 (53.96%) of all found proteins. As shown in Figure 2C, the largest overlap of proteins was observed between IAA and ETHY+IAA at 8 DAH, with 1,212 (67.07%) identified in both groups. In contrast, the smallest overlap of common proteins was observed between the proteomes at 0 DAH and at 8 DAH treated with auxin, corresponding to 1103 proteins (61.04%). Tomato fruits without hormone treatment presented a total of 1385 proteins (76.65%) at 0 DAH and 1333 proteins (73.77%) at 8 DAH, with 1165 and 1122 proteins differently expressed, respectively. In relation to the treat fruits, found proteins ranged from 1310 (72.50%) to 1421 (78.64%), with 1097-1204 proteins differently expressed. Among the groups, a greater number of proteins were upregulated (903-1097) than downregulated (526-662).

Table 1 – Summary protein identification data of tomato (*Solanum lycopersicum* L. cv. Micro-Tom) fruit samples at different ripening stages (0 and 8 days after harvest) and hormone treatments

DAH	Hormone treatment	Protein quantification				$p < 0.05$[a]	Protein regulation	
		Identified	Absent	Marginal	Present		Up	Down
0	-	2332	1372	947	1385	1165	935	526
8	CTRL	1897	1807	564	1333	1122	966	662
8	ETHY	2010	1694	700	1310	1097	903	639
8	IAA	1928	1776	588	1340	1125	1014	641
8	ETHY+IAA	2135	1569	714	1421	1204	1097	634
Total		3704	0	1897	1807	1547	nd	nd

DAH: Days after harvest. CTRL: Control fruits. ETHY: Ethylene-treated fruits. IAA: Indole-3-acetic acid-treated fruits. ETHY+IAA: Fruits treated with both hormones. nd: not determined. [a]Number of proteins with p value < 0.05 calculated using one-way ANOVA analysis (Tukey HSD).

GO functional classification was performed on tomato proteins to reveal the biological processes they were involved in. The results revealed that found proteins were associated with a diverse range of biological processes, molecular functions and cellular component (Figure 2D, Table S3, and Table S4). The distribution of protein frequency per GO term indicated a significant enrichment in specific functional groups

with high and low coverage (Table S5). Enrichment analysis results suggested that the identified proteins represent a functionally defined subset of the theoretical tomato proteome associated with tomato fruit ripening. On the basis of biological processes (1188 proteins), the two largest classes of proteins participated in metabolic processes (77.86%) and cellular processes (63.97%). In relation to the molecular function (1369 proteins), the largest class of proteins are involved in catalytic activities (71.22%) and consisted of binding proteins (58.66%). The classification based on subcellular location revealed that proteins of all cellular compartments were identified, as well as that found in extracellular space. secreted proteins. The largest classes of proteins were in cytoplasm (35.45%), nucleus (18.66%), and plastids (chloroplasts, chromoplasts, and amyloplasts; 19.78%) (Figure 2D, Table S3, and Table S4). Finally, KEGG pathways analysis was performed for a more comprehensive understanding of the metabolic processes in tomato fruits. Results showed that multiple metabolic pathways were highly represented in the tomato proteome, being mainly grouped in carbohydrate metabolism (44.80%), as well as in amino acid (22.87%), lipid (13.23%), and energy metabolisms (18.34%). As also observed by Szymanski et al. (2017) for Micro-Tom proteomic analysis, the primary metabolism was characterized by high proteome coverage of their annotated genes, while the secondary metabolism and other categories were highly overrepresented.

3.3 Tomato fruit proteomic profiles at early and middle ripening stages

Before investigating the changes that happened in tomato fruit proteomes in response to ethylene-auxin crosstalk, proteomes from 0 and 8 DAH were compared to identify natural changes of proteomic profiles during fruit ripening (Figure 3). Out of the set of 1807 proteins, 1130 were overlapped between the two ripening stages, but only 38.32% (433) of them presented expression at significantly different levels ($p < 0.05$) when both stages were compared. Similarity between stages was 62.53%, greater than the 58% and 59% found by ROCCO et al. (2006) for tomatoes cv. Ailsa Craig and SM2, respectively.

Figure 3 – Identity of the tomato (*Solanum lycopersicum* L. cv. Micro-Tom) fruit proteome at two ripening stages (0 and 8 DAH)

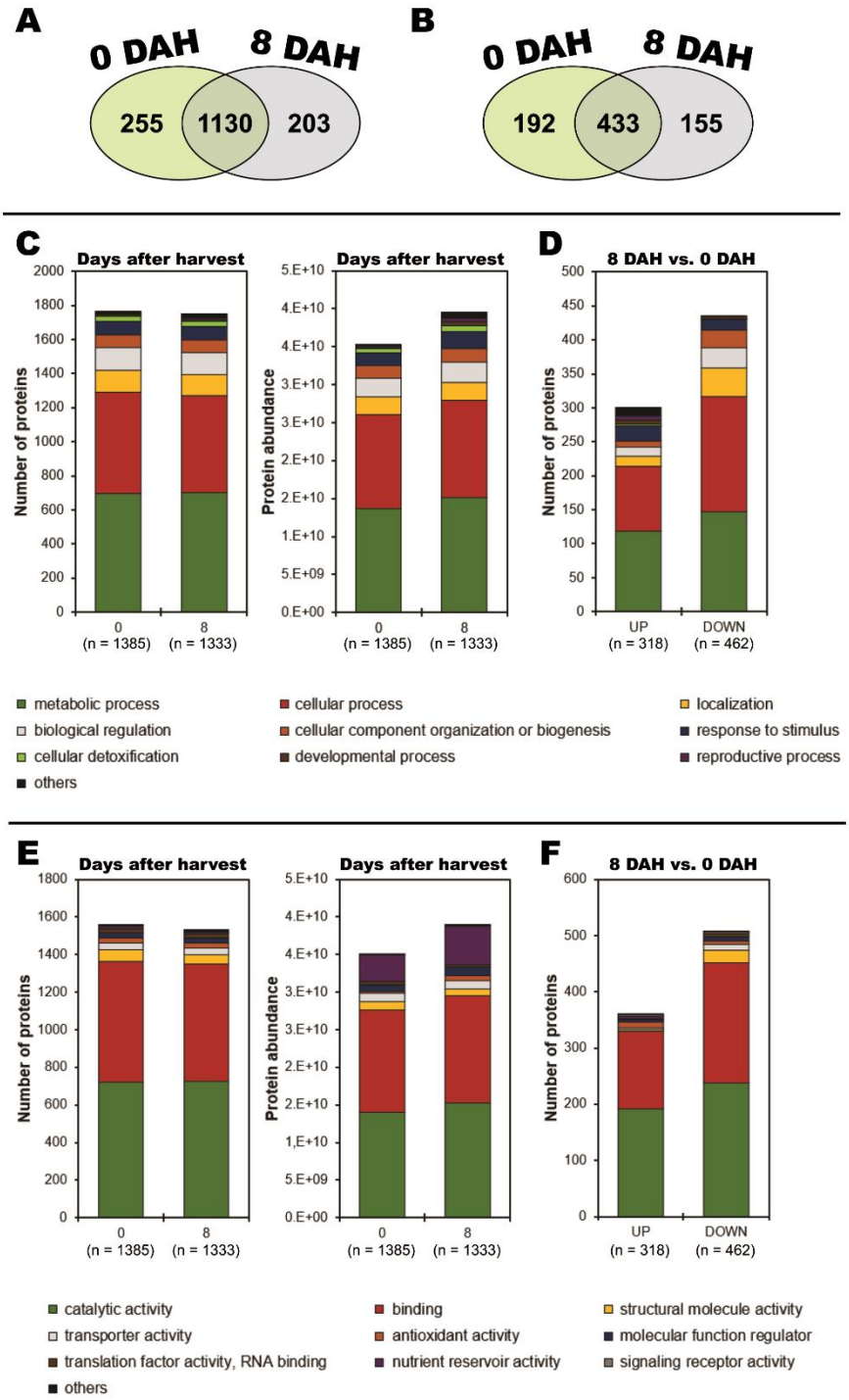

(A) Venn diagram presenting the number of overlapping and individual proteins of the 0 and 8 DAH proteomes. (B) Venn diagram presenting the number of overlapping and individual proteins that were significantly different between 0 and 8 DAH. (C) Bar chart showing the number and abundance of proteins per GO biological process annotation for 0 and 8 DAH proteomes. (D) Bar chart showing the number of proteins per GO biological process annotation that were common to both ripening stages and had their abundances increased (UP) or decreased (DOWN). (E) Bar chart showing the number and abundance of proteins per GO molecular function annotation for 0 and 8 DAH proteomes. (F) Bar chart showing the number of proteins per GO molecular function annotation that were common to both ripening stages and had their abundances increased (UP) or decreased (DOWN). DAH: Days after harvest.

According to KOK et al. (2008), the large number of proteins with significantly different expression may be a reflection of tomato fruits at breaker stage (8 DAH) be metabolically very active. In relation to the proteins exclusively found at a specific ripening stage, 255 were found at 0 DAH and 203 at 8 DAH, and approximately 76.00% of them presented significantly different expression levels. All the 1588 proteins found at 0 and 8 DAH were analyzed within Perseus to identify significant changes in protein abundance, resulting in the identification of 318 proteins with increased abundance and 462 proteins with reduced levels at 8 DAH. Contrary to what was observed by Szymanski et al. (2017), the analysis of differentially expressed proteins between ripening stages (8 DAH vs. 0 DAH) highlighted a greater number of downregulated that upregulated. However, when the total abundance of the two proteomes was compared, it was observed that the proteome at 8 DAH presented proteins with greater abundance than at 0 DAH, although the number of proteins was close.

According to GO biological process classification, proteins that participated in developmental and reproductive process presented the greatest abundance variations, with 194.81% and 221.88% of increasement, respectively. Among the proteins expressed with significant difference, 44.74% of the proteins that participate in metabolic process and 35.85% of that participating in cellular process were upregulated. Proteins that participate in localization and cellular component organization were predominantly downregulated (73.68% and 74.29%, respectively). All the proteins that participate in reproductive process with significantly different expression levels were upregulated. These results were expected, mainly the metabolic process-related, once that the fruit ripening process reflect the protein expression changes and the sequential activation and repression of specific biological processes. In relation to the molecular function, proteins involved in antioxidant activity and signaling receptor activity presented the greatest abundance increasement (101.89% and 87.42%, respectively), while proteins involved in structural molecule activity presented the greatest abundance reduction (28.54%). Proteins involved in antioxidant activity with significantly different expression levels were predominantly upregulated (66.67%), while proteins involved in structural molecule and translation factor activity were predominantly repressed (92.00% and 75.00%, respectively). All the proteins with significantly different expression levels that are involved in nutrient reservoir activity were upregulated.

These 1588 proteins are mainly located in cytoplasm, nucleus and plastids (chloroplasts, chromoplasts, and amyloplasts), and, according to KEGG pathways classification, mapped in primary metabolisms of carbohydrates (34,04%) and amino acids (18,09%), as well as in energy metabolism (13.40%). These results are according to that observed by Szymanski et al. (2017). Among the proteins differentially expressed, 57.58% of the proteins mapped in lipid metabolism were upregulated, while 55.14% of the proteins mapped in carbohydrate metabolisms and 53.19% of that mapped in amino acid metabolism were downregulated. The changes that were observed in proteins related to primary metabolism regulation are directly involved in important biochemical changes that occurs during the ripening. Knowing the natural process of ripening, proteomes of treated groups could be compared to CTRL (8 DAH), in order to better understand how both hormones affect the key processes during ripening progress.

3.4 Changes of tomato fruit protein levels in response to ethylene and auxin crosstalk

To assess the effects that ethylene and auxin treatments have on the tomato fruit ripening, the proteins identified in CTRL and treated fruits proteomes were compared. In total, 1696 tomato proteins were identified in at least one experimental group, although each group has between 1310 and 1421 proteins. As shown in Figure 4A and Figure 4B, 1049 proteins were overlapped among CTRL and the three treated groups and 69.21% (726) of them presented expression at significantly different levels ($p < 0.05$) when any two groups were compared. In relation to the proteins exclusively found at a specific group, 63 were found at CTRL, 54 at ETHY, 64 at IAA, and 96 at ETHY+IAA, and 75.00%-85.71% of them presented significantly different expression levels.

To evaluate the measurement reproducibility for the different biological replicates, all the 1696 tomato proteins were subjected to PLS-DA. The results indicated that the biological replicates for each group were always clustered together (Figure 4C), simultaneously demonstrating the high reproducibility of the different treatments and the significance of their effects on the proteome profiles.

Figure 4 – Identity of the tomato (*Solanum lycopersicum* L. cv. Micro-Tom) fruit proteomes modified by treatment with ethylene, auxin, or both hormones

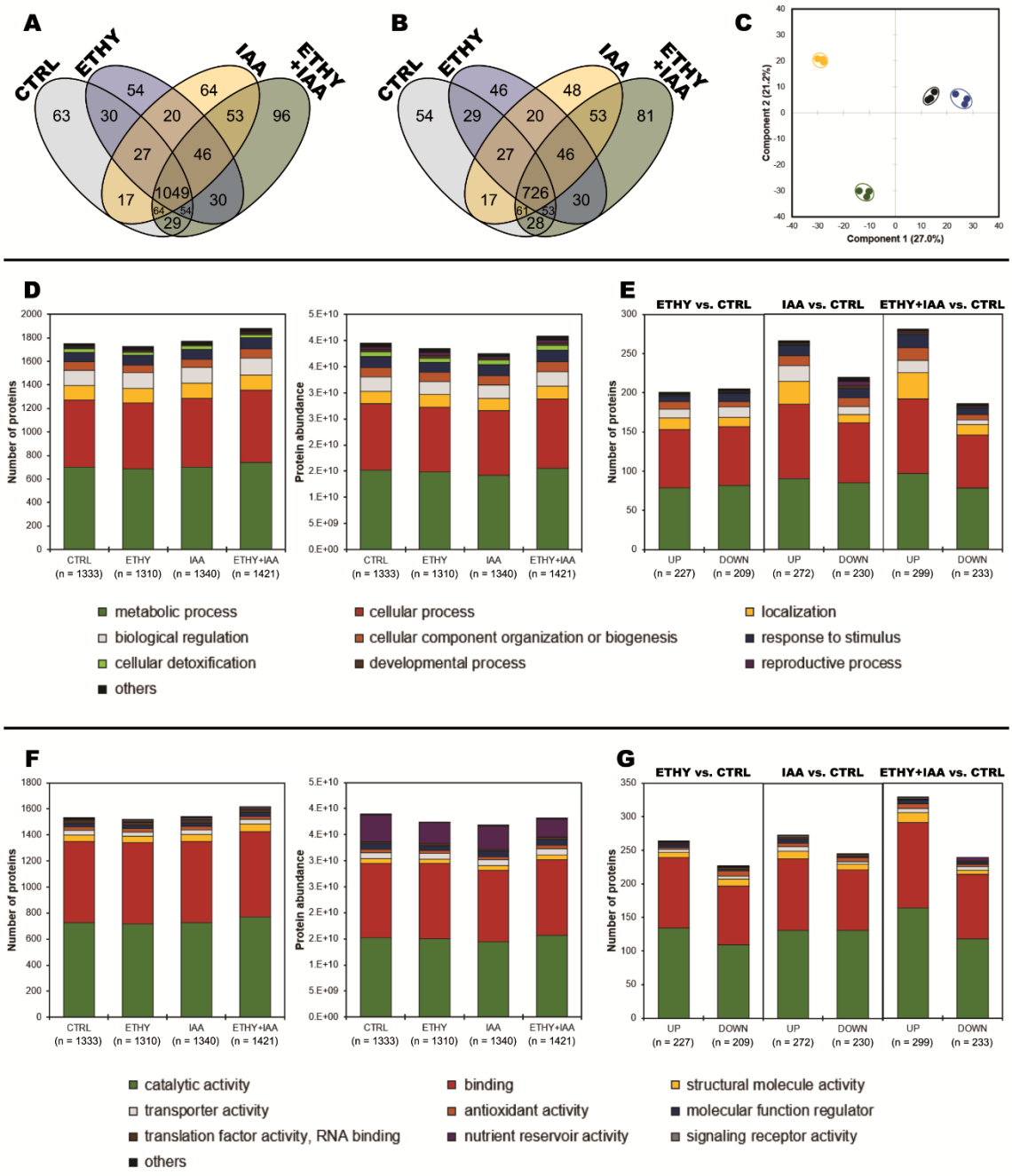

(A) Venn diagram presenting the number of overlapping and individual proteins of CTRL and treated groups. (B) Venn diagram presenting the number of overlapping and individual proteins that were significantly different between CTRL and treated groups. (C) Partial least squares discriminant analysis (PLS-DA) of proteins identified in proteomes of CTRL and treated groups. (D) Bar chart showing the number and abundance of proteins per GO biological process annotation for CTRL, ETHY, IAA, and ETHY+IAA proteomes. (E) Bar chart showing the number of proteins per GO biological process annotation that were common to CTRL and treated groups and had their abundances increased (UP) or decreased (DOWN). (F) Bar chart showing the number and abundance of proteins per GO molecular function annotation for CTRL, ETHY, IAA, and ETHY+IAA proteomes. (G) Bar chart showing the number of proteins per GO molecular function annotation that were common to CTRL and treated groups and had their abundances increased (UP) or decreased (DOWN). CTRL: Control group. ETHY: Ethylene-treated group. IAA: Indole-3-acetic acid-treated group. ETHY+IAA: Group treated with both hormones.

The PLS-DA explained 48.2% (component 1, 27.0%; component 2, 21.2%) of the total variance between the CTRL and the treated fruits (ETHY, IAA, and ETHY+IAA), revealing a clear separation according to the hormone treatments. As shown in Figure 4C, component 1 separated CTRL and ETHY from IAA and ETHY+IAA, and component 2 separated the ETHY+IAA from the other groups.

Tomato proteins found at ETHY, IAA, and ETHY+IAA were compared with CTRL within Perseus to identify significant changes in protein abundance, resulting in the identification of dysregulated proteins. In relation to CTRL, ETHY, IAA and ETHY+IAA presented 227, 272, and 299 proteins upregulated and 209, 230, and 233 proteins downregulated, respectively. These differences can be seen in Figure 4E and Figure 4G classified according to GO biological process and molecular function. Although treated fruits presented more proteins upregulated than downregulated, ETHY and IAA had 4.61% and 5.44% of abundance reduction in comparison to CTRL, respectively, suggesting a high abundance reduction due to both hormone treatments. On the other hand, ETHY+IAA proteome present greater protein number and abundance.

GO analysis revealed a similar proportion of functional categories of proteins based on their biological process and molecular function between CTRL and treated fruits suggesting no major differences in protein function in these fruits. Figure 4D to Figure 4G shows the protein distribution over the GO categories. According to GO biological process (Figure 4D, Figure 4E) classification, proteins that participate in metabolic and cellular processes presented 1.88% and 3.03% of abundance reduction in fruits treated with ethylene, 6.07% and 3.83% of abundance reduction in fruits treated with auxin, but 2.56% and 3.39% of increasing when treated with both hormones, respectively. Among the dysregulated proteins, proteins that participate in metabolic and cellular processes were predominantly downregulated in ETHY (50.93% and 50.34%) and upregulated in IAA (51.43% and 55.56%) and in ETHY+IAA (55.43% and 58.28%). Proteins that participate in biological regulation presented the same pattern: 54.17% downregulated in ETHY, 66.67% upregulated in IAA, and 72.73% upregulated in ETHY+IAA. In relation to the catalytic activity (GO molecular function), participating proteins presented 1.23% abundance reduction in fruits treated with ethylene, 5.00% of reduction in fruits treated with auxin, but 3.47% of increasing when treated with both hormones. Dysregulated proteins that participate of this activity were

predominantly upregulated in ETHY (55.14%) and in ETHY+IAA (58.16%), while the percentage of upregulation in IAA was 50% (Figure 4F, Figure 4G).

As with untreated fruits, the proteins in ETHY, IAA and ETHY+IAA are mainly located in cytoplasm, nucleus and plastids (chloroplasts, chromoplasts, and amyloplasts), and, according to KEGG pathways classification, mapped in primary metabolisms of carbohydrates, amino acids and lipids, as well as in energy metabolism. As shown in Figure S2A (data available in Table S6), dysregulated enzymes involved in carbohydrate and terpenoid metabolisms were mostly upregulated by ethylene (61.11% and 71.43%) and downregulated by auxin (53.13% and 66.67%) and at ETHY+IAA (51.61% and 60.00%). Enzymes involved in amino acid metabolism were mostly downregulated by both treatments (ETHY, 55.88%; IAA, 57.58%), but upregulated at ETHY+IAA (51.72%). Finally, enzymes involved in lipid metabolism were mostly upregulated at the three treated groups (ETHY, 75.00%; IAA, 55.00%; ETHY+IAA, 63.16%). Proteomes of ETHY+IAA and isolated treatments (ETHY or IAA) were also compared (Figure S2B, Table S6) to better understand the ethylene-auxin crosstalk. ETHY+IAA and ETHY presented 1180 overlapped proteins and 855 of them have significantly different expression. Among the ETHY+IAA proteins annotated by KEGG pathways, 51.59% were had their abundances decreased in relation to ETHY. Dysregulated enzymes involved in amino acid and lipid metabolisms were mostly upregulated, with 64.29% and 57.89%, while the enzymes involved in carbohydrate and terpenoid metabolisms were mostly downregulated. With 60.94% and 60.00%, respectively. On the other side, ETHY+IAA and IAA presented 1212 overlapped proteins and 886 of them have significantly different expression. ETHY+IAA proteins annotated by KEGG pathways mostly had their abundance increased in relation to IAA (53.22%). Dysregulated enzymes involved in carbohydrate, amino acid and terpenoid metabolisms were mostly upregulated, with 53.73%, 57.58%, and 66.67%, while the 55.00% of enzymes involved in lipid metabolism were downregulated.

These results reinforce not only the effect of ethylene and auxin regulation, but also the role of the ethylene-auxin crosstalk in regulating the tomato fruit metabolism during ripening. To further clarify the role of each hormone in regulating the tomato fruit aroma, the direct links between primary metabolism and VOC biosynthesis were studied considering the identified enzymes involved in important metabolic pathways

and other factors that can affect the production and release of tomato aroma compounds.

3.5 Ethylene and auxin effects in tomato aroma reflected by protein expression dynamics

As hormone regulation play an important role in the tomato fruit aroma formation, it was interesting to examine proteins directly and indirectly related the VOC biosynthesis in the proteomes of ETHY, IAA and ETHY+IAA. Firstly, changes were observed in the expression levels of enzymes involved in the biosynthesis of ethylene, typical ripening-promotion hormone in climacteric fruits, methyl jasmonate and abscisic acids (ABA), other hormones involved in ripening regulation. Enzymes involved in auxin biosynthesis were not found. Ethylene is biosynthesized from S-adenosylmethionine (SAM) having aminocyclopropane-1-carboxylic acid (ACC) as intermediary compound. In tomatoes, SAM synthases (SAMS) 1 and 3, and ACC oxidase (ACO) 1 and 4 display are crucial enzymes in ethylene biosynthesis. RNA-seq data available in TomExpress (ZOUINE et al., 2017) for tomato cv. Micro-Tom gene expression shows that SAMS3 levels does not change during the ripening, while SAMS1 is upregulated between mature green and breaker ripening stages. As shown in Figure 5A and in Table 2, SAMS1 abundance was increased while SAMS3 was not found in ETHY and opposite results were found in IAA and ETHY+IAA. The result was interesting because it highlights the effect of exogenous ethylene treatment in the normal expression pattern these enzymes. SAMS1 levels increased to detectable levels after treatment with ethylene, while ethylene's effect on SAMS3 is perceptible in ETHY+IAA, since its abundance is greater than in IAA. TomExpress also demonstrated that ACO1 and ACO4 present two peaks of gene expression. The first peak occurs between mature green and breaker stages and the second between breaker and red stages, with greater second peak of ACO4. In this study, the enzyme ACO4 presented increased expression at ETHY, while ACO1 was increased at IAA. In both ACO1 and ACO4, ETHY+IAA showed the same result pattern of ETHY.

Table 2 – Tomato (*Solanum lycopersicum* L. cv. Micro-Tom) fruit proteins involved in hormone and volatile compounds biosynthesis whose abundance changes specifically as a result of ethylene, auxin, and both treatments

Protein ID	Functional description	Protein Abbrev.	Ripening stage (0 DAH *vs*. 8 DAH)		Hormonal treatment									
					ETHY *vs*. CTRL		IAA *vs*. CTRL		ETHY+IAA *vs*. CTRL		ETHY+IAA *vs*. ETHY		ETHY+IAA *vs*. IAA	
			Reg[a]	*p* value	Reg[a]	*p* value	Reg[a]	*p* value	Reg[a]	*p* value	Reg[a]	*p* value	Reg[a]	*p* value
Ethylene biosynthesis and signaling														
P43280	S-adenosylmethionine synthase 1	SAMS1	↓	**9.96E-04**	↑	**4.15E-03**	nd		nd		↓	**2.38E-03**	nd	
P43282	S-adenosylmethionine synthase 3	SAMS3	=	5.18E-01	↓	**5.17E-07**	=	9.24E-02	=	2.57E-01	=	1.00E-01	=	6.86E-02
P05116	1-aminocyclopropane-1-carboxylate oxidase 1	ACO1	↑	**1.18E-02**	=	9.18E-01	=	9.07E-02	=	6.14E-01	=	8.22E-01	=	3.06E-01
P24157	1-aminocyclopropane-1-carboxylate oxidase 4	ACO4	nd		=	2.28E-01	nd		↑	**6.77E-03**	=	1.76E-01	↑	**6.88E-03**
Abscisic acid biosynthesis and conjugation														
A0A3Q7FC15	zeaxanthin epoxidase	ZEP	↑	**7.37E-04**	=	3.14E-01	↓	**2.94E-02**	=	8.55E-01	=	4.09E-01	↑	**2.36E-02**
K4D422	UDP-glucosyltransferase 73C	UGT73C4	↑	**1.43E-03**	↑	**2.45E-02**	=	2.65E-01	=	3.00E-01	↓	**3.49E-02**	=	7.22E-01
Jasmonate biosynthesis														
Q9LEG5	allene oxide cyclase	AOC	=	6.96E-02	=	1.51E-01	=	8.71E-02	=	2.54E-01	=	3.37E-01	=	1.56E-01
Q9LLB0	allene oxide synthase 2	AOS2	↑	**3.31E-03**	=	4.70E-01	↓	**1.40E-03**	=	6.83E-01	=	3.70E-01	↑	**1.87E-02**
Lipid metabolism														
A0A3Q7ERA8	lipoxygenase C	LoxC	↑	**3.15E-03**	=	2.18E-01	=	1.10E-01	↑	**3.89E-02**	=	8.18E-01	↑	**9.72E-03**
K4CF70	hydroperoxide lyase	HPL	↓	**2.33E-02**	=	8.77E-02	=	1.31E-01	↑	**4.33E-02**	=	9.70E-01	↑	**2.87E-02**
P28032	alcohol dehydrogenase 2	ADH2	↑	**6.94E-03**	=	2.61E-01	=	6.31E-01	=	6.99E-02	=	8.68E-01	=	8.48E-02
Amino acid metabolism														
A0A3Q7JCI1	branched-chain-amino-acid aminotransferase 1	BCAT1	=	2.03E-01	=	9.23E-01	↓	**1.42E-02**	=	3.29E-01	=	3.85E-01	↑	**2.28E-03**
A0A3Q7E8Y5	phenylacetaldehyde reductase 2	PAR2	nd		nd		↑	**3.04E-02**	↑	**1.99E-02**	↑	**2.07E-02**	=	5.41E-01
A0A3Q7HWL4	l-phenylalanine ammonia lyase	PAL	=	7.31E-02	=	1.81E-01	↓	**4.14E-02**	=	1.49E-01	=	3.43E-01	=	6.86E-01
A0A3Q7IJX7	aromatic amino acid decarboxylase	AADC	↑	**1.57E-04**	=	9.10E-01	↓	**3.34E-02**	=	2.00E-01	=	3.21E-01	=	5.36E-02
Metabolism of carotenoid and other terpenoids														
A8WBX7	diphosphomevalonate decarboxylase	MPDC	=	7.26E-01	=	8.33E-01	=	9.93E-01	=	2.58E-01	=	5.57E-02	↑	**3.18E-02**
Q8GZR6	(E)-4-hydroxy-3-methylbut-2-enyl-diphosphate synthase	HDS	↓	**1.66E-03**	↑	**6.78E-03**	↑	**4.81E-03**	↑	**2.68E-02**	=	7.77E-01	=	5.84E-01
A0A3Q7EA63	4-diphosphocytidyl-2-C-methyl-D-erythritol kinase	ispE	nd		↑	**1.08E-03**	nd		nd		↓	**4.85E-04**	nd	
D0VNY3	4-hydroxy-3-methylbut-2-en-1-yl diphosphate reductase	ispH	↑	**3.48E-02**	↑	**4.39E-02**	↓	**2.16E-02**	↓	**1.92E-02**	↓	**7.76E-04**	nd	
A0A3Q7GXR4	Isopentenyl-diphosphate-isomerase	IDI (1)	=	7.76E-01	↓	**1.27E-02**	=	7.04E-01	=	4.89E-01	↑	**5.32E-03**	=	8.99E-01

Table 2 – (Continued)

Protein ID	Functional description	Protein Abbrev.	Ripening stage (0 DAH *vs*. 8 DAH)		Hormonal treatment									
					ETHY *vs*. CTRL		IAA *vs*. CTRL		ETHY+IAA *vs*. CTRL		ETHY+IAA *vs*. ETHY		ETHY+IAA *vs*. IAA	
			Reg[a]	*p* value	Reg[a]	*p* value	Reg[a]	*p* value	Reg[a]	*p* value	Reg[a]	*p* value	Reg[a]	*p* value
Metabolism of carotenoid and other terpenoids														
A9LRT7	Isopentenyl-diphosphate-isomerase	IDI $_{(2)}$	=	3.72E-01	=	7.51E-01	=	5.77E-02	=	8.03E-02	=	1.74E-01	=	7.67E-01
O65004	farnesyl pyrophosphate synthase	FPPS	=	2.40E-01	=	9.32E-01	=	6.12E-01	=	2.84E-01	=	1.92E-01	=	3.46E-01
P08196	phytoene synthase 1	PSY1	↑	**5.93E-04**	↑	**1.46E-02**	↓	**1.92E-03**	↓	**6.06E-04**	=	6.72E-02	nd	
Q9SE20	zeta-carotene desaturase	ZDS	nd		=	5.59E-01	nd		nd		=	3.45E-01	nd	
Cell wall structure														
Q42872	endo-1,4-β-glucanase	Cel2	↑	**1.01E-04**	=	6.91E-01	=	4.05E-01	=	2.42E-01	=	1.70E-01	=	5.42E-01
Q8L5J1	endo-1,4-β-mannosidase 4	LeMAN4a	=	7.57E-02	=	9.14E-01	=	9.54E-02	=	2.28E-01	=	3.12E-01	=	6.86E-01
A7X331	expansin-like protein precursor	LeEXLA1	↑	**5.92E-06**	↑	**2.61E-04**	↓	**4.07E-05**	↓	**6.64E-06**	↓	**1.42E-04**	nd	
A0A3Q7IEQ9	Fn3_like domain-containing protein	LeXYL1	=	8.57E-02	=	1.02E-01	=	1.04E-01	↓	**6.27E-03**	nd		nd	
P05117	polygalacturonase 2a	PG2a	↑	**1.35E-04**	=	5.61E-01	↓	**1.48E-04**	=	9.56E-01	=	5.67E-01	=	5.83E-01
A0A3Q7I883	pectinesterase	PME	↓	**2.04E-04**	↑	**2.86E-04**	nd		↑	**2.78E-04**	=	1.87E-01	↑	**2.86E-04**
P14280	pectinesterase 1.9	PME1.9	=	2.12E-01	=	6.53E-01	=	8.81E-01	=	8.49E-01	=	7.79E-01	=	9.38E-01
Q9FZ05	xyloglucan endotransglucosylase	SlXTH2	=	3.09E-01	=	4.76E-01	=	8.02E-01	=	6.47E-01	=	5.77E-01	=	3.27E-01
A0A3Q7J3R3	β-galactosidase	TBG4	↑	**3.18E-04**	=	3.91E-01	↓	**3.22E-04**	=	8.46E-01	=	2.34E-01	↑	**3.03E-04**

DAH: Days after harvest. CTRL: Control fruits. ETHY: Ethylene-treated fruits. IAA: Indole-3-acetic acid-treated fruits. ETHY+IAA: Fruits treated with both hormones. nd: not determined. *p* value calculated using T-test between ripening stages or treatment groups. Values in bold letters indicate statistical significance ($p < 0.05$). [a] Protein regulation. ↑: Upregulated. ↓: Downregulated. =: Without change.

Figure 5 – Tomato (*Solanum lycopersicum* L. cv. Micro-Tom) fruit enzymes involved in hormone and volatile compounds biosynthetic pathways whose abundance changes during fruit ripening or in response to ethylene, auxin, and both treatments

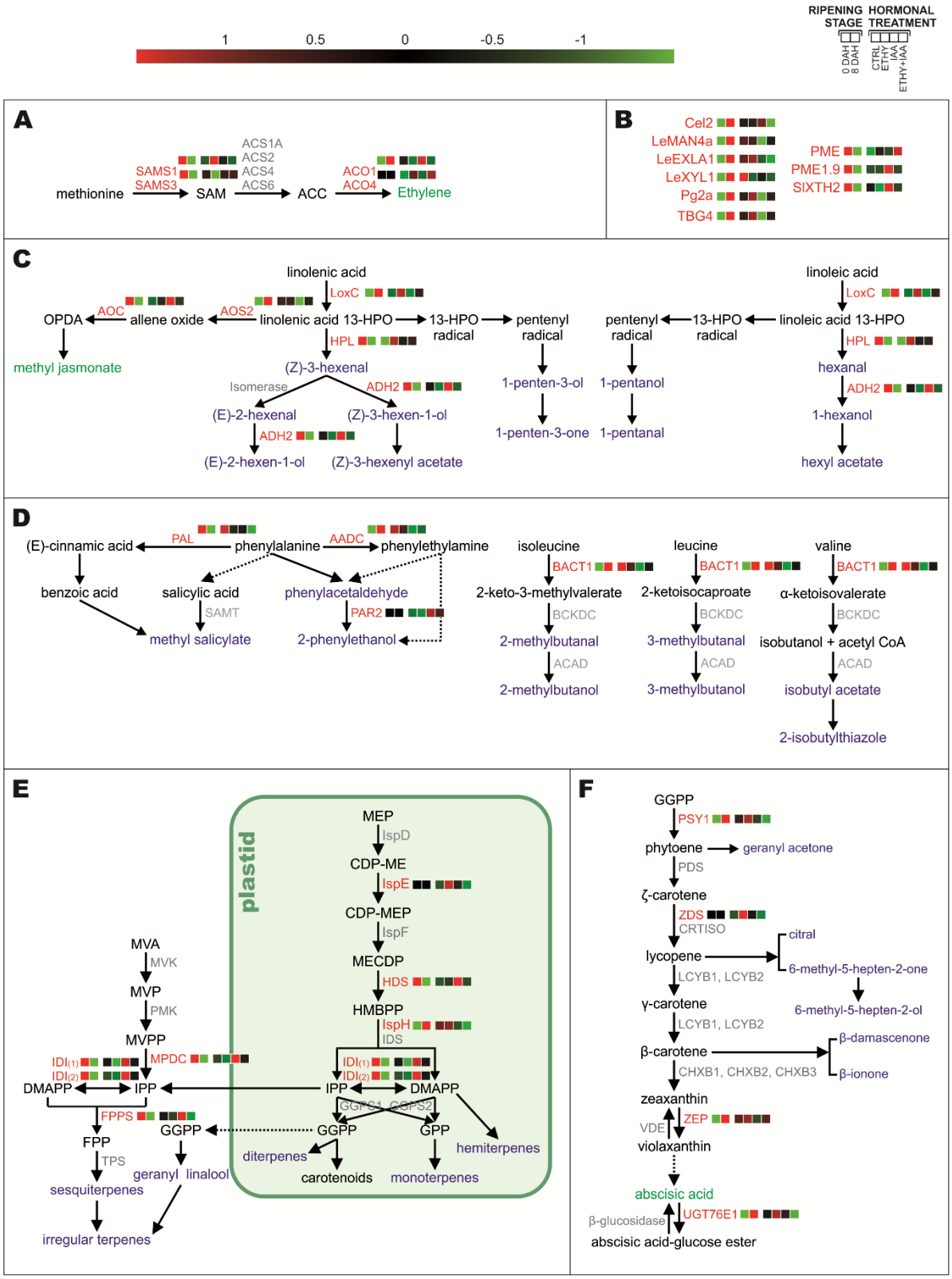

Enzymes with at least one putative isoform identified in tomato fruit proteomes are highlighted in red with its heatmap representation for each ripening stage and hormone treatment. Hormones are shown in green and volatile compounds (TIEMAN et al., 2017; KLEE; TIEMAN, 2018) are shown in blue. (A) Ethylene biosynthesis and signaling. (B) Enzymes related to cell wall structures. (C) Lipid metabolism

and jasmonate biosynthesis. (D) Amino acid metabolism. (E) Terpenoid metabolism. (F) Carotenoids metabolism and abscisic acid biosynthesis and conjugation. CTRL: Control group. ETHY: Ethylene-treated group. IAA: Indole-3-acetic acid-treated group. ETHY+IAA: Group treated with both hormones. AADC: aromatic amino acid decarboxylase. ACO1: 1-aminocyclopropane-1-carboxylate oxidase 1. ACO4: 1-aminocyclopropane-1-carboxylate oxidase 4. ADH2: alcohol dehydrogenase 2. AOC: allene oxide cyclase. AOS2: allene oxide synthase 2. BCAT1: branched-chain-amino-acid aminotransferase. Cel2: endo-1,4- β-glucanase. FPPS: farnesyl pyrophosphate synthase. HDS: (E)-4-hydroxy-3-methylbut-2-enyl-diphosphate synthase. HPL: hydroperoxide lyase. IDI: Isopentenyl-diphosphate-isomerase. IspE: 4-diphosphocytidyl-2-C-methyl-D-erythritol kinase. IspH: 4-hydroxy-3-methylbut-2-en-1-yl diphosphate reductase. LoxC: lipoxygenase C. LeEXLA1: expansin-like protein precursor. LeMAN4a: endo-1,4-β-mannosidase 4. LeXYL1: Fn3_like domain-containing protein. MPDC: diphosphomevalonate decarboxylase. PAL: phenylalanine ammonia-lyase. PAR2: phenylacetaldehyde reductase 2. PG2a: polygalacturonase 2a. PME: pectinesterase. PME1.9: pectinesterase 1.9. PSY1: phytoene synthase 1. SAMS1: S-adenosylmethionine synthase 1. SAMS3: S-adenosylmethionine synthase 3. SlXTH2: xyloglucan endotransglucosylase. TBG4: β-galactosidase. UGT73C4: UDP-glucosyltransferase 73C. ZDS: zeta-carotene desaturase. ZEP: zeaxanthin epoxidase.

In relation to jasmonates biosynthesis, allene oxide cyclase (AOC) and allene oxide synthase 2 (AOS2) are enzymes involved in fatty acid metabolism that have crucial importance to this hormone production. AOS2 appears to have its protein expression levels increased between 0 and 8 DAH and the opposite is observed to AOC. Because of this, the results in the comparisons between treated groups and CTRL also present opposite patters, making it clear that ethylene accelerated and auxin delayed the jasmonates biosynthesis (Figure 5C). Additionally, the similar results observed for ETHY+IAA and ETHY suggest that, in this case, ethylene regulation overlaps the auxin regulatory system. About ABA biosynthesis, the first step specific of this hormone biosynthetic pathway is catalyzed by a zeaxanthin epoxidase (ZEP). As shown in Figure 5F, ZEP did not appear to have been directly affected by ethylene or auxin, although it levels were reduced at 8 DAH in ETHY+IAA. On the other hand, the UDP-glycosyltransferase 73C4 (UGT73C4), an important enzyme in the ABA conjugation process, presented increased expression in fruits treated with ethylene, no changes in IAA, and reduction in ETHY+IAA.

The synthesis of aroma compounds occurs mainly during fatty acid, amino acid and carotenoid metabolism, but other important VOCs are directly derived from terpenoid metabolism (ZHANG et al., 2015). Figure 5C to Figure 5F shows biosynthetic pathways of VOCs that are important to the tomato aroma (TIEMAN et al., 2017; KLEE; TIEMAN, 2018) and the enzymes catalyzing each pathway step. Fatty acid derivative VOCs constitute the most abundant volatiles produced in tomato fruits. Lipoxygenase

C (LoxC), hydroperoxide lyase (HPL), and alcohol dehydrogenase 2 (ADH2) are the crucial enzymes involved in these pathway (Figure 5C, Table 2). The biosynthesis of these fatty acid derivatives begins with the oxidation of linoleic and linolenic acids to 13-hydroperoxides (13-HPO) by the action of lipoxygenase C followed by oxidative cleavage catalyzed by HPL to generate hexanal and (Z)-3-hexenal, that can be isomerized to (E)-2-hexenal. ADH2 catalyzes the reduction of hexanal, (Z)-3-hexenal, and (E)-2-hexenal to 1-hexanol, (Z)-3-hexen-1-ol, and (E)-2-hexen-1-ol, respectively (SPEIRS et al., 1998; CHEN et al., 2004; BAI et al., 2011; RAMBLA et al., 2014). In the current study, LoxC was upregulated in ETHY and ETHY+IAA. This result is in accordance with previous studies by this research group, by Xue et al. (2009), and by Wu et al. (2018), since LoxC is also known as a ripening-related gene and has expression induced by ethylene (GIOVANNONI, 2001). Wu et al. (2018) analyzed LoxC, HPL, and ADH2 gene expressions, and fatty acid-derived VOCs in Sweet Grape tomatoes (cv. Xin Taiyang) treated with 2,4-dichlorophenoxyacetic acid (synthetic auxin). The lower gene expressions were accompanied by the lower VOC contents in auxin-treated tomato fruit at 7 DAH. In the present study, LoxC and HPL was also downregulated in IAA, while ADH2 expression levels were not significantly different (Figure 6, Table 2), which was in accordance with the study previously described. The aroma compounds are known as C5 volatiles (1-pentanal, 1-pentanol, and 1-penten-3-one) and C6 volatiles (hexanal, 1-hexanol, (Z)-3-hexenal, (E)-2-hexenal, and (Z)-3-hexen-1-ol), are classified as green-leaf volatiles due to their characteristic aroma of freshly cut grass, and their production increases during fruit ripening (RAMBLA et al., 2014).

Aroma compounds derived from amino acids are important for tomato fruit aroma and are grouped into two categories (phenolic and branched-chain compounds) (SELLI et al., 2014; RAMBLA et al., 2014). Phenolic VOCs are directly derived from the aromatic amino acid phenylalanine (Phe) and the first step in their biosynthesis is catalyzed by l-phenylalanine ammonia lyase (PAL), which deaminates Phe to (E)-cinnamic acid, or by aromatic amino acid decarboxylase (AADC), which decarboxylates Phe to phenylethylamine. Other important enzyme in this pathway is the phenylacetaldehyde reductase 2 (PAR2), which catalyzes the conversion of phenylacetaldehyde to 2-phenylethanol (DUDAREVA et al., 2013).

Figure 6 – Tomato (*Solanum lycopersicum* L. cv. Micro-Tom) fruit proteins involved in hormone and volatile compounds biosynthetic pathways whose abundance changes specifically as a result of ethylene, auxin, and both treatments

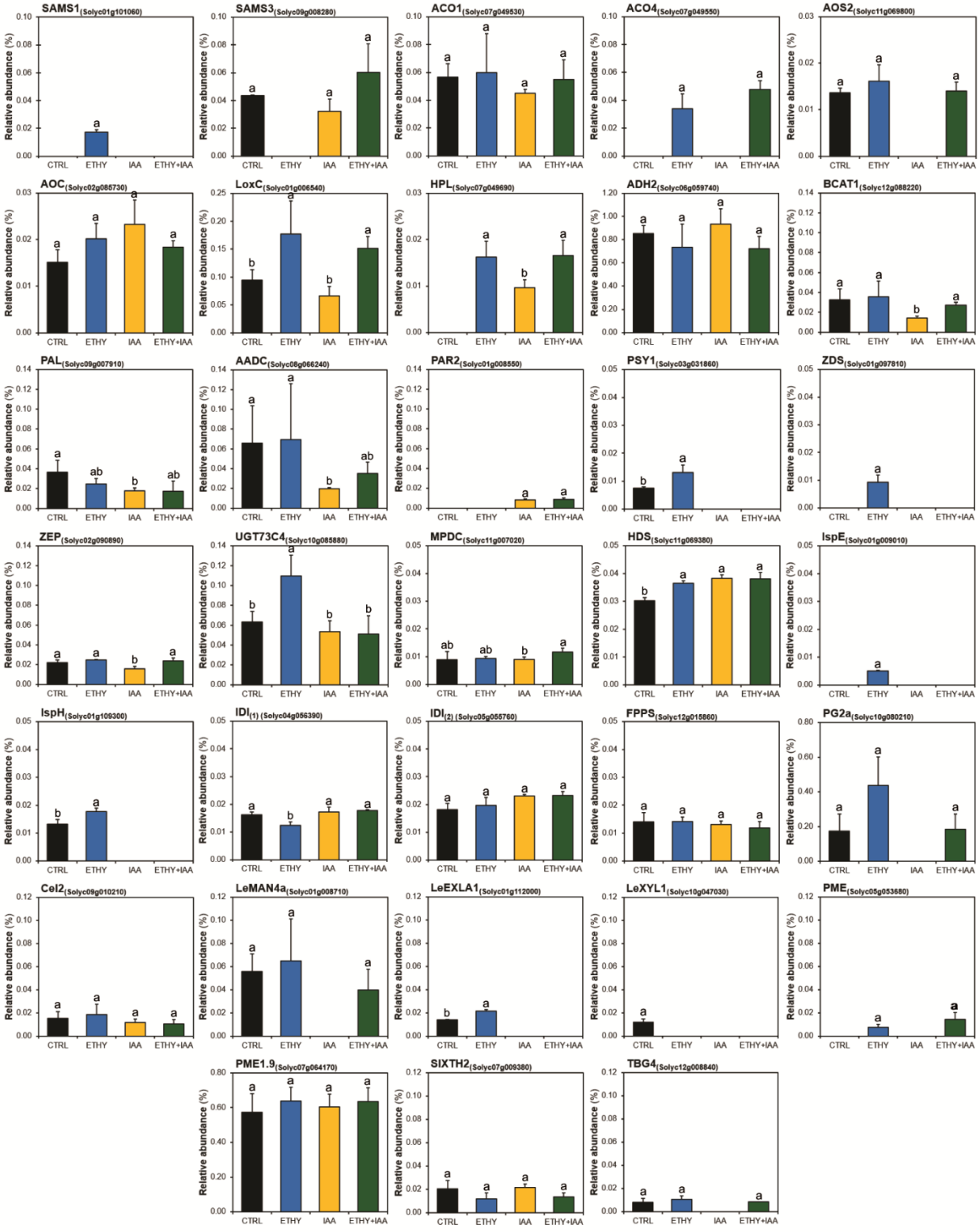

Different superscript letters indicate statistical significance ($p < 0.05$) at the same DAH (n = 4). CTRL: Control group. ETHY: Ethylene-treated group. IAA: Indole-3-acetic acid-treated group. ETHY+IAA: Group treated with both hormones. AADC: aromatic amino acid decarboxylase. ACO1: 1-aminocyclopropane-1-carboxylate oxidase 1. ACO4: 1-aminocyclopropane-1-carboxylate oxidase 4. ADH2: alcohol dehydrogenase 2. AOC: allene oxide cyclase. AOS2: allene oxide synthase 2. BCAT1:

branched-chain-amino-acid aminotransferase. Cel2: endo-1,4- β-glucanase. FPPS: farnesyl pyrophosphate synthase. HDS: (E)-4-hydroxy-3-methylbut-2-enyl-diphosphate synthase. HPL: hydroperoxide lyase. IDI: Isopentenyl-diphosphate-isomerase. IspE: 4-diphosphocytidyl-2-C-methyl-D-erythritol kinase. IspH: 4-hydroxy-3-methylbut-2-en-1-yl diphosphate reductase. LoxC: lipoxygenase C. LeEXLA1: expansin-like protein precursor. LeMAN4a: endo-1,4-β-mannosidase 4. LeXYL1: Fn3_like domain-containing protein. MPDC: diphosphomevalonate decarboxylase. PAL: phenylalanine ammonia-lyase. PAR2: phenylacetaldehyde reductase 2. PG2a: polygalacturonase 2a. PME: pectinesterase. PME1.9: pectinesterase 1.9. PSY1: phytoene synthase 1. SAMS1: S-adenosylmethionine synthase 1. SAMS3: S-adenosylmethionine synthase 3. SlXTH2: xyloglucan endotransglucosylase. TBG4: β-galactosidase. UGT73C4: UDP-glucosyltransferase 73C. ZDS: zeta-carotene desaturase. ZEP: zeaxanthin epoxidase.

As shown in Figure 5D and Figure 6, PAL was downregulated in the three treated group, but IAA presents the lowest expression levels. AADC was upregulated in ETHY and downregulated in IAA and ETHY+IAA, white PAR2 was found with reduced levels only in IAA and ETHY+IAA.

Numerous tomato aroma compounds are derived from branched-chain amino acids (leucine, isoleucine, and valine) and their biosynthesis begins with an initial deamination or transamination catalyzed by branched-chain-amino-acid aminotransferase 1 (BACT1), the crucial enzyme of the pathway (DUDAREVA et al., 2013). In the current study (Figure 6, Table 2), BACT1 was upregulated by ETHY and downregulated by IAA. ETHY+IAA presented intermediate expression levels between ETHY and IAA. AADC and BCAT1 gene expressions and amino acid-derived VOCs were analyzed by Wu et al. (2018) in Sweet Grape tomato treated with auxin and the results observed for AADC and BCAT1 protein expression in the present study seems to agree with that obtained by Wu et al. (2018). VOCs derived from phenylalanine (phenylacetaldehyde, 2-phenylethanol, methyl salicylate), leucine (3-methylbutanal, 3-methylbutanol), isoleucine (2-methylbutanal, 2-methylbutanol), and valine (isobutyl acetate, 2-isobutylthiazole) contribute significantly to the tomato aroma with distinct aromatic notes, especially 2-isobutylthiazole, which individually presents a characteristic tomato-like aroma (BALDWIN et al., 1998; RAMBLA et al., 2014).

Although aroma compounds derived from carotenoids are well known, terpenoids constitute a larger and more diverse class of secondary metabolites with many more volatile constituents, which are derived from two common five-carbon precursors, isopentenyl diphosphate (IPP) and dimethylallyl diphosphate (DMAPP) (MCGARVEY; CROTEAU, 1995; DUDAREVA et al., 2013)., two independent, and compartmentally separated, pathways are responsible for the formation of these C5-

isoprene building units in plants: mevalonic acid (MVA) and methylerythritol phosphate (MEP) (Figure 5e). The MVA pathway consists of six enzymatic reactions and is initiated by a stepwise condensation of three molecules of acetyl-CoA, while the MEP pathway involves seven enzymatic steps and begins with the condensation of d-glyceraldehyde 3-phosphate and pyruvate (LANGE et al., 2000; RAMBLA et al., 2014). Seven enzymes related to both of these pathways were found in the current study and all of them were upregulated by auxin treatment, excepting 4-diphosphocytidyl-2-C-methyl-D-erythritol kinase (IspE) and 4-hydroxy-3-methylbut-2-en-1-yl diphosphate reductase (IspH) that were not found in IAA and ETHY+IAA (Figure 6, Table 2). The MVA pathway gives rise to volatile sesquiterpenes, geranyl linalool and other irregular terpenes, while the MEP pathway provides precursors to volatile hemiterpenes, monoterpenes, diterpenes and carotenoids (RAMBLA et al., 2014).

Carotenoids are directly derived from geranylgeranyl pyrophosphate (GGPP) and the first step in their biosynthesis is catalyzed by phytoene synthase 1 (PSY1), ripening-related enzyme that has expression induced by ethylene (GIOVANNONI, 2001). Phytoene undergoes a series of sequential steps to biosynthesize lycopene, β-carotene, other carotenoids, ABA and other carotenoid-derived products, such as aroma compounds (FRASER; BRAMLEY, 2004; ENFISSI et al., 2016). In addition to PSY1, the current study also identified the ζ-carotene desaturase (ZDS) (Figure 5F, Figure 6). PSY1 was found in CTRL and ETHY proteomes, while ZDS was found only in ETHY (Table 2). Su et al. (2015) observed similar results analyzing PSY1 and ZDS genes and phytoene and lycopene concentrations after tomato cv. Micro-Tom treated with ACC (ethylene precursor), indole-3-acetic acid and both hormones. Gene expressions and carotenoid concentrations were increated in ACC-treated fruits and reduced in IAA. The results obtained in this study for PSY1 and ZDS complement that of Su et al. (2015), explaining the effect of both hormones on carotenoid metabolism.

Carotenoid derivative VOCs are biosynthesized by the action of carotenoid cleavage dioxygenases (CCD1A and CCD1B) in different carotenoids. Geranyl acetone is derived from phytoene, while citral, 6-methyl-5-hepten-2-one, and 6-methyl-5-hepten-2-ol are derived from lycopene; β-damascenone and β-ionone are both important apocarotenoids derived from β-carotene (RAMBLA et al., 2014; ENFISSI et al., 2016). These compounds are produced at low levels in ripe fruit but are important in tomato aroma due to their low perception threshold and positively association with

flavor and overall liking of tomato fruit (BUTTERY et al., 1971; RAMBLA et al., 2014; TIEMAN et al., 2017).

Additionally, several cell wall related enzymes were also identified in the current study and their patterns also suggested that they had their expression levels dysregulated by the exogenous hormone treatments. The antagonistic roles of ethylene and auxin in the cell wall degradation during the tomato fruit ripening was already individually established. Fruit softening is accelerated by exogenous ethylene (TUCKER et al., 2017) and delayed by auxin treatment (LI et al., 2016). Polygalacturonase (PG) 2a, endo-1,4-β-glucanase (Cel2), pectinesterase (PME), β-D-xylosidase 1 (LeXYL1), xyloglucan endo-transglucosylase (SlXTH2), mannan endo-1,4-β-mannosidase (LeMAN4a), β-galactosidase (TBG4), and expansin-like protein (LeEXLA1), crucial enzymes in cell wall degradation and fruit softening, were found in the present study with increased or reduced expression levels in treated fruits (Figure 5B, Figure 6). Among these enzymes, PG is also known as a ripening-related gene and is especially important due to the induced expression by ethylene (SITRIT; BENNETT, 1998; GIOVANNONI, 2001; XUE et al., 2009). PG2a, Cel2, LeMAN4a, LeEXLA1 PME1.9, and TBG4 were upregulated in ETHY and downregulated in IAA, while, SlXTH2 presented opposite profiles (Figure 6, Table 2). When treated with both hormones, the abundances of these enzymes differ from ETHY, with values similar to IAA or intermediate. In addition to the changes directly occurring in VOC metabolism, the perception of the fruit aroma can be indirectly affected by the change in fruit firmness. The cell wall degradation, responsible for fruit softening, can facilitate the release of free and conjugated VOC present inside the fruit in the final ripening stages or even during chewing, thus affecting the aroma of tomato fruits.

4 CONCLUSIONS

Fruit ripening is a complex developmental process accompanied by a huge amount of metabolic changes. Knowledge of the involved proteins in this process is extensive, but their hormone regulation remains unclear. Most of the 1807 proteins identified in the current study are involved in metabolic processes, participate in catalytic activities and are differently expressed ($p < 0.05$) between at least two

analyzed conditions (ripening stage and hormone treatment). The effects of ethylene and auxin treatments were observed in the primary and secondary metabolic profiles, with an emphasis on the aroma compounds formation. Important enzymes of hormones and VOCs biosynthetic pathways were identified and analyzed, providing a presumptive explanation for the effects of both hormones on these compounds in tomato fruit during the ripening. As in the case of the various enzymes in the terpenoids pathway, which were upregulated by auxin and downregulated by ethylene. In addition to contributing to elucidating ethylene and auxin regulatory mechanisms in VOC pathways, the generated proteomic data can be useful in later studies, on how both hormones regulate the metabolism of tomato fruits during ripening.

SUPPLEMENTARY MATERIAL

Supplementary tables of this chapter are available on a virtual drive (link below) for download since the table sizes make them unfeasible to be presented in this printed thesis.

Table S1 – Identification of tomato (*Solanum lycopersicum* L. cv. Micro-Tom) fruit protein results

Link: Table S1

Table S2 – Tomato (*Solanum lycopersicum* L. cv. Micro-Tom) fruit proteins whose abundance changes specifically during ripening or as a result of ethylene, auxin, and both treatments

Link: Table S2

Table S3 – Gene ontology classification for tomato (*Solanum lycopersicum* L. cv. Micro-Tom) fruit proteome at 0 and 8 days after harvest (DAH) and different hormone treatments

Link: Table S3

Table S6 – Tomato (*Solanum lycopersicum* L. cv. Micro-Tom) fruit proteins involved in primary and secondary metabolisms whose abundance changes specifically during fruit ripening or as a result of ethylene, auxin, and both treatments

Link: Table S6

Figure S1 – Schematic representation of the experiment design and the proteomic analysis workflow

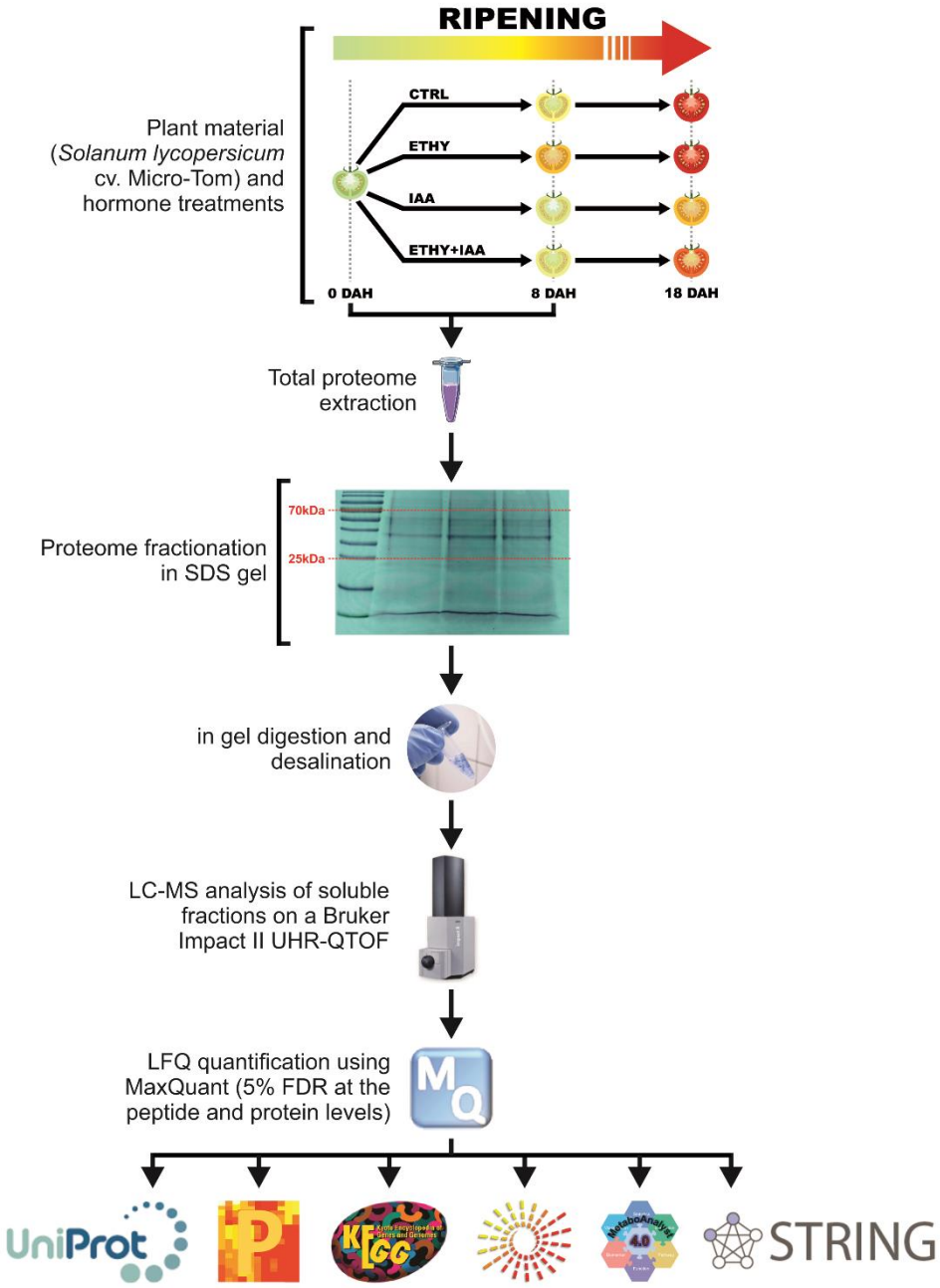

All presented steps have been described in detail in the Materials and methods section. They include the following. Tomato (*Solanum lycopersicum* cv. Micro-tom) fruits were collected at 0 and 8 days after harvest in four biological replicates. Ethylene emission and surface color were evaluated daily as ripening parameters. Proteomes were extracted, quantified, fractionated, and subjected to in-gel tryptic digestion using Shevchenko et al. (2006) protocol. After cleanup, digested peptides were analyzed by liquid chromatography-mass spectrometry (LC-MS). The MS data were analyzed using MaxQuant v. 1.6.6.0 and bioinformatics analysis was performed using Perseus v. 1.6.6.0, Uniprot, MetaboAnalyst 4.0 and STRING.

Figure S2 – Differently expressed proteins were grouped according to KEGG pathways

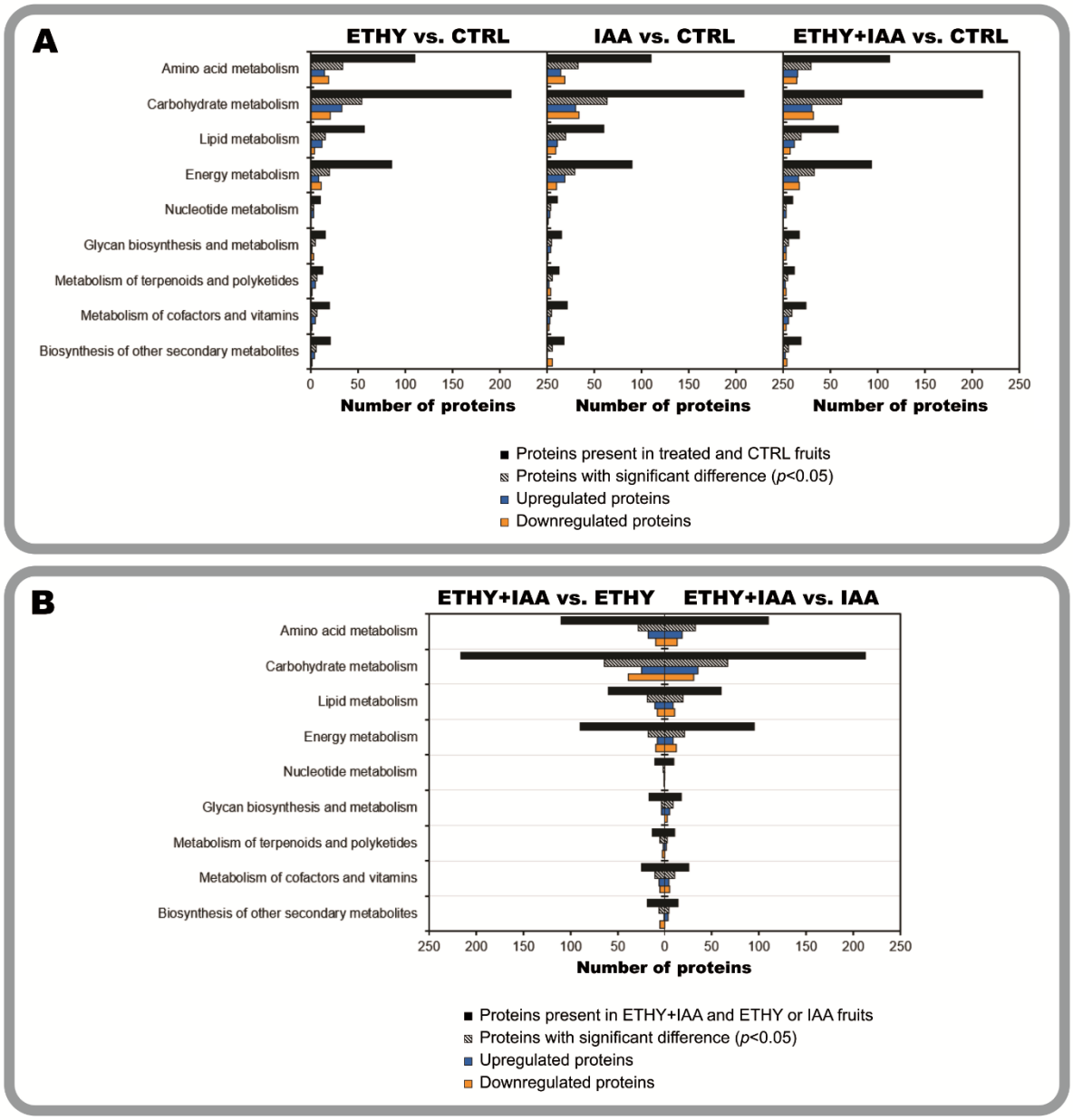

(A) Number of proteins present, significantly different expressed (p < 0.05), upregulated, and downregulated between CTRL and treated treated groups. (B) Number of proteins present, significantly different expressed (p < 0.05), upregulated, and downregulated between ETHY+IAA and fruits treated with ethylene or auxin. CTRL: Control group. ETHY: Ethylene-treated group. IAA: Indole-3-acetic acid-treated group. ETHY+IAA: Group treated with both hormones.

Table S4 – Summary of gene ontology and KEGG pathway classifications for tomato (*Solanum lycopersicum* L. cv. Micro-Tom) fruit proteome at 0 and 8 days after harvest (DAH) and different hormone treatments

Class name	Total	0 DAH	8 DAH			
			CTRL	ETHY	IAA	ETHY+IAA
Biological process						
metabolic process	925	697	700	688	700	740
cellular process	760	595	570	560	584	613
biological regulation	172	132	129	131	133	141
localization	162	130	127	123	132	133
response to stimulus	111	79	79	82	84	94
cellular component organization or biogenesis	95	75	72	67	69	78
cellular detoxification	38	29	28	26	29	28
developmental process	16	10	11	12	11	13
multicellular organismal process	14	7	10	11	8	11
reproductive process	12	4	9	9	6	9
multi-organism process	12	3	10	9	9	9
immune system process	3	1	2	2	2	3
others	9	3	7	7	4	6
Molecular function						
catalytic activity	975	722	728	719	726	772
binding	803	640	620	622	622	655
structural molecule activity	66	62	53	49	55	57
transporter activity	42	38	35	33	36	34
antioxidant activity	36	27	26	24	27	26
molecular function regulator	34	24	25	28	27	27
translation factor activity, RNA binding	27	25	23	21	22	23
nutrient reservoir activity	12	11	11	12	11	12
signaling receptor activity	6	4	5	6	6	6
others	8	7	7	6	8	7
Cellular component						
transmembrane	202	156	129	132	137	147
cytoplasm	107	94	92	95	94	94
nucleus	65	53	51	50	52	55
chloroplast	37	29	30	32	29	27
cell	33	27	27	23	26	25
ribosome	32	31	25	24	28	26
cytosol	29	24	20	23	23	22
extracellular space	29	11	23	24	18	24
membrane	19	15	16	14	15	18
others	460	382	360	352	374	388

Table S4 – (Continued)

Class name	Total	0 DAH	8 DAH			
			CTRL	ETHY	IAA	ETHY+IAA
Subcellular location						
cytoplasm	95	83	81	83	80	81
nucleus	50	40	40	42	41	44
plastid	53	40	41	42	43	42
membrane	23	19	18	13	13	15
secreted (extracellular space)	26	11	22	21	16	23
mitochondrion	18	13	15	15	15	16
endoplasmic reticulum	18	15	13	15	13	15
golgi apparatus	11	8	7	8	9	8
cytoplasmic vesicle	13	12	10	9	10	12
vacuole	4	3	3	2	3	3
others	5	4	5	4	3	4
KEGG Pathways						
carbohydrate metabolism	237	191	199	199	187	203
amino acid metabolism	121	95	100	94	97	101
lipid metabolism	70	56	50	55	54	54
energy metabolism	97	84	83	78	84	88
glycan biosynthesis and metabolism	19	12	14	13	14	15
nucleotide metabolism	14	12	8	10	10	9
metabolism of cofactors and vitamins	29	17	17	17	20	23
metabolism of terpenoids and polyketides	16	8	11	12	11	9
biosynthesis of other secondary metabolites	24	16	18	19	13	15

DAH: Days after harvest. CTRL: Control fruits. ETHY: Ethylene-treated fruits. IAA: Indole-3-acetic acid-treated fruits. ETHY+IAA: Fruits treated with both hormones.

Table S5 – Gene ontology (GO) and KEGG pathway enrichment analysis of the identified proteins in tomato (*Solanum lycopersicum* L. cv. Micro-Tom) fruit proteomes

ID	Term description	Mapping	Background	FDR
Biological process				
GO:0008152	metabolic process	67	276	1.09e-33
GO:0009987	cellular process	65	261	1.68e-33
GO:0044237	cellular metabolic process	61	237	3.24e-32
GO:0071704	organic substance metabolic process	57	223	5.08e-30
GO:0044238	primary metabolic process	50	205	1.60e-25
GO:1901564	organonitrogen compound metabolic process	33	121	5.92e-18
GO:0006807	nitrogen compound metabolic process	34	148	1.34e-16
GO:0055114	oxidation-reduction process	27	85	4.06e-16
GO:0044281	small molecule metabolic process	25	70	6.18e-16
GO:0009058	biosynthetic process	31	143	1.22e-14
GO:1901576	organic substance biosynthetic process	30	141	5.18e-14
GO:0044249	cellular biosynthetic process	29	131	5.80e-14
GO:0043436	oxoacid metabolic process	17	45	3.31e-11
GO:0015979	photosynthesis	17	46	3.83e-11
GO:0043170	macromolecule metabolic process	24	116	4.25e-11
GO:0017144	drug metabolic process	16	40	5.88e-11
GO:0019752	carboxylic acid metabolic process	16	44	1.80e-10
GO:0050896	response to stimulus	19	82	1.43e-09
GO:0032787	monocarboxylic acid metabolic process	12	22	1.78e-09
GO:0005975	carbohydrate metabolic process	14	38	2.78e-09
GO:0044260	cellular macromolecule metabolic process	20	99	3.26e-09
GO:0006091	generation of precursor metabolites and energy	14	41	5.77e-09
GO:0018298	protein-chromophore linkage	11	20	8.69e-09
GO:0044283	small molecule biosynthetic process	13	37	1.73e-08
GO:0072330	monocarboxylic acid biosynthetic process	10	18	4.71e-08
GO:0006796	phosphate-containing compound metabolic process	12	33	5.21e-08
GO:0019538	protein metabolic process	16	73	6.12e-08
GO:0006464	cellular protein modification process	12	34	6.18e-08
GO:0046394	carboxylic acid biosynthetic process	11	29	1.37e-07
GO:0044248	cellular catabolic process	11	30	1.72e-07
GO:1901135	carbohydrate derivative metabolic process	10	25	3.87e-07
GO:0044267	cellular protein metabolic process	14	67	7.41e-07
GO:1901575	organic substance catabolic process	10	28	8.75e-07
GO:0019684	photosynthesis, light reaction	9	22	1.53e-06
GO:0044255	cellular lipid metabolic process	10	31	1.83e-06
GO:0006950	response to stress	12	52	2.28e-06
GO:0008610	lipid biosynthetic process	10	32	2.28e-06
GO:0005976	polysaccharide metabolic process	8	17	3.04e-06
GO:0071554	cell wall organization or biogenesis	8	17	3.04e-06
GO:0009057	macromolecule catabolic process	8	18	4.09e-06
GO:0016310	phosphorylation	8	18	4.09e-06
GO:0090407	organophosphate biosynthetic process	7	12	5.27e-06
GO:1901360	organic cyclic compound metabolic process	13	75	1.09e-05
GO:0009152	purine ribonucleotide biosynthetic process	6	8	1.17e-05
GO:0016052	carbohydrate catabolic process	7	15	1.42e-05

Table S5 – (Continued)

ID	Term description	Mapping	Background	FDR
GO:1901362	organic cyclic compound biosynthetic process	11	54	1.61e-05
GO:1901566	organonitrogen compound biosynthetic process	12	67	1.73e-05
GO:0006633	fatty acid biosynthetic process	6	10	2.48e-05
GO:0022900	electron transport chain	7	17	2.48e-05
GO:0042737	drug catabolic process	7	18	3.30e-05
GO:0006631	fatty acid metabolic process	6	11	3.57e-05
GO:0044265	cellular macromolecule catabolic process	6	11	3.57e-05
GO:0051188	cofactor biosynthetic process	6	11	3.57e-05
GO:0044271	cellular nitrogen compound biosynthetic process	12	75	4.37e-05
GO:0044272	sulfur compound biosynthetic process	5	6	4.99e-05
GO:0051186	cofactor metabolic process	7	21	6.80e-05
GO:1901565	organonitrogen compound catabolic process	6	13	6.80e-05
GO:0009206	purine ribonucleoside triphosphate biosynthetic process	5	7	8.01e-05
GO:0000272	polysaccharide catabolic process	6	14	8.76e-05
GO:0019438	aromatic compound biosynthetic process	9	44	9.99e-05
GO:0019637	organophosphate metabolic process	7	23	9.99e-05
GO:0009150	purine ribonucleotide metabolic process	6	15	0.00012
GO:0044036	cell wall macromolecule metabolic process	5	8	0.00012
GO:0016043	cellular component organization	8	36	0.00016
GO:0006952	defense response	7	26	0.00017
GO:0065007	biological regulation	11	76	0.00018
GO:0009772	photosynthetic electron transport in photosystem II	4	4	0.00021
GO:0018130	heterocycle biosynthetic process	8	38	0.00021
GO:0006790	sulfur compound metabolic process	5	10	0.00022
GO:0009205	purine ribonucleoside triphosphate metabolic process	5	10	0.00022
GO:0009416	response to light stimulus	6	18	0.00022
GO:1901615	organic hydroxy compound metabolic process	6	21	0.00042
GO:0034654	nucleobase-containing compound biosynthetic process	7	32	0.00046
GO:0006754	ATP biosynthetic process	4	6	0.00054
GO:0009168	purine ribonucleoside monophosphate biosynthetic process	4	6	0.00054
GO:0006520	cellular amino acid metabolic process	6	23	0.00060
GO:0044262	cellular carbohydrate metabolic process	5	14	0.00065
GO:0016998	cell wall macromolecule catabolic process	4	7	0.00077
GO:0009835	fruit ripening	5	15	0.00082
GO:0055085	transmembrane transport	5	15	0.00082
GO:0009108	coenzyme biosynthetic process	4	8	0.0010
GO:0031407	oxylipin metabolic process	4	8	0.0010
GO:0031408	oxylipin biosynthetic process	4	8	0.0010
GO:0006810	transport	6	28	0.0013
GO:0009167	purine ribonucleoside monophosphate metabolic process	4	9	0.0014
GO:0046034	ATP metabolic process	4	9	0.0014
GO:1902600	proton transmembrane transport	4	9	0.0014
GO:0071555	cell wall organization	4	10	0.0018
GO:0006030	chitin metabolic process	3	4	0.0025
GO:0006032	chitin catabolic process	3	4	0.0025
GO:0009768	photosynthesis, light harvesting in photosystem I	4	12	0.0028
GO:0006139	nucleobase-containing compound metabolic process	7	49	0.0030

Table S5 – (Continued)

ID	Term description	Mapping	Background	FDR
GO:0009064	glutamine family amino acid metabolic process	3	5	0.0034
GO:0015986	ATP synthesis coupled proton transport	3	5	0.0034
GO:1901605	alpha-amino acid metabolic process	4	13	0.0034
GO:0006721	terpenoid metabolic process	4	14	0.0041
GO:0016114	terpenoid biosynthetic process	4	14	0.0041
GO:0044264	cellular polysaccharide metabolic process	3	6	0.0047
GO:0006508	proteolysis	3	8	0.0087
GO:0051716	cellular response to stimulus	5	31	0.0089
GO:0006066	alcohol metabolic process	3	9	0.0112
GO:0016051	carbohydrate biosynthetic process	3	9	0.0112
GO:0099131	ATP hydrolysis coupled ion transmembrane transport	3	9	0.0112
GO:0099132	ATP hydrolysis coupled cation transmembrane transport	3	9	0.0112
GO:0006081	cellular aldehyde metabolic process	2	2	0.0123
GO:0006090	pyruvate metabolic process	2	2	0.0123
GO:0006165	nucleoside diphosphate phosphorylation	2	2	0.0123
GO:0006749	glutathione metabolic process	2	2	0.0123
GO:0006750	glutathione biosynthetic process	2	2	0.0123
GO:0006955	immune response	2	2	0.0123
GO:0061024	membrane organization	2	2	0.0123
GO:0009636	response to toxic substance	3	10	0.0131
GO:0009607	response to biotic stimulus	3	11	0.0163
GO:0016125	sterol metabolic process	3	11	0.0163
GO:0065008	regulation of biological quality	4	23	0.0164
GO:0006073	cellular glucan metabolic process	2	3	0.0186
GO:0006556	S-adenosylmethionine biosynthetic process	2	3	0.0186
GO:0010207	photosystem II assembly	2	3	0.0186
GO:0034404	nucleobase-containing small molecule biosynthetic process	2	3	0.0186
GO:0042446	hormone biosynthetic process	3	13	0.0228
GO:0042221	response to chemical	4	27	0.0255
GO:0006595	polyamine metabolic process	2	4	0.0260
GO:0006596	polyamine biosynthetic process	2	4	0.0260
GO:0006730	one-carbon metabolic process	2	4	0.0260
GO:0009853	photorespiration	2	4	0.0260
GO:0010383	cell wall polysaccharide metabolic process	2	4	0.0260
GO:0019253	reductive pentose-phosphate cycle	2	4	0.0260
GO:0042545	cell wall modification	2	4	0.0260
GO:0043254	regulation of protein complex assembly	2	4	0.0260
GO:0046500	S-adenosylmethionine metabolic process	2	4	0.0260
GO:0051603	proteolysis involved in cellular protein catabolic process	2	4	0.0260
GO:0097164	ammonium ion metabolic process	2	4	0.0260
GO:1901617	organic hydroxy compound biosynthetic process	3	14	0.0260
GO:0006468	protein phosphorylation	2	5	0.0327
GO:0006575	cellular modified amino acid metabolic process	2	5	0.0327
GO:0019439	aromatic compound catabolic process	2	5	0.0327
GO:1901361	organic cyclic compound catabolic process	2	5	0.0327
GO:0050794	regulation of cellular process	5	53	0.0490

Table S5 – (Continued)

ID	Term description	Mapping	Background	FDR
Molecular function				
GO:0003824	catalytic activity	60	212	1.35e-33
GO:0005488	binding	60	250	1.59e-30
GO:0043167	ion binding	50	154	1.59e-30
GO:0043168	anion binding	34	88	8.33e-23
GO:0046872	metal ion binding	32	101	2.09e-19
GO:0097159	organic cyclic compound binding	38	166	5.04e-19
GO:1901363	heterocyclic compound binding	38	166	5.04e-19
GO:0016491	oxidoreductase activity	26	77	1.48e-16
GO:0008144	drug binding	22	53	1.35e-15
GO:0036094	small molecule binding	24	78	1.26e-14
GO:0005524	ATP binding	19	39	1.42e-14
GO:0097367	carbohydrate derivative binding	20	55	1.68e-13
GO:0000166	nucleotide binding	20	60	5.16e-13
GO:0048037	cofactor binding	22	78	5.16e-13
GO:0046906	tetrapyrrole binding	16	38	8.01e-12
GO:0016787	hydrolase activity	15	53	3.93e-09
GO:0016740	transferase activity	14	49	1.28e-08
GO:0016168	chlorophyll binding	10	18	1.62e-08
GO:0005515	protein binding	13	43	2.52e-08
GO:0016301	kinase activity	7	11	2.02e-06
GO:0019904	protein domain specific binding	7	11	2.02e-06
GO:0009055	electron transfer activity	7	13	4.37e-06
GO:0046914	transition metal ion binding	8	22	7.10e-06
GO:0016829	lyase activity	9	34	1.36e-05
GO:0004553	hydrolase activity, hydrolyzing O-glycosyl compounds	6	14	6.75e-05
GO:0016773	phosphotransferase activity, alcohol group as acceptor	5	9	0.00013
GO:0020037	heme binding	6	20	0.00032
GO:0045156	electron transporter, transferring electrons within the cyclic electron transport pathway of photosynthesis activity	4	5	0.00032
GO:0004497	monooxygenase activity	5	13	0.00048
GO:0050662	coenzyme binding	6	28	0.0014
GO:0015078	proton transmembrane transporter activity	4	9	0.0015
GO:0005506	iron ion binding	4	10	0.0020
GO:0004568	chitinase activity	3	4	0.0025
GO:0016830	carbon-carbon lyase activity	4	11	0.0025
GO:0042623	ATPase activity, coupled	4	11	0.0025
GO:0031409	pigment binding	4	12	0.0029
GO:0016765	transferase activity, transferring alkyl or aryl (other than methyl) groups	4	13	0.0037
GO:0140096	catalytic activity, acting on a protein	4	13	0.0037
GO:0000287	magnesium ion binding	4	14	0.0043
GO:0016705	oxidoreductase activity, acting on paired donors, with incorporation or reduction of molecular oxygen	4	14	0.0043
GO:0019842	vitamin binding	4	15	0.0050
GO:0016874	ligase activity	3	7	0.0065
GO:0016702	oxidoreductase activity, acting on single donors with incorporation of molecular oxygen, incorporation of two atoms of oxygen	2	2	0.0105
GO:0016831	carboxy-lyase activity	3	9	0.0105
GO:0016881	acid-amino acid ligase activity	2	2	0.0105

Table S5 – (Continued)

ID	Term description	Mapping	Background	FDR
GO:0019829	cation-transporting ATPase activity	3	9	0.0105
GO:0004478	methionine adenosyltransferase activity	2	3	0.0160
GO:0016984	ribulose-bisphosphate carboxylase activity	2	4	0.0232
GO:0030599	pectinesterase activity	2	4	0.0232
GO:0031418	L-ascorbic acid binding	2	4	0.0232
GO:0038023	signaling receptor activity	2	4	0.0232
GO:0045330	aspartyl esterase activity	2	4	0.0232
GO:0046910	pectinesterase inhibitor activity	2	4	0.0232
GO:0046933	proton-transporting ATP synthase activity, rotational mechanism	2	4	0.0232
GO:0051539	4 iron, 4 sulfur cluster binding	2	4	0.0232
GO:0016835	carbon-oxygen lyase activity	3	15	0.0240
GO:0004672	protein kinase activity	2	5	0.0271
GO:0016836	hydro-lyase activity	2	5	0.0271
GO:0004601	peroxidase activity	2	6	0.0340
GO:0070011	peptidase activity, acting on L-amino acid peptides	2	6	0.0340
GO:0042803	protein homodimerization activity	2	7	0.0409
Cellular component				
GO:0044464	cell part	60	293	3.03e-27
GO:0005737	cytoplasm	52	234	2.02e-25
GO:0005622	intracellular	54	270	1.31e-24
GO:0044444	cytoplasmic part	45	195	7.61e-23
GO:0043227	membrane-bounded organelle	41	214	2.57e-18
GO:0009507	chloroplast	34	141	6.25e-18
GO:0043229	intracellular organelle	41	225	7.98e-18
GO:0043231	intracellular membrane-bounded organelle	40	212	7.98e-18
GO:0044434	chloroplast part	24	78	5.96e-15
GO:0016020	membrane	25	101	9.10e-14
GO:0009535	chloroplast thylakoid membrane	20	61	4.54e-13
GO:0044446	intracellular organelle part	26	123	4.99e-13
GO:0031984	organelle subcompartment	21	73	6.71e-13
GO:0098796	membrane protein complex	17	45	3.08e-12
GO:0044425	membrane part	21	85	6.41e-12
GO:0032991	protein-containing complex	21	95	3.83e-11
GO:0009521	photosystem	13	33	8.87e-10
GO:0009523	photosystem II	11	26	1.12e-08
GO:0016021	integral component of membrane	16	74	1.27e-08
GO:0005576	extracellular region	10	38	2.08e-06
GO:0009570	chloroplast stroma	7	20	2.02e-05
GO:0009941	chloroplast envelope	7	22	3.20e-05
GO:0071944	cell periphery	7	32	0.00022
GO:0010287	plastoglobule	5	13	0.00025
GO:0005618	cell wall	5	16	0.00054
GO:0005829	cytosol	6	27	0.00060
GO:0009522	photosystem I	5	17	0.00064
GO:1902494	catalytic complex	5	18	0.00078
GO:0009509	chromoplast	3	5	0.0022

Table S5 – (Continued)

ID	Term description	Mapping	Background	FDR
GO:0045259	proton-transporting ATP synthase complex	3	5	0.0022
GO:0005615	extracellular space	3	9	0.0075
GO:0045261	proton-transporting ATP synthase complex, catalytic core F(1)	2	2	0.0081
GO:0005768	endosome	2	3	0.0128
GO:0009654	photosystem II oxygen evolving complex	2	3	0.0128
GO:0005777	peroxisome	2	5	0.0234
GO:0031969	chloroplast membrane	2	6	0.0296
GO:0048046	apoplast	2	6	0.0296
GO:0005773	vacuole	2	8	0.0438
KEGG pathway				
sly01100	Metabolic pathways	281	2050	1.78e-100
sly01110	Biosynthesis of secondary metabolites	161	1192	7.14e-54
sly01200	Carbon metabolism	79	266	1.28e-46
sly01230	Biosynthesis of amino acids	58	232	9.09e-31
sly00010	Glycolysis / Gluconeogenesis	38	132	5.12e-22
sly04141	Protein processing in endoplasmic reticulum	40	213	1.82e-17
sly00520	Amino sugar and nucleotide sugar metabolism	32	132	8.01e-17
sly00710	Carbon fixation in photosynthetic organisms	25	76	7.82e-16
sly00020	Citrate cycle (TCA cycle)	22	54	1.35e-15
sly00620	Pyruvate metabolism	26	91	2.60e-15
sly00630	Glyoxylate and dicarboxylate metabolism	24	74	3.11e-15
sly03050	Proteasome	20	49	2.43e-14
sly00195	Photosynthesis	20	72	8.76e-12
sly00051	Fructose and mannose metabolism	19	70	4.22e-11
sly00270	Cysteine and methionine metabolism	22	107	9.80e-11
sly00260	Glycine, serine and threonine metabolism	18	69	2.33e-10
sly03010	Ribosome	34	290	4.07e-10
sly01210	2-Oxocarboxylic acid metabolism	16	61	2.39e-09
sly00030	Pentose phosphate pathway	15	55	5.06e-09
sly04144	Endocytosis	25	182	6.44e-09
sly00190	Oxidative phosphorylation	20	130	5.05e-08
sly00500	Starch and sucrose metabolism	20	132	6.07e-08
sly00970	Aminoacyl-tRNA biosynthesis	12	51	8.11e-07
sly00480	Glutathione metabolism	16	108	2.07e-06
sly00670	One carbon pool by folate	8	19	2.38e-06
sly03013	RNA transport	19	159	3.31e-06
sly00061	Fatty acid biosynthesis	10	46	1.37e-05
sly00250	Alanine, aspartate and glutamate metabolism	10	50	2.53e-05
sly03018	RNA degradation	14	111	4.73e-05
sly00052	Galactose metabolism	10	58	7.42e-05
sly00400	Phenylalanine, tyrosine and tryptophan biosynthesis	9	48	0.00010
sly00603	Glycosphingolipid biosynthesis - globo and isoglobo series	5	9	0.00010
sly01212	Fatty acid metabolism	11	77	0.00013
sly00053	Ascorbate and aldarate metabolism	9	55	0.00024
sly00561	Glycerolipid metabolism	11	84	0.00024
sly00460	Cyanoamino acid metabolism	8	45	0.00034

Table S5 – (Continued)

ID	Term description	Mapping	Background	FDR
sly00220	Arginine biosynthesis	7	36	0.00055
sly00350	Tyrosine metabolism	8	49	0.00055
sly00920	Sulfur metabolism	7	36	0.00055
sly04145	Phagosome	10	82	0.00075
sly00410	beta-Alanine metabolism	8	53	0.00082
sly00640	Propanoate metabolism	7	41	0.00098
sly00280	Valine, leucine and isoleucine degradation	8	60	0.0017
sly00910	Nitrogen metabolism	6	34	0.0021
sly00330	Arginine and proline metabolism	8	65	0.0024
sly00591	Linoleic acid metabolism	5	23	0.0024
sly00592	alpha-Linolenic acid metabolism	7	49	0.0024
sly00230	Purine metabolism	13	159	0.0029
sly00196	Photosynthesis - antenna proteins	5	25	0.0032
sly00290	Valine, leucine and isoleucine biosynthesis	5	26	0.0036
sly00360	Phenylalanine metabolism	8	71	0.0038
sly00750	Vitamin B6 metabolism	4	15	0.0038
sly00130	Ubiquinone and other terpenoid-quinone biosynthesis	6	42	0.0046
sly04146	Peroxisome	9	92	0.0046
sly00450	Selenocompound metabolism	4	17	0.0052
sly00770	Pantothenate and CoA biosynthesis	5	30	0.0056
sly00780	Biotin metabolism	4	19	0.0071
sly00340	Histidine metabolism	4	20	0.0081
sly00071	Fatty acid degradation	6	52	0.0108
sly00310	Lysine degradation	5	39	0.0143
sly00040	Pentose and glucuronate interconversions	9	117	0.0174
sly00650	Butanoate metabolism	4	27	0.0193
sly00604	Glycosphingolipid biosynthesis - ganglio series	2	4	0.0195
sly00511	Other glycan degradation	3	14	0.0196
sly00600	Sphingolipid metabolism	4	28	0.0206
sly00564	Glycerophospholipid metabolism	8	102	0.0215
sly01040	Biosynthesis of unsaturated fatty acids	4	29	0.0220
sly03015	mRNA surveillance pathway	9	124	0.0220
sly03040	Spliceosome	11	182	0.0347
sly00906	Carotenoid biosynthesis	4	35	0.0375
sly00940	Phenylpropanoid biosynthesis	12	210	0.0381
sly00900	Terpenoid backbone biosynthesis	5	56	0.0442
sly00730	Thiamine metabolism	3	21	0.0443

ID: GO or KEGG identification. FDR: False discovery rate

5 CONCLUSIONS

Fruit ripening is a complex developmental process accompanied by a huge number of metabolic changes. Knowledge of hormonal regulation is extensive; however, the role of each hormone in fruit aroma formation remains unclear. The metabolomic and proteomic approaches described in this study were highly effective in elucidating ethylene and auxin regulatory mechanisms in VOC pathways, demonstrating how different hormone treatments changed the primary and secondary metabolic profiles and therefore the tomato fruit aroma.

Although the tomato fruits were visually similar when fully ripe, we identified significant changes in various metabolite classes, indicating reprogramming of specific pathways after treatments with exogenous ethylene and auxin. Most of the 126 primary metabolites, 1,807 proteins, and 40 important VOCs identified in the present study showed significantly changed abundances in response to at least one hormone treatment. The effects of ethylene and auxin treatments were observed in the primary and secondary metabolic profiles, with an emphasis on the aroma compound formation. Thus, a systemic view of the VOC changes during ripening indicated that related pathways reacted differently to each hormone as well as to the crosstalk between them, providing a presumptive explanation for the effects of both hormones on these compounds during tomato fruit ripening.

In addition to enabling elucidation of the ethylene and auxin regulatory mechanisms in VOC pathways, the generated metabolomic and proteomic data may be useful in further studies on how both hormones regulate the metabolism of tomato fruits during ripening. Furthermore, the findings in this study encourage the application of other omics approaches to studying hormonal regulation of fruit metabolism.

The obtained results stimulated further studies adopting different approaches to confirming the role of auxin in regulating the VOC metabolism. Tomato mutants can be used as a tool for visualizing phenotype changes by modifying the genes of interest. This approach is a common practice in studies that highlight the role of ethylene and the master regulators (*rin, nor, cnr*) during ripening, but it has not yet been used in studies related to auxin and aroma metabolism. Another possible approach to continuing this study is the treatment of tomato fruits with α-(phenylethyl-2-one)-indole-

3-acetic acid (PEO-IAA), an auxin antagonist that competes for its binding domain and prevents the degradation of Aux/IAA.

REFERENCES

ADAMS-PHILLIPS, L. *et al*. Evidence that CTR1-mediated ethylene signal transduction in tomato is encoded by a multigene family whose members display distinct regulatory features. **Plant Molecular Biology**, v. 54, p. 387-404, 2004.

ARAGÜEZ, I.; FERNÁNDEZ, V.V. Metabolic engineering of aroma components in fruits. **Plant Biotechnology**, v. 8, i. 10, p. 1144-58, 2013

ARORA, A. Ethylene receptors and molecular mechanism of ethylene sensitivity in plants. **Current science**, v. 89, p. 1348-61, 2005.

BAI, J. *et al*. Chilling and heating may regulate C6 volatile aroma production by different mechanisms in tomato (*Solanum lycopersicum*) fruit. **Postharvest Biology and Technology**, v. 60, i. 2, p. 111-20, 2011.

BALDWIN, E.A. *et al*. Flavor trivia and tomato aroma: biochemistry and possible mechanisms for control of important aroma components. **Hortscience**, v. 35, p. 1013-22, 2000.

BALDWIN, E.A. *et al*. Relationship between Sensory and Instrumental Analysis for Tomato Flavor. **Journal of the American Society for Horticultural Science**, v. 123, i. 5, p. 906-15, 1998.

BARGMAN, B.O.R.; ESTELLE, M. Auxin perception: in the IAA of the beholder. **Physiologia Plantarum**, v. 151, p. 52-61, 2014.

BARSAN, C. *et al*. Proteomic analysis to chloroplast to chromoplast transition in tomato reveals metabolic shifts coupled with disrupted thylakoid biogenesis machinery and elevated energy-production components. **Plant Physiology**, v. 160, p. 708-25, 2012.

BAUCHET, G. *et al*. Identification of major loci and genomic regions controlling acid and volatile content in tomato fruit: implications for flavor improvement. **The New Phytologist**, v. 215, i. 2, p. 624-41, 2017.

BERGOUGNOUX, V. The history of tomato: From domestication to biopharming. **Biotechnology Advances**, v. 32, i. 1, p. 170-89, 2014.

BIALE, J.B.; YOUNG, R.E. Respiration and ripening in fruits: retrospective and prospect. In: FRIEND, J.; RHODES, M.J.C. **Recent advances in the biochemistry of fruits and vegetables**. London: Academic, 1981. p. 1-39.

BLIGH, E.G.; DYER, W.J. A rapid method for total lipid extraction and purification. **Canadian Journal Biochemistry and Physiology**, v. 37, p. 911-7, 1959.

BÖTTCHER, C. *et al*. Sequestration of auxin by the indole-3-acetic acid-amido synthetase GH3-1 in grape berry (*Vitis vinifera* L.) and the proposed role of auxin conjugation during ripening. **Journal of Experimental Botany**, v. 61, p. 3615-25, 2010.

BUSTIN, S.A. *et al*. The MIQE guidelines: Minimum information for publication of quantitative real-time PCR experiments. **Clinical Chemistry**, v. 55, i. 4, p. 611-22, 2009.

BUTTERY, R.G. et al. Characterization of additional volatile components of tomato. **Journal of Agricultural and Food Chemistry**, v. 19, i. 3, p. 524-9, 1971.

CHEN, G. *et al*. Identification of a specific isoform of tomato lipoxygenase (TomloxC) involved in the generation of fatty acid-derived flavor compounds. **Plant Physiology**, v. 136, p. 2641-51, 2004.

CHEN, K.H. *et al*. A rapid and simple procedure for purification of indole-3-acetic-acid prior to GC-SIM-MS analysis. **Plant Physiology**, v. 86, i. 3, p. 822-5, 1988.

CHEN, Y. *et al*. Ethylene receptors and related proteins in climacteric and non-climacteric fruits. **Plant Science**, v. 276, p. 63-72, 2018.

CHONG, J.; WISHART, D.S.; XIA, J. Using MetaboAnalyst 4.0 for Comprehensive and Integrative Metabolomics Data Analysis. **Current Protocols in Bioinformatics**, v. 68, i. 1, p. 1-128, 2019.

DAVIES, P.J. **Plant Hormones: Biosynthesis, Signal Transduction, Action!** London: Kluwer Academic Publishers, 2004.

DAVIES, P.J. **Plant Hormones—Physiology, Biochemistry and Molecular Biology**. Netherlands: Kluwer Academic Publishers, 1995.

DÍAZ DE LEÓN-SÁNCHEZ, F. *et al*. Effect of refrigerated storage on aroma and alcohol dehydrogenase activity in tomato fruit. **Postharvest Biology and Technology**, v. 54, p. 93-100, 2009.

DU, X. *et al*. Identification of sulphur volatiles and GC-olfactometry aroma profiling in two fresh tomato cultivars. **Food Chemistry**, v. 171, p. 306-14, 2015.

DUDAREVA, N. *et al*. Biosynthesis, function and metabolic engineering of plant volatile organic compounds. **New Phytologist**, v. 198, p. 16-32, 2013.

EGEA, I. *et al*. Chloroplast to chromoplast transition in tomato fruit: spectral confocal microscopy analyses of carotenoids and chlorophylls in isolated plastids and time-lapse recording on intact live tissue. **Annals of Botany**, v. 108, p. 291-7, 2011.

ENFISSI, E.M.A. *et al*. The regulation of carotenoid formation in tomato fruit. **The Plant Journal**, v. 89, p. 774-88, 2017.

EXPOSITO-RODRIGUEZ, M. *et al*. Gene structure and spatiotemporal expression profile of tomato genes encoding YUCCA-like flavin monooxygenases: the ToFZY gene family. **Plant Physiology and Biochemistry**, v. 49, i. 7, p. 782-91, 2011.

EXPOSITO-RODRIGUEZ, M. *et al*. Selection of internal control genes for quantitative real-time RT-PCR studies during tomato development process. **BMC Plant Biology**, v. 8, i. 131, p. 1-12, 2008.

FABI, J.P. *et al*. Analysis of ripening-related gene expression in papaya using an Arabidopsis-based microarray. **BMC Plant Biology**, v. 12, i. 242, p. 1-19, 2012.

FABI, J.P. *et al*. Papaya fruit ripening: response to ethylene and 1-methylcyclopropene (1-MCP). **Journal of Agricultural and Food Chemistry**, v. 55, i. 15, p. 6118-23, 2007.

FIEHN, O. *et al*. Metabolite profiling for plant functional genomics. **Nature Biotechnology**, v. 18, i. 11, p. 1157-61, 2000.

FRASER, P.D; BRAMLEY, P.M. The biosynthesis and nutritional uses of carotenoids. **Progress in Lipid Research**, v. 43, p. 228-65, 2004.

GAPPER, N.E.; MCQUINN, R.P.; GIOVANNONI, J.J. Molecular and genetic regulation of fruit ripening. **Plant Molecular Biology**, v. 82, i. 6, p. 575-91, 2013.

GIOVANNONI, J.J. Fruit ripening mutants yield insights into ripening control. **Current Opinion Plant Biology**, v. 10, p. 283-9, 2007.

GIOVANNONI, J.J. Genetic regulation of fruit development and ripening. **Plant Cell**, v. 16, p. S170–S80, 2004.

GIOVANNONI J.J. Molecular biology of fruit maturation and ripening. **Annual Review of Plant Physiology and Plant Molecular Biology**, v. 52, p. 725-49, 2001.

GIVEN, N.K.; VENIS, M.A.; GIERSON, D. Hormonal regulation of ripening in the strawberry, a non-climacteric fruit. **Planta**, v. 174, p. 402–6, 1988.

GOFF, S.A.; KLEE, H.J. Plant volatile compounds: sensory cues for health and nutritional value? **Science**, v. 311, p. 815-9, 2006.

GOULET, C. *et al*. Role of an esterase in flavor volatile variation within the tomato clade. **Proceedings of the National Academy of Sciences**, v. 109, i. 46, p. 19009-14, 2012.

GRIERSON, D. Ethylene and the control of fruit ripening. In: **The molecular Biology and Biochemistry of Fruit Ripening**. Ed. Wiley-Blackwell, 2013. p. 43-68.

GRIFFITHS, A. *et al*. Ethylene and developmental signals regulate expression of lipoxygenase genes during tomato fruit ripening. **Journal of Experimental Botany**, v. 50, i. 335, p. 793-8, 1999.

HAYASHI, K. The interaction and integration of auxin signaling components. **Plant and Cell Physiology**, v. 53, p. 965-75, 2012.

ICHIHARA, K.I.; FUKUBAYASHI, Y. Preparation of fatty acid methyl esters for gas-liquid chromatography. **Journal of Lipid Research**, v. 51, p. 635-40, 2010.

ILG, A. *et al*. Tomato carotenoid cleavage dioxygenases 1A and 1B: Relaxed double bond specificity leads to a plenitude of dialdehydes, mono-apocarotenoids and isoprenoid volatiles. **FEBS Open Bio**, v. 4, p. 584-93, 2014.

JIYUAN, S. *et al*. A 13-lipoxygenase, TomloxC, is essential for synthesis of C5 flavour volatiles in tomato. **Journal of Experimental Botany**, v. 65, p. 419-28, 2014.

JONES, B. *et al*. Down-regulation of DR12, an auxin-response-factor homolog, in the tomato results in a pleiotropic phenotype including dark green and blotchy ripening fruit. **The Plant Journal**, v. 32, p. 603-13, 2002.

JU, C. *et al*. CTR1 phosphorylates the central regulator EIN2 to control ethylene hormone signaling from the ER membrane to the nucleus in Arabidopsis. **Proceedings of the National Academy of Sciences**, v. 109, i. 47, p. 19486-91, 2012.

KARLOVA, R. *et al*. Transcriptional control of fleshy fruit development and ripening. **Journal of Experimental Botany**, v. 65, i. 16, p. 4527-41, 2014.

KEVANY, B.M. *et al*. Ethylene receptor degradation controls the timing of ripening in tomato fruit. **Plant Journal**, v. 51, p. 458-67, 2007.

KEVANY, B.M.; TAYLOR, M.G.; KLEE, H.J. Fruit-specific suppression of the ethylene receptor LeETR4 results in early-ripening tomato fruit. **Plant Biotechnology Journal**, v. 6, i. 3, p. 295-300, 2008.

KIEBER, J.J. *et al*. CTR1, a negative regulator of the ethylene response pathway in Arabidopsis, encodes a member of the Raf family of protein kinases. **Cell**, v. 72, i. 3, p. 427-41, 1993.

KIND, T. *et al*. FiehnLib: mass spectral and retention index libraries for metabolomics based on quadrupole and time-of-flight gas chromatography/mass spectrometry. **Analytical Chemistry**, v. 81, i. 24, p. 10038-48, 2009.

KLEE, H.J. Improving the flavor of fresh fruits: genomics, biochemistry, and biotechnology. **New Phytologist**, v. 187, i. 1, p. 44-56, 2010.

KLEE, H.J.; GIOVANNONI, J.J. Genetics and control of tomato fruit ripening and quality attributes. **Annual Review of Genetics**, v. 45, p. 41-59, 2011.

KLEE, H.J.; TIEMAN, D.M. Genetic challenges of flavor improvement in tomato. **Trends in Genetics**, v. 29, p. 257-62, 2013.

KLEE, H.J.; TIEMAN, D.M. The genetics of fruit flavor preferences. **Nature reviews**, v. 19, p. 347-56, 2018.

KOK, E.J. *et al*. Changes in Gene and Protein Expression during Tomato Ripening – Consequences for the Safety Assessment of New Crop Plant Varieties. **Food Science and Technology International**, v. 14, n. 6, 503-18, 2008.

KORASICK, D.A.; ENDERS, T.A.; STRADER, L.C. Auxin biosynthesis and storage forms. **Journal of Experimental Botany**, v. 64, p. 2541-55, 2013.

KUMAR, R. *et al*. Genome-wide investigation and expression analysis suggest diverse roles of auxin-responsive GH3 genes during development and response to different stimuli in tomato (*Solanum lycopersicum*). **Molecular Genetics and Genomics**, v. 287, p. 221-35, 2012.

KUMAR, R.; KHURANA, A.; SHARMA, A.K. Role of plant hormones and their interplay in development and ripening of fleshy fruits. **Journal of Experimental Botany**, v. 65, i. 16, p. 4561-75, 2014.

LANGE, B.M. *et al*. Isoprenoid biosynthesis: the evolution of two ancient and distinct pathways across genomes. **Proceedings of the National Academy of Sciences**, v. 97, p. 13172-7, 2000.

LELIEVRE, J.M. *et al*. Ethylene and fruit ripening. **Physiologia Plantarum**, v. 101, p. 727-39, 1997.

LI, J. *et al*. Comprehensive RNA-Seq Analysis on the Regulation of Tomato Ripening by Exogenous Auxin. **PLoS ONE**, v. 11, i. 5, p. 1-22, 2016.

LI, J. *et al*. Effects of exogenous auxin on pigments and primary metabolite profile of postharvest tomato fruit during ripening. **Scientia Horticulturae**, v. 219, p. 90-7, 2017.

LIBIN, W.; BALDWIN, E.A.; JINHE, B. Recent advance in aromatic volatile research in tomato fruit: the metabolisms and regulations. **Food and Bioprocess Technology**, v. 9, p. 203-16, 2016.

LISEC, J. *et al*. Gas chromatography mass spectrometry–based metabolite profiling in plants. **Nature Protocols**, v. 1, i. 1, p. 387-96, 2006.

LIU, M. *et al*. A dominant repressor version of the tomato Sl-ERF.B3 gene confers ethylene hypersensitivity via feedback regulation of ethylene signaling and response components. **The Plant Journal**, v. 76, p. 406-19, 2013.

LIU, M. *et al*. Comprehensive Profiling of Ethylene Response Factor Expression Identifies Ripening-Associated ERF Genes and Their Link to Key Regulators of Fruit Ripening in Tomato. **Plant Physiology**, v. 170, i. 3, p. 1732-44, 2016.

LIU, M. *et al.* Ethylene Control of Fruit Ripening: Revisiting the Complex Network of Transcriptional Regulation. **Plant Physiology**, v. 169, i. 4, p. 2380-90, 2015.

LIU, Y.; SCHIFF, M.; DINESH-KUMAR, S.P. Virus-induced gene silencing in tomato. **Plant Journal**, v. 31, p. 777-86, 2002.

LIU, Z.; KARMARKAR, V. Groucho/Tup1 family co-repressors in plant development. **Trends in Plant Science**, v. 13, i. 3, p. 137-44, 2008.

LUDWIG-MÜLLER, J.; GEORGIEV, M.; BLEY, T. Metabolite and hormonal status of hairy root cultures of Devil's claw (*Harpagophytum procumbens*) in flasks and in a bubble column bioreactor. **Process Biochemistry**, v. 43, i. 1, p. 15-23, 2008.

MAGEROY, M.H. *et al*. A Solanum lycopersicum catechol-Omethyltransferase involved in synthesis of the flavor molecule guaiacol. **Plant Journal**, v. 69, i. 6, p. 1043-51, 2012.

MATHIEU, S. *et al*. Flavour compounds in tomato fruits: identification of loci and potential pathways affecting volatile composition. **Journal of Experimental Botany**, v. 60, i. 1, p. 325-37, 2009.

MCATEE, P. *et al*. A dynamic interplay between phytohormones is required for fruit development, maturation, and ripening. **Frontiers in Plant Science**, v. 4, p. 79, 2013.

MCGARVEY, D.J.; CROTEAU, R. Terpenoid metabolism. **Plant Cell**, v. 7, i. 7, p. 1015-26, 1995.

MEIR, S. *et al*. Microarray Analysis of the Abscission-Related Transcriptome in the Tomato Flower Abscission Zone in Response to Auxin Depletion. **Plant Physiology**, v. 154, i. 4, p. 1929-56, 2010.

MUDAY, G.K.; RAHMAN, A.; BINDER, B.M. Auxin and ethylene: collaborators or competitors? **Trends in Plant Science**, v. 17, i. 4, p. 181-95, 2012.

NEGI, S. *et al*. Genetic dissection of the role of ethylene in regulating auxin-dependent lateral and adventitious root formation in tomato. **Plant Journal**, v. 61, i. 1, p. 3-15; 2010.

NORMANLY, J.; SLOVIN, J.P.; COHEN, J.D. Rethinking auxin biosynthesis and metabolism. **Plant Physiology**, v. 107, p. 323-9, 1995.

OMS-OLIU, G. *et al*. Metabolic characterization of tomato fruit during preharvest development, ripening, and postharvest shelf-life. **Postharvest Biology and Technology**, v. 62, i. 1, p. 7-16, 2011.

PALEY, S. *et al*. The Omics Dashboard for interactive exploration of gene-expression data. **Nucleic Acids Research**, v. 45, i. 21, p. 12113-24, 2017.

PATTISON, R.J.; CATALA, C. Evaluating auxin distribution in tomato (*Solanum lycopersicum*) through an analysis of the PIN and AUX/LAX gene families. **The Plant Journal**, v. 70, p. 585-98, 2012.

PÉREZ, A.G.; SANZ, C. Formation of fruit flavor. In: Bruckner B, Wyllie SG**. Fruit and Vegetable Flavour – Recent advances and future prospects**. Woodhead Publishing, 2008. p. 41-70.

PESARESI, P. *et al*. Genetic regulation and structural changes during tomato fruit development and ripening. **Frontiers in Plant Science**, v. 5, i. 124, p. 1-14, 2014.

PFAFFL, M.W. A new mathematical model for relative quantification in real-time RT-PCR. **Nucleic Acids Research**, v. 29, i. 9, p. 2002-7, 2001.

POEL, B.V. *et al*. Targeted Systems Biology Profiling of Tomato Fruit Reveals Coordination of the Yang Cycle and a Distinct Regulation of Ethylene Biosynthesis during Post climacteric Ripening. **Plant Physiology**, v. 160, i. 3, p. 1498-514, 2012.

POTUSCHAK, T. *et al*. EIN3-dependent regulation of plant ethylene hormone signaling by two Arabidopsis F box proteins: EBF1 and EBF2. **Cell**, v. 115, i. 6, p. 679-89, 2003.

PURGATTO, E*. et al*. Inhibition of β-amylase activity, starch degradation and sucrose formation by indole-3-acetic acid during banana ripening. **Planta**, v. 212, p. 823-8, 2001.

QIN, G. *et al*. Unraveling the regulatory network of the MADS box transcription factor RIN in fruit ripening. **The Plant Journal**, v. 70, i. 2, p. 243-55, 2012.

QUINET, M. *et al.* Tomato Fruit Development and Metabolism. **Frontiers in Plant Science**, v.10, p. 1-23, 2019.

RAMBLA, J.L. *et al*. The expanded tomato fruit volatile landscape. **Journal of Experimental Botany**, v. 65, i. 16, p. 4613-23, 2014.

ROCCO, M. *et al*. Proteomic analysis of tomato fruits from two ecotypes during ripening. **Proteomics**, v. 6, i. 13, p. 3781-91, 2006.

ROSS, J.J. *et al*. Plant hormone interactions: how complex are they? **Physiologia Plantarum**, v. 141, p. 299-309, 2011.

RUGKONG, A. *et al*. Expression of ripening-related genes in cold-stored tomato fruit. **Postharvest Biology and Technology**, v. 61, i. 1, p. 1-14, 2011.

SCHWAB, W.; RIKANATI, R.D.; LEWINSOHN, E. Biosynthesis of plant-derived flavor compounds. **The Plant Journal**, v. 54, p. 712-32, 2008.

SELLI, S., *et al*. Characterization of the most aroma-active compounds in cherry tomato by application of the aroma extract dilution analysis. **Food Chemistry**, v. 165, p. 540-6, 2014.

SÉRINO, S. *et al*. HPLC Assay of Tomato Carotenoids: Validation of a Rapid Microextraction Technique. **Journal of Agricultural and Food Chemistry**, v. 57, i. 19, p. 8753-60, 2009.

SEYMOUR, G.B. *et al*. Down-regulation of two non-homologous endogenous tomato genes with a single chimaeric sense gene construct. **Plant Molecular Biology**, v. 23, i. 1, p. 1-9, 1993.

SEYMOUR, G.B. *et al*. Regulation of ripening and opportunities for control in tomato and other fruit. **Plant Biotechnology Journal**, v. 11, i. 3, p. 269-78, 2013.

SHEN, J. *et al*. A 13-lipoxygenase, TomloxC, is essential for synthesis of C5 flavour volatiles in tomato. **Journal of Experimental Botany**, v. 65, i. 2, p. 419-28, 2014.

SHEVCHENKO, A. *et al*. In-gel digestion for mass spectrometric characterization of proteins and proteomes. **Nature Protocols,** v. 1, i. 6, p. 2856-60, 2006.

SIMKIN, A. *et al*. The tomato carotenoid cleavage dioxygenase 1 genes contribute to the formation of the flavor volatiles b-ionone, pseudo ionone, and geranyl acetone. **The Plant Journal**, v. 40, p. 882-92, 2004.

SITRIT, Y.; BENNETT, A.B. Regulation of Tomato Fruit Polygalacturonase mRNA Accumulation by Ethylene: A Re-Examination. **Plant Physiology**, v.116, i. 3, p. 1145-50, 1998.

SORREQUIETA, A. *et al*. Free amino acid production during tomato fruit ripening: a focus on L-glutamate. **Amino Acids**, v. 38, i. 5, p. 1523-32, 2010.

SOUZA, M.A.S. *et al.* Changes in flavonoid and carotenoid profiles alter volatile organic compounds in purple and orange cherry tomatoes obtained by allele introgression. **Journal of the Science of Food and Agriculture**, v. 100, i. 4, p. 1662-70, 2019.

SPEIRS, J. *et al*. Genetic manipulation of alcohol dehydrogenase levels in ripening tomato fruit affects the balance of some flavor aldehydes and alcohols. **Plant Physiology**, v. 117, i. 3, p. 1047-58, 1998.

SU, L*. et al*. Carotenoid accumulation during tomato fruit ripening is modulated by the auxin-ethylene balance. **BMC Plant Biology**, v. 15, i. 114, p. 1-12, 2015.

SZYMANSKI, J*. et al*. Label-free deep shotgun proteomics reveals protein dynamics during tomato fruit tissues development. **The Plant Journal**, v. 90, p. 396-417, 2017.

TAIZ, L.; ZEIGER, E. **Fisiologia Vegetal [Plant physiology]**. Porto Alegre: Artmed Editora, 2004.

TANDON, K.N. *et al*. Characterization of fresh tomato aroma volatiles using GC-olfactometry. **Proceedings of the Florida State Horticultural Society**, v. 114, p.142-4, 2001.

TEALE, W.D.; PAPONOV, I.A.; PALME, K. Auxin in action: signalling, transport and the control of plant growth and development. **Nature Reviews Molecular Cell Biology**, v. 7, i. 11, p. 847-59, 2006.

THE TOMATO GENOME CONSORTIUM. The tomato genome sequence provides insights into fleshy fruit evolution. **Nature**, v. 485, p. 635-41, 2012.

THEOLOGIS, A. *et al.* Modification of fruit ripening by suppressing gene-expression. **Plant Physiology**, v. 100, i. 2, p. 549-51, 1992.

TIEMAN, D.M. *et al*. A chemical genetic roadmap to improved tomato flavor. **Science**, v. 355, i. 6323, p. 391-4, 2017.

TIEMAN, D.M*. et al*. Functional analysis of a tomato salicylic acid methyl transferase and its role in synthesis of the flavor volatile methyl salicylate. **Plant Physiology**, v. 62, i. 1, p. 113-23, 2010.

TIEMAN, D.M*. et al*. Identification of loci affecting flavor volatile emissions in tomato fruits. **Journal of Experimental Botany**, v. 57, p. 887-96, 2006.

TIEMAN, D.M. *et al*. The tomato ethylene receptors NR and LeETR4 are negative regulators of ethylene response and exhibit functional compensation within a multigene family. **Proceedings of the National Academy of Sciences**, v. 97, p. 5663-8, 2000.

TIEMAN, D.M*. et al*. Tomato phenylacetaldehyde reductases catalyze the last step in the synthesis of the aroma volatile 2- phenylethanol. **Phytochemistry**, v. 68, i. 21, p. 2660-9, 2007.

TIEMAN, D.M.; KLEE, H.J. Differential expression of two novel members of the tomato ethylene receptor family. **Plant Physiology**, v. 120, p.165-72, 1999.

TRAINOTTI, L.; TADIELLO, A.; CASADORO, G. The involvement of auxin in the ripening of climacteric fruits comes of age: the hormone plays a role of its own and has an intense interplay with ethylene in ripening peaches. **Journal of Experimental Botany**, v. 58, i. 12, p. 3299-308, 2007.

TUCKER, G. *et al*. Ethylene and fruit softening. **Food Quality and Safety**, v. 1, i. 4, p. 253-67, 2017.

TYANOVA, S. *et al.* The Perseus computational platform for comprehensive analysis of (prote)omics data. **Nature Methods**, v. 13, i. 9, p. 731-40, 2016.

TYANOVA, S.; TEMU, T.; COX, J. The MaxQuant computational platform for mass spectrometry-based shotgun proteomics. **Nature Protocols**, v. 11, i. 12, p. 2301-19, 2016.

VAN DE POEL, B. *et al*. Targeted systems biology profiling of tomato fruit reveals coordination of the yang cycle and a distinct regulation of ethylene biosynthesis during post climacteric ripening. **Plant Physiology**, v. 160, p. 1498-514, 2012.

VOGEL, J.T. *et al*. Carotenoid content impacts flavor acceptability in tomato (*Solanum lycopersicum*). **Journal of the Science of Food and Agriculture**, v. 90, i. 13, p. 2233-40, 2010.

WANG, L. *et al.* Suppression of volatile production in tomato fruit exposed to chilling temperature and alleviation of chilling injury by a pre-chilling heat treatment. **LWT—Food Science and Technology**, v. 62, i. 1, p. 115-21, 2015.

WU, Q. *et al.* Effect of exogenous auxin on aroma volatiles of cherry tomato (*Solanum lycopersicum* L.) fruit during postharvest ripening. **Postharvest Biology and Technology**, v. 146, p. 108-16, 2018.

XUE, Z. *et al*. Effect of ethylene on polygalacturonase, lipoxygenase and expansin in ripening of tomato fruits. **Transactions of Tianjin University**, v. 15, 173, 2009.

YANAGISAWA, S.; YOO, S.D.; SHEEN, J. Differential regulation of EIN3 stability by glucose and ethylene signalling in plants. **Nature**, v. 425, p. 521-5, 2003.

YANG, S.F.; HOFFMAN, N.E. Ethylene biosynthesis and its regulation in higher plants. **Annual Review of Plant Biology**, v. 35, p. 155-89, 1984.

YANG, S.O. *et al*. Four divergent Arabidopsis ethylene-responsive element-binding factor domains bind to a target DNA motif with a universal CG step core recognition and different flanking bases preference. **The FEBS Journal**, v. 276, p. 7177-86, 2009.

YUE, P. *et al*. Ethylene promotes IAA reduction through PuERFs-activated PuGH3.1 during fruit ripening in pear (*Pyrus ussuriensis*). **Postharvest Biology and Technology**, v. 157, 2019.

ZAHARAH, S.S. *et al*. Role of Brassinosteroids, Ethylene, Abscisic Acid, and Indole-3-Acetic Acid in Mango Fruit Ripening. **Journal of Plant Growth Regulation**, v. 31, p. 363-72, 2012.

ZHANG, J. *et al*. Genome-wide association mapping for tomato volatiles positively contributing to tomato flavor. **Frontiers in Plant Science**, v. 6, 1042, 2015.

ZOUINE, M. *et al*. Characterization of the Tomato ARF Gene Family Uncovers a Multi-Levels Post-Transcriptional Regulation Including Alternative Splicing. **PLOS ONE**, v. 9, i. 1, p. e84203, 2014.

ZOUINE, M. *et al*. TomExpress, a unified tomato RNA-Seq platform for visualization of expression data, clustering and correlation networks. **The Plant Journal**, v. 92, p. 727-35, 2017.